Université de Montréal

Étude par pharmacologie quantitative du système dopaminergique des ganglions de la base pour l'optimisation de la pharmacothérapie. Modèle unificateur pour la maladie de Parkinson et le TDAH

par

Florence Véronneau-Veilleux

Faculté de pharmacie

Thèse présentée en vue de l'obtention du grade de
Philosophiæ Doctor (Ph.D.)
en sciences pharmaceutiques

14 décembre 2021

Université de Montréal

Cette thèse intitulée

Étude par pharmacologie quantitative du système dopaminergique des ganglions de la base pour l'optimisation de la pharmacothérapie. Modèle unificateur pour la maladie de Parkinson et le TDAH

présentée par

Florence Véronneau-Veilleux

a été évaluée par un jury composé des personnes suivantes :

Amélie Marsot
(présidente-rapporteuse)

Fahima Nekka
(directrice de recherche)

Janelle Drouin-Ouellet
(membre du jury)

Laurent Pujo-Menjouet
(examinateur externe)

(représentant du doyen de la FESP)

Résumé

La dopamine est un neurotransmetteur important dans le fonctionnement des ganglions de la base, région du cerveau impliquée dans la fonction motrice et l'apprentissage. Un dérèglement de la dynamique de la dopamine peut être à l'origine de différentes pathologies neurologiques, telles que la maladie de Parkinson et le trouble de déficit de l'attention avec ou sans hyperactivité (TDAH). La lévodopa, un précurseur de la dopamine, est utilisée pour réduire les symptômes associés à la maladie de Parkinson, sans action directe sur ses causes. La lévodopa est très efficace au début de la maladie, mais la durée de son effet ainsi que son index thérapeutique diminuent avec la progression de la dénervation induite par la maladie. Ces changements compliquent considérablement l'optimisation des régimes posologiques. Le méthylphénidate, quant à lui, est administré pour réduire les symptômes du TDAH et agit entre autres en bloquant la recapture de la dopamine. Bien que les données confirment une certaine implication de la dopamine dans le TDAH, son étiologie exacte demeure inconnue.

Peu d'études ont cerné l'effet de la lévodopa sur le système dopaminergique des ganglions de la base et son évolution avec la progression de la maladie. Aussi, bien que le TDAH ait suscité beaucoup d'intérêt, rares sont les études quantitatives de nature mécanistiques sur le sujet. L'approche de modélisation mathématique utilisée dans cette thèse s'inscrit dans un effort global visant l'optimisation de la lévodopa et du méthylphénidate, appuyé par l'élucidation des mécanismes impliqués dans la maladie de Parkinson et dans le TDAH. En adoptant une approche de pharmacologie quantitative des systèmes (QSP), nous avons développé un modèle intégratif du système dopaminergique des ganglions de la base, avec l'objectif d'élucider les mécanismes impliqués, d'évaluer l'impact de la dopamine chez des

sujets souffrant de Parkinson ou de TDAH, et recevant ou non un traitement, et enfin de guider objectivement l'exercice d'optimisation des régimes posologiques. À notre connaissance, c'est le premier cadre unificateur de modélisation qui s'adresse à ces deux pathologies.

Le modèle développé dans cette thèse est composé de trois sous-modèles : le premier décrit la pharmacocinétique du médicament concerné, soit la lévodopa ou le méthylphénidate ; le deuxième exprime mathématiquement les différents mécanismes impliqués dans la dynamique de la dopamine ; le troisième représente la complexité de la neurotransmission dans les ganglions de la base. Avec des adaptations appropriées, nous avons appliqué ce même modèle au contexte de la maladie de Parkinson et au TDAH, ainsi qu'à leurs thérapies respectives.

Pour représenter physiologiquement la maladie de Parkinson, nous avons intégré dans le modèle l'évolution de la perte neuronale ainsi que les différents mécanismes de compensation qui en résultent. La fréquence de tapotement des doigts est utilisée comme mesure clinique de la bradykinésie, définie comme le ralentissement des mouvements chez les patients parkinsoniens. Le modèle développé se base sur les connaissances actuelles de la pathophysiologie et pharmacologie du Parkinson, assurant ainsi sa validité en comparaison à des observations expérimentales et cliniques. Ensuite, à l'aide de ce modèle, les relations non-linéaires entre la concentration plasmatique de lévodopa, la concentration en dopamine dans le cerveau et la réponse à une tâche motrice sont étudiées. Le rétrécissement de l'index thérapeutique de la lévodopa au cours de la progression de la maladie dû à ces non-linéarités est investigué. Enfin, pour assurer l'aspect translationnel de notre approche, nous avons développé une application web à laquelle ce modèle a été intégré. Cette application sert de preuve de concept à un outil facilitant l'optimisation et l'individualisation des régimes posologiques.

Pour l'étude du TDAH, nous avons adapté le modèle du système dopaminergique en y intégrant la libération tonique et phasique de la dopamine, cette dernière se produisant durant une tâche d'apprentissage par renforcement. Des individus virtuels ont été créés avec et sans déséquilibre du ratio tonique/phasique de la dopamine. En simulant une tâche de

réponse à des stimuli dans un contexte de déséquilibre de la dopamine, le modèle nous a permis d'observer des symptômes similiaires à ceux de patients réels souffrant de TDAH. Finalement, la réponse au méthylphénidate résultant de l'inhibition de la recapture de la dopamine, à travers différents scénarios d'apprentissage a aussi été étudiée. Le développement d'une métrique nous a permis de différencier les répondants des non-répondants, et ainsi de mettre en évidence l'implication possible d'un apprentissage excessif chez les non-répondants. Une meilleure compréhension de la réponse au méthylphénidate permettrait d'éviter la surmédication chez les non-répondants et d'aider les cliniciens dans leur pratique.

Malgré la complexité du système dopaminergique et des traitements associés, cette thèse est un pas en avant dans la compréhension des mécanismes sous-jacents et de leur implication dans la thérapie. Ces avancées ont été réalisées en adoptant une approche de pharmacologie quantitative des systèmes, associée à une modélisation neurocomputationnelle du domaine du génie électrique, et complétée par un aspect de transfert au chevet du patient. Ce n'est qu'en transcendant ainsi les frontières disciplinaires qu'une visée aussi globale et intégrative est possible, afin de faire face aux défis multidimensionnels du système de la santé.

Mots-clés : Pharmacologie quantitative des systèmes (QSP), pharmacométrie, ganglions de la base, système dopaminergique, Parkinson, lévodopa, TDAH, méthylphénidate.

Abstract

Dopamine is an important neurotransmitter of the basal ganglia, a region of the brain involved in motor function and learning. Disruption of dopamine dynamics can cause various neurological conditions, such as Parkinson's disease and attention deficit hyperactivity disorder (ADHD). Levodopa, a dopamine precursor, is used to reduce the symptoms associated with Parkinson's disease, without directly alleviating its causes. Levodopa is very effective in the early stages of the disease, but its effect duration along with its therapeutic index decrease with disease-induced denervation. These modifications further challenge determination of optimal dosing regimens of levodopa. In the case of ADHD, methylphenidate is administered to reduce its symptoms by, among other things, blocking dopamine recapture. Although evidence supports involvement of dopamine in ADHD, its exact etiology remains unknown.

Few studies have investigated the effect of levodopa on the basal ganglia dopaminergic system and how it evolves with disease progression. Also, although ADHD has received a lot of interest, few quantitative studies of a mechanistic nature have been conducted on the subject. The mathematical modeling approach used in this thesis is part of an overall effort to optimize levodopa and methylphenidate, supported by the elucidation of the mechanisms involved in Parkinson's disease and ADHD. Using a quantitative systems pharmacology (QSP) approach, we have developed an integrative model of the basal ganglia dopaminergic system, with the objective of elucidating the mechanisms involved, assessing the impact of dopamine in subjects with Parkinson's or ADHD, with and without treatment, and objectively guiding the dosing regimens optimization. To the best of our knowledge, this is the

first unifying modeling framework that addresses at the same time these two pathologies and their therapies.

The model developed in this thesis includes three sub-models: the first one describes the drug pharmacokinetics, either levodopa or methylphenidate; the second one translates mathematically the different mechanisms involved in the dopamine dynamics; the third one is a computational representation of the complexity of neurotransmission in the basal ganglia. With appropriate adaptations, we have applied this same model to the context of Parkinson's disease and ADHD, as well as to their respective pharmacotherapies.

In order to physiologically represent Parkinson's disease, we have integrated the denervation process in the model as well as the resulting compensation mechanisms. The finger tapping frequency is used as a clinical endpoint of bradykinesia, defined as the slowing of movements. The developed model is based on up-to-date knowledge of the pathophysiology and pharmacology of Parkinson's disease, thus ensuring its validity in comparison with experimental and clinical observations. Using this model, the non-linear relationships between plasma levodopa concentration, dopamine concentration in the brain and response to a motor task were studied. The narrowing of levodopa therapeutic index during the progression of the disease due to these non-linearities was investigated. Finally, to ensure the translational aspect of our approach, we developed a web application in which this model was integrated. This application serves as a proof of concept for a tool aimed to facilitate the optimization and individualization of dosing regimens.

For the study of ADHD, we adapted the developed model by integrating tonic and phasic dopamine release, the latter occurring during a reinforcement learning task. Virtual individuals were created with and without dopamine imbalance in the tonic/phasic ratio. By simulating a stimulus-response task, we observe ADHD-like symptoms among virtual patients with dopamine imbalance. Finally, the response to methylphenidate resulting from dopamine recapture inhibition, through different learning scenarios, was also studied. The

development of a metric allowed us to differentiate responders from non-responders, and thus to highlight the possible implication of excessive learning in non-responders. A better understanding of methylphenidate response would help avoid overmedication in non-responders and assist clinicians in their practice.

Despite the complexity of the dopaminergic system and its associated therapies, this thesis is a step forward in understanding the underlying mechanisms and their involvement in pharmacotherapy. These advances were achieved by adopting a quantitative systems pharmacology approach, combined with neurocomputational modeling borrowed from the electrical engineering field, and complemented by a translational bedside aspect. It is only by transcending disciplinary boundaries and adopting such an integrative approach that this ultimate goal of having a real impact on the multifaceted health system is possible.

Keywords: Quantitative Systems Pharmacology (QSP), pharmacometrics, neurocomputational modeling, basal ganglia, dopaminergic system, Parkinson's disease, levodopa, ADHD, methylphenidate.

Table des matières

Liste des tableaux

Table des figures

Liste des sigles et des abréviations

ADHD	Attention deficit hyperactivity disorder
ADME	Absorption, distribution, métabolisme, élimination
A2A	Récepteurs de l'adénosine
BG	Basal ganglia
ChI	Interneurone cholinergique - *cholinergic interneurons*
CNS	Système nerveux central - *central nervous system*
COMT	Catéchol-O-méthyltransférase
CPT	Tâche de performance continue - *continuous performance task*
DOPA	3,4-dihydroxyphénylalanine
D1	Récepteurs dopaminergiques D1
D2	Récepteurs dopaminergiques D2
DA	Dopamine

DAT	*Dopamine active transporter*
DSM	*Diagnostic and Statistical Manual of Mental Disorders*
EC50	Concentration pour l'obtention de 50% de l'effet maximal *Half maximal effective concentration*
GABA	Acide gamma-aminobutyrique
GB	Ganglions de la base
GPe	Globus pallidus externe - *Globus pallidus extern*
GPi	Globus pallidus interne - *Globus pallidus intern*
H&Y	Échelle de Hoehn et Yahr - *Hoehn and Yahr scale*
IV	Intraveineuse - *intravenous*
LD	Lévodopa
m-santé	Santé mobile
MPH	Méthylphénidate - *methylphenidate*
MSN	Neurones épineux de taille moyenne - *Medium sized spiny neurons*
NET	Transporteurs de la noradrénaline

PD	Pharmacodynamique - *pharmacodynamic*
PK	Pharmacocinétique - *pharmacokinetic*
PK/PD	Pharmacocinétique/pharmacodynamique - *pharmacokinetic/pharmacodynamic*
QSP	Pharmacologie quantitative des systèmes - *Quantitative systems pharmacology*
Std	*Standard deviation*
STN	Noyau subthalamique - *Subthalamic nucleus*
T	Thalamus
TDAH	Trouble de déficit de l'attention avec ou sans hyperactivité
TH	Tyrosine hydroxylase
UPDRS	*Unified Parkinson's disease rating scale*
UPDRS3	Partie 3 de l'échelle UPDRS
VMAT	Transporteurs vésiculaires de monoamine
5-HT2A	Récepteurs sérotoninergiques

À ma famille et mes amis qui ont contribué sans
l'ombre d'un doute à cette thèse.

Remerciements

Cette thèse est le résultat de beaucoup d'années de travail, de réflexion, de discussion et de remise en question pendant lesquelles j'ai été entourée de nombreuses personnes envers lesquelles je souhaite témoigner ma reconnaissance.

J'aimerais d'abord remercier ma directrice de recherche, Dre Fahima Nekka, d'avoir su me guider et m'encourager durant toutes ces années. J'admire votre passion et votre dévouement pour la science, mais encore plus envers vos étudiants. Vous avez fait de moi la chercheuse que je suis aujourd'hui grâce à votre soutien moral et scientifique (et vos nombreuses corrections de mes textes). Je me considère très chanceuse de faire partie de votre laboratoire. Je ne me doutais pas que présenter au séminaire d'été du CAMBAM me mènerait jusqu'ici !

Je tiens à remercier Dr Philippe Robaey pour toutes les discussions enrichissantes que nous avons eues, sans vous ma compréhension du TDAH aurait été beaucoup plus lente et pénible. Merci pour votre rigueur scientifique toujours bienveillante et vos sages réflexions. Les réunions avec vous et Fahima sont toujours un réel plaisir !

J'aimerais aussi remercier Dr Mauro Ursino, à qui j'ai écrit, naïvement, au début de mon parcours doctoral, pensant ne jamais recevoir de réponse. Ce fut finalement le début d'une belle collaboration. *Un ringraziamento speciale al Dr. Ursino per il sostegno fornitomi.*

Merci Dr Daniel Lévesque d'avoir répondu à toutes mes questions, surtout durant les premières années pendant lesquelles la maladie de Parkinson ne m'était pas familière, ce fut précieux pour moi de pouvoir compter sur vous.

J'aimerais évidemment remercier les membres du jury, Dre Janelle Drouin-Ouellet, Dre Amélie Marsot et Dr Laurent Pujo-Menjouet d'avoir accepté d'évaluer ma thèse.

Je souhaite aussi remercier mes collègues de la Faculté de pharmacie qui ont su mettre du soleil dans mes journées, Abdullah, Anaëlle, Augusto, Cassandre, Churny, Fatéma, Frédérique, Imad, Jeffery, Miriam, Paul-Antoine, Guillaume, Sara, Stéphanie, Steven et Vivian. Le confinement m'a fait réaliser à quel point j'appréciais nos pauses discussion de l'après-midi. Merci aussi à mes collègues enseignants de mathématiques du Collège André-Grasset qui ont toujours su respecter ma position étrange d'enseignante-étudiante.

Je remercie aussi mes amies rencontrées à Lyon, en particulier Gwladys et Marion, de vos conseils et encouragements à distance tout au long de ma thèse. Mes remerciements vont aussi à mes amies, Camille, Geneviève, Justine, Laure, Laurence et Manuela, à qui j'ai dit d'innombrables fois « Désolé, je ne peux pas, je travaille sur ma thèse ! ». Merci de votre compréhension et de votre patience, j'ai hâte de pouvoir vous retrouver avec plus de liberté !

J'aimerais remercier tous les membres de ma famille élargie de m'avoir toujours encouragée, vous m'avez manqué pendant le confinement. En particulier, merci à mes parents, France et Paul et ma sœur Marianne, qui ont toujours été présents, qu'il s'agisse de réviser mon introduction, de me préparer des repas pour que je puisse me concentrer sur ma thèse ou de démolir notre plancher en céramique. Vous êtes et serez toujours des piliers dans ma vie. Vous m'inspirez à travers votre façon d'être et vos conseils, même si je ne les suis pas toujours ! J'aimerais exprimer un merci spécial à mon grand-papa qui nous a quitté durant mon doctorat, et qui m'a toujours encouragée dans mes études. Je n'ai pas guéri la maladie de Parkinson comme tu le pensais, j'espère que tu es fier quand même. J'aurais aimé que tu sois là pour pouvoir partager et célébrer la fin de mes études avec toi.

Finalement, merci à Dmitri, le dernier mais non le moindre, avec qui je partage ma vie. Merci pour tout, les réflexions scientifiques, les encouragements, les corrections, la prise en charge des tâches ménagères pendant ma rédaction... Merci aussi de m'aider à remettre les choses en perspective. Ton intelligence n'a d'égal que ta gentillesse, et ce n'est pas peu dire ! Tu as su partager mes joies et mes angoisses, j'espère que ça ne s'arrêtera jamais. Je t'aime.

Introduction

L'objectif principal de la présente thèse est d'élucider les mécanismes impliqués dans le dysfonctionnement du système dopaminergique des ganglions de la base engendrant différentes pathologies ainsi que dans l'effet des thérapies associées, pour des fins d'optimisation de leurs posologies. Deux pathologies distinctes en apparence, mais partageant des mécanismes physiologiques communs, sont étudiées : la maladie de Parkinson et le trouble de déficit de l'attention avec ou sans hyperactivité (TDAH). En effet, ces deux pathologies affectent des mécanismes impliqués dans la dynamique de la dopamine des ganglions de la base et sont associées à une réduction du niveau de base de la dopamine dans cette région. Les médicaments les plus couramment prescrits pour traiter chacune de ces pathologies sont inclus dans cette étude : la lévodopa, pour la maladie de Parkinson, et le méthylphénidate, pour le TDAH. La modélisation mathématique et l'approche computationnelle ont été choisies comme outil principal pour l'atteinte des objectifs de cette thèse.

La maladie de Parkinson est la deuxième maladie neurodégénérative la plus répandue au monde après la maladie d'Alzheimer [**142**]. En effet, uniquement au Canada, l'agence de la santé publique dénombrait 84 000 individus vivant avec la maladie de Parkinson en 2013-2014 [**37**]. De plus, entre 0.001 et 0.002% de la population européenne, principalement les personnes âgées de 60 ans et plus, est touchée par la maladie de Parkinson [**133**]. Malgré l'usage très répandu de la lévodopa pour traîter les symptômes de cette maladie, l'optimisation du régime posologique de ce médicament représente un véritable casse-tête pour les cliniciens lorsque la maladie atteint un stade plus avancé.

De son côté, le TDAH est le trouble neurocomportemental le plus commun chez les jeunes. Au Québec, la prévalence dans la seule période de 2015-2016 était de 240 000 jeunes (pour la tranche d'âge de 1 à 24 ans) [**70**]. La prévalence mondiale du TDAH est estimée à 5,29% [**98**]. Malgré le grand nombre de recherches, l'étiologie exacte de cette pathologie demeure inconnue. Le méthylphénidate est le médicament vedette utilisé pour diminuer les symptômes du TDAH.

Au cours des dernières années, des approches très variées ont été utilisées pour mieux comprendre les étiologies de ces pathologies et en améliorer le traitement, allant d'études expérimentales aux pures modélisations théoriques, en passant par tout le spectre compris entre ces extrémités. La modélisation mathématique et computationnelle représente une option prometteuse, prenant de plus en plus d'envergure parmi l'arsenal d'approches utilisées en pharmacologie. Combinée à des données et connaissances physiologiques, elle se distingue par son caractère non-invasif et sa capacité à tester et valider rapidement de nombreuses hypothèses et scénarios cliniques, des qualités qui la rendent particulièrement adaptée à l'investigation de pathologies mal comprises telles la maladie de Parkinson et le TDAH.

Afin de mettre en contexte les contributions de la présente thèse, les prochaines sections présenteront dans l'ordre le fonctionnement des ganglions de la base et du système dopaminergique, puis l'état actuel des connaissances liées à la maladie de Parkinson et au TDAH, et finalement les différentes approches utilisées dans le domaine de la modélisation mathématique .

0.1. La neurotransmission et les ganglions de la base

Puisque la maladie de Parkinson et le TDAH affectent les ganglions de la base, débuter par une description du fonctionnement des différentes régions de cette partie du cerveau apparaît essentiel.

0.1.1. La neurotransmission

Le cerveau est un des organes les plus complexes du corps humain. Il est composé d'environ 100 milliards de neurones [**137**], des cellules nerveuses dont on peut mesurer le potentiel électrique de la membrane, connectés entre eux et transmettant de l'information. Cette transmission permet d'assurer le bon déroulement des différentes fonctions du cerveau, telles la mémoire, le mouvement, la cognition, l'attention, le langage, les émotions, etc. Avec le vieillissement des populations occidentales, on assiste à une croissance de la prévalence de maladies affectant le fonctionnement du cerveau et engendrant des symptômes nuisibles à la qualité de vie des patients. L'étude du cerveau, autant dans son état physiologique que pathologique, s'avère donc plus que jamais pertinente.

Lorsqu'on étudie le phénomène de neurotransmission en se concentrant sur une paire de neurones, on distingue le neurone présynaptique envoyant le signal, du neurone postsynaptique qui le reçoit. En effet, l'espace se trouvant entre les neurones est connu sous le nom de synapse. Dans cet espace, les neurotransmetteurs, c'est à dire les molécules permettant la transmission de l'information d'un neurone à l'autre, sont libérés du neurone présynaptique et captés par les récepteurs du neurone postsynaptique tel qu'illustré à la Figure 1. Évidemment, puisque chaque neurone est connecté à plusieurs autres, il est à la fois pré- et postsynaptique.

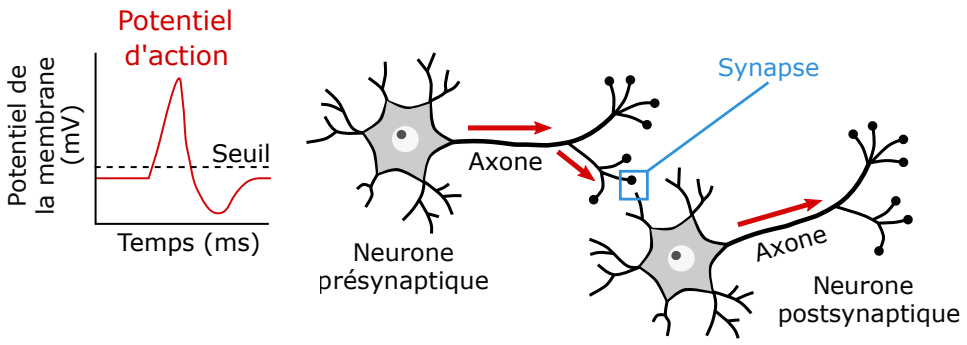

Figure 1. Représentation de la transmission d'un signal électrique entre deux neurones, le neurone pré- et postsynaptique et représentation graphique du potentiel d'action déclenché après l'atteinte d'un seuil.

La libération des neurotransmetteurs survient lorsque le potentiel membranaire du neurone présynaptique dépasse un certain seuil, pouvant varier d'un neurone à l'autre. Un potentiel d'action est alors déclenché et se propage le long de son axone. Les neurotransmetteurs libérés peuvent se lier à la portion postsynatique d'autres neurones, ce qui induit différentes réactions à l'intérieur de ces derniers, dont des modifications de leur potentiel membranaire. Lorsque leur potentiel électrique dépasse leur seuil, ils déclenchent à leur tour un potentiel d'action menant à la libération d'autres neurotransmetteurs. Cet effet en cascade, d'un neurone à l'autre, porte le nom de signal bioélectrique. Selon leur nature, les neurotransmetteurs peuvent exciter ou inhiber les neurones, c'est-à-dire qu'ils peuvent respectivement favoriser ou retenir la création d'un potentiel d'action qui permettra de transmettre l'information au prochain neurone.

Afin de simplifier l'étude du cerveau, les neurones sont souvent regroupés en régions caractérisées selon les fonctions effectuées. Les ganglions de la base, impliquées dans les deux pathologies à l'étude, constituent une de ces régions.

0.1.2. Ganglions de la base

Les ganglions de la base forment une région souvent associée à la fonction motrice du cerveau. Ils sont par ailleurs également impliqués dans les fonctions cognitives, émotionnelles et exécutives du cerveau [**78**].

Afin d'assurer leurs nombreuses fonctions, les ganglions de la base sont divisés en différents noyaux sous-corticaux, sous-régions en dessous du cortex, qui communiquent par différentes voies de neurotransmission. Les principaux noyaux sont le striatum, le globus pallidus, le noyau subthalamique et la substance noire. Le cortex et le thalamus sont également connectés à plusieurs de ces noyaux par des voies de neurotransmission tel que représenté à la Figure 2.

Puisque c'est au striatum que l'information provenant du cortex est reçue, pour ensuite être acheminée aux autres noyaux, celui-ci est parfois qualifié de noyau d'entrée. Alimenté

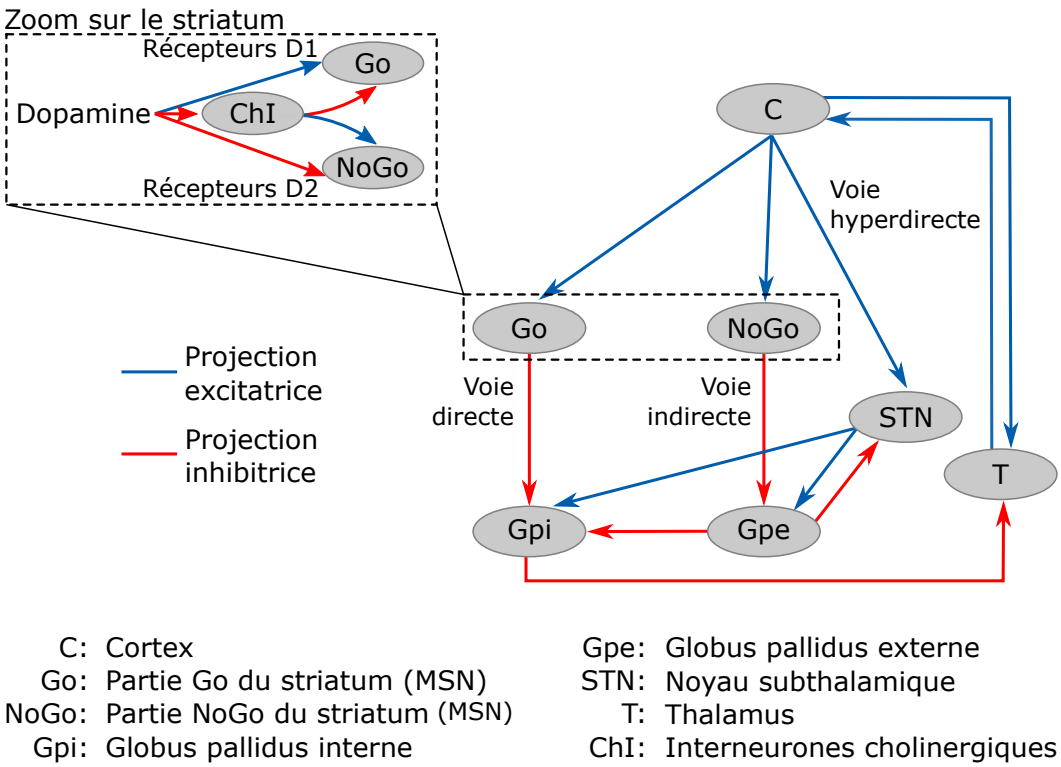

Figure 2. Représentation des différentes régions des ganglions de la base ainsi que des trois voies de neurotransmission : directe, indirecte et hyperdirecte.

en dopamine par la substance noire, dont la mort des neurones dopaminergiques caractérise justement la maladie de Parkinson [**78**], le striatum est composé de neurones épineux de taille moyenne (*medium sized spiny neurons* (MSN)) et d'interneurones. Alors qu'ils utilisent l'acide gamma-aminobutyrique (GABA) comme neurotransmetteur inhibiteur [**78**], les MSN ont des récepteurs dopaminergiques de type D1 et D2, pour lesquels la dopamine a respectivement un effet excitateur ou inhibiteur. En fonction du type de récepteurs majoritairement présents sur les MSN, ceux-ci sont divisés au sein du striatum en neurones faisant partie de la voie directe (D1) ou de la voie indirecte (D2). Par ailleurs, les MSN sont également affectés par l'activité des interneurones cholinergiques. Ces cellules, utilisant l'acétylcholine comme neurotransmetteur et inhibées par la dopamine [**128**], ont respectivement un effet inhibiteur et excitateur sur les MSN de la voie directe et de la voie indirecte (effet dans les deux cas inverse à celui de la dopamine).

Le globus pallidus, quant à lui, est composé de neurones GABAergiques et reçoit des projections inhibitrices du striatum par les deux voies mentionnées précédemment. Plus précisément, les neurones du striatum à récepteur majoritairement D1 sont connectées au globus pallidus interne par la voie directe, alors que les neurones à récepteur majoritairement D2 affectent plutôt le globus pallidus externe, qui inhibe de surcroît le globus pallidus interne. Par ailleurs, ces deux parties du globus pallidus reçoivent également des projections excitatrices du noyau subthalamique.

Ce noyau subthalamique est en effet composé de neurones GABAergique excitateurs recevant de l'information directement en provenance du cortex, tout en étant lui aussi inhibé par le globus pallidus externe. Il a fait l'objet de plusieurs études dans les dernières années, étant donné qu'il s'agit d'une des régions des ganglions de la base pouvant être stimulées par des électrodes lors de l'intervention chirurgicale nommée la stimulation cérébrale profonde (deep brain stimulation) qui sera abordée à la Section 0.3.1.4.

Le thalamus ne fait pas partie des noyaux des ganglions de la base, mais il est nécessaire à la transmission de l'information dans les différentes voies de neurotransmission. Il reçoit des projections inhibitrices du globus pallidus interne et transmet l'information au cortex [**78**].

Le modèle classique de l'organisation fonctionnelle des ganglions de la base fut élaboré dans les années 1980 [**78**]. C'est ce modèle qui a introduit les termes *voie directe* et *voie indirecte* pour faire référence aux connections entre les différents noyaux, selon leurs effets opposés sur la sortie des ganglions de la base. Les termes direct et indirect ont été utilisés au départ pour décrire l'aspect moteur des ganglions de la base. En effet, en termes de fonction motrice, l'inhibition du globus pallidus interne par la voie directe favorise le mouvement, alors que la voie indirecte inhibe plutôt l'inhibition de ce noyau, nuisant au final au mouvement. C'est pourquoi on nomme la portion du striatum faisant partie de la voie directe (avec récepteurs D1) le « Go », et celle faisant partie de la voie indirecte (avec récepteurs D2) le « NoGo ». Dans le modèle classique, une balance entre les deux voies de neurotransmission est nécessaire afin de permettre des mouvements appropriés.

La voie hyperdirecte est le fruit d'études plus récentes [**88**], et relie le cortex au globus pallidus en passant par le noyau subthalamique plutôt que le striatum. Cette voie permet, lors de la réception par les ganglions de la base d'informations conflictuelles ou contradictoires, d'envoyer un signal d'arrêt, le temps que le conflit se règle.

Une hypothèse répandue stipule que les ganglions de la base sont séparés en trois boucles fonctionnelles distinctes : les boucles « limbique », « motrice », et « associative ». Il demeure toutefois incertain que ces trois boucles touchent vraiment des régions physiologiquement séparées des différents noyaux des ganglions de la base [**61**]. La boucle motrice permet de contrôler et d'initier le mouvement et impliquerait le cortex moteur et prémoteur ainsi que la partie dorsale latérale du striatum [**59**]. La boucle limbique serait quant à elle impliquée dans les processus affectifs, les récompenses et les punitions [**69**]. Elle contiendrait le nucleus accumbens faisant partie du striatum ventral [**59**]. Finalement, la boucle associative serait impliquée dans les processus cognitifs plus complexes et comprendrait la partie dorsale médiale du striatum et le cortex associatif.

0.1.3. Problématique

Bien que le modèle des ganglions de la base présenté précédemment ait permis de nombreuses avancées, certains questionnements demeurent [**78**]. En effet, des données sur les effets des lésions dans les ganglions de la base entrent en contradiction avec le modèle classique des voies directes et indirectes. Par exemple, lors d'une pallidotomie, une partie du GPi est détruite par la chaleur induite par une sonde. Ces lésions au niveau du GPi ont mené à une amélioration de la fonction motrice de patients parkinsoniens [**92, 93**] plutôt qu'à la détérioration attendue.

De plus, la force de connexion entre les neurones des différents noyaux peut changer au cours du temps, tel que plus amplement discuté à la Section 0.2.2. Étant donné la complexité de la neurotransmission dans les ganglions de la base et son implication dans différentes fonctions (motrices, cognitives,...), les impacts d'une telle modification des connections entre les noyaux restent encore incertains.

La complexité des ganglions de la base ainsi que l'acquisition constante de nouvelles données les concernant rendent nécessaire la création de cadres théoriques afin de les étudier, tâche pour laquelle les modèles mathématiques représentent une approche de choix.

0.2. Système dopaminergique des ganglions de la base

Vu son rôle majeur dans le fonctionnement des ganglions de la base en raison de sa liaison aux récepteurs du striatum, en plus de son effet démontré sur l'apprentissage, la motivation et l'attention, la dopamine est un neurotransmetteur dont la dynamique est au coeur du projet réalisé dans cette thèse.

0.2.1. Dynamique de la dopamine

Tel que mentionné précédemment, la dopamine est produite par les neurones de la substance noire avant d'être libérée dans la fente synaptique, où elle peut se lier aux récepteurs des neurones du striatum pour en moduler l'activité. Différents mécanismes interviennent dans son cycle de vie, incluant la synthèse, la recapture et l'élimination. Ces processus, illustrés à la Figure 3, régulent la concentration en dopamine dans la fente synaptique.

La tyrosine, un précurseur de la dopamine provenant de l'alimentation (fromage, soja, boeuf, haricots,...[**76**]), est transformée en DOPA par la tyrosine hydroxylase (TH) des neurones. La DOPA se retrouve alors dans le cytoplasme des neurones et peut être décarboxylée en dopamine par la DOPA-décarboxylase. Si elle n'est pas éliminée à l'intérieur du neurone [**13**], la dopamine est ensuite emmagasinée dans des vésicules grâce aux transporteurs de monoamine vésiculaire (VMAT). La dopamine à l'intérieur des vésicules peut par la suite être libérée sous l'action des potentiels d'action, par fusion des vésicules avec la membrane du neurone.

On distingue deux types de libération, soit la libération tonique et phasique. La libération tonique fait référence à une libération soutenue de dopamine qui permet de maintenir une concentration de base, la fréquence de stimulation est alors d'environ 5 Hz [**17**]. La libération phasique, quant à elle, est due à une décharge sous forme de rafales (*bursts*) d'une fréquence

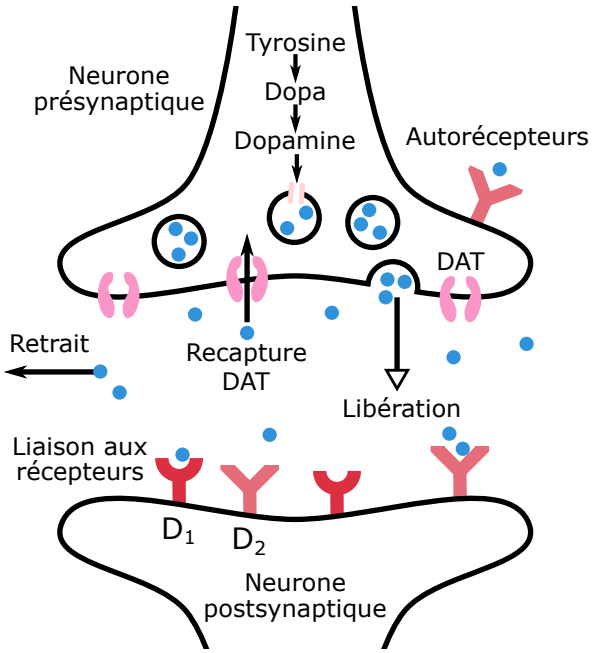

Figure 3. Représentation de la dynamique de la dopamine dans les neurones pré- et postsynaptiques et dans la fente synaptique.

de 15 à 30 Hz [**17, 55**]. Elle n'est pas continue, mais plutôt transitoire et est causée par un évènement comme une récompense. En effet, une augmentation de la libération de la dopamine fut observée chez les rats et les singes lors de la réception d'une récompense imprévue, alors que l'absence d'une récompense attendue entraîne, quant à elle, une diminution de la dopamine [**113**]. À la lumière de cet effet, il est logique que la dopamine soit souvent décrite comme étant l'erreur de prédiction de récompense (*reward prediction error*) qui quantifie la différence entre la récompense attendue après un choix et celle réellement obtenue.

Une fois dans la fente synaptique, la dopamine peut bien entendu se lier aux récepteurs dopaminergiques des neurones postsynaptiques, en particulier les récepteurs D1 et D2, qui ont été considérés dans le cadre de cette thèse. Il existe cependant d'autres mécanismes : elle peut se lier aux autorécepteurs de type D2 du neurone présynaptique, être recapturée par les transporteurs DATs se trouvant sur le neurone présynaptique, ou être dégradée par la catéchol-O-méthyltransférase (COMT). Le principal mécanisme de retrait de la fente synaptique est la recapture [**13**], à la suite de laquelle la dopamine est de nouveau emmagasinée dans les vésicules ou éliminée dans le cytoplasme du neurone.

En cas de liaison aux autorécepteurs, un effet de régulation de la libération de la dopamine a été démontré [**12, 15, 45**]. En effet, ces autorécepteurs modifient la synthèse de la dopamine, la fréquence de décharge (*firing rate*) du neurone ainsi que la libération de la dopamine. Selon le modèle développé par Grace [**55, 57**], la diminution de la liaison des autorécepteurs amènerait une augmentation de la libération phasique permettant ainsi de compenser une diminution du niveau de dopamine tonique.

Puisque la dopamine est essentielle au bon fonctionnement des ganglions de la base, différents processus sont mis en place afin de maintenir une certaine concentration lorsque des perturbations surviennent. D'abord, les autorécepteurs permettent une telle autorégulation, tel que discuté précédemment. De plus, il fût démontré que la dénervation de la substance noire, entraînant la perte des neurones dopaminergiques, produit une diminution de la libération, mais aussi de la recapture de la dopamine [**16, 103**]. Le terme *stabilisation passive* fut utilisé pour décrire ce phénomène. Toutefois, lorsque la dénervation est trop avancée, le maintien de l'homéostasie n'est plus possible. Il a aussi été avancé qu'avec la dénervation, l'élimination de la dopamine de la fente synaptique est augmentée [**16, 103**]. Dans un cerveau sain, les neurones dopaminergiques sont très denses, laissant peu de place à la diffusion de la dopamine dans l'espace synaptique pouvant mener à une éliminination. C'est plutôt la recapture par les transporteurs qui domine la dynamique. Par contre, avec la dénervation, les neurones sont plus espacés, permettant ainsi la diffusion de la dopamine avant sa recapture.

0.2.2. Plasticité synaptique

Des études ont démontré que les ganglions de la base sont impliqués dans l'apprentissage stimulus-réponse, soit l'association d'un stimulus à une réponse adéquate [**44**]. Cet apprentissage peut se faire à l'aide de punitions et de récompenses reçues lorsque, respectivement, une mauvaise et une bonne réponse est associée à un stimulus. Le rôle de la dopamine, en particulier, a été mis en évidence dans ce processus de récompenses et de punitions menant à l'apprentissage [**5, 44**]. En effet, il fut démontré, tant chez les animaux [**112**] que chez l'humain [**146**], que le signal de la dopamine phasique représente les erreurs de prédiction

des récompenses (*reward prediction error*). L'existence d'une corrélation entre l'amplitude de la libération phasique et la taille de la récompense inattendue fut également démontrée [**39**]. Cette amplitude, qui dépend du taux de décharge phasique du neurone allant de 20 à 100 Hz [**43**], peut atteindre une concentration aussi grande que $1\mu mol/L$ [**138**]. Un arrêt du taux de décharge (*firing rate*) des neurones dopaminergiques fut, quant à lui, observé lorsqu'une récompense est omise ou est moins satisfaisante que celle attendue [**89**].

Ces variations de la dopamine phasique induiraient des modulations de la configuration et de l'intensité des connexions synaptiques, qu'on regroupe sous le terme "plasticité". Cette intensité peut être modifiée au niveau postsynaptique, par le biais d'un changement du nombre ou des propriétés des récepteurs postsynaptiques, ou au niveau présynaptique, impliquant alors une augmentation ou une diminution de la libération de neurotransmetteurs [**143**]. La variation de la connexion des synapses peut être à court terme et durer seulement une fraction de seconde, ou bien durer quelques minutes, heures, jours ou même années, auquel cas elle est connue sous le nom de plasticité synaptique à long terme.

Dans les années 1940, Donald Hebb a émis l'hypothèse que la force des connexions synaptiques est modifiée lorsque des neurones pré- et postsynaptiques sont activés en même temps [**83**], hypothèse résumée par l'expression *"Cells that fire together, wire together"*. Cette plasticité permettrait l'apprentissage par l'association d'un stimuli à une réponse adéquate.

Des chercheurs ont par ailleurs avancé l'hypothèse qu'un dysfonctionnement dans le système dopaminergique pourrait aussi engendrer de la plasticité synaptique aberrante, c'est-à-dire que la modification des connexions synaptiques mènerait alors à des effets négatifs, tels que de mauvaises associations entre stimulus et réponse. Il s'agit notamment d'une explication proposée pour les symptômes moteurs de la maladie de Parkinson [**14**]. Il est aussi à noter que des études ont établi un lien entre le dysfonctionnement du système de récompense et le TDAH [**136**].

0.2.3. Pathologies du système dopaminergique

Un dysfonctionnement du système dopaminergique peut entraîner différentes pathologies et déficits. À titre d'exemple, il est largement reconnu qu'une libération trop grande de dopamine dans le striatum et une trop faible dans le cortex pourraient être en cause dans la schizophrénie [**23**]. Par ailleurs, un excès de dopamine dans le noyau accumbens, faisant partie du striatum, est avancé comme hypothèse sous-jacente à l'addiction aux drogues en raison d'un possible apprentissage excessif du comportement de consommation [**34**].

Pour ce qui est de la maladie de Parkinson la dénervation caractéristique des neurones dopaminergiques de la substance noire des ganglions de la base, entraînant une diminution de la concentration en dopamine dans le striatum, est une cause des symptômes moteurs observés [**86**].

Des études ont également démontré qu'une variation de différents gènes associés au système dopaminergique serait impliquée dans le TDAH [**40**]. Cependant, bien que l'implication de la dopamine dans le TDAH fasse consensus, la nature de cette implication est encore matière à débat, et il n'est pas même certain que les symptômes résultent d'un surplus ou d'un manque de ce neurotransmetteur. Pour réconcilier les données contradictoires, détaillées dans la section 0.3.2.2 portant plus spécifiquement sur le TDAH, l'hypothèse d'une réduction du niveau de la dopamine tonique menant à une augmentation de la dopamine phasique fut émise [**9, 56**].

0.2.4. Problématique

Des questions ouvertes subsistent relativement au fonctionnement du système dopaminergique et aux effets de différentes lésions l'affectant. Tout d'abord, l'effet des mécanismes de compensation de la dynamique de la dopamine sur les symptômes de la maladie de Parkinson, ainsi que leur interaction avec la médication et avec les effets secondaires des médicaments ne sont pas encore complètement élucidés. En outre, il est encore incertain si le TDAH est associé à une diminution ou plutôt à une augmentation de la dopamine. Enfin, l'impact de la plasticité synaptique induite par la dopamine sur les ganglions de la base et sur les

symptômes des pathologies associées est mal connu. Ces interrogations nous ont amenés à adopter une approche holistique intégrant les mécanismes importants de la dynamique de la dopamine et leurs implications pour ces deux pathologies et leur pharmacothérapie associée.

0.3. La maladie de Parkinson et le TDAH

Dans la présente thèse, un modèle intégratif combinant la dynamique de la dopamine et la neurotransmission dans les ganglions de la base a été développé afin d'étudier indépendamment la maladie de Parkinson et le TDAH. En plus de la simulation des symptômes, la pharmacothérapie associée à chacune de ces pathologies a pu être étudiée. Pour mettre en évidence les caractéristiques clés que les modèles doivent saisir, les éléments fondamentaux de ces deux pathologies seront discutés dans les prochaines sections.

0.3.1. La maladie de Parkinson

Entre 0.001 et 0.002% de la population européenne, principalement les personnes âgées de 60 ans et plus, est touchée par la maladie de Parkinson [**133**]. Au Canada, plus de 84 000 personnes vivaient avec cette maladie en 2013-2014. Elle est caractérisée par la perte des neurones dopaminergiques de la substance noire des ganglions de la base, menant à l'apparition de différents symptômes moteurs.

0.3.1.1. Historique.

La maladie de Parkinson fut décrite pour la première fois en 1817 par le chirurgien anglais James Parkinson, dans un livre intitulé *"An Essay on the Shaking Palsy"*. Il y décrit des symptômes tels que le tremblement, le ralentissement des mouvements, la posture voûtée et les problèmes de démarche. Ce n'est qu'en 1872 que le terme maladie de Parkinson fait son entrée dans la nomenclature médicale.

Le rôle de la dopamine dans cette maladie est mis en lumière dans les années 1960. Des expériences sur des animaux permettent de démontrer que l'administration de la lévodopa, un précurseur de la dopamine, permet d'augmenter la concentration en dopamine et donne lieu à une activité motrice accrue. Par la suite, les déficits caractéristiques en dopamine dans

la substance noire et le striatum ont été mis en évidence chez des humains atteints de la maladie de Parkinson [**99**]. Des travaux ultérieurs ont démontré que, bien que l'administration de la lévodopa chez les humains permette de réduire les symptômes, elle entraîne également des effets secondaires tels que des hallucinations et des mouvements involontaires nommées dyskinésies [**99**]. Ces effets secondaires sont potentiellement causés par une stimulation pulsatile des neurones du striatum. Pour pallier ces effets secondaires, de nouvelles formulations (comme celles avec ajout d'inhibiteurs) et voies d'administration (telles l'infusion duodénale et intraveineuse) de la lévodopa ont été mises au point à partir des années 1970.

D'autres études ont été réalisées en parallèle afin de comprendre le fonctionnement des ganglions de la base. Dans les années 1980, le modèle classique propose que les ganglions de la base soient constitués de deux voies de neurotransmission, soit la voie directe, qui promeut le mouvement, et la voie indirecte, qui l'inhibe [**99**].

Enfin, c'est en 1995 que la stimulation cérébrale profonde du noyau subthalamique *(deep brain stimulation)* commence à être utilisée dans le but d'atténuer les symptômes de la maladie de Parkinson.

0.3.1.2. Symptômes et biomarqueurs.

La maladie de Parkinson est souvent associée à ses symptômes moteurs : le tremblement au repos, les problèmes de posture, la rigidité musculaire et la bradykinésie, cette dernière référant au ralentissement des mouvements. Toutefois, des symptômes non-moteurs sont aussi présents, les plus incommodants étant des problèmes de sommeil, d'odorat, de constipation, des troubles de la vessie, des hallucinations ainsi que des troubles de l'humeur, pour n'en nommer que quelques uns [**24, 142**].

La *Movement Disorder Society* (MDS) propose quatre étapes permettant d'établir un diagnostic de Parkinson. D'abord, il est nécessaire de vérifier si le patient présente des signes de bradykinésie combinés à des tremblements au repos ou à de la rigidité musculaire. Ensuite, d'autres observations doivent être présentes afin d'appuyer le diagnostic, par exemple une réponse à la lévodopa, la présence de tremblements au repos ou une perte olfactive. L'étape suivante consiste à déterminer si tout autre diagnostic pourrait expliquer ces symptômes,

puisque certains médicaments tels des agents bloquant les récepteurs de la dopamine pourraient induire des symptômes similaires à ceux de la maladie de Parkinson. Enfin, la dernière étape consiste en l'étude de l'historique du patient afin de vérifier la présence de symptômes précurseurs qui pourraient orienter vers la maladie de Parkinson [**105**].

Généralement, lorsque la maladie de Parkinson est diagnostiquée chez un patient, la perte neuronale a déjà atteint 60 à 90 % [**4, 148**]. Ce retard dans l'apparition des symptômes s'explique par le fait que des processus de compensation agissent au niveau du cerveau, que ce soit pour maintenir un niveau adéquat de dopamine ou pour permettre aux neurones de fonctionner malgré un niveau réduit de dopamine.

Plusieurs équipes de chercheurs tentent donc d'identifier des biomarqueurs précliniques qui permettraient un diagnostic précoce et une meilleure prise en charge des patients en ce qui à trait à leur traitement. Le tremblement essentiel, qui se traduit par un tremblement des mains, de la tête ou des jambes, pourrait servir de marqueur pré-clinique puisque des études épidémiologiques ont démontré la présence d'une corrélation importante entre le nombre de patients ayant un tremblement essentiel et ceux ayant la maladie de Parkinson. Jusqu'à 90% des patients atteints de Parkinson souffrent de perte de l'odorat et présentent également des troubles du sommeil. Des problèmes au niveau de la saccade oculaire ainsi que des problèmes de constipation ont aussi été observés chez ces patients. On rapporte également qu'environ 30 à 35% des patients souffrent de dépression [**74, 106**]. Les symptômes mentionnés précédemment pourraient donc servir d'indices précurseurs de la maladie de Parkinson.

0.3.1.3. Échelles de mesure des symptômes.

Les symptômes associés à la maladie de Parkinson étant multiples, plusieurs échelles ont été développées afin de les quantifier. Celles-ci sont aussi utilisées afin d'étudier la progression de la maladie et la réponse aux traitements. L'*Unified Parkinson's Disease Rating Scale* (UPDRS) et l'échelle Hoehn et Yahr (H & Y) sont largement utilisées.

L'échelle UPDRS, développée en 1980, est divisée en quatre parties qui comportent des questions et évaluations. Les parties 1 et 2 concernent respectivement les problèmes non moteurs de la vie courante, tels que les problèmes cognitifs ou les symptômes reliés à l'anxiété,

et les problèmes moteurs, comme de la difficulté à écrire ou à tenir des objets de la vie courante. La partie 3 a trait à l'évaluation des symptômes moteurs tels que le tremblement au repos, la rigidité, les problèmes de posture et la bradykinésie, en plus d'évaluer les expressions faciales et le langage. Enfin, c'est dans la partie 4 que sont étudiées les complications motrices telles que les dyskinésies [**53**]. La réponse aux questions de chaque partie se situe sur une échelle de 0 à 4, référant respectivement à un état normal, léger, modéré, important et sévère. Certaines questions portant sur les effets secondaires, doivent être répondues par un oui ou par un non. À partir des réponses données, un score est attribué aux patients. Certains items de la partie 3 sont mesurés à l'aide de tests moteurs comme le test de tapotement des doigts (*finger tapping test*), le test de pronation/supination du poignet ou le test de la fréquence de tapotement des orteils [**53**]. Dans le cadre de la présente thèse, la fréquence de tapotement des doigts est la mesure utilisée afin d'évaluer le niveau de bradykinésie.

L'échelle de Hoehn et Yahr (H&Y) publiée en 1967 pour décrire la progression de la maladie de Parkinson, divise la maladie en cinq stades. Au stade 1, les patients présentent des symptômes légers sur un seul côté du corps, qui n'affectent pas leur vie quotidienne. Au stade 2, les symptômes affectent les deux côtés du corps, mais les patients ne présentent pas de problèmes d'équilibre. Au stade 3 commencent à apparaître les problèmes de posture ainsi qu'un ralentissement des mouvements. Les patients dont les symptômes entravent leur autonomie sont classés au stade 4. Le stade 5, quant à lui, est attribué aux patients devant utiliser une chaise roulante ou étant alités [**52**].

Peu d'études ont analysé le lien entre les deux échelles, UPDRS et H&Y. Une d'entre elles a démontré que les scores pour les quatre parties de l'échelle UPDRS augmentent avec chaque stade de l'échelle H&Y [**122**].

0.3.1.4. Traitements de la maladie de Parkinson.

Malgré les efforts de recherche déployés depuis des décennies, aucun traitement permettant de guérir ou d'arrêter la progression de la maladie de Parkinson n'a encore vu le jour. Les traitements actuellement utilisés permettent cependant d'atténuer l'intensité des symptômes, améliorant ainsi la qualité de vie des patients.

Parmi les traitements disponibles, la référence est la lévodopa, en raison de l'effet plus significatif que ce médicament a sur les symptômes moteurs, effet se traduisant par une diminution du score UPDRS. Tel que mentionné précédemment, la réponse à la lévodopa est même utilisée comme outil diagnostique en raison de son étroite association avec la maladie de Parkinson.

La dopamine ne peut pas traverser la barrière hématoencéphalique en raison de sa faible solubilité lipidique et de l'absence de transporteurs spécifiques [**95**]. La tyrosine et la lévodopa, un précurseur de la dopamine,sont capables de traverser la barrière hématoencéphalique grâce aux transporteurs LAT1 [**81, 147**]. Se retrouvant alors dans le cerveau, la lévodopa peut être décarboxylée en dopamine par les neurones dopaminergiques de la substance noire et, parfois également par les neurones sérotoninergiques [**97**]. Cette transformation, qui permet d'augmenter la concentration en dopamine et d'induire une réduction des symptômes parkinsoniens, peut s'effectuer après une phase de stockage créant un effet tampon (*buffering effect*) et ce, lorsque le nombre de neurones dopaminergiques restant est suffisant. Cet effet tampon permet de maintenir l'effet de la lévodopa entre deux doses [**1, 97**].

Comme il est également possible que la lévodopa soit décarboxylée en dopamine avant de traverser la barrière hématoencéphalique, une transformation périphérique non souhaitable en raison de la diminution de l'effet thérapeutique, elle est combinée à un inhibiteur de la décarboxylase, souvent la carbidopa, qui fait passer la demi-vie de la lévodopa de 60 à 90 minutes [**1**]. Ce traitement combiné permet de diminuer de 75 à 80% les doses de lévodopa [**84**]. En outre, pour permettre à une plus grande quantité de lévodopa d'atteindre le cerveau et ainsi augmenter la durée de son effet, des inhibiteurs de la catéchol-O-méthyltransférase (COMT) tels que l'entacapone ou la tolcapone peuvent également être ajoutés à l'utilisation de la lévodopa et la carbidopa [**1**].

Aux premiers stades de la maladie de Parkinson, la lévodopa s'avère très efficace pour réduire les symptômes, et ce, avec un nombre limité de doses quotidiennes. Cette phase est désignée comme la période de "lune de miel" [**65**]. Avec la progression de la maladie, la durée de l'effet diminue et peut mener à des périodes où le médicament est même inefficace.

Ceci serait attribuable à la perte de l'effet tampon des neurones. En effet, avec la perte de neurones dopaminergiques, ceux-ci ne sont plus en mesure d'assurer un taux suffisant de dopamine et n'emmagasinent donc plus la lévodopa, mais la transforment et libèrent la dopamine résultante immédiatement. La courbe de l'effet dans le temps devient alors similaire à la courbe de concentration dans le temps et l'effet n'est plus maintenu entre les doses. Afin de pallier cette atténuation de l'effet de la lévodopa, les doses et/ou leurs fréquences d'administration doivent être augmentées.

Au fur et à mesure que le niveau de dénervation augmente, des effets secondaires tels que les dyskinésies, des mouvements involontaires, apparaissent. Des fluctuations *on-off*, caractérisées par des périodes d'effet suivies de périodes où les symptômes sont de retour, surviennent également [**123**]. Dans plusieurs études, on dénombre qu'entre 50 à 55% des patients parkinsoniens ont développé des dyskinésies après 5 à 6 ans de traitement avec la lévodopa [**96**]. Différents facteurs sont impliqués dans l'apparition des dyskinésies, dont l'âge à l'apparition des premiers symptômes ainsi que la durée de la maladie. En effet, il y a un risque plus grand de développer des dyskinésies si les symptômes se sont déclarés à un plus jeune âge. Les dyskinésies étant directement reliées à la prise de lévodopa, le risque associé augmente avec l'augmentation des doses.

Les causes exactes de l'apparition de ces dyskinésies demeurent pourtant mal comprises. Selon une hypothèse répandue, lorsque la dénervation de la substance noire est très avancée, les neurones sérotoninergiques pourraient capter la lévodopa, ce qui mènerait à une libération irrégulière de la dopamine et pourrait ainsi contribuer à l'apparition des effets secondaires [**114**]. La stimulation pulsatile plutôt que continue des récepteurs dopaminergiques pourrait également être en cause [**97**], en plus d'induire une modification de la plasticité synaptique [**96**]. Il a été observé que les traitements qui diminuent la stimulation pulsatile font aussi diminuer les risques de développer des dyskinésies [**96**]. Ceci explique pourquoi, en plus de la voie orale la plus courante, d'autres voies d'administration ont été développées telles que l'infusion duodénale et intraveineuse, afin d'assurer un maintien à un accès plus continu à la lévodopa.

Il est par ailleurs important de noter qu'avec la progression de la maladie, l'index thérapeutique de la lévodopa est réduit, tel qu'illustré qualitativement à la Figure 4. Les doses produisant un effet thérapeutique se rapprochent de celles menant à des effets secondaires, compliquant ainsi considérablement l'optimisation des régimes posologiques des patients.

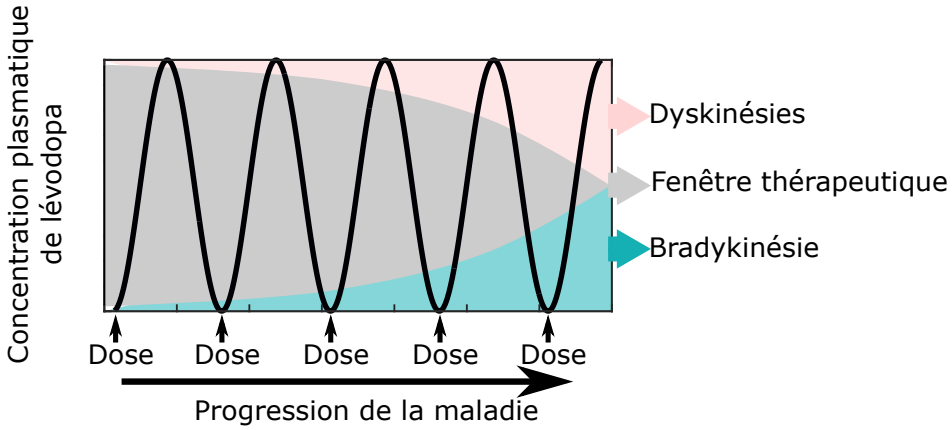

Figure 4. Représentation de la réduction de l'index thérapeutique de la lévodopa avec la progression de la maladie.

De façon générale, on distingue trois phases dans le processus de titrage de la lévodopa. D'abord, le régime posologique standard est offert aux patients en début de maladie. Lorsque les patients commencent à ressentir une diminution de la durée de l'effet, des fluctuations de l'effet ou des effets secondaires, un régime posologique personnalisé est proposé. Finalement, lorsque surviennent des effets secondaires ou de longues périodes sans effet thérapeutique, et que le régime personnalisé ne convient plus, on peut alors avoir recours à la lévodopa sous forme non-orale [**130**].

L'usage des agonistes de la dopamine afin de réduire les symptômes de la maladie de Parkinson fait également partie de la pratique clinique. Ils sont principalement utilisés afin de différer l'administration de la lévodopa et ainsi tenter de retarder l'apparition des dyskinésies [**21**]. En l'absence de dopamine, les agonistes peuvent se lier aux récepteurs dopaminergiques du striatum et ainsi imiter l'action de celle-ci. Les effets secondaires potentiels des agonistes comprennent des hallucinations, de la somnolence et de l'insuffisance cardiaque [**21**].

La stimulation cérébrale profonde (*deep brain stimulation*, DBS) est aussi pratiquée dans le but de réduire les symptômes de la maladie de Parkinson. Durant cette opération chirurgicale, des électrodes sont placées à des endroits stratégiques dans les ganglions de la base, généralement au niveau du noyau subthalamique, du globus pallidus interne ou du thalamus [**77**]. La stimulation électrique induite par ces électrodes permet de réduire les symptômes. Étant donné son aspect invasif, le DBS est généralement offert aux patients à des stades avancés de la maladie chez qui, même si la lévodopa fonctionne, elle cause des effets secondaires très incommodants [**46**].

0.3.1.5. Problématique.

L'utilisation chronique de la lévodopa combinée à la dénervation mène à l'apparition d'effets secondaires ainsi qu'à des fluctuations motrices qui diminuent la qualité de vie des patients. Il importe donc d'optimiser les régimes posologiques de la lévodopa afin de tenter de réduire les doses administrées tout en maintenant un effet thérapeutique et en retardant les effets secondaires. Toutefois, cette optimisation devient de plus en plus difficile avec la progression de la maladie, puisque l'index thérapeutique est graduellement réduit. Le développement d'outils quantitatifs permettant de tester différents régimes posologiques et différentes voies d'administration de la lévodopa afin d'en identifier les plus optimaux serait d'une grande aide pour la pratique clinique et pour l'amélioration de la qualité de vie des patients.

0.3.2. Le trouble du déficit de l'attention avec ou sans hyperactivité

Le TDAH est le trouble neurocomportemental le plus commun chez les jeunes. Ce trouble est principalement caractérisé par un comportement inattentif et/ou impulsif omniprésent, inadéquat en fonction de l'âge du patient[**100**].

Le diagnostic, difficile à poser, repose essentiellement sur des questionnaires ou des autoévaluations. Il est ainsi difficile de connaître avec exactitude la prévalence du TDAH, on estime tout de même qu'elle oscillerait entre 2% et 18% [**108**]. L'âge médian auquel le diagnostic est posé est 7 ans [**135**], et 60 à 80% des symptômes persistent à l'âge adulte [**100, 117**].

0.3.2.1. Historique du TDAH.

Des troubles au niveau de l'attention ont été décrits dès 1798 par le médecin Alexander Crichton, qui dépeint des patients souvent distraits, ayant de la difficulté à maintenir une attention soutenue [**79**]. En 1902, George Frederic Still, quant à lui, décrit des enfants ayant *"the particular psychical conditions [...] which are concerned with an abnormal defect of moral control"* [**127**]. Il mentionne qu'un trait commun de ces enfants est la recherche de la gratification immédiate plutôt qu'à long terme, trait similaire aux patients ayant de nos jours un diagnostic de TDAH [**79**].

Kramer et Pollnow décrivent en 1932 ce qui ressemble le plus au TDAH tel que défini actuellement dans le *Diagnostic and Statistical Manual of Mental Disorders* (DSM). Ils nomment alors ce trouble "maladie hyperkinétique de l'enfance". Des symptômes tels qu'une activité motrice intense parfois sans but, des difficultés d'apprentissage dues à l'inattention et des difficultés à porter attention aux détails, y sont mentionnés. Le terme "réaction hyperkinétique de l'enfance" sera introduit dans le DSM-II de 1968 [**79**]. En 1937, des effets positifs suite à l'utilisation de stimulants auprès d'enfants avec des troubles du comportement sont remarqués par Charles Bradley. Il faudra toutefois attendre 1944 avant que le méthylphénidate, médicament très utilisé de nos jours, soit synthétisé pour la première fois par Leandro Panizzon [**79**].

Dans les années 1930-1940, plusieurs études appuient l'hypothèse selon laquelle des troubles du comportement tels l'inattention pourraient être reliés à des dommages au cerveau [**79**]. En 1987, le terme TDAH est introduit dans le DSM III. Puis, dans le DSM-IV de 1994, on fait une distinction entre les patients avec trouble de l'attention avec ou sans hyperactivité.

0.3.2.2. Symptômes et étiologie.

Parmi les patients atteints de TDAH, on distingue trois sous-catégories : ceux qui sont surtout inattentifs, ceux qui sont plutôt hyperactifs et ceux qui présentent une combinaison des deux [**100**]. Ces symptômes engendrent différents problèmes tels des difficultés scolaires,

un risque plus élevé d'accident de voiture, une faible estime de soi, ou encore un risque accru de développer une dépendance aux drogues [**117**].

Le comportement des patients souffrant de TDAH peut être évalué à travers plusieurs tests leur demandant d'accomplir des tâches précises. Ainsi, dans le cas de la tâche de performance continue (*continuous performance task*, CPT), la réponse des patients à différents stimuli ayant au préalable reçu des indications est évaluée. On pourrait demander à un patient, par exemple, de cliquer sur le bouton gauche de sa souris si une flèche apparaît à gauche de son écran d'ordinateur et de cliquer à droite si elle apparaît à droite. Le taux de bonnes réponses et le temps de réaction des patients sont respectivement plus bas et plus lents chez les patients souffrant de TDAH.

Pour ce qui est de la tâche du "*Go/NoGo*", la capacité des patients à ne pas répondre à certains stimuli est évaluée. Durant cette tâche, une série de stimuli est présentée aux patients et ce, généralement, à l'aide d'un ordinateur. Au préalable, on indique aux patients à quel sous-ensemble des stimuli ils doivent réagir, typiquement en cliquant sur la souris de l'ordinateur et ceux auxquels il ne doivent pas réagir. Chaque stimulus est présenté rapidement. On peut alors évaluer le nombre d'erreurs de commission ou de d'omission, dénotant respectivement des clics superflus et des clics manquants. Bien que le nombre d'erreurs des deux types soit plus grand chez les patients souffrant de TDAH, la nature des erreurs apporte une information additionnelle. En effet, les erreurs de commission indiquent typiquement l'impulsivité alors que et les erreurs d'omission reflètent l'inattention [**18**].

Peu importe la nature de la tâche, les patients souffrant de TDAH commettent habituellement plus d'erreurs que les sujets du groupe contrôle, sont davantage sensibles au bruit, et ont des temps de réaction plus longs et plus variables [**68, 75**].

Les causes exactes du TDAH sont inconnues. Des études pointent vers l'implication du cortex préfrontal, du noyau caudé (partie du striatum) et du cerebellum, car une maturation plus lente, un volume ou une activité réduite y ont été observés chez des patients souffrant de TDAH [**6**]. Le TDAH comporterait une composante héréditaire et serait associé à des variations de gènes reliés à la dopamine [**40**]. Des différences quant aux gènes en lien avec les

récepteurs dopaminergiques et les transporteurs DATs ont été observées [**51**] ainsi que des perturbations au niveau du fonctionnement des récepteurs noradrénergiques [**116**]. Tant la dopamine que la noradrénaline, des neurotransmetteurs présents dans les zones du cerveau listées précédemment, seraient donc impliquées dans ce trouble. Dans la présente thèse, nous nous concentrerons uniquement sur l'implication du système dopaminergique dans le TDAH.

De manière contradictoire, certains auteurs décrivent le TDAH comme un état hypodopaminergique alors que d'autres le décrivent comme un état hyperdopaminergique. En effet, des indicateurs tels la réduction du flux sanguin dans le striatum chez les patients souffrant de TDAH, l'efficacité du méthylphénidate à diminuer les symptômes en augmentant les niveaux de dopamine, ainsi que la réduction des marqueurs synaptiques de la dopamine semblent indiquer que le TDAH soit lié à une réduction du niveau de dopamine. Les perturbations fonctionnelles au niveau des récepteurs noradrénergiques indiqueraient aussi une réduction du niveau de la noradrénaline chez ces patients [**117**]. Par contre, d'autres études indiquent plutôt qu'une augmentation des niveaux de dopamine et de noradrénaline serait impliquée dans le TDAH. En effet, des signes d'hyperactivité et d'inattention ont été remarqués chez des souris ayant des niveaux de dopamine plus élevés que la normale [**9, 80**]. De plus, des mutations faisant augmenter la libération en dopamine et en diminuant la recapture ont été identifiées chez des patients souffrant de TDAH. Une augmentation de la concentration en noradrénaline a aussi été observée dans un modèle de rats du TDAH [**109**].

Cette apparente contradiction a mené certains auteurs à poser l'hypothèse que le TDAH soit en fait associé à une réduction du niveau de dopamine tonique, correspondant au niveau de base, mais à une augmentation du niveau de dopamine phasique [**9, 55**]. Cette modification de l'équilibre entre le niveau de dopamine tonique et phasique dans le TDAH entraînerait un dysfonctionnement du système de récompenses et de la motivation dans la voie limbique des ganglions de la base [**82**]. Le système des récompenses étant très important dans l'apprentissage stimulus-réponse, on associe souvent le TDAH à des problèmes au niveau de cet apprentissage.

0.3.2.3. Échelle de mesure des symptômes.

En raison de la complexité du TDAH, il n'est pas possible, à ce jour de poser, un diagnostic à l'aide de tests d'imagerie cérébrale [**117**]. Des questionnaires utilisant différentes échelles basées sur les symptômes décrits dans le DSM, complétés par les patients eux-même, les cliniciens, leurs parents et/ou leurs enseignants, sont plutôt utilisés pour poser un diagnostic. Une des échelles très utilisée est la *Conner's rating scale*. Celle-ci s'appuie sur un questionnaire dont chaque question doit être répondue par un nombre allant de 0 (pas du tout) à 3 (très fréquemment). Les scores associés à cette échelle sont ensuite convertis en percentiles ou en cotes statistiques (*T-score*) pour évaluer à quel point les problèmes cliniques sont significatifs [**124**].

D'autres échelles peuvent aussi être utilisées, notamment : *"Inattention/Overactivity With Aggression (IOWA)", "Swanson, Nolan, and Pelham-IV (SNAP-IV) Questionnaire", "Swanson, Kotkin, Agler, M-Flynn, and Pelham (SKAMP) rating scale", "ADHD Rating Scale-IV", "Vanderbilt ADHD Rating Scale"* et *"ADHD Symptom Rating Scale"*, qui sont basées sur les critères diagnostiques du DSM [**117**].

0.3.2.4. Traitement du TDAH.

Il existe trois grandes classes de traitement destinés à diminuer les symptômes et les effets néfastes associés au TDAH : la médication, la thérapie comportementale ou une combinaison des deux.

Deux types de médicaments peuvent être utilisés : les stimulants et les non-stimulants. Les psychostimulants sont les plus prescrits et regroupent deux catégories de médicaments [**58**], le méthylphénidate et les sels d'amphétamine. Ces médicaments inhibent tous deux les transporteurs DATs de la dopamine et les transporteurs de la noradrénaline, et permettent donc de diminuer la recapture de ces neurotransmetteurs [**117**], ce qui se traduit par une normalisation de l'attention chez l'enfant. Les effets secondaires qui leur sont associés sont de l'insomnie, des maux de tête, de l'irritabilité, de l'anxiété et de la perte de poids. Malgré leur efficacité similaire, les amphétamines auraient une plus grande probabilité de mener à de l'addiction, ce qui diminue leur intérêt thérapeutique [**71**].

Le méthylphénidate, dont une étude est réalisée dans le Chapitre 5 de la présente thèse, existe sous forme de libération immédiate et prolongée. La demi-vie du méthylphénidate à libération immédiate est de 2 à 3h, ce qui signifie que les patients doivent prendre leur médication en moyenne deux à trois fois par jour afin d'en maintenir l'effet [**126**]. Le méthylphénidate à libération prolongée fut développé dans les années 2000 dans le but de diminuer le nombre d'administrations du médicament. Cependant, comme l'effet du méthylphénidate à libération prolongée n'est pas nécessairement le même que celui à libération immédiate, une combinaison des deux peut également être recommandée. Cette médication existe sous forme orale ou sous forme de patch transdermique [**117**].

Lorsque des patients souffrant de TDAH ne répondent pas aux psychostimulants ou sont trop incommodés par leurs effets secondaires, des médicaments non stimulants comme l'atomoxetine, la clonidine et la guanafacine peuvent être prescrits. L'atomoxetine permet, comme les psychostimulants, d'augmenter les niveaux de dopamine et de noradrénaline au niveau du cerveau, mais son effet peut prendre jusqu'à quelques semaines avant d'apparaître. La guanafacine et la clonidine agissent sur des récepteurs noradrénergiques post-synaptiques, ce qui permet également de diminuer les symptômes [**117**]. Comme ces médicaments sont reconnus pour être moins efficaces que les psychostimulants, ils sont utilisés en deuxième ligne.

Par ailleurs, différentes sortes de thérapies comportementales ont été développées afin d'aider les patients atteints de TDAH, en combinaison ou pas avec la médication. Les parents d'enfants ayant un diagnostic de TDAH peuvent par exemple participer à des programmes tels le *"Triple P-Positive Parenting Program"*, qui les amène à développer des habiletés afin d'aider leur enfant au niveau comportemental à travers le lien parent-enfant [**7, 141**]. Ils peuvent également collaborer avec les professionnels de l'école fréquentée par leur enfant, afin de faciliter son apprentissage.

0.4. Les approches par modélisation mathématique du système dopaminergique

La maladie de Parkinson et le TDAH sont des pathologies complexes qui touchent un organe qui l'est tout autant, le cerveau, et pour lequel l'obtention de données est difficile. De nombreux besoins subsistent, qu'il s'agisse de déterminer plus efficacement les doses de lévodopa dans le cas de la maladie de Parkinson ou de mettre en évidence le lien exact entre le système dopaminergique et le TDAH. Les approches présentement utilisées pour l'analyse de ces pathologies comportent des études précliniques, in vivo ainsi qu'in silico. L'approche adoptée dans le cadre de cette thèse repose essentiellement sur la modélisation mathématique et computationnelle, fortement basée sur la réalité pharmacologique et clinique.

Afin de représenter un phénomène, un modèle mathématique se compose d'une série d'équations qui sont développées en fonction des objectifs de l'étude. Ces équations contiennent des éléments d'entrée (*input*), impactant le comportement du phénomène étudié en sortie (*output*). Dans le contexte d'un modèle mathématique représentant la concentration plasmatique du méthylphénidate, par exemple, la dose constituerait l'entrée alors que la concentration plasmatique serait la sortie. Différents paramètres se retrouvent dans les équations faisant le pont entre l'entrée et la sortie. Leurs valeurs peuvent être estimées à partir de données ou encore trouvées dans la littérature. Afin de vérifier la validité de ces modèles, ils sont comparés de manière quantitative à des données du phénomène à l'étude ou de manière qualitative au comportement général du phénomène.

L'utilisation de modèles mathématiques comporte de nombreux avantages. En effet, ces modèles permettent de contrôler précisément et connaître tous les paramètres de l'étude, ce qui peut être impossible en laboratoire. De plus, en raison de leur rapidité d'utilisation, ils permettent de faire une variété de tests qui seraient impossibles à faire avec des sujets humains. Par exemple, un modèle mathématique peut être utilisé pour étudier la concentration plasmatique d'un médicament pour une multitudes de doses ou de régimes posologiques, et ce en très peu de temps. Les résultats de tels modèles doivent être interprétés avec précautions, car ils représentent une simplification du phénomène à l'étude. De plus, ces modèles

ne sont jamais une représentation parfaite de la réalité étudiée et ne peuvent que compléter les études pré-cliniques et cliniques.

Il existe différents types de modèles mathématiques utilisés en pharmacométrie, ceux retenus dans le cadre de cette thèse sont les modèles de pharmacologie quantitative des systèmes (mécanistiques) décrits aux sections suivantes. Les modèles pharmacocinétiques font aussi partie intégrante de l'approche holistique considérée ici.

0.4.1. Modèles mathématiques

0.4.1.1. Modèles pharmacocinétiques et pharmacodynamiques.

Les modèles pharmacocinétiques portent sur l'étude de l'absorption, la distribution, le métabolisme et l'élimination d'un médicament, processus regroupés sous l'acronyme ADME. Ces modèles permettent de simuler l'évolution dans le temps de la concentration plasmatique du médicament en fonction de la dose et des autres paramètres impliqués.

Dans les modèles pharmacocinétiques compartimentaux, le corps humain est représenté par une série de compartiments qui communiquent entre eux par des constantes de transfert. Le médicament se distribue à travers chacun des compartiments. La concentration plasmatique est déterminée par la concentration dans le compartiment central où le médicament est diffusé rapidement. Lorsque le principe actif se distribue plus lentement dans d'autres tissus, d'autres compartiments peuvent être ajoutés. Ainsi, le compartiment central représente la circulation systémique et les tissus hautement perfusés, alors que les autres compartiments représentent les tissus qui le sont moins [**20**]. Par contre, l'interprétation physiologique des compartiments de ces modèles est limitée.

La quantité de médicament dans chacun des compartiments est exprimée par une équation différentielle permettant de calculer la quantité qui transite par les compartiments en termes d'entrées et de sorties. On considère généralement que le transfert du médicament d'un compartiment à l'autre suit une cinétique d'ordre 1, c'est-à-dire que la vitesse de sortie d'un compartiment est proportionnelle à la concentration dans celui-ci. Un exemple typique de modèle pharmacocinétique à deux compartiments pour une administration intraveineuse est

illustré à la Figure 5. Celui-ci comprend des micro-constante de transfert telles k_{12}, k_{21} et k_{el}, agissant en tant que constantes de proportionnalité. Les paramètres k_{12} et k_{21} sont associés à la distribution du principe actif et k_{el} à son élimination. Des macro-constantes comme la clairance (CL), avec $k_{el} = CL/V_1$ où V_1 est le volume de distribution du compartiment central, peuvent également être définies.

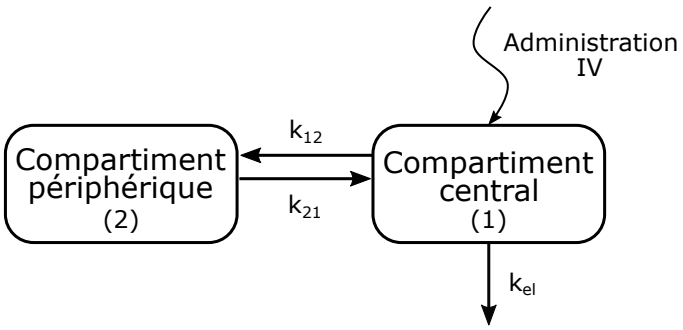

Figure 5. Représentation d'un modèle PK à deux compartiments pour une administration intraveineuse.

Certaines études ont pour objectif d'étudier non seulement le devenir du médicament dans l'organisme, mais aussi son effet. Ainsi de nouvelles équations sont nécessaire afin de caractériser l'effet dans le temps du médicament, soit sa pharmacodynamique (PD). Plusieurs relations exposition-réponse existent et donnent lieu à différentes équations (linéaires, logarithmiques, Emax,...) [**42**]. Le modèle Emax est un exemple de modèle pharmacodynamique classique. Il est utilisé, entre autres, lorsque l'on peut présumer que les concentrations plasmatiques du médicament sont en équilibre rapide avec le site d'effet. Dans ce modèle, on fait l'hypothèse que l'effet du médicament (E) est proportionnel à l'occupation des récepteurs [**42**].

L'effet dans le temps peut alors être décrit par la fonction suivante :

$$E(t) = E_0 + \frac{E_{max} C_1^n(t)}{EC_{50}^n + C_1^n(t)}, \tag{0.4.1}$$

où E_0 est l'effet de base (si applicable), E_{max} l'effet maximal du médicament, C_1 la concentration dans le compartiment central (aussi appelé compartiment 1), EC_{50} la concentration pour avoir 50% de l'effet maximal et n le coefficient de Hill. Ce dernier représente l'inclinaison de la pente de l'effet en fonction de la concentration [**42**].

Évidemment plusieurs autres modèles PD existent pour permettre de modéliser une diversité de relations exposition-réponse.

Ces modèles sont simples et comportent un nombre limité de paramètres, ce qui permet leur estimation à partir de données de concentration et d'effet. Toutefois, ils ne permettent pas de décrire ni d'étudier les mécanismes d'action des médicaments de façon plus détaillée. C'est pourquoi, un modèle plus proche des mécanismes du système dopaminergique impliqués dans la maladie de Parkinson et le TDAH, fut utilisé dans cette thèse en remplacement des modèles PD classiques afin d'étudier l'effet de la lévodopa et du méthyphénidate.

La structure des modèles pharmacocinétiques/pharmacodynamiques (PK/PD) décrite précédemment peut être utilisée pour étudier non seulement les concentrations et les effets d'un médicament chez un individu, mais aussi dans une population. En effet, l'approche PK/PD de population a été développée en 1972 par Sheiner [**31**] et permet d'inclure dans les modèles la variabilité intra- et inter-individuelle. Pour ce faire, un modèle statistique de régression à effets mixtes est ajouté au modèle structurel décrit précédemment [**118**]. Ce modèle statistique intègre les effets moyens (fixes) et aléatoires, ces derniers permettant de représenter la variabilité expliquée (inter-individuelle et intra-individuelle) et la variabilité inexpliquée. Ainsi, un paramètre quelconque θ des modèles présentés précédemment (par exemple k_{12}, $Emax$,...) proviendra d'une distribution statistique, le plus fréquemment exponentielle. Ce paramètre θ sera alors décrit par l'équation suivante pour l'individu i, dans le cas d'une distribution exponentielle :

$$\theta_i = \theta^* e^{\eta_i}, \tag{0.4.2}$$

où θ^* est la valeur moyenne du paramètre dans la population, et η_i est une variable aléatoire provenant d'une distribution, souvent normale, de moyenne 0 et de variance ω_θ^2, $\eta_i \sim \mathcal{N}(0, \omega_\theta^2)$.

Les modèles PK/PD de population ont été standardisés puis adoptés par les industries pharmaceutiques et les agences réglementaires telles Santé Canada. Le logiciel NONMEM a

même été développé pour permettre l'utilisation de tels modèles et en faire l'estimation des paramètres.

Dans la présente thèse, des modèles PK individuels ont été utilisés par souci de clarté. En effet, l'objectif initial était de mettre en évidence et permettre l'étude des différents mécanismes, sans interférence avec la variabilité inter-individuelle. Une fois les bases du modèle bien établies, il serait envisageable d'y intégrer une approche PK de population.

0.4.1.2. Modèles de pharmacologie quantitative des systèmes (QSP).

Les modèles de pharmacologie quantitative des systèmes (*Quantitative Systemes Pharmacology, QSP*), de nature plus mécanistique, permettent de mettre en équations les différents mécanismes impliqués dans le phénomène à l'étude. Afin de développer de tels modèles, il convient de bien définir les objectifs à atteindre et de tenir compte de l'information et des données disponibles. Ceci détermine aussi l'échelle à laquelle le modèle peut être construit, allant de l'échelle moléculaire, cellulaire, en passant par celle de l'organe, jusqu'au niveau de l'organisme et enfin de la population. Un modèle QSP, et plus généralement un modèle mécanistique, peut être comparé à un casse-tête. Selon les objectifs de recherche, il n'est pas toujours nécessaire d'assembler toutes les pièces du casse-tête afin de pouvoir deviner ses contours, ses détails et les formes qu'il représente. Par analogie, une pièce de casse-tête sur le système dopaminergique pourrait être utilisée afin d'étudier le TDAH. Au besoin et selon les objectifs, d'autres pièces pourraient être ajoutées comme celle du système noradrénergique par exemple. Un modèle ne repose pas uniquement sur l'information du jour, mais se bâtit sur les réussites du passé, en ce sens qu'il a recours aux connaissances accumulées au fil des années et à travers les disciplines, afin de remplir, voir même deviner les pièces manquantes [**30**].

Un des avantages de ces modèles dits *"systems-based"* est leur adaptabilité et leur modularité, puisqu'ils se prêtent à un démontage de certaines pièces (sous-modèles) afin d'être remplacées par d'autres, selon le besoin. Considérons par exemple un modèle contenant deux

sous-modèles, l'un représentant un modèle PK de la lévodopa orale et l'autre, l'effet du médicament sur les ganglions de la base. Ce modèle pourrait être réutilisé afin d'investiguer l'effet de l'infusion duodénale de la lévodopa et ce, en changeant uniquement le modèle PK.

Évidemment, ces modèles ne sont jamais une représentation parfaite de la réalité et ne peuvent que compléter les études pré-cliniques et cliniques, essentiellement lorsque certaines conditions ou scénarios ne peuvent pas être testés dans la réalité sur le plan éthique ou pratique. En effet, ces modèles basés sur la physiologie et la pharmacologie des systèmes sont typiquement utilisés pour tenter de comprendre les différents mécanismes impliqués dans un phénomène complexe, vérifier la validité d'hypothèses de recherche ou encore étudier le comportement du modèle dans des situations qui n'ont pas été testées expérimentalement [**110**].

Les modèles mécanistiques développés en pharmacométrie, lorsque calqués sur la réalité clinique et traduits en outils conviviaux, peuvent aussi aider les cliniciens dans leur prise de décisions. Leur usage se popularise de plus en plus, particulièrement avec la disponibilité de logiciels tels R-Shiny et Matlab, qui permettent de développer des applications Web ou mobiles, sans avoir une expertise en programmation. L'ère de la m-santé, aussi appelée santé mobile, est commencée [**90**].

0.4.1.3. Modèles mathématiques en m-santé.

Avec l'accès grandissant à internet et aux téléphones cellulaires dans la vie quotidienne, l'utilisation d'applications mobiles pour une médecine de précision est rendue possible. Ces outils mobiles peuvent être utilisés afin de recueillir, avec bien sûr le consentement du patient, des données transmises par la suite à un professionnel de la santé [**139**]. En outre, les patients auraient la possibilité par le biais d'une telle application, de subir un examen médical ou de discuter de leur état avec leurs professionnels de la santé, ce qui permet de les responsabiliser et de les impliquer dans leur propre santé [**90**].

L'utilisation adéquate de ces applications permettrait de recueillir, à plus faible coût, différentes données médicales et allégerait la charge pesant sur le système de santé [**73**]. L'intégration de modèles mathématiques dans ces applications leur assurerait un niveau de

rigueur souhaitable et les rendrait aptes à simuler une variété de scénarios pour en faire un outil d'aide à la décision clinique. Ces applications d'aide à la décision permettent donc de faire la transition vers une médecine personnalisée. À titre d'exemples, des applications ont déjà été implémentées pour l'optimisation des régimes posologiques de la chimiothérapie ou encore pour guider le traitement des patients atteints de septicémie [**90**].

Plus près des enjeux concernant cette thèse, l'utilisation de "journaux moteurs" dans lesquels les patients décrivent leurs symptômes ont largement été utilisés comme moyens de mesure des effets secondaires de la lévodopa. Ils sont par contre loin de faire l'unanimité quant à leur précision, puisque les patients oublient fréquemment de les compléter ou y répondent avec un certain délai, souvent de plus 4 heures après l'apparition des symptômes [**38**]. Afin de palier à ce problème d'adhésion à l'inscription des effets dans leurs journaux, des enregistrements vidéos des patients ont été réalisés afin d'avoir une évaluation plus juste des symptômes et des effets secondaires. L'utilité de ces enregistrements, particulièrement pour révéler des problèmes de posture et de démarche, a été démontrée [**38**]. Récemment, le recours à des outils plus modernes, tels que le port, par les patients, de capteurs aux poignets a permis la cueillette efficace de données. Ainsi, des données d'accélérométrie ont été obtenues pendant un test de pronation-supination de la main. L'analyse de ces données, à l'aide d'un algorithme d'apprentissage machine, a permis de quantifier l'état moteur des patients [**131**]. Les évaluations du niveau moteur, obtenues à l'aide de l'algorithme, furent similaires à celles déterminées par des professionnels de la santé [**131**]. De plus, ces données obtenues durant une tâche de pronation-supination de la main ont servi à estimer de façon personnalisée les paramètres d'un modèle PK/PD de la lévodopa/carbidopa. Ce modèle personnalisé a par la suite été utilisé dans un algorithme d'optimisation afin de déterminer le régime posologique optimal des microcomprimés de lévodopa/carbidopa de chaque patient [**130**]. Il a été démontré qu'il n'y avait pas de différence statistiquement significative entre la recommandation du clinicien et celle de l'algorithme.

Une application utilisant un modèle pharmacocinétique de population fut aussi implémentée afin d'optimiser le régime posologique du méthylphénidate à libération immédiate

dans le traitement du TDAH. L'optimisation nécessitait d'évaluer plusieurs régimes posologiques potentiels à l'aide de "boîtes thérapeutiques", tenant compte non seulement de la fenêtre thérapeutique (une concentration minimale afin d'assurer l'efficacité du médicament, une concentration maximale afin d'éviter les effets indésirables), mais également des contraintes temporelles personnalisées des patients. Les régimes posologiques avaient été évalués en fonction du pourcentage de temps pendant lequel la concentration plasmatique associée à ce régime se trouvait dans les boîtes thérapeutiques, ainsi que du pourcentage de profils pharmacocinétiques qui s'y retrouvaient [**19**].

Les modèles mathématiques en santé mobile commencent donc à faire partie intégrante des outils d'aide à la décision clinique. Ces modèles permettent d'effectuer des simulations qui vont bien au delà de celles réalisables auprès de patients. Afin de permettre l'acceptabilité sociale et l'utilité clinique de tels outils, la validité des modèles et de leurs recommandations doivent d'abord faire l'objet d'études où pharmacométriciens, professionnels de la santé et potentiellement patients, en font l'essai de façon collaborative et itérative.

0.4.2. Modèles mathématiques de la maladie de Parkinson

L'étude de la maladie de Parkinson a suscité beaucoup d'intérêt à travers les années, et a fait intervenir diverses intentions et approches. L'utilisation de modèles mathématiques a contribué à la compréhension des mécanismes pathophysiologiques impliqués dans la maladie. Ce n'est cependant que récemment que la combinaison de ces approches à des modèles PK/PD a commencé à se retrouver dans la littérature. En effet, historiquement, les études PK et/ou PD de la lévodopa, celles sur la dynamique de la dopamine ou sur la neurotransmission dans les ganglions de la base ont co-existé de façon séparée.

0.4.2.1. Modèles PK/PD de la lévodopa.

Dans le but d'étudier les différents effets de la lévodopa et les transformations qu'elle subit dans l'organisme, des modèles PK et/ou PD de la lévodopa ont été développés. Afin d'obtenir une disponibilité continue de la lévodopa dans l'organisme et ainsi tenter de limiter les effets secondaires, différentes voies d'administration sont utilisées. Des modèles PK de ces

voies d'absorption de la lévodopa ont été proposés : voie orale [**8, 26, 29, 72, 94, 121, 132**], infusion intraveineuse [**27, 91**] et infusion duodénale [**94, 140**].

Les modèles PK développés étaient typiquement composés d'un [**72, 121, 132**] ou de deux compartiments [**26, 27, 94, 91, 140**].

Différentes mesures ont été utilisées dans les modèles PD pour la quantification de l'effet de la lévodopa, telles que la fréquence de tapotement des doigts [**26, 29, 91, 132**], l'évaluation des dyskinésies [**29, 121**], ainsi que les scores sur différentes échelles motrices [**8, 121, 140**].

Les modèles PK/PD ont permis de mettre en lumière différentes facettes de la lévodopa. La réponse à long terme de la lévodopa, c'est-à-dire celle qui s'échelonne sur plusieurs jours, a été étudiée pour divers groupes de patients : ceux naïfs de traitement, ceux ayant une réponse stable à la lévodopa et ceux qui présentent des fluctuations motrices. Une réponse à long terme était présente chez les patients stables. La réponse à court terme, soit en terme d'heures, était quant à elle présente chez tous les patients. De plus, une augmentation de la réponse à la lévodopa, combinée à l'apparition des dyskinésies, augmentait les fluctuations motrices [**91**]. Une autre étude a fait ressortir que la lévodopa permettait d'augmenter la fréquence de tapotement des doigts, utilisée comme mesure de la bradykinésie, tant à court terme qu'à long terme (fréquence de base) [**26**].

L'influence de la combinaison typique lévodopa - inhibiteur de COMT a également été étudiée à l'aide de modèles pharmacocinétiques [**8, 72**]. Il a été démontré que cet inhibiteur, la tolcapone, permet de diminuer la quantité de lévodopa métabolisée, et donc d'en diminuer la clairance [**72**] tout en augmentant sa concentration maximale ainsi que l'aire sous sa courbe de concentration plasmatique [**8**].

Un autre modèle PK/PD a été élaboré afin d'étudier à la fois l'effet de la lévodopa sur le score de l'échelle UPDRS et sur le niveau de dyskinésie. Ce modèle a servi à démontrer qu'aucun des paramètres PK de l'infusion intraveineuse n'est associé aux fluctuations motrices [**27**], et que le score UPDRS et la réponse motrice maximale étaient associés à l'apparition des dyskinésies [**121**].

Des modèles PK/PD de la lévodopa sous forme d'infusion duodénale ont aussi été proposés, et ont mis en évidence le fait que la variabilité inter-individuelle du temps à l'atteinte de l'effet maximal était considérable [**140**]. L'absorption de lévodopa sous forme de gel intestinal est par ailleurs plus rapide, représente une variabilité intra-individuelle plus petite, tout en possédant une biodisponibilité similaire à la forme orale [**94**].

Des modèles PK/PD ont aussi été développés pour l'étude spécifique de l'effet de la lévodopa en fonction de la progression de la maladie. Il a ainsi été notamment démontré que la durée de la maladie et le score sur l'échelle H&Y influencent les paramètres pharmacodynamiques tels la concentration pour avoir 50% d'effet (EC50) et le coefficient de Hill du modèle Emax [**132**]. Une autre étude réalisée chez des patients à des stades avancés de la maladie a fait ressortir que le EC50 était augmenté et que la durée de l'effet était réduite [**29**]. Aux stades précoces de la maladie, la concentration thérapeutique était plus basse que celle associée aux dyskinésies, tandis que ces concentrations se confondaient lorsque la maladie atteignait des stades plus avancés [**29**].

Ces nombreuses études PK/PD ont permis de mettre en lumière la complexité de la lévodopa et de son effet. Différentes solutions ont été proposées afin de tenter d'augmenter l'effet de la lévodopa tout en minimisant l'apparition des effets secondaires, notamment par la variation des voies d'administration ou par l'utilisation simultanée d'inhibiteurs de COMT. De plus, ces études ont permis de démontrer l'importance de tenir compte de la progression de la maladie dans la modélisation pharmacodynamique de la lévodopa. En prenant en considération ces études, il nous apparaît nécessaire que ce domaine pharmacologique soit approfondi, en développant une approche holistique qui intégrerait non seulement les différents aspects reliés aux mécanismes de la maladie mais aussi la complexité de sa thérapie. C'est donc dans cette optique que nous avons développé un modèle intégratif de pharmacologie quantitative des systèmes (QSP) permettant d'étudier l'effet de la lévodopa avec la progression de la maladie, tout en restant assez flexible pour envisager les autres voies d'administration de la lévodopa, ainsi que ses différentes combinaisons.

0.4.2.2. Modèles de la dynamique de la dopamine.

Puisque des dysfonctionnements au niveau de la dynamique de la dopamine sont responsables de différentes pathologies, plusieurs groupes de recherche se sont intéressés à la modélisation de cette dynamique, que ce soit pour identifier de nouvelles cibles thérapeutiques, identifier les paramètres reliés au maintien de l'homéostasie, ou pour étudier l'effet de médicaments existants.

Un modèle probabiliste, incluant la dopamine dans les vésicules et la fente synaptique, a ainsi été développé afin d'investiguer les fluctuations motrices chez les patients parkinsoniens. Ce modèle a identifié le taux de libération vésiculaire comme étant un paramètre important dans l'apparition des effets secondaires [**33**]. La libération, la recapture et l'élimination de la dopamine dans la fente synaptique ont également été modélisées afin d'étudier les processus de compensation qui permettent de maintenir un certain niveau en dopamine, même après 85% de dénervation [**103**]. Dans ce modèle, le rôle du processus de modification de la recapture dans le maintien de l'homéostasie a été mis en évidence. D'autres modèles, incluant la dynamique dans le neurone et dans la fente synaptique, ont aussi permis d'identifier la synthèse de la tyrosine comme étant un paramètre important dans le maintien de l'homéostasie [**101**], de quantifier le rôle des autorécepteurs dans la préservation d'un certain niveau de dopamine face aux fluctuations [**17**], d'identifier des cibles potentielles pour le traitement de la maladie de Parkinson [**102**], ou d'étudier les effets de la lévodopa combinés à un traitement d'inhibition de l'auto-oxydation de la dopamine [**111**]. En particulier, cette dernière étude a démontré que cette combinaison permettait d'augmenter la concentration en dopamine vésiculaire ainsi que la libération de dopamine.

Avec la progression de la dénervation, les neurones sérotoninergiques pourraient eux aussi capter la lévodopa pour la libérer, par la suite, sous forme de dopamine. Un modèle de dynamique de la dopamine combiné à un modèle de la dynamique de la sérotonine ont permis d'étudier l'effet de la lévodopa sur le système sérotoninergique et la libération pulsatile de dopamine [**104**]. Des simulations avec ce modèle ont permis d'émettre l'hypothèse que l'augmentation de la libération de dopamine par les neurones sérotoninergiques, ainsi que la diminution de la recapture par les transporteurs, toutes deux causées par la mort des neurones

dopaminergiques, créeraient des fluctuations importantes dans le niveau de dopamine entre les doses. Cette stimulation pulsatile serait impliquée dans l'apparition des dyskinésies.

Moins détaillé que les précédents, mais ajoutant l'aspect spatiotemporel dans sa modélisation, un modèle de la dopamine dans la fente synaptique [**36, 35**] a permis d'étudier plus spécifiquement la transmission avec ou sans lévodopa. Cette étude a démontré que la dopamine phasique augmente particulièrement la liaison aux récepteurs D1, et qu'une dénervation des neurones dopaminergiques non homogène dans l'espace entraînerait une modification de sa signalisation.

Finalement, l'ajout de la dynamique de l'insuline, qui selon certaines études, influence la dénervation dans la maladie de Parkinson, à un modèle de la dopamine a permis de démontrer les bénéfices associés au fait de commencer le traitement rapidement au début de la maladie [**22**].

Ces modèles ont permis d'identifier les mécanismes importants dans la dynamique de la dopamine. Ils ont aussi permis de démontrer que la dénervation affecte non seulement la libération, mais aussi la recapture et l'élimination de la dopamine. Cependant, l'effet de cette modification de la dynamique de la dopamine sur la neurotransmission dans les ganglions de la base n'était pas l'objet de ces études. De plus, ces modèles simulent des biomarqueurs difficilement mesurables chez les patients, tels la concentration de la dopamine vésiculaire, et donc plus difficilement applicables dans un contexte clinique. À cet effet, notre modèle, qui inclut la dynamique de la dopamine et la neurotransmission dans les ganglions de la base, peut être utilisé pour simuler des biomarqueurs cliniques afin d'étudier plus facilement l'impact de la dénervation chez les patients.

0.4.2.3. Modèles neurocomputationnels des ganglions de la base.

Les modèles neurocomputationnels des ganglions de la base représentent une autre approche dans l'étude de la maladie de Parkinson, se rattachant au sillage tracé dans les années 1950 par Hodgkin et Huxley. Leur modèle mécanistique détaillé de la création de potentiels d'action dans un neurone à la suite de l'induction d'un courant a permis de décrire fidèlement des données recueillies sur des neurones de calmars [**64**]. Par la suite, plusieurs modèles

simplifiés ont été développés entre autres par FitzHugh, Nagumo et Morris, ou Lecar. Le modèle *"leaky-integrate-and-fire"* développé subséquemment par Lapicque représente le neurone comme un circuit composé d'une résistance et d'un condensateur en série et permet ainsi de simuler le potentiel de la membrane du neurone dans le temps [**64**]. C'est de ce type de modèle qu'est inspiré le modèle neurocomputationnel des ganglions de la base utilisé dans cette thèse.

Des modèles neurocomputationnels, mettant en équations non plus un neurone isolé mais plutôt un réseau, ont aussi été développés, notamment pour étudier la maladie de Parkinson. Dans le cas des ganglions de la base, il devient ainsi possible de décrire mathématiquement les différentes régions et les différentes voies de neurotransmission, i.e. les voies directes, indirectes et hyperdirectes [**11, 10, 25, 32, 48, 50, 60, 62, 87, 125, 107, 134, 144**]. Différentes mesures des symptômes ont été considérés dans la formulation de ces modèles, tels que le tremblement [**62, 125, 144**], le score UPDRS [**107**], la fréquence de tapotement des doigts [**10, 134**], le mouvement des bras [**32**], et la modification de l'écriture [**50**].

Des modèles neurocomputationnels axés sur l'étude de traitements existants ou potentiels ont également été développés pour les ganglions de la base. Ainsi, une plateforme contenant un modèle de compétition de récepteurs et un modèle de neurones a été développée afin d'étudier l'effet de 95 médicaments reconditionnés. Cinq composés sérotoninergiques ont été identifiés comme étant des médicaments prometteurs [**125**]. Ce modèle a ensuite été étendu afin d'étudier de nouvelles cibles thérapeutiques, ce qui a permis d'identifier le caractère prometteur de la combinaison de lévodopa avec des antagonistes des récepteurs sérotoninergiques ou de l'adénosine (5-HT2A ou A2A) [**107**] pour le traitement de la maladie de Parkinson. L'effet sur le tremblement de la lévodopa et du neurotransmetteur GABA ont aussi été évalués [**62**]. Un autre modèle a reproduit le comportement oscillatoire des neurones de la substance noire, qui serait à l'origine des symptômes, et l'effet des inhibiteurs calciques de type L sur ceux-ci [**47**]. Ces simulations ont permis de démontrer que les inhibiteurs calciques peuvent réduire ou éliminer ces oscillations, ce qui pourrait contribuer à la diminution des symptômes.

Les effets de la stimulation cérébrale profonde (*deep brain stimulation*) ont été étudiés à l'aide d'un modèle [**144**] des ganglions de la base, ayant précédemment servi dans l'étude du tremblement essentiel [**145**] et des oscillations [**85**]. Il a été démontré que la stimulation cérébrale profonde remplace les oscillations de petites fréquences et de grandes amplitudes des neurones dopaminergiques, par des oscillation de grandes fréquences et petites amplitudes. Un autre modèle a toutefois conclu que la stimulation cérébrale profonde chez les Parkinsoniens peut les conduire à faire des choix impulsifs [**25**].

Différents impacts de la dénervation sur le mouvement volontaire des bras ont aussi fait l'objet d'études par modélisation neuronale [**32**]. Cette approche a permis de reproduire l'augmentation du temps de réaction et la variabilité plus importante dans le mouvement observées chez les patients parkinsoniens. Une approche semblable a porté sur l'évolution de l'écriture des patients parkinsoniens avec la progression de la maladie. Il a été démontré que la réduction de la concentration en dopamine mène à une réduction de la taille de l'écriture [**50**].

L'apprentissage avec ou sans médication chez les patients parkinsoniens a aussi été étudié, en simulant différents niveaux de dopamine tonique et phasique [**60**]. Il a été démontré que le nombre d'erreurs commises dans la tâche à apprendre augmente avec la diminution de la dopamine tonique et phasique. Cette diminution a aussi été simulée pour étudier l'apprentissage par renforcement chez les patients ayant reçu ou non de la médication [**87**]. Il a été démontré que l'apprentissage pourrait être compromis, même sous thérapie, puisque le ratio entre la dopamine tonique et phasique ne serait pas rétabli. Il a aussi été démontré que, grâce à l'apprentissage réalisé pendant son administration, la lévodopa pourrait avoir un effet à court et à long terme [**134**].

Ces modèles sont une illustration de l'utilité de la modélisation mathématique dans l'étude des effets thérapeutiques des traitements sur les ganglions de la base, lesquels sont difficiles d'accès chez les patients. Toutefois, les modèles précédents ne tenaient pas compte de la progression de la maladie de Parkinson et du changement dans la réponse à la lévodopa qui en découle. Pour reproduire cet effet, il est nécessaire de combiner les deux approches

décrites précédemment, à savoir la modélisation de la dynamique de la dopamine et celle des ganglions de la base. En particulier, les travaux réalisés dans le cadre de cette thèse ont été inspirés par le modèle des ganglions de la base développé par l'équipe du Dr. M. Ursino [**11, 10**].

0.4.3. Les modèles mathématiques du TDAH

Tout comme pour la maladie de Parkinson, un dysfonctionnement au niveau de la dynamique de la dopamine dans les ganglions de la base serait impliqué dans le TDAH. Ainsi, dans le cadre de cette thèse, le modèle développé initialement pour l'étude de la maladie de Parkinson a été adapté pour étudier le TDAH et les effets du méthylphénidate.

Par le passé, le TDAH et sa médication ont été étudiés, entre autres, à l'aide de modèles PK/PD et de modèles représentant la prise de décisions. Cependant, très peu de ces études ont décrit les mécanismes sous-jacents de façon quantitative.

0.4.3.1. Modèles PK/PD du méthylphénidate.

Des études PK/PD impliquant le méthylphénidate ne manquent pas dans la littérature, en raison du grand usage de ce médicament sous différentes formes, et ont bien servi à identifier les paramètres importants pour l'optimisation de sa posologie.

À titre d'exemples, citons la mise en évidence, par un modèle PK, du poids comme covariable importante à considérer pour moduler la dose prescrite [**115**], ou encore une attribution à des profils d'absorption différents des différences existant entre la cinétique du méthylphénidate avec multicouches à libération prolongée et celle à libération immédiate [**2**].

Comme mentionné précédemment, une optimisation du régime posologique du méthylphénidate à libération immédiate a aussi été réalisée dans un contexte de pharmacocinétique de population [**19**], en se basant sur l'optimisation des concentrations plasmatiques soumises à des seuils minimaux et maximaux et à des contraintes temporelles définies par les activités quotidiennes du patient.

Un modèle pharmacodynamique d'une nouvelle formulation du méthylphénidate à libération prolongée de type Emax a été développé en utilisant le score sur différentes échelles

comme mesure de l'effet. De nouveau, un lien direct entre le poids et la dose efficace a été trouvé [**129**]. Ce modèle fut subséquemment réutilisé pour le méthylphénidate sous forme de capsules multicouches à libération prolongée et il a été démontré que le médicament avait alors un profil d'absorption double [**3**].

L'atteinte d'un effet maximal après 12h fut démontrée pour le méthylphénidate à libération prolongée et retardée à l'aide d'un modèle PK/PD utilisant différents scores pour en mesurer l'effet [**54**]. La durée de l'effet augmentait alors avec la dose.

Un modèle PK/PD intégrant l'occupation des transporteurs DATs a permis de démontrer que la concentration plasmatique en méthylphénidate et la concentration en dopamine augmentent avec l'augmentation des doses [**119**].

Ainsi, des modèles PK/PD ont permis l'étude de différentes facettes du méthylphénidate, sans toutefois représenter les mécanismes sous-jacents à son effet. Les travaux réalisés dans la présente thèse se distinguent par leur approche mécanistique de l'effet de ce médicament sur le système dopaminergique.

0.4.3.2. Modèles pour l'étude du TDAH.

La modélisation mécanistique du TDAH n'a reçu que peu d'intérêt, probablement dû à l'incertitude quant aux causes exactes impliquées.

Dans une des rares études comprenant un modèle neurocomputationnel des ganglions de la base ainsi qu'une modélisation de l'apprentissage sous l'effet de la dopamine et de la noradrénaline, une diminution de la dopamine tonique et phasique a mené à un apprentissage erroné dans la voie directe des ganglions de la base, pouvant toutefois être inversé grâce à la médication [**49**].

Les modèles les plus utilisés pour étudier le TDAH sont ceux de type *"drift-diffusion"* et *"reinforcement learning"*, ou "apprentissage par renforcement". Ces deux types de modèles permettent de simuler le choix entre différentes réponses face à un stimulus, réponses classées "correctes" ou "incorrectes". Il est ainsi possible de quantifier le nombre d'erreurs commises et le temps de réaction après la réception d'un stimulus.

Les modèles de type *"drift diffusion"* représentent la prise de décision entre deux options comme étant l'accumulation de justifications en faveur des différents choix jusqu'à ce qu'un seuil soit franchi. Un modèle de ce type a été utilisé pour l'étude de l'effet de la dopamine phasique sur l'apprentissage, et a conduit à la conclusion qu'un apprentissage asymétrique (i.e. avec davantage d'apprentissage positif), pourrait être responsable des symptômes du TDAH [**28**]. Ce type de modèle a aussi permis d'étudier les différences chez les enfants souffrant ou non de TDAH [**41**], en montrant que le paramètre de rythme d'accumulation de justifications était plus lent chez le groupe souffrant de TDAH [**41, 67**]. Même commencer avec un biais en faveur de la bonne décision ne permet pas de contrebalancer la diminution du rythme d'accumulation des justifications. Il a aussi été démontré que ce rythme augmente chez les patients souffrant de TDAH de manière corrélée avec le temps qu'ils passent à accomplir la tâche [**66**]. De plus, ces patients avaient plus de difficulté à distinguer les stimuli auxquels ils devaient répondre de ceux auxquels ils ne devaient pas répondre [**66**].

Les modèles de type "apprentissage par renforcement" permettent de simuler l'apprentissage stimulus-réponse. Ce modèle comprend un terme qui permet de quantifier la différence entre la récompense attendue après un choix et celle réellement obtenue. On appelle ce terme "l'erreur de prédiction de la récompense" *("reward prediction errror").* À partir de la valeur de ce terme, la probabilité de réponse à différents stimuli est calculée. Encore une fois, selon le stimulus reçu, certaines réponses sont qualifiés de "correctes" ou "incorrectes". Le nombre d'erreurs commises peut donc être calculé.

Une estimation des valeurs des paramètres de ce modèle chez les sujets sains et souffrant de TDAH a été effectuée, et il a été constaté que le paramètre associé au ratio du comportement qualifié d'"exploration" sur celui d'"exploitation" était modifié. Les patients souffrant de TDAH auraient donc un comportement plus exploratoire [**63**] que les sujets sains.

Par ailleurs, la combinaison de ce type de modèle à un modèle des ganglions de la base a été réalisée à des fins de simulation de l'effet d'une lésion du système dopaminergique dans différents contextes d'apprentissage, et il a été démontré que celle-ci mènerait à des problèmes au niveau de la motivation [**120**].

Ces différents modèles ont permis de mettre en lumière le comportement plus exploratoire des patients souffrant de TDAH, en plus d'associer certaines paramètres aux symptômes. Par contre, ces modèles n'incluent pas les composantes mécanistiques du TDAH, ce qui limite leur utilité concernant l'étude des causes et des processus impliqués dans ce trouble, ainsi que leur pouvoir prédictif.

0.5. Objectifs

De par leur similarité au niveau de l'impact qu'elles ont sur le système dopaminergique des ganglions de la base, deux pathologies, ainsi que leurs pharmacothérapies, seront étudiées dans cette thèse, soient la maladie de Parkinson et le TDAH.

L'objectif principal de cette thèse est d'élucider les mécanismes impliqués dans l'effet des médicaments associés au système dopaminergique des ganglions de la base, plus précisément sur la lévodopa dans le contexte de la maladie de Parkinson et le méthylphénidate dans le cas du TDAH.

Cet objectif se décline en cinq sous-objectifs, présentés sous forme d'articles, parus, soumis ou en préparation :

— Développer un modèle QSP de la maladie de Parkinson intégrant la dynamique de la dopamine et la neurotransmission dans les ganglions de la base pour étudier l'effet de la lévodopa avec la progression de la maladie.

— Étudier les effets non-linéaires de la dénervation sur la pharmacodynamique de la lévodopa qui compliquent son optimisation.

— Développer, en tant que preuve de concept, une application Web pour aider les cliniciens à identifier les régimes posologiques optimaux de la lévodopa.

— Évaluer, à l'aide d'un modèle QSP, les impacts possibles d'un débalancement de la dopamine tonique et phasique sur les ganglions de la base et sur la réponse à un stimulus dans le cadre du TDAH.

— Évaluer l'effet du méthylphénidate sur la performance après apprentissage, en utilisant un modèle de TDAH de débalancement de la dopamine tonique et phasique selon différents scénarios d'apprentissage.

La conclusion et les perspectives futures sont présentées dans la discussion.

Bibliographie

[1] Alison Abbott : Levodopa : the story so far. *Nature*, 466:S6–S7, août 2010.

[2] Akwete Adjei, Nathan S Teuscher, Robert J Kupper, Wei-Wei Chang, Laurence Greenhill, Jeffrey H Newcorn, Daniel F Connor et Sharon Wigal : Single-dose pharmacokinetics of methylphenidate extended-release multiple layer beads administered as intact capsule or sprinkles versus methylphenidate immediate-release tablets (ritalin(®)) in healthy adult volunteers. *Journal of child and adolescent psychopharmacology*, 24:570–578, décembre 2014.

[3] Akwete L Adjei, Inder Chaudhary, Scott H Kollins et Americo Padilla : A pharmacokinetic study of methylphenidate hydrochloride multilayer extended-release capsules (aptensio xr, javax.xml.bind.jaxbelement@138346bb,) in preschool-aged children with attention-deficit/hyperactivity disorder. *Paediatric drugs*, 22:561–570, octobre 2020.

[4] Y Agid : Parkinson's disease : pathophysiology. *Lancet (London, England)*, 337:1321–1324, juin 1991.

[5] Oscar Arias-Carrión, Maria Stamelou, Eric Murillo-Rodríguez, Manuel Menéndez-González et Ernst Pöppel : Dopaminergic reward system : a short integrative review. *International archives of medicine*, 3:24, octobre 2010.

[6] Amy F T Arnsten et Steven R Pliszka : Catecholamine influences on prefrontal cortical function : relevance to treatment of attention deficit/hyperactivity disorder and related disorders. *Pharmacology, biochemistry, and behavior*, 99:211–216, août 2011.

[7] Joseph Austerman : Adhd and behavioral disorders : Assessment, management, and an update from dsm-5. *Cleveland Clinic journal of medicine*, 82:S2–S7, novembre 2015.

[8] H Baas, F Zehrden, R Selzer, R Kohnen, J Loetsch et S Harder : Pharmacokinetic-pharmacodynamic relationship of levodopa with and without tolcapone in patients with parkinson's disease. *Clinical pharmacokinetics*, 40:383–393, 2001.

[9] Rajendra D Badgaiyan, Sampada Sinha, Munawwar Sajjad et David S Wack : Attenuated tonic and enhanced phasic release of dopamine in attention deficit hyperactivity disorder. *PloS one*, 10:e0137326, 2015.

[10] Chiara Baston, Manuela Contin, Giovanna Calandra Buonaura, Pietro Cortelli et Mauro Ursino : A mathematical model of levodopa medication effect on basal ganglia in parkinson's disease : An application to the alternate finger tapping task. *Frontiers in human neuroscience*, 10:280, 2016.

[11] Chiara Baston et Mauro Ursino : A biologically inspired computational model of basal ganglia in action selection. *Computational intelligence and neuroscience*, 2015:187417, 2015.

[12] Jean-Martin Beaulieu et Raul R Gainetdinov : The physiology, signaling, and pharmacology of dopamine receptors. *Pharmacological reviews*, 63:182–217, mars 2011.

[13] Desroches J Du Souich P Beaulieu P, Pichette V : *Précis de Pharmacologie, Du fondamental à la clinique*. Les Presses de l'Université de Montréal, 2015.

[14] Jeff A Beeler : Preservation of function in parkinson's disease : what's learning got to do with it ? *Brain research*, 1423:96–113, novembre 2011.

[15] M Benoit-Marand, E Borrelli et F Gonon : Inhibition of dopamine release via presynaptic d2 receptors : time course and functional characteristics in vivo. *The Journal of neuroscience : the official journal of the Society for Neuroscience*, 21:9134–9141, décembre 2001.

[16] Brian P Bergstrom et Paul A Garris : "passive stabilization" of striatal extracellular dopamine across the lesion spectrum encompassing the presymptomatic phase of parkinson's disease : a voltammetric study in the 6-ohda-lesioned rat. *Journal of neurochemistry*, 87:1224–1236, décembre 2003.

[17] Janet A Best, H Frederik Nijhout et Michael C Reed : Homeostatic mechanisms in dopamine synthesis and release : a mathematical model. *Theoretical biology & medical modelling*, 6:21, septembre 2009.

[18] Serena Bezdjian, Laura A Baker, Dora Isabel Lozano et Adrian Raine : Assessing inattention and impulsivity in children during the go/nogo task. *The British journal of developmental psychology*, 27:365–383, juin 2009.

[19] Guillaume Bonnefois, Philippe Robaey, Olivier Barrière, Jun Li et Fahima Nekka : An evaluation approach for the performance of dosing regimens in attention-deficit/hyperactivity disorder treatment. *Journal of child and adolescent psychopharmacology*, 27:320–331, mai 2017.

[20] Mehdi Boroujerdi : *Pharmacokinetics and toxicokinetics*. 2015.

[21] Josip Anđelo Borovac : Side effects of a dopamine agonist therapy for parkinson's disease : a mini-review of clinical pharmacology. *The Yale journal of biology and medicine*, 89:37–47, mars 2016.

[22] Elise M Braatz et Randolph A Coleman : A mathematical model of insulin resistance in parkinson's disease. *Computational biology and chemistry*, 56:84–97, juin 2015.

[23] Ralf Brisch, Arthur Saniotis, Rainer Wolf, Hendrik Bielau, Hans-Gert Bernstein, Johann Steiner, Bernhard Bogerts, Katharina Braun, Anna Katharina Braun, Zbigniew Jankowski, Jaliya Kumaratilake, Jaliya Kumaritlake, Maciej Henneberg et Tomasz Gos : The role of dopamine in schizophrenia from a neurobiological and evolutionary perspective : old fashioned, but still in vogue. *Frontiers in psychiatry*, 5:47, 2014.

[24] Parkinson Canada : Symptômes de la maladie de parkinson. https ://www.parkinson.ca/fr/la-maladie/frsymptoms/, 2021.

[25] James F Cavanagh, Thomas V Wiecki, Michael X Cohen, Christina M Figueroa, Johan Samanta, Scott J Sherman et Michael J Frank : Subthalamic nucleus stimulation reverses mediofrontal influence over decision threshold. *Nature neuroscience*, 14:1462–1467, septembre 2011.

[26] Phylinda L S Chan, John G Nutt et Nicholas H G Holford : Modeling the short- and long-duration responses to exogenous levodopa and to endogenous levodopa production in parkinson's disease. *Journal of pharmacokinetics and pharmacodynamics*, 31:243–268, juin 2004.

[27] Phylinda L S Chan, John G Nutt et Nicholas H G Holford : Importance of within subject variation in levodopa pharmacokinetics : a 4 year cohort study in parkinson's disease. *Journal of pharmacokinetics and pharmacodynamics*, 32:307–331, août 2005.

[28] Jeffrey Cockburn et Clay B Holroyd : Focus on the positive : computational simulations implicate asymmetrical reward prediction error signals in childhood attention-deficit/hyperactivity disorder. *Brain research*, 1365:18–34, décembre 2010.

[29] M Contin, R Riva, P Martinelli, F Albani, P Avoni et A Baruzzi : Levodopa therapy monitoring in patients with parkinson disease : a kinetic-dynamic approach. *Therapeutic drug monitoring*, 23:621–629, décembre 2001.

[30] M Craig, M González-Sales, J Li et F Nekka : Approaching pharmacometrics as a paleontologist would : Recovering the links between drugs and the body through reconstruction. *CPT : pharmacometrics & systems pharmacology*, 5:158–160, mars 2016.

[31] Chantal Csajka et Davide Verotta : Pharmacokinetic-pharmacodynamic modelling : history and perspectives. *Journal of pharmacokinetics and pharmacodynamics*, 33:227–279, juin 2006.

[32] Vassilis Cutsuridis et Stavros Perantonis : A neural network model of parkinson's disease bradykinesia. *Neural networks : the official journal of the International Neural Network Society*, 19:354–374, mai 2006.

[33] Raúl de la Fuente-Fernández, Michael Schulzer, Edwin Mak, Donald B Calne et A Jon Stoessl : Presynaptic mechanisms of motor fluctuations in parkinson's disease : a probabilistic model. *Brain : a journal of neurology*, 127:888–899, avril 2004.

[34] Gaetano Di Chiara, Valentina Bassareo, Sandro Fenu, Maria Antonietta De Luca, Liliana Spina, Cristina Cadoni, Elio Acquas, Ezio Carboni, Valentina Valentini et Daniele Lecca : Dopamine and drug addiction : the nucleus accumbens shell connection. *Neuropharmacology*, 47 Suppl 1:227–241, 2004.

[35] Jakob K Dreyer : Three mechanisms by which striatal denervation causes breakdown of dopamine signaling. *The Journal of neuroscience : the official journal of the Society for Neuroscience*, 34:12444–12456, septembre 2014.

[36] Jakob K Dreyer, Kjartan F Herrik, Rune W Berg et Jørn D Hounsgaard : Influence of phasic and tonic dopamine release on receptor activation. *The Journal of neuroscience : the official journal of the Society for Neuroscience*, 30:14273–14283, octobre 2010.

[37] Gouvernement du Canada : Le parkinsonisme au canada, y compris la maladie de parkinson. https ://www.canada.ca/fr/sante-publique/services/publications/maladies-et-affections/parkinsonisme.html, 2019.

[38] M Kelley Erb, Daniel R Karlin, Bryan K Ho, Kevin C Thomas, Federico Parisi, Gloria P Vergara-Diaz, Jean-Francois Daneault, Paul W Wacnik, Hao Zhang, Tairmae Kangarloo, Charmaine Demanuele, Chris R Brooks, Craig N Detheridge, Nina Shaafi Kabiri, Jaspreet S Bhangu et Paolo Bonato : mhealth and wearable technology should replace motor diaries to track motor fluctuations in parkinson's disease. *NPJ digital medicine*, 3:6, 2020.

[39] Neir Eshel, Ju Tian, Michael Bukwich et Naoshige Uchida : Dopamine neurons share common response function for reward prediction error. *Nature neuroscience*, 19:479–486, mars 2016.

[40] Stephen V Faraone et Henrik Larsson : Genetics of attention deficit hyperactivity disorder. *Molecular psychiatry*, 24:562–575, avril 2019.

[41] Jason S Feldman et Cynthia Huang-Pollock : A new spin on spatial cognition in adhd : A diffusion model decomposition of mental rotation. *Journal of the International Neuropsychological Society : JINS*, 27:472–483, mai 2021.

[42] Melanie A Felmlee, Marilyn E Morris et Donald E Mager : Mechanism-based pharmacodynamic modeling. *Methods in molecular biology (Clifton, N.J.)*, 929:583–600, 2012.

[43] Ashley M Fennell, Elizabeth G Pitts, Lacey L Sexton et Mark J Ferris : Phasic dopamine release magnitude tracks individual differences in sensitization of locomotor response following a history of nicotine exposure. *Scientific reports*, 10:173, janvier 2020.

[44] Karin Foerde et Daphna Shohamy : The role of the basal ganglia in learning and memory : insight from parkinson's disease. *Neurobiology of learning and memory*, 96:624–636, novembre 2011.

[45] C P Ford : The role of d2-autoreceptors in regulating dopamine neuron activity and transmission. *Neuroscience*, 282:13–22, décembre 2014.

[46] The Michael J. Fox Foundation : Deep brain stimulation. https ://www.michaeljfox.org/deep-brain-stimulation, 2021.

[47] Febe Francis, Míriam R García et Richard H Middleton : A single compartment model of pacemaking in dissasociated substantia nigra neurons : stability and energy analysis. *Journal of computational neuroscience*, 35:295–316, décembre 2013.

[48] Michael J Frank : Dynamic dopamine modulation in the basal ganglia : a neurocomputational account of cognitive deficits in medicated and nonmedicated parkinsonism. *Journal of cognitive neuroscience*, 17:51–72, janvier 2005.

[49] Michael J Frank, Amy Santamaria, Randall C O'Reilly et Erik Willcutt : Testing computational models of dopamine and noradrenaline dysfunction in attention deficit/hyperactivity disorder. *Neuropsychopharmacology : official publication of the American College of Neuropsychopharmacology*, 32:1583–1599, juillet 2007.

[50] G Gangadhar, D Joseph, A V Srinivasan, D Subramanian, R G Shivakeshavan, N Shobana et V S Chakravarthy : A computational model of parkinsonian handwriting that highlights the role of the indirect pathway in the basal ganglia. *Human movement science*, 28:602–618, octobre 2009.

[51] Ian R Gizer, Courtney Ficks et Irwin D Waldman : Candidate gene studies of adhd : a meta-analytic review. *Human genetics*, 126:51–90, juillet 2009.

[52] Christopher G Goetz, Werner Poewe, Olivier Rascol, Cristina Sampaio, Glenn T Stebbins, Carl Counsell, Nir Giladi, Robert G Holloway, Charity G Moore, Gregor K Wenning, Melvin D Yahr, Lisa Seidl et Movement Disorder Society Task Force on Rating Scales for Parkinson's Disease : Movement disorder society task force report on the hoehn and yahr staging scale : status and recommendations. *Movement disorders : official journal of the Movement Disorder Society*, 19:1020–1028, septembre 2004.

[53] Christopher G Goetz, Barbara C Tilley, Stephanie R Shaftman, Glenn T Stebbins, Stanley Fahn, Pablo Martinez-Martin, Werner Poewe, Cristina Sampaio, Matthew B Stern, Richard Dodel,

Bruno Dubois, Robert Holloway, Joseph Jankovic, Jaime Kulisevsky, Anthony E Lang, Andrew Lees, Sue Leurgans, Peter A LeWitt, David Nyenhuis, C Warren Olanow, Olivier Rascol, Anette Schrag, Jeanne A Teresi, Jacobus J van Hilten, Nancy LaPelle et Movement Disorder Society UPDRS Revision Task Force : Movement disorder society-sponsored revision of the unified parkinson's disease rating scale (mds-updrs) : scale presentation and clinimetric testing results. *Movement disorders : official journal of the Movement Disorder Society*, 23:2129–2170, novembre 2008.

[54] Roberto Gomeni, Marina Komolova, Bev Incledon et Stephen V Faraone : Model-based approach for establishing the predicted clinical response of a delayed-release and extended-release methylphenidate for the treatment of attention-deficit/hyperactivity disorder. *Journal of clinical psychopharmacology*, 40:350–358, 2020.

[55] A A Grace : Phasic versus tonic dopamine release and the modulation of dopamine system responsivity : a hypothesis for the etiology of schizophrenia. *Neuroscience*, 41:1–24, 1991.

[56] Anthony A. Grace : Psychostimulant actions on dopamine and limbic system function : Relevance to the pathophysiology and treatment of adhd., 2001.

[57] Anthony A Grace : Dysregulation of the dopamine system in the pathophysiology of schizophrenia and depression. *Nature reviews. Neuroscience*, 17:524–532, août 2016.

[58] Laurence L Greenhill, Steven Pliszka, Mina K Dulcan, William Bernet, Valerie Arnold, Joseph Beitchman, R Scott Benson, Oscar Bukstein, Joan Kinlan, Jon McClellan, David Rue, Jon A Shaw, Saundra Stock, American Academy of Child et Adolescent Psychiatry : Practice parameter for the use of stimulant medications in the treatment of children, adolescents, and adults. *Journal of the American Academy of Child and Adolescent Psychiatry*, 41:26S–49S, février 2002.

[59] C M Gremel et D M Lovinger : Associative and sensorimotor cortico-basal ganglia circuit roles in effects of abused drugs. *Genes, brain, and behavior*, 16:71–85, janvier 2017.

[60] M Guthrie, C E Myers et M A Gluck : A neurocomputational model of tonic and phasic dopamine in action selection : a comparison with cognitive deficits in parkinson's disease. *Behavioural brain research*, 200:48–59, juin 2009.

[61] S N Haber : The place of dopamine in the cortico-basal ganglia circuit. *Neuroscience*, 282:248–257, décembre 2014.

[62] Mohammad Haeri, Yashar Sarbaz et Shahriar Gharibzadeh : Modeling the parkinson's tremor and its treatments. *Journal of theoretical biology*, 236:311–322, octobre 2005.

[63] Tobias U Hauser, Reto Iannaccone, Juliane Ball, Christoph Mathys, Daniel Brandeis, Susanne Walitza et Silvia Brem : Role of the medial prefrontal cortex in impaired decision making in juvenile attention-deficit/hyperactivity disorder. *JAMA psychiatry*, 71:1165–1173, octobre 2014.

[64] Thomas Heiberg, Birgit Kriener, Tom Tetzlaff, Gaute T Einevoll et Hans E Plesser : Firing-rate models for neurons with a broad repertoire of spiking behaviors. *Journal of computational neuroscience*, 45:103–132, octobre 2018.

[65] Nick Holford et John G Nutt : Disease progression, drug action and parkinson's disease : why time cannot be ignored. *European journal of clinical pharmacology*, 64:207–216, février 2008.

[66] Cynthia Huang-Pollock, Roger Ratcliff, Gail McKoon, Alexandra Roule, Tyler Warner, Jason Feldman et Shane Wise : A diffusion model analysis of sustained attention in children with attention deficit hyperactivity disorder. *Neuropsychology*, 34:641–653, septembre 2020.

[67] Cynthia Huang-Pollock, Roger Ratcliff, Gail McKoon, Zvi Shapiro, Alex Weigard et Hilary Galloway-Long : Using the diffusion model to explain cognitive deficits in attention deficit hyperactivity disorder. *Journal of abnormal child psychology*, 45:57–68, janvier 2017.

[68] Cynthia L Huang-Pollock, Sarah L Karalunas, Helen Tam et Amy N Moore : Evaluating vigilance deficits in adhd : a meta-analysis of cpt performance. *Journal of abnormal psychology*, 121:360–371, mai 2012.

[69] Satoshi Ikemoto, Chen Yang et Aaron Tan : Basal ganglia circuit loops, dopamine and motivation : A review and enquiry. *Behavioural brain research*, 290:17–31, septembre 2015.

[70] INSPQ : Surveillance du trouble du déficit de l'attention avec ou sans hyperactivité (tdah) au québec. https ://www.inspq.qc.ca/publications/2535, 2019.

[71] P S Jensen, V S Bhatara, B Vitiello, K Hoagwood, M Feil et L B Burke : Psychoactive medication prescribing practices for u.s. children : gaps between research and clinical practice. *Journal of the American Academy of Child and Adolescent Psychiatry*, 38:557–565, mai 1999.

[72] K Jorga, L Banken, B Fotteler, P Snell et J L Steimer : Population pharmacokinetics of levodopa in patients with parkinson's disease treated with tolcapone. *Clinical pharmacology and therapeutics*, 67:610–620, juin 2000.

[73] Cheng-Kai Kao et David M Liebovitz : Consumer mobile health apps : Current state, barriers, and future directions. *PM & R : the journal of injury, function, and rehabilitation*, 9:S106–S115, mai 2017.

[74] E M Khedr, A A Abdelrahman, Y Elserogy, AF Zaki et Gamea A : Depression and anxiety among patients with parkinson's disease : frequency, risk factors, and impact on quality of life. *The Egyptian Journal of Neurology, Psychiatry and Neurosurgery*, 56(116), 2020.

[75] Michael J Kofler, Mark D Rapport, Dustin E Sarver, Joseph S Raiker, Sarah A Orban, Lauren M Friedman et Ellen G Kolomeyer : Reaction time variability in adhd : a meta-analytic review of 319 studies. *Clinical psychology review*, 33:795–811, août 2013.

[76] Simone Kühn, Sandra Düzel, Lorenza Colzato, Kristina Norman, Jürgen Gallinat, Andreas M Brandmaier, Ulman Lindenberger et Keith F Widaman : Food for thought : association between dietary tyrosine and cognitive performance in younger and older adults. *Psychological research*, 83:1097–1106, septembre 2019.

[77] Chantelle Lachance, Carolyn Spry et Danielle MacDougall : Deep brain stimulation for parkinson's disease : A review of clinical effectiveness, cost-effectiveness, and guidelines. décembre 2018.

[78] José L Lanciego, Natasha Luquin et José A Obeso : Functional neuroanatomy of the basal ganglia. *Cold Spring Harbor perspectives in medicine*, 2:a009621, décembre 2012.

[79] Klaus W Lange, Susanne Reichl, Katharina M Lange, Lara Tucha et Oliver Tucha : The history of attention deficit hyperactivity disorder. *Attention deficit and hyperactivity disorders*, 2:241–255, décembre 2010.

[80] Damiana Leo, Ilya Sukhanov, Francesca Zoratto, Placido Illiano, Lucia Caffino, Fabrizio Sanna, Giulia Messa, Marco Emanuele, Alessandro Esposito, Mariia Dorofeikova, Evgeny A Budygin, Liudmila Mus, Evgenia V Efimova, Marco Niello, Stefano Espinoza, Tatyana D Sotnikova, Marius C Hoener, Giovanni Laviola, Fabio Fumagalli, Walter Adriani et Raul R Gainetdinov : Pronounced hyperactivity, cognitive dysfunctions, and bdnf dysregulation in dopamine transporter knock-out rats. *The Journal of neuroscience : the official journal of the Society for Neuroscience*, 38:1959–1972, février 2018.

[81] Renata P Lerner, Veronica Francardo, Koji Fujita, Zisis Bimpisidis, Vincent A Jourdain, Chris C Tang, Stephen L Dewey, Thomas Chaly, M Angela Cenci et David Eidelberg : Levodopa-induced abnormal involuntary movements correlate with altered permeability of the blood-brain-barrier in the basal ganglia. *Scientific reports*, 7:16005, novembre 2017.

[82] Marjolein Luman, Jaap Oosterlaan et Joseph A Sergeant : The impact of reinforcement contingencies on ad/hd : a review and theoretical appraisal. *Clinical psychology review*, 25:183–213, février 2005.

[83] Mojtaba Madadi Asl, Abdol-Hossein Vahabie et Alireza Valizadeh : Dopaminergic modulation of synaptic plasticity, its role in neuropsychiatric disorders, and its computational modeling. *Basic and clinical neuroscience*, 10:1–12, 2019.

[84] Merck.

[85] Robert Merrison-Hort, Nada Yousif, Felix Njap, Ulrich G Hofmann, Oleksandr Burylko et Roman Borisyuk : An interactive channel model of the basal ganglia : bifurcation analysis under healthy and parkinsonian conditions. *Journal of mathematical neuroscience*, 3:14, août 2013.

[86] Diane B Miller et James P O'Callaghan : Biomarkers of parkinson's disease : present and future. *Metabolism : clinical and experimental*, 64:S40–S46, mars 2015.

[87] Ahmed A Moustafa et Mark A Gluck : A neurocomputational model of dopamine and prefrontal-striatal interactions during multicue category learning by parkinson patients. *Journal of cognitive neuroscience*, 23:151–167, janvier 2011.

[88] Atsushi Nambu, Hironobu Tokuno et Masahiko Takada : Functional significance of the cortico-subthalamo-pallidal 'hyperdirect' pathway. *Neuroscience research*, 43:111–117, juin 2002.

[89] Helen M Nasser, Donna J Calu, Geoffrey Schoenbaum et Melissa J Sharpe : The dopamine prediction error : Contributions to associative models of reward learning. *Frontiers in psychology*, 8:244, 2017.

[90] Fahima Nekka, Chantal Csajka, Mélanie Wilbaux, Sachin Sanduja, Jun Li et Marc Pfister : Pharmacometrics-based decision tools facilitate mhealth implementation. *Expert review of clinical pharmacology*, 10:39–46, janvier 2017.

[91] J G Nutt, W R Woodward, J H Carter et S T Gancher : Effect of long-term therapy on the pharmacodynamics of levodopa. relation to on-off phenomenon. *Archives of neurology*, 49:1123–1130, novembre 1992.

[92] J A Obeso, M Jahanshahi, L Alvarez, R Macias, I Pedroso, L Wilkinson, N Pavon, B Day, S Pinto, M C Rodríguez-Oroz, J Tejeiro, J Artieda, P Talelli, O Swayne, R Rodríguez, K Bhatia, M Rodriguez-Diaz, G Lopez, J Guridi et J C Rothwell : What can man do without basal ganglia motor output ? the effect of combined unilateral subthalamotomy and pallidotomy in a patient with parkinson's disease. *Experimental neurology*, 220:283–292, décembre 2009.

[93] Jose A Obeso, J Guridi, A Nambu et A R Crossman : Motor manifestations and basal ganglia output activity : the paradox continues. *Movement disorders : official journal of the Movement Disorder Society*, 28:416–418, avril 2013.

[94] Ahmed A Othman et Sandeep Dutta : Population pharmacokinetics of levodopa in subjects with advanced parkinson's disease : levodopa-carbidopa intestinal gel infusion vs. oral tablets. *British journal of clinical pharmacology*, 78:94–105, juillet 2014.

[95] Richa Pahuja, Kavita Seth, Anshi Shukla, Rajendra Kumar Shukla, Priyanka Bhatnagar, Lalit Kumar Singh Chauhan, Prem Narain Saxena, Jharna Arun, Bhushan Pradosh Chaudhari, Devendra Kumar Patel, Sheelendra Pratap Singh, Rakesh Shukla, Vinay Kumar Khanna, Pradeep Kumar, Rajnish Kumar Chaturvedi et Kailash Chand Gupta : Trans-blood brain barrier delivery of dopamine-loaded nanoparticles reverses functional deficits in parkinsonian rats. *ACS nano*, 9:4850–4871, mai 2015.

[96] Sanjay Pandey et Prachaya Srivanitchapoom : Levodopa-induced dyskinesia : Clinical features, pathophysiology, and medical management. *Annals of Indian Academy of Neurology*, 20:190–198, 2017.

[97] Werner Poewe, Angelo Antonini, Jan Cm Zijlmans, Pierre R Burkhard et François Vingerhoets : Levodopa in the treatment of parkinson's disease : an old drug still going strong. *Clinical interventions in aging*, 5:229–238, septembre 2010.

[98] Guilherme Polanczyk, Maurício Silva de Lima, Bernardo Lessa Horta, Joseph Biederman et Luis Augusto Rohde : The worldwide prevalence of adhd : a systematic review and metaregression analysis. *The American journal of psychiatry*, 164:942–948, juin 2007.

[99] Serge Przedborski : The two-century journey of parkinson disease research. *Nature reviews. Neuroscience*, 18:251–259, mars 2017.

[100] Diane Purper-Ouakil, Nicolas Ramoz, Aude-Marie Lepagnol-Bestel, Philip Gorwood et Michel Simonneau : Neurobiology of attention deficit/hyperactivity disorder. *Pediatric research*, 69:69R–76R, mai 2011.

[101] Zhen Qi, Gary W Miller et Eberhard O Voit : Computational systems analysis of dopamine metabolism. *PloS one*, 3:e2444, juin 2008.

[102] Zhen Qi, Gary W Miller et Eberhard O Voit : Computational analysis of determinants of dopamine (da) dysfunction in da nerve terminals. *Synapse (New York, N.Y.)*, 63:1133–1142, décembre 2009.

[103] Michael C. Reed, Janet Best et H. Frederik Nijhout : Passive and active stabilization of dopamine in the striatum. *Bioscience Hypotheses*, 2(4):240 – 244, 2009.

[104] Michael C Reed, H Frederik Nijhout et Janet A Best : Mathematical insights into the effects of levodopa. *Frontiers in integrative neuroscience*, 6:21, 2012.

[105] Stephen G Reich et Joseph M Savitt : Parkinson's disease. *The Medical clinics of North America*, 103:337–350, mars 2019.

[106] Jennifer S A M Reijnders, Uwe Ehrt, Wim E J Weber, Dag Aarsland et Albert F G Leentjens : A systematic review of prevalence studies of depression in parkinson's disease. *Movement disorders : official journal of the Movement Disorder Society*, 23:183–9 ; quiz 313, janvier 2008.

[107] Patrick Roberts, Athan Spiros et Hugo Geerts : A humanized clinically calibrated quantitative systems pharmacology model for hypokinetic motor symptoms in parkinson's disease. *Frontiers in pharmacology*, 7:6, 2016.

[108] Andrew S Rowland, Catherine A Lesesne et Ann J Abramowitz : The epidemiology of attention-deficit/hyperactivity disorder (adhd) : a public health view. *Mental retardation and developmental disabilities research reviews*, 8:162–170, 2002.

[109] V Russell, S Allie et T Wiggins : Increased noradrenergic activity in prefrontal cortex slices of an animal model for attention-deficit hyperactivity disorder–the spontaneously hypertensive rat. *Behavioural brain research*, 117:69–74, décembre 2000.

[110] Steven Sanche : *Effet des antirétroviraux sur la pathogénèse du VIH : une étude par modélisation mathématique intégrant la cinétique du virus, de l'immunité, du médicament, et le comportement d'adhésion avec leurs variabilités interindividuelles*. Thèse de doctorat, Université de Montréal, 2018.

[111] Matthew B Sass, Alyson N Lorenz, Robert L Green et Randolph A Coleman : A pragmatic approach to biochemical systems theory applied to an alpha-synuclein-based model of parkinson's disease. *Journal of neuroscience methods*, 178:366–377, avril 2009.

[112] Wolfram Schultz : Dopamine reward prediction error coding. *Dialogues in clinical neuroscience*, 18:23–32, mars 2016.

[113] Wolfram Schultz : Recent advances in understanding the role of phasic dopamine activity. *F1000Research*, 8, 2019.

[114] Rhyomi C Sellnow, Jordan H Newman, Nicole Chambers, Anthony R West, Kathy Steece-Collier, Ivette M Sandoval, Matthew J Benskey, Christopher Bishop et Fredric P Manfredsson : Regulation of dopamine neurotransmission from serotonergic neurons by ectopic expression of the dopamine d2 autoreceptor blocks levodopa-induced dyskinesia. *Acta neuropathologica communications*, 7:8, janvier 2019.

[115] R I Shader, J S Harmatz, J R Oesterheld, D X Parmelee, F R Sallee et D J Greenblatt : Population pharmacokinetics of methylphenidate in children with attention-deficit hyperactivity disorder. *Journal of clinical pharmacology*, 39:775–785, août 1999.

[116] Chi-Yung Shang, Hsiang-Yuan Lin et Susan Shur-Fen Gau : The norepinephrine transporter gene modulates intrinsic brain activity, visual memory, and visual attention in children with attention-deficit/hyperactivity disorder. *Molecular psychiatry*, 26:4026–4035, août 2021.

[117] Alok Sharma et Justin Couture : A review of the pathophysiology, etiology, and treatment of attention-deficit hyperactivity disorder (adhd). *The Annals of pharmacotherapy*, 48:209–225, février 2014.

[118] L B Sheiner, B Rosenberg et K L Melmon : Modelling of individual pharmacokinetics for computer-aided drug dosage. *Computers and biomedical research, an international journal*, 5:411–459, octobre 1972.

[119] Ryosuke Shimizu, Naotaka Horiguchi, Koji Yano, Masashi Sakuramoto, Naoki Kanegawa, Shunji Shinohara et Shuichi Ohnishi : Pharmacokinetic-pharmacodynamic modeling of brain dopamine levels based on dopamine transporter occupancy after administration of methylphenidate in rats. *The Journal of pharmacology and experimental therapeutics*, 369:78–87, avril 2019.

[120] Massimo Silvetti, Jan R Wiersema, Edmund Sonuga-Barke et Tom Verguts : Deficient reinforcement learning in medial frontal cortex as a model of dopamine-related motivational deficits in adhd. *Neural networks : the official journal of the International Neural Network Society*, 46:199–209, octobre 2013.

[121] N Simon, F Viallet, A Boulamery, A Eusebio, D Gayraud et J-P Azulay : A combined pharmacokinetic/pharmacodynamic model of levodopa motor response and dyskinesia in parkinson's disease patients. *European journal of clinical pharmacology*, 72:423–430, avril 2016.

[122] Matej Skorvanek, Pablo Martinez-Martin, Norbert Kovacs, Mayela Rodriguez-Violante, Jean-Christophe Corvol, Pille Taba, Klaus Seppi, Oleg Levin, Anette Schrag, Thomas Foltynie, Mario Alvarez-Sanchez, Tomoko Arakaki, Zsuzsanna Aschermann, Iciar Aviles-Olmos, Eve Benchetrit, Charline Benoit, Alberto Bergareche-Yarza, Amin Cervantes-Arriaga, Anabel Chade, Florence Cormier, Veronika Datieva, David A Gallagher, Nelida Garretto, Zuzana Gdovinova, Oscar Gershanik, Milan Grofik, Vladimir Han, Jing Huang, Liis Kadastik-Eerme, Monica M Kurtis, Graziella Mangone, Juan Carlos Martinez-Castrillo, Amelia Mendoza-Rodriguez, Michal Minar, Henry P Moore, Mari Muldmaa, Christoph Mueller, Bernadette Pinter, Werner Poewe, Karin Rallmann, Eva Reiter, Carmen Rodriguez-Blazquez, Carlos Singer, Barbara C Tilley, Peter Valkovic, Christopher G Goetz et Glenn T Stebbins : Differences in mds-updrs scores based on hoehn and yahr stage and disease duration. *Movement disorders clinical practice*, 4:536–544, 2017.

[123] Lance A Smith, Michael J Jackson, Matthew J Hansard, Eleni Maratos et Peter Jenner : Effect of pulsatile administration of levodopa on dyskinesia induction in drug-naïve mptp-treated common marmosets : effect of dose, frequency of administration, and brain exposure. *Movement disorders : official journal of the Movement Disorder Society*, 18:487–495, mai 2003.

[124] Alyssa C Smyth et Scott T Meier : Evaluating the psychometric properties of the conners adult adhd rating scales. *Journal of attention disorders*, 23:1111–1118, août 2019.

[125] Athan Spiros, Patrick Roberts et Hugo Geerts : Phenotypic screening of the prestwick library for treatment of parkinson's tremor symptoms using a humanized quantitative systems pharmacology platform. *Journal of Parkinson's disease*, 3:569–580, 2013.

[126] M A Stein, T A Blondis, E R Schnitzler, T O'Brien, J Fishkin, B Blackwell, E Szumowski et N J Roizen : Methylphenidate dosing : twice daily versus three times daily. *Pediatrics*, 98:748–756, octobre 1996.

[127] G F Still : Some abnormal psychical conditions in children. *Lancet*, 1902.

[128] Christoph Straub, Nicolas X Tritsch, Nellwyn A Hagan, Chenghua Gu et Bernardo L Sabatini : Multiphasic modulation of cholinergic interneurons by nigrostriatal afferents. *The Journal of neuroscience : the official journal of the Society for Neuroscience*, 34:8557–8569, juin 2014.

[129] Nathan S Teuscher, Carolyn R Sikes, Russ McMahen et Dorothy Engelking : Population pharmacokinetic-pharmacodynamic modeling of a novel methylphenidate extended-release orally disintegrating tablet in pediatric patients with attention-deficit/hyperactivity disorder. *Journal of clinical psychopharmacology*, 38:467–474, octobre 2018.

[130] Ilias Thomas, Moudud Alam, Filip Bergquist, Dongni Johansson, Mevludin Memedi, Dag Nyholm et Jerker Westin : Sensor-based algorithmic dosing suggestions for oral administration of levodopa/carbidopa microtablets for parkinson's disease : a first experience. *Journal of neurology*, 266:651–658, mars 2019.

[131] Ilias Thomas, Jerker Westin, Moudud Alam, Filip Bergquist, Dag Nyholm, Marina Senek et Mevludin Memedi : A treatment-response index from wearable sensors for quantifying parkinson's disease motor states. *IEEE journal of biomedical and health informatics*, 22:1341–1349, septembre 2018.

[132] E J Triggs, B G Charles, M Contin, P Martinelli, P Cortelli, R Riva, F Albani et A Baruzzi : Population pharmacokinetics and pharmacodynamics of oral levodopa in parkinsonian patients. *European journal of clinical pharmacology*, 51:59–67, 1996.

[133] Ole-Bjørn Tysnes et Anette Storstein : Epidemiology of parkinson's disease. *Journal of neural transmission (Vienna, Austria : 1996)*, 124:901–905, août 2017.

[134] Mauro Ursino et Chiara Baston : Aberrant learning in parkinson's disease : A neurocomputational study on bradykinesia. *The European journal of neuroscience*, 47:1563–1582, juin 2018.

[135] Susanna N Visser, Benjamin Zablotsky, Joseph R Holbrook, Melissa L Danielson et Rebecca H Bitsko : Diagnostic experiences of children with attention-deficit/hyperactivity disorder. *National health statistics reports*, pages 1–7, septembre 2015.

[136] N D Volkow, G-J Wang, J H Newcorn, S H Kollins, T L Wigal, F Telang, J S Fowler, R Z Goldstein, N Klein, J Logan, C Wong et J M Swanson : Motivation deficit in adhd is associated with dysfunction of the dopamine reward pathway. *Molecular psychiatry*, 16:1147–1154, novembre 2011.

[137] Christopher S von Bartheld, Jami Bahney et Suzana Herculano-Houzel : The search for true numbers of neurons and glial cells in the human brain : A review of 150 years of cell counting. *The Journal of comparative neurology*, 524:3865–3895, décembre 2016.

[138] Matthew J Wanat, Ingo Willuhn, Jeremy J Clark et Paul E M Phillips : Phasic dopamine release in appetitive behaviors and drug addiction. *Current drug abuse reviews*, 2:195–213, mai 2009.

[139] Ronald S Weinstein, Elizabeth A Krupinski et Charles R Doarn : Clinical examination component of telemedicine, telehealth, mhealth, and connected health medical practices. *The Medical clinics of North America*, 102:533–544, mai 2018.

[140] Jerker Westin, Dag Nyholm, Sven Pålhagen, Thomas Willows, Torgny Groth, Mark Dougherty et Mats O Karlsson : A pharmacokinetic-pharmacodynamic model for duodenal levodopa infusion. *Clinical neuropharmacology*, 34:61–65, 2011.

[141] Tamera L Wiggins, Kate Sofronoff et Matthew R Sanders : Pathways triple p-positive parenting program : effects on parent-child relationships and child behavior problems. *Family process*, 48:517–530, décembre 2009.

[142] Yuncheng Wu, Weidong Le et Joseph Jankovic : Preclinical biomarkers of parkinson disease. *Archives of neurology*, 68:22–30, janvier 2011.

[143] Ying Yang et Nicole Calakos : Presynaptic long-term plasticity. *Frontiers in synaptic neuroscience*, 5:8, octobre 2013.

[144] Nada Yousif, Peter G Bain, Dipankar Nandi et Roman Borisyuk : A population model of deep brain stimulation in movement disorders from circuits to cells. *Frontiers in human neuroscience*, 14:55, 2020.

[145] Nada Yousif, Michael Mace, Nicola Pavese, Roman Borisyuk, Dipankar Nandi et Peter Bain : A network model of local field potential activity in essential tremor and the impact of deep brain stimulation. *PLoS computational biology*, 13:e1005326, janvier 2017.

[146] Kareem A Zaghloul, Justin A Blanco, Christoph T Weidemann, Kathryn McGill, Jurg L Jaggi, Gordon H Baltuch et Michael J Kahana : Human substantia nigra neurons encode unexpected financial rewards. *Science (New York, N.Y.)*, 323:1496–1499, mars 2009.

[147] Jingshun Zhang, Ying Xu, Dandan Li, Lulu Fu, Xueying Zhang, Yigang Bao et Lianwen Zheng : Review of the correlation of lat1 with diseases : Mechanism and treatment. *Frontiers in chemistry*, 8:564809, 2020.

[148] M J Zigmond, E D Abercrombie, T W Berger, A A Grace et E M Stricker : Compensations after lesions of central dopaminergic neurons : some clinical and basic implications. *Trends in neurosciences*, 13:290–296, juillet 1990.

Premier chapitre.

An Integrative Model of Parkinson's Disease Treatment Including Levodopa Pharmacokinetics, Dopamine Kinetics, Basal Ganglia Neurotransmission and Motor Action throughout Disease Progression

par

Florence Véronneau-Veilleux [1], Philippe Robaey[2], Mauro Ursino[3] et Fahima Nekka[4]

([1]) Faculté de Pharmacie, Université de Montréal, Montréal, Québec, Canada

([2]) Faculty of Medicine, University of Ottawa, Ottawa, Ontario, Canada

([3]) Department of Electrical, Electronic and Information Engineering "Guglielmo Marconi", University of Bologna, 40136 Bologna, Italy

([4]) Faculté de Pharmacie, Université de Montréal
Centre de recherches mathématiques, Université de Montréal,
Centre for Applied Mathematics in Bioscience and Medicine (CAMBAM), McGill University, Montréal, Québec, Canada

Cet article a été publié dans *Journal of Pharmacokinetics and Pharmacodynamics* vol. 48, 1 (2021): 133-148. Le matériel supplémentaire associé à cet article se trouve à l'annexe A de la présente thèse .

Dans ce premier chapitre, l'objectif est de développer un modèle représentant les mécanismes importants impliqués dans la pharmacodynamique de la lévodopa ainsi que l'impact de la dénervation sur ceux-ci. Le modèle développé est conçu sur la base des connaissances actuelles de la physiopathologie et de la pharmacologie de la maladie de Parkinson et intègre la pharmacocinétique de la lévodopa, la dynamique de la dopamine et la neurotransmission dans les ganglions de la base. Grâce à ce modèle, la fréquence de tapotement des doigts dans le temps, utilisé comme indicateur clinique de la bradykinésie, pour une dose de lévodopa à différents stades de la maladie a pu être étudiée.

Abstract. Levodopa is considered the gold standard treatment of Parkinson's disease. Although very effective in alleviating symptoms at their onset, its chronic use with the progressive neuronal denervation in the basal ganglia leads to a decrease in levodopa's effect duration and to the appearance of motor complications. This evolution challenges the establishment of optimal regimens to manage the symptoms as the disease progresses. Based on up-to-date pathophysiological and pharmacological knowledge, we developed an integrative model for Parkinson's disease to evaluate motor function in response to levodopa treatment as the disease progresses. We combined a pharmacokinetic model of levodopa to a model of dopamine's kinetics and a neurocomputational model of basal ganglia. The parameter values were either measured directly or estimated from human and animal data. The concentrations and behaviors predicted by our model were compared to available information and data. Using this model, we were able to predict levodopa plasma concentration, its related dopamine concentration in the brain and the response performance to a motor task for different stages of disease.

Keywords: Parkinson's disease, levodopa, dopamine kinetics, basal ganglia, denervation

1. Introduction

Parkinson's disease is the second most common neurodegenerative disorder after Alzheimer's [**69**]. Its generated motor symptoms are associated with the loss of dopaminergic neurons in the substantia nigra in the nigrostriatal pathway [**69**], leading to dopamine depletion in the striatum (caudate putamen). Symptoms of Parkinson's disease include rigidity, tremor at rest, postural disabilities, and bradykinesia, which is a disabling symptom defined by the slowness of the movements. The complexity of the disease and its involved mechanisms calls for the development of an integrative approach using mathematical modeling.

Going beyond a descriptive role, the main objective of the current study is to develop a holistic approach that integrates a mechanistic model of basal ganglia, levodopa kinetics and dopamine kinetics in order to help understanding the underlying mechanisms of Parkinson therapy as the disease progresses and to design proper therapeutic interventions. With this

objective in mind, we put within the same framework a pharmacokinetic (PK) model of levodopa that we interface with a neurocomputational model of basal ganglia, where dopamine kinetics is mechanistically described. The temporal profiles of levodopa concentration in plasma and brain, as well as dopamine concentration in the brain are derived. The model presented here could be used in future studies to optimize levodopa's regimen in an individualized manner.

To assess the degree of severity of the disease, numerous tests are used and expressed in different scales, the most common being the Unified Parkinson's Disease Rating Scale (UPDRS). The finger tapping task is generally used as a clinical biomarker since it has been shown to correlate with bradykinesia subscore in terms of UPDRS scale [**43, 73**]. The tapping frequency was used here as an output of the model to study the motor activity of patients and the severity of bradykinesia.

Levodopa, considered as a gold standard treatment, is one of the most effective drugs to relieve motor symptoms of Parkinson's disease [**56**]. While levodopa appears to slow disease progression [**41**] and to have long duration response [**16**], it does not completely stop the progression of denervation [**65**]. Denervation is therefore an important aspect of the present work. Levodopa is converted to dopamine and acts in reducing the disease symptoms[**19**]. Unfortunately, while levodopa is very effective during the first years of therapy, its effect is altered with the progression of the disease. The initial period of long-lasting effect with almost complete suppression of symptoms is referred to as the "honeymoon period" [**42**]. After several years of treatment, the effect duration and the delay between plasma concentration and effect both shorten [**42**], leading to more frequent administration of levodopa and higher doses. This is thought to induce disabling side effects such as involuntary movements called dyskinesias [**71**]. These complications call for a better understanding of the modification of the mechanisms involved in disease progression and the response to therapy.

The integrative model developed here presents three novelties. First, our model takes into account levodopa's, dopamine's and basal ganglia's kinetics all together with physiologically interpretable parameters. Second, the effect of nigrostriatal denervation throughout

the model is represented. Finally, each model component is separately verified through comparison with available data, providing reliability of its predictions. Altogether, this leads to an integrative and physiologically realistic model that helps understanding Parkinson's disease's progression and its medication.

Previous studies have looked separately at the effect of levodopa, the dopamine kinetics and the neurotransmission in the basal ganglia.

The evolution of the therapeutic effect of levodopa during the progression of the disease was previously evaluated using empirical equations, namely the E_{max} models [**15, 18, 42, 55, 75**]. Disease progression was correlated with pharmacodynamic parameters and levodopa duration effect [**75**]. Studies were conducted to assess the difference in the pharmacodynamic parameters between early and advanced parkinsonian patients. Modifications in parameters such as endogenous effect of dopamine [**15**], endogenous release [**42**], maximal change in response [**15**], maximal effect [**42**], concentration to 50% effect (EC_{50}) [**18**] and steepness of effect curve [**75**] were observed. Although these studies highlight the importance of incorporating disease progression into pharmacodynamic modeling of levodopa, they do not provide mechanistic explanation. In the current work, the influence of disease progression on release, recapture and elimination of dopamine in the brain is explicitly modeled to enable a better understanding of the evolution of levodopa's effects with the disease.

Previous studies focused exclusively on the modeling of dopamine kinetics with and without levodopa in Parkinson's disease [**9, 25, 26, 61, 62**]. Although more complex and detailed, these models did not include the effect of dopamine on the basal ganglia. Since dopamine concentration does not invariably reflect the effect of levodopa throughout the disease, it was important to include the neuronal activity in the model. Other models were more concerned with dopamine kinetics in normal and pathological states and did not address therapy [**9, 25, 26**]. Compared to these models, the use of the present model can be extended to understand the impact of different mechanisms (such as modification of receptor's density, of DATs recapture, of neurotransmission,...) on the disease progression and its medication.

Other studies have focused their work on understanding Parkinson's disease through neurocomputational models of basal ganglia, which is the extrapyramidal center of control, selection and initiation of movement [**5, 7, 6, 14, 21, 28, 37, 29, 35, 51, 66, 76, 79**]. Basal ganglia are composed of subregions and include the striatum, the globus pallidus, the substantia nigra and subthalamic nucleus. The neurotransmission is carried out through the direct, the indirect and the hyperdirect striatal output, where the former promotes the movement, the second decreases it, and the latter is responsible for suppression of erroneous movements. In the classical models [**3, 20, 22**], a proper action selection is thought to be the result of a balance between these pathways. Dopamine (DA) loss involved in Parkinson's disease is reported to disrupt this natural balance at the striatal level [**3**]. Although the above mentionned model of basal ganglia included the nuclei and the neurotransmission pathways, neither of them included dopamine kinetics as ours.

The current study focuses on the modeling of levodopa and its effect on both dopamine kinetics and basal ganglia function through a quantitative systems pharmacology approach. It is aimed to provide a more thorough understanding of levodopa kinetics and action. The model here developed tries to keep a good balance between simplicity and accuracy. The paper is organized as follows. The description of the three submodels and the role of neuronal death in the evolution of the different involved mechanisms are given in Section 2. The validation of the whole model using available data is presented in Section 3.1. Simulation of a virtual patient and the effect of the progression of the disease on the motor task are presented in section 3.2 and 3.3 respectively. Details on the model and the scaling of some equations are given in the Supplementary material.

2. Methods

The whole model is divided into three parts, each of which is detailed in a separate section below. It represents the different mechanisms relevant to understand the effect of levodopa and the progression of the disease on dopamine kinetics and neurotransmission in the basal ganglia. This physiological integrative model is a combination and an extension of three

models previously proposed [**6, 7, 25**]. The first part consists in a pharmacokinetic model of levodopa, adapted from Baston et al. [**6**]. The dopamine kinetics model is detailed in the second part. The processes of dopamine's release, recapture by dopamine transporters (DATs), elimination and occupancy of the dopaminergic receptors are included, along with their interrelationship with nigrostriatal denervation. In the third part, the neuronal activity of each region of the basal ganglia is reproduced by simulating the direct, indirect and hyper-direct neurotransmission pathways, which respectively promotes the movement, decreases it and suppresses erroneous movement, and their response to dopamine concentrations. The finger tapping frequency as an output of the integral model is assessed. Figure 6 depicts the three models and their connections.

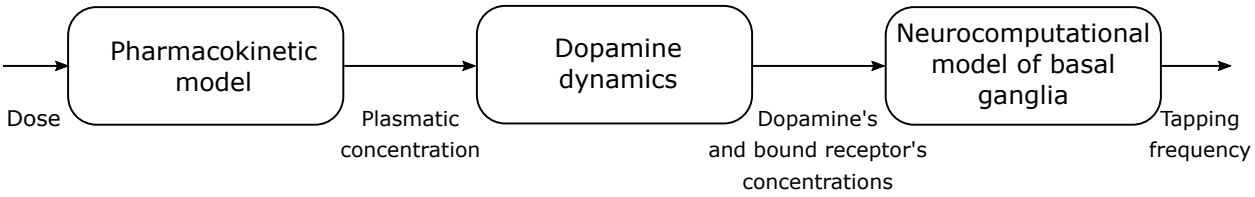

Figure 6. Representation of the three parts of the whole model

Disease progression is represented here by the degree of nigrostriatal denervation, described with the fraction of neurons alive in the substantia nigra, denoted f, which alters the mechanisms involved in the three different parts of the model. When a linear regression between the neural density and the UPDRS3 score was performed [**33**], it was shown that neuronal density in the substantia nigra is inversely correlated with UPDRS3 score [**33**], so would be the case for the fraction f.

2.1. Modeling the pharmacokinetics of levodopa

The dopamine precursor levodopa is one of the most effective treatments of Parkinson's disease. Unlike dopamine, it is able to cross the blood brain barrier to reach the basal ganglia. Levodopa is then decarboxylated into dopamine by the neurons of the substantia nigra, enhancing dopamine release by the remaining dopaminergic neurons. Levodopa has been shown to successfully alleviate symptoms for many years following the initial diagnosis. With disease progression, the effect duration and the delay in the effect are thought to be shorter

because of the loss of buffering capacity of the neurons [**27, 57, 60**]. In early stages of the disease, the neurons, which are still in sufficient quantity, store dopamine and release it into the synaptic cleft as required. This allows the effect of levodopa to last longer than its plasma concentration. With the progression of the disease and the loss of dopaminergic neurons, this storage capacity is presumably lost and dopamine is released almost immediately. At this stage, levodopa effect starts to mimic the plasma concentration. Pharmacodynamics studies using an E_{max} model have shown an increase in EC_{50} and the Hill coefficient n with progression of the disease measured by Hoehn and Yahr (H&Y) stages [**1, 18**]. This increase in pharmacodynamic parameters with disease progression is however still subject to debate [**16**]. It does not however concern the model developed in this work because the E_{max} model is substituted by a dopamine kinetics model combined to a neurocomputational model of basal ganglia. The dopamine kinetics model is used to represent the different processes regulating dopamine concentration in the striatum (release, recapture and removal). This model is linked to a neurocomputational model to represent the dopamine action on the neurotransmission pathways.

Pharmacokinetic (PK) studies [**6, 15, 68**] have shown that two-compartment models are good fit of levodopa concentrations. The herein PK model was adapted from [**6**], which was used with the neurocomputational model of basal ganglia to represent the PK of a typical patient. Figure 7 is a schematic representation of the PK model for an intravenous infusion.

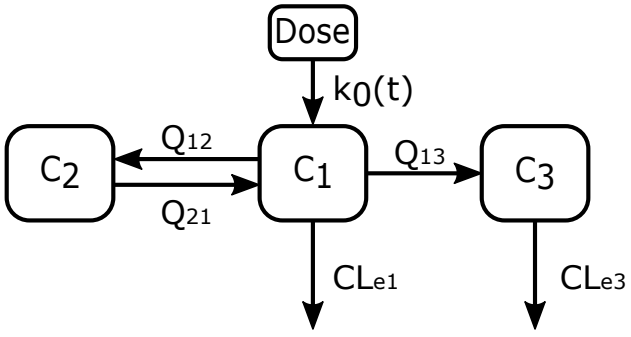

Figure 7. Representation of the two compartment pharmacokinetic model of levodopa with a third compartment for levodopa in the brain

Concentrations C_1 and C_2 in the central and peripheral compartments are respectively given by:

$$V_1 \frac{dC_1}{dt} = k_0(t) + Q_{21}C_2 - (Q_{12} + CL_{etot})C_1, \tag{2.1}$$

$$V_2 \frac{dC_2}{dt} = Q_{12}C_1 - Q_{21}C_2, \tag{2.2}$$

where Q_{ij} is the inter-compartment clearance between the ith and the jth compartments. As mentioned in [**6**], Q_{12} and Q_{21} take slightly different values to provide good fitting of individual plasma concentrations. This raises a problem of identifiability of parameters Q_{12} and Q_{21} that was not addressed in the present work. The total clearance is given by the parameter CL_{etot} with $CL_{etot} = CL_{e1} + Q_{13}$. The infusion rate is $k_0(t)$. As the disease progresses, the PK of levodopa remains the same, so the parameters of equations 2.1 and 2.2 are not affected by the fraction f of neurons alive [**18**]. Levodopa brain concentrations in the third compartment C_3 are given by:

$$V_3 \frac{dC_3}{dt} = Q_{13}C_1 - CL_{e3}C_3. \tag{2.3}$$

At early stages of the disease, dopamine is still functionally released in the synaptic cleft, modulated by the need in dopamine. With disease progression, this buffering effect of the neurons is increasingly lost, leading to a rapid and pulsatile rather than continuous release of dopamine in the synaptic cleft [**74**]. This loss of buffering effect was previously modeled by assuming that the value of CL_{e3} is increased with the loss in dopamine [**18, 38, 55, 54, 75**]. The parameter CL_{e3} which represents the clearance from the effect compartment (here the brain) was shown to be correlated with nigrostriatal denervation [**24**]. Parameter Q_{13} was also previously correlated with denervation [**11, 18, 77**]. In the current model, we assumed that both CL_{e3} and Q_{13} are correlated with the loss of neurons. Indeed, since dopamine is released more rapidly due to the loss of buffering capacity in the synaptic cleft, Q_{13} is assumed to become higher with denervation. It is as if levodopa fills a reservoir that slowly leaks and becomes leakier with denervation, hence CL_{e3} and Q_{13} are higher with denervation. With the progression of the disease, equation 2.3 is modified and the concentration in the

brain is given by:

$$V_3 \frac{dC_3}{dt} = \frac{1}{f} \cdot Q_{13} C_1 - \frac{1}{f} \cdot CL_{e3} C_3. \tag{2.4}$$

The denervation progresses with disease, resulting in a smaller fraction f of neurons alive (higher values of $1/f$.) In a previous work, an exponential function was used to describe the denervation with symptom duration in years [**45**].

The value of parameter CL_{e1} is much larger than the value of Q_{13}, hence the value of CL_{etot} is almost equal to CL_{e1}. For the sake of simplicity, the total elimination parameter ($CL_{etot} = CL_{e1} + Q_{13}$) of the first compartment has been maintained constant throughout the disease even if Q_{13} is modifed by f. This choice is supported by the observation that denervation does not impair the pharmacokinetics, hence the total elimination remains unchanged [**18**]. The parameters V_i in the previous equations represent the volume of compartment i. The initial condition for C_1, C_2 and C_3 is zero. Most parameter values were taken from patient 1 in [**6**], estimated from plasma concentrations and effect (measured as finger tapping frequency) by considering $f = 0.30$. Only parameter Q_{13} was estimated to obtain a maximal levodopa brain concentration close to the one presented in [**53**]. Patient 1 was chosen since he exhibits quite a stable response to levodopa, with just a moderate decrease in tapping frequency during the first hours after drug administration. The behavior of more unstable patients presented in [**6**] can be simulated via a reduction in f, as demonstrated below. No significant difference was seen in pharmacokinetics between patients with or without motor fluctuations in previous studies [**6, 27, 55**]. The parameter values are presented in Table 1.

2.2. Modeling the Dopamine Kinetics

The extracellular dopamine concentration in the striatum is regulated by different processes. It is synthesized by dopaminergic neurons of the substantia nigra and released in the striatum. It can then be recaptured by DATs on the presynaptic neurons and eliminated or removed from the synaptic cleft. The remaining dopamine molecules can bind to dopaminergic receptors (D1 and D2 receptors are considered here) on the postsynaptic

Table 1. Parameter values of the PK model

Parameter	Description	Value	Reference
Q_{12}	Inter-compartmental clearance from compartment 1 to 2	9.11 L/min*	[**6**]
Q_{21}	Inter-compartmental clearance from compartment 2 to 1	10 L/min*	[**6**]
Q_{13}	Inter-compartmental clearance from compartment 1 to 3	0.0021 L/min	estimated
CL_{e3}	Clearance from compartment 3	0.006 L/min	[**6**]
CL_{e1}	Clearance from compartment 1	0.7979 L/min	[**6**]
V_1	Volume of compartment 1	12 L	[**6**]
V_2	Volume of compartment 2	32 L	[**6**]
V_3	Volume of compartment 3	2 L	[**6**]
$k_0(t)$	Infusion rate	3.33 mg/min for $0 \leq t \leq 30$min 0 mg/min for $t \geq 30$min	[**6**]

* The values of Q_{12} and Q_{21} are not identifiably different.

neurons. To maintain simplicity of the model, not all reactions in the neurons nor interactions with enzymes are detailed, but only the main processes for which information and data are accessible. Indeed, dopamine metabolism and DAT density were evaluated through both positron emission tomography (PET) and single-photon emission computed tomography (SPECT) [**34**]. Distruption in the L-Tyrosine to vesicular dopamine pathway was not modeled here as in [**62**]. Focus was kept on release, reuptake and elimination of dopamine in the synaptic cleft and their influence on dopamine concentration.

Figure 8 illustrates the processes of dopamine kinetics included in the model.

We here explicitly add the influence of removal that can be affected in different ways by the loss of dopaminergic neurons. The processes of release, recapture and elimination were described in the current model using the following relation to express dopamine concentration

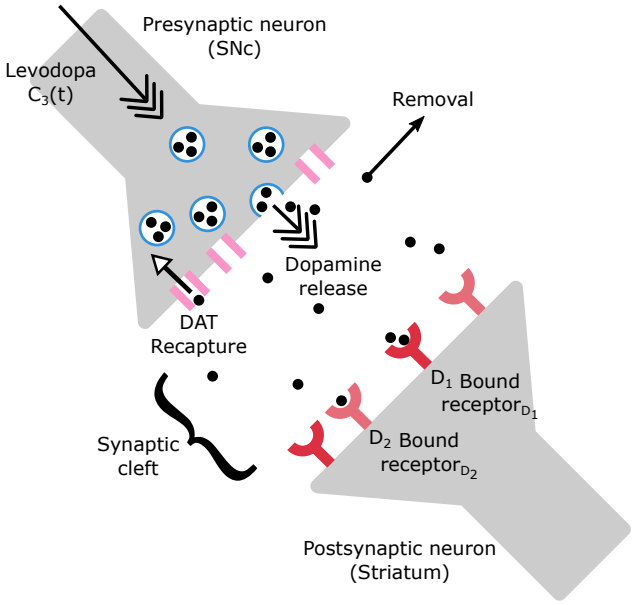

Figure 8. Schematic representation of release, recapture by DATs, binding to receptors and elimination of the dopamine in the synaptic space.

$C_{dop}(t)$ in μmol/L in the synaptic space:

$$\underbrace{V_{SC}\frac{dC_{dop}(t)}{dt}}_{\text{Dopamine concentration}} = \underbrace{\tilde{I}_{DA}(t)}_{\text{Dopamine Release}} - \underbrace{\frac{\tilde{V}_{max}C_{dop}(t)}{(k_m + C_{dop}(t))}}_{\text{Recapture by DATs}} - \underbrace{CL_{rem}C_{dop}(t)}_{\text{Removal}} \tag{2.5}$$

where V_{SC} is the volume of the synaptic cleft. It is possible to rewrite equation 2.6 as the following:

$$\frac{dC_{dop}}{dt} = \frac{\tilde{I}_{DA}(t)}{V_{SC}} - \frac{\tilde{V}_{max}C_{dop}(t)}{V_{SC}(k_m + C_{dop}(t))} - \frac{CL_{rem}}{V_{SC}}C_{dop}(t) \tag{2.6}$$

$$= I_{DA}(t) - \frac{V_{max}C_{dop}(t)}{k_m + C_{dop}(t)} - k_{rem}C_{dop}(t) \tag{2.7}$$

where the values of parameters V_{max}, k_m and k_{rem} are given in Table 2. The binding of dopamine to receptors was neglected in equation 2.6 as in [**44**] because dopamine kinetics are dominated by transporters uptake rather than by binding to receptors. Indeed, the removal of dopamine from synaptic cleft by receptors binding is much slower than from re-uptake by transporters DATs [**44**]. The variable $I_{DA}(t)$ could account for dopamine release from serotoninergic terminals in future studies. In the current study, $I_{DA}(t)$ only expresses release by dopaminergic neurons. The details of the determination of the variable $I_{DA}(t)$ are

presented in Section A.2 of the Supplementary Material. This release variable is the sum of the endogenous and exogenous dopamine. In the present model, levodopa brain concentration needs to be converted into its equivalent increase in dopamine release. Exogenous dopamine release by levodopa is assumed to be proportionnal to concentration C_3:

$$I_{DA}(t) = I_{DAendogenous} + I_{DAlevodopa}(t) \tag{2.8}$$

$$= I_{DAendogenous} + k_{3dop}C_3(t). \tag{2.9}$$

The value of $I_{DAendogenous}$ is given in Table 2. $I_{DAendogenous}$ is considered to be the constant tonic release of dopamine and $I_{DAlevodopa}$ is changing in time as concentration of levodopa in the brain C_3 is changing. $I_{DAendogenous}$ and $I_{DAlevodopa}$ are proportional to the terminal density, the vesicular release probability, the number of molecules released per vesicule fusion and the average firing rate of dopaminergic neurons. They are inversely proportional to the extracellular volume fraction and the Avogadro's constant [**25**]. The parameter k_{3dop} also contains the conversion factor of C_3 from $\mu g/mL$ to $\mu mol/L$. More details are given in section A.2 of Supplementary material. The scaling of levodopa brain concentration into its related release of dopamine is presented in section A.1 of Supplementary material. Recapture by DATs is a saturable process given by a Michaelis-Menten equation. All other processes leading to the removal of dopamine such as diffusion far from the release site, or metabolism by the Catechol-O-methyltransferase (COMT) in glial cells or neurons, are considered linear [**13, 25**]. Equation 2.7 was proposed in several papers dedicated to dopamine kinetics [**9, 25, 61**]. The merit of this equation lies in the physiological interpretation of its involved parameters, readily measurable from experimental data.

As the disease progresses, neurons will die in the substantia nigra, leading to changes in the dopamine kinetics. Considering f as the fraction of neurons alive, equation 2.6 becomes:

$$\frac{dC_{dop}(t)}{dt} = f \cdot I_{DA}(t) - \frac{f \cdot V_{max}C_{dop}(t)}{(k_m + C_{dop}(t))} - \frac{1}{f} \cdot k_{rem}C_{dop}(t). \tag{2.10}$$

It is assumed that the release variable $I_{DA}(t)$ decreases linearly with the loss of neurons. While the exact relation is not known, the recapture by DATs is also assumed to decrease

linearly with the loss of neurons in the present model since the transporters are located on the dying neurons [**25, 61**]. The linear removal from the synaptic cleft is usually lower compared to reuptake because the neurons of the substantia nigra are densely packed, so the dopamine molecules are recaptured by DATs from neighboring terminals before they have had time to be removed by other mechanisms. As the disease progresses and the terminals become sparser, it gets easier for the dopamine molecules to be removed, justifying the assumption of inverse proportionality to the fraction of neurons alive for linear removal [**61**]. As shown in Figure 9, the main route of dopamine elimination from the synaptic cleft is through recapture by DATs until too many neurons have died. The contribution of enzymatic elimination or of the other removal processes increases with denervation and it becomes the dominant one when $f < 0.05$.

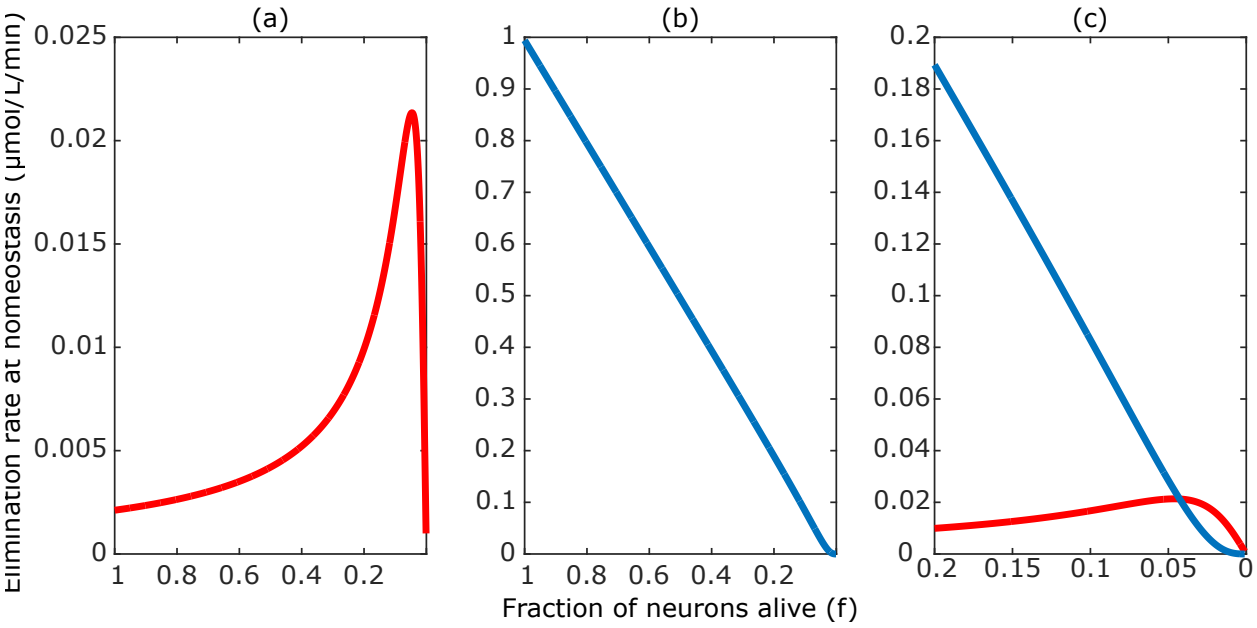

Figure 9. (a) Rate of dopamine linear removal at homeostasis, (b) Rate of dopamine's recapture by DATs transporters at homeostasis and as function of fraction of neurons alive (f) (c) Both recapture and removal routes for f below 0.2

Once in the synaptic cleft, dopamine can bind to dopaminergic receptors D1 and D2. The concentration of bound receptors to dopamine of type i with $i \in \{D1, D2\}$ is given by

Table 2. Parameter values for the dopamine kinetics model

Parameter	Descrition	Value	Reference
$I_{DAendogenous}$	Endogenous release rate	0.9963 μmol/L/s	[**25**]
V_{max}	Maximal reuptake rate by DATs	4 μmol/L/s	[**25**]
k_m	DATs dissociation constant	0.16 μmol/L	[**25, 61**]
k_{rem}	Removal rate	0.04 1/s	[**13, 25**]
k_D^{D1}	D1 receptor dissociation constant	1 μmol/L	[**49**]
k_D^{D2}	D2 receptor dissociation constant	0.01 μmol/L	[**49**]
B_{max}^{D1}	D1 receptor maximal density	0.007 μmol/L	[**17**]
B_{max}^{D2}	D2 receptor maximal density	0.015 μmol/L	[**46**]

the following equation:

$$\text{Bound receptor}_i = \frac{B_{max}^i C_{dop}}{k_D^i + C_{dop}}. \tag{2.11}$$

The maximal concentration of receptors of type i is given by B_{max}^i. The dissociation constant k_D^i of the receptors changes according to receptors' affinity. k_D^i is approximatively 1 μM for low affinity state and 0.01 μM for high affinity state [**52, 63**]. In the striatum, we considered that most of the $D1$ receptors are in low affinity state and $D2$ receptors are in high affinity state [**63**]. The parameter values of equations 2.7 and 2.11 are given in Table 2 with the references from which they were drawn. The bound receptor concentration will be considered representative of the postsynaptic effect of dopamine [**39**]. In the neurocomputational model of basal ganglia, Bound receptorD_1 and Bound receptorD_2 act on the activity of neurons in the striatum. Bound receptorD_1 acts on the Go pathway and Bound receptorD_2 on the NoGo and cholinergic pathways.

2.3. Modeling the Basal Ganglia

The basal ganglia are the control center for movement's selection and initiation [**50**]. They are composed of subcortical nuclei such as the striatum, the globus pallidus, the substantia nigra and the subthalamic nucleus. They are divided in three main neurotransmission pathways: the direct pathway which promotes the movement, the indirect pathway which decreases the movement and the hyperdirect pathway which suppresses erroneous movement.

The direct pathway connects the striatum, the globus pallidus internal (GPi) and the thalamus. The indirect pathway connects the striatum, the globus pallidus external (GPe), the GPi and the thalamus. The dopaminergic receptors present on the neurons of the striatum are mainly D1 (Go or G) and D2 (NoGo or N). Neurons presenting D1 and D2 receptors will be considered separately in the model since direct-pathway striatal neurons contain more D1 receptors, while indirect-pathway striatal neurons contain more D2 receptors [**30**]. Finally, the hyperdirect pathway connects the cortex to the subthalamic nucleus. In the classical model [**3, 20, 22**], correct motor responses are the result of balance between these three neurotransmission pathways. This classical model states that, in Parkinson's disease, this balance is lost. Dopamine acts on the neurotransmission pathways. It is mainly excitatory for D1 and inhibitory for D2. In the current model, dopamine also acts on the striatal cholinergic interneurons. In this model, dopamine inhibits cholinergic interneurons, which in turn provides inhibition to the Go neurons and excitation to the NoGo neurons, with an opposing role compared with dopamine. The thalamus and cortex are also included in the current model to complete the neurotransmission loops. A schematic representation of the basal ganglia nuclei and the three neurotransmission pathways of the model is given in Figure 10.

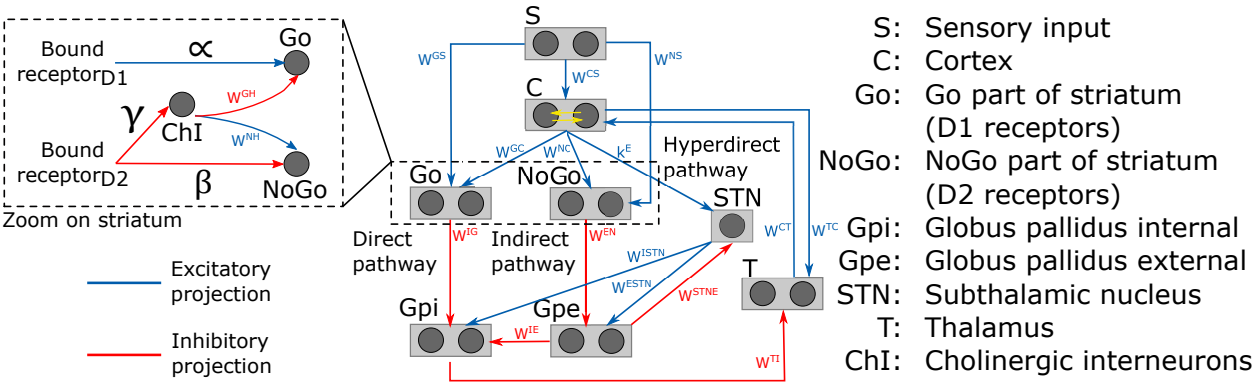

Figure 10. Schematic representation of the basal ganglia and the three neurotransmission pathways [**6**]

The neurocomputational model of basal ganglia was previously developed to investigate the motor function in the finger tapping task [**6, 7**]. Each subcortical nuclei of the basal ganglia is divided in two "neurons" to represent the two binary actions of the task: rising the

finger and lowering the finger. Firing rate type equations were used to represent the neural activity in each region. The equations and details of this model are presented in Section A.3 of the Supplementary material. In the neurocomputational model of basal ganglia, Bound receptor$_{D1}$ and Bound receptor$_{D2}$ act on the activity of neurons in the striatum. In particular, Bound receptor$_{D1}$ excites activity of the Go pathway and Bound receptor$_{D2}$ inhibits activity of the NoGo one. Moreover, Bound receptor$_{D2}$ acts on the cholinergic system which, in turn, amplifies the effect of the dopaminergic term. As a consequence, a dopamine increase activates the Go pathway, favoring action selection, while a decrease in dopamine activates the NoGo pathway, preventing action selection. The finger tapping task was simulated as a choice between two actions (finger down, finger up) which are alternatively given as input to the model. At the end of each action, before starting the new one, a time lag of 115 ms is inserted [**6**], to simulate the time necessary to perform the action. Hence, the tapping frequency depends on the balance between the direct, indirect and hyperdirect pathways, which, in turn, are a function of bound receptors.

2.4. Connecting the three submodels

The plasma concentration of levodopa is given by the pharmacokinetic model. Once it crosses the blood brain barrier, levodopa is decarboxylated into dopamine by the neurons of the substantia nigra. The release of exogenous dopamine will be added to the endogenous one. Indeed, the release term $I_{DA}(t)$ is the sum of the endogenous and exogenous dopamine, which is related to the concentration in the third compartment $C_3(t)$. Dopamine will then bind to receptors D_1 and D_2. Its post-synaptic effect will be given by the concentration of bound receptors through the variables Bound ReceptorD_1 and Bound ReceptorD_2, respectively. These variables will affect the neurotransmission in the basal ganglia nuclei and thus will modify the final motor response. Dopamine and levodopa concentrations, both in plasma and brain, are given in $\mu mol/L$ and $\mu g/mL$, respectively. Their equivalent concentrations in different units could be obtained by considering dopamine's molar mass of 153,18 g/mol

and levodopa's molar mass of 197,1879 g/mol. Figure 11 is a schematic representation of the whole model with the connections between the three submodels.

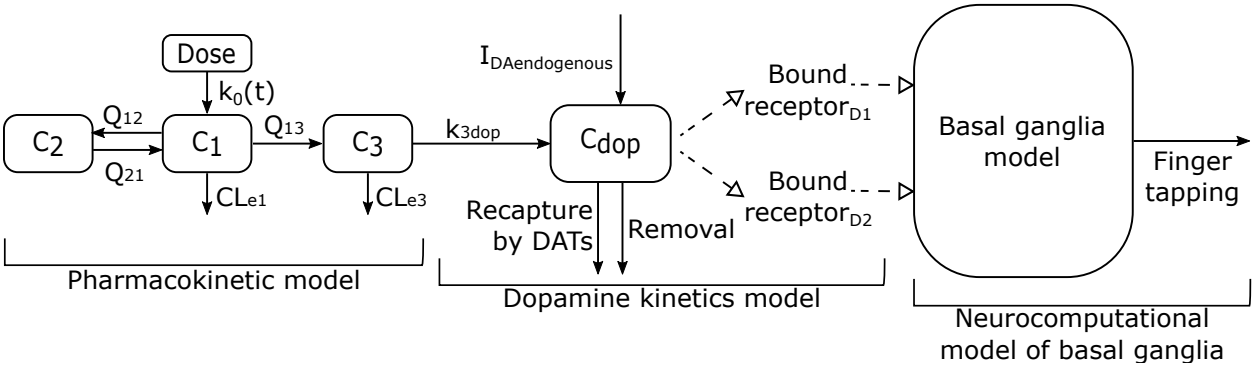

Figure 11. Schematic representation of the three submodels connected

All simulations were performed with Matlab R2018a using standard libraries.

3. Results

The processes involved in the progression of Parkinson's disease and the effect of levodopa are not still fully understood. The current model is based on the up-to-date pathophysiological and pharmacological knowledge. Several physiological parameters were measured either in animals or humans. The parameters of the neurocomputational model of basal ganglia were previously fitted [**6**] to tapping frequency data recorded 12 times over 200 minutes for a group of six patients.

3.1. Representation of physiological data

In the following, the output of each submodel was either compared with available physiological data or to well-documented behaviour.

3.1.1. PK model.

Pharmacokinetic parameters previously fitted to data taken from patient 1 in this study [**6**] were used here. This patient received 100 mg of levodopa for a 30 minutes intravenous infusion. The PK parameters were estimated to fit the data of nine samples

over a 200-minutes period.

Levodopa concentration in the basal ganglia is given by the concentration in the third compartment of the PK model (C_3). This concentration has been measured in humans by microdialysis [**53**]. Using our model, the simulated maximal levodopa concentration in the brain is ~ 1 μmol/L, which is close to the one measured in humans (~ 0.8 μmol/L) [**53**].

3.1.2. Dopamine kinetics model.

Parkinson's disease symptoms do not appear until only about 10% to 40% of neurons (represented by the parameter f in the present model) of the substantia nigra remain alive [**2, 80**]. Dopamine concentration does not decrease significantly until approximatively 15% of the neurons are alive [**8, 10, 23**]. Before reaching this threshold of denervation, adjustment of the different processes involved in dopamine kinetics allows the dopamine concentration to remain constant. This compensation phenomenon is represented in the model. Indeed, while the fraction of neurons alive f decreases, dopamine concentration does not change until approximatively only 30% subsists. The endogenous concentration of dopamine as a function of the fraction f of neurons alive is simulated using equation 2.10 and shown in Figure 12.

Only endogenous dopamine is considered here so the parameter $I_{DAlevodopa}(t)$ of equation 2.8 was set to zero.

The decarboxylation of levodopa in the brain will contribute to the increase in dopamine release. The resulting dopamine concentration in the synaptic cleft (C_{Dop}) is given by the dopamine kinetics model. It was reported that dopamine concentration increases to 0.17 μmol/L with levodopa medication close to therapeutic dose compared to 0.07 μmol/L without the medication [**25**]. In [**72**], dopamine concentrations without medication were on the order of $0.01-0.03$ μmol/L. Similar dopamine concentrations were obtained with the current model, increasing from ~ 0.05 μmol/L in the absence of medication to ~ 0.1 μmol/L with levodopa, in the case where only a 30% fraction of neurons are still alive.

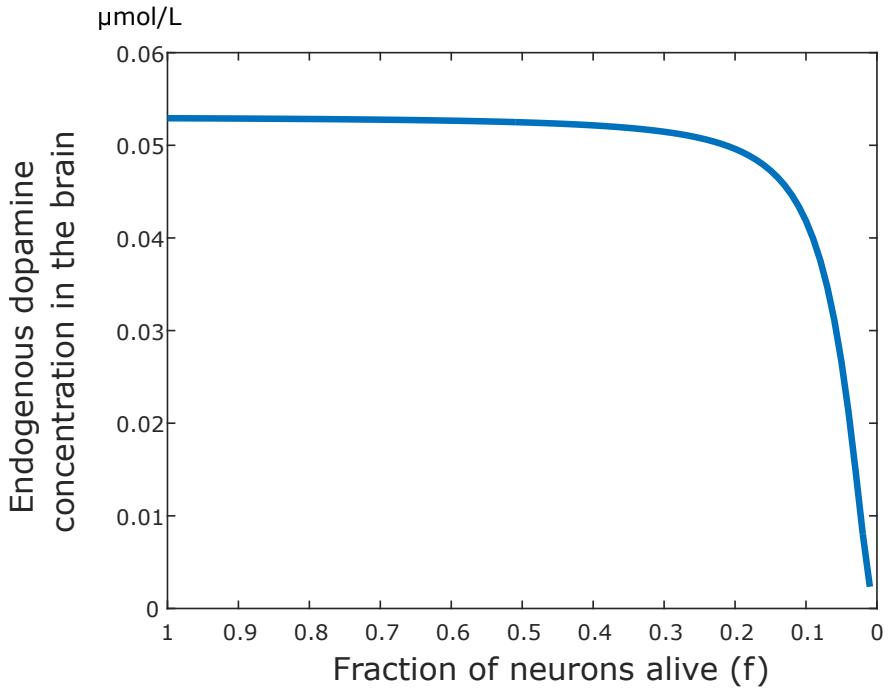

Figure 12. Endogenous dopamine concentration in the brain as a function of the fraction of neurons alive (f)

At an early stage of the disease, the buffering capacity of the neurons allows dopamine concentration in the brain to be maintained at a constant level even when levodopa plasma concentration is fluctuating [**60**]. This buffering capacity of the neurons is progressively lost with denervation. Fluctuations in dopamine concentration are then appearing and tend to mimic levodopa plasma concentration. This phenomenon is simulated using the combination of the PK model with the dopamine kinetics model. Figure 13 depicts the plasma concentration of levodopa and the related dopamine concentration in the brain for different fractions of neurons alive. This observed pattern [**60**] is reproduced here with our model.

As seen in Figure 13, basal dopamine concentration is smaller than $\sim$ 0.05 μmol/L. This is due to a feedback that decreases dopamine release when levodopa is taken [**25**]. Autoreceptors are not explicitly modeled in this work, but their influence on dopamine release is represented. Details are found in Supplementary material section A.2. Basal dopamine concentration is also decreased due to denervation, especially in the case of $f = 0.1$.

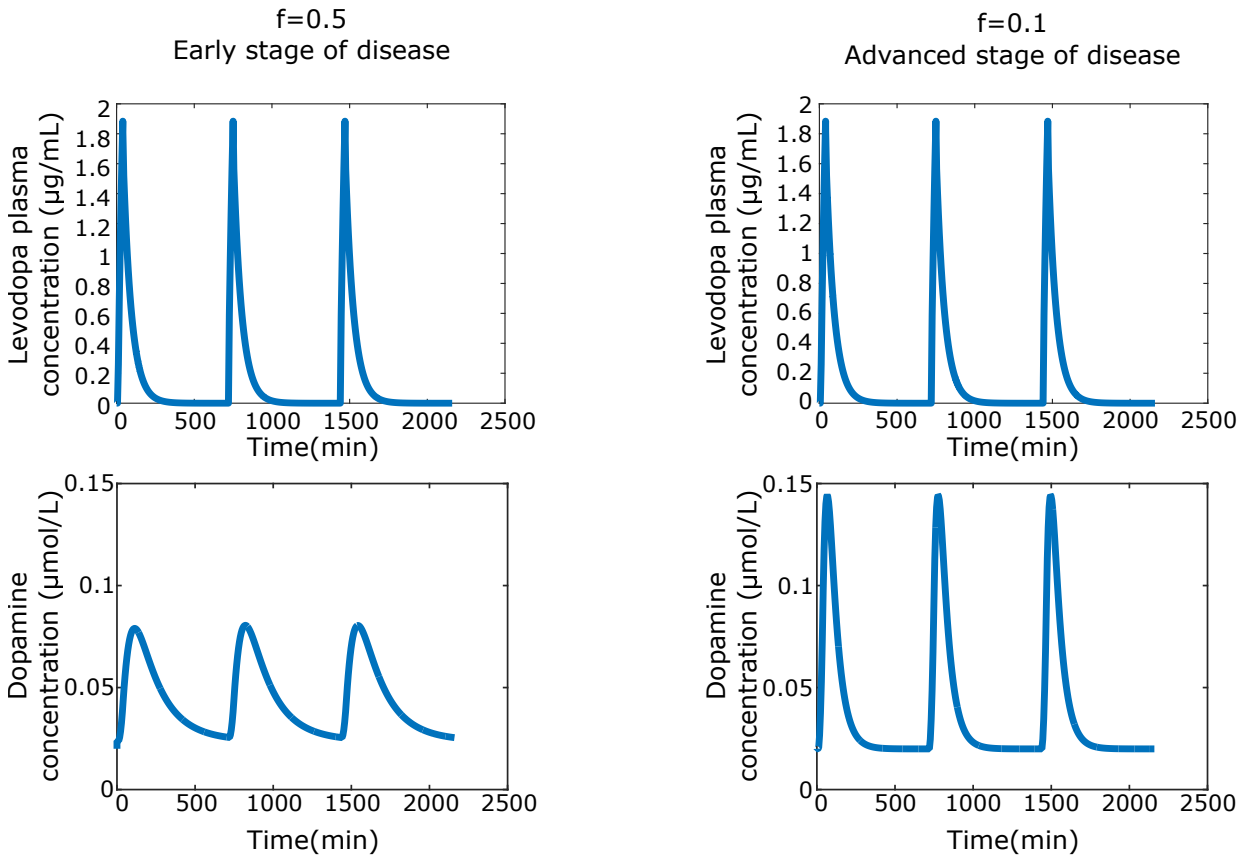

Figure 13. Levodopa plasma concentration and related dopamine brain concentration in time. Left: Concentrations for early stage of disease with a fraction of neurons alive of 50%; Right: Concentrations for advanced stage of disease with a fraction of neurons alive of 10%.

3.2. Simulation of a patient

Using the whole model, simulations were performed with the set of parameter values given above. The effect of dopamine in the basal ganglia, assigned in [**6**] to fit the finger tapping data, is simulated here assuming a fraction of neurons alive of 30%, $f = 0.3$. The model allows the plasma concentration, the concentration of levodopa in the brain, the corresponding dopamine concentration in the brain and the fraction of occupied receptors D1 and D2 to be expressed as a function of time. The fractions of occupied receptors are calculated as follows: Bound receptor$_i/B^i_{max}$ with $i = \{D_1, D_2\}$. The resulting simulations are shown in Figure 14. The patient was simulated using the whole model with $f = 0.3$. With these simulations, the maximal tapping frequency, the levodopa plasma concentration at 50% of effect (EC50) and the baseline tapping were estimated to 175 taps/min, 0.78

$\mu g/mL$ and 118 taps/min, respectively. These values can be visually deduced from Figure 14 (a) and (e) put together.

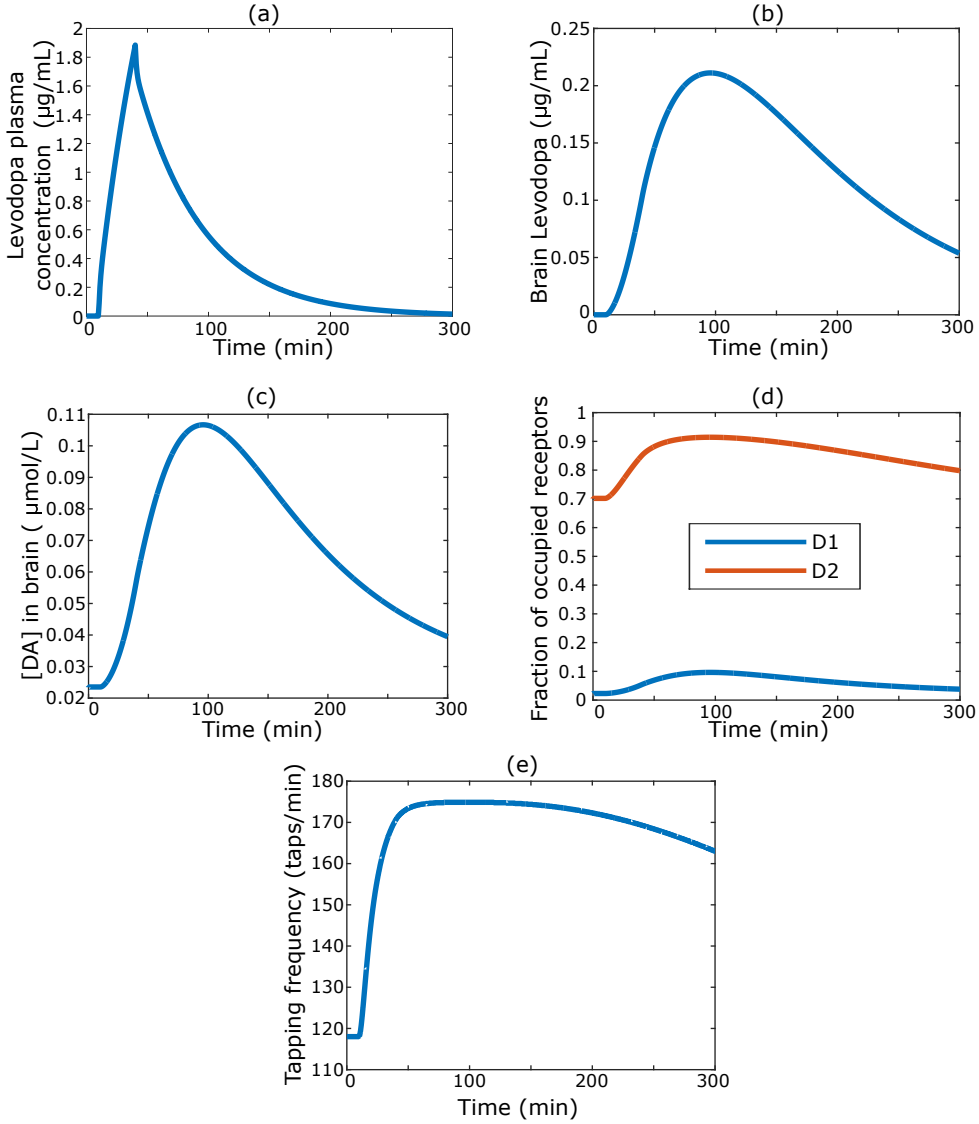

Figure 14. (a) Levodopa plasma concentration, (b) levodopa brain concentration, (c) dopamine concentration, (d) fraction of occupied dopaminergic receptors D1 and D2 and (e) tapping frequency in time.

3.3. Progression of the disease

At early stages of the disease, levodopa's effect duration extends beyond the duration of the drug in the plasma concentration. As the disease progresses, the onset of levodopa's effect is quicker and the effect duration is shorter. This phenomenon is well reproduced by

the model. Simulations were performed for different fractions of neurons alive (f) in order to represent the progression of the disease. The values of all parameters were kept constant but the fraction f. The results obtained for the tapping frequency over time with the whole model (PK model, dopamine kinetics model and neurocomputational model of basal ganglia) are shown in Figure 15. The fraction of neurons alive was varied between 80% and 5% as observed in experimental studies on animals [**48**]. A denervation of 5% would represent a score of approximately 73 on the UPDRS3 scale [**33**].

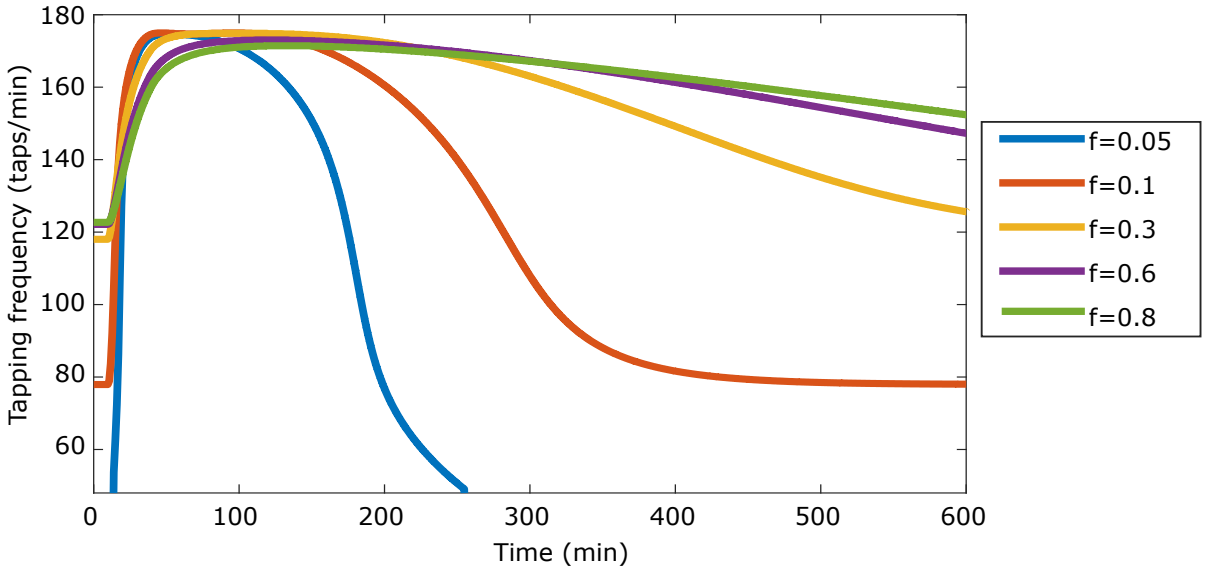

Figure 15. Tapping frequency in time for different fractions of neurons alive, frequencies before 10 minutes are the basal frequencies before taking the dose

In Figure 15, baseline frequencies, which are those at 10 minutes before taking the dose, decrease with denervation. This is in line with what is reported in the literature [**43, 58, 73**]. Our model does not include long duration response of levodopa which could lead to an increase in this baseline tapping frequency [**16**]. Long duration response could be added in future studies to better capture the effect of levodopa chronic use.

3.4. Receptor's sensitivity analysis

Dopaminergic receptor's density has been shown to change with aging [**46**] and with nigrostriatal denervation and may be involved in the development of levodopa induced dyskinesia [**36, 47, 64, 67**]. The maximal density of receptors D_1 and D_2 is represented in the

current model by the parameter $B_{max}^{D_1}$ and $B_{max}^{D_2}$ respectively. In an attempt to investigate the impact of a change in each receptor's density, a variation of more or less 40% was applied to each of the parameters $B_{max}^{D_1}$ and $B_{max}^{D_2}$ individually. The resulting tapping frequency as a function of f is given in Figures 16(a) and 17(a). As reported in the literature [**32, 64**], a change in receptor D2 density has a bigger impact on the motor action than that of receptor D1.

Contrary to the maximal receptor density, the affinity of the receptors is not modified with denervation [**64**]. However, dopamine agonists and antagonists could [**12, 40, 59**] modify the affinity of receptors D_1 and D_2, represented here by parameters $k_D^{D_1}$ and $k_D^{D_2}$, respectively. Dopamine receptor agonists are used to delay the starting of levodopa therapy and in advanced stages of Parkinson's disease, they are also used in combination with levodopa [**32**].

In order to study the impact of each receptor, their affinities were changed independently. A variation of more or less 40% was added to the affinity of receptor D_1 and then of D_2. The tapping frequency as a function of the fraction of neurons alive was computed and the results are shown in Figures 16(b) and 17(b). The tapping frequency is more affected by a modification in receptor D2 affinity.

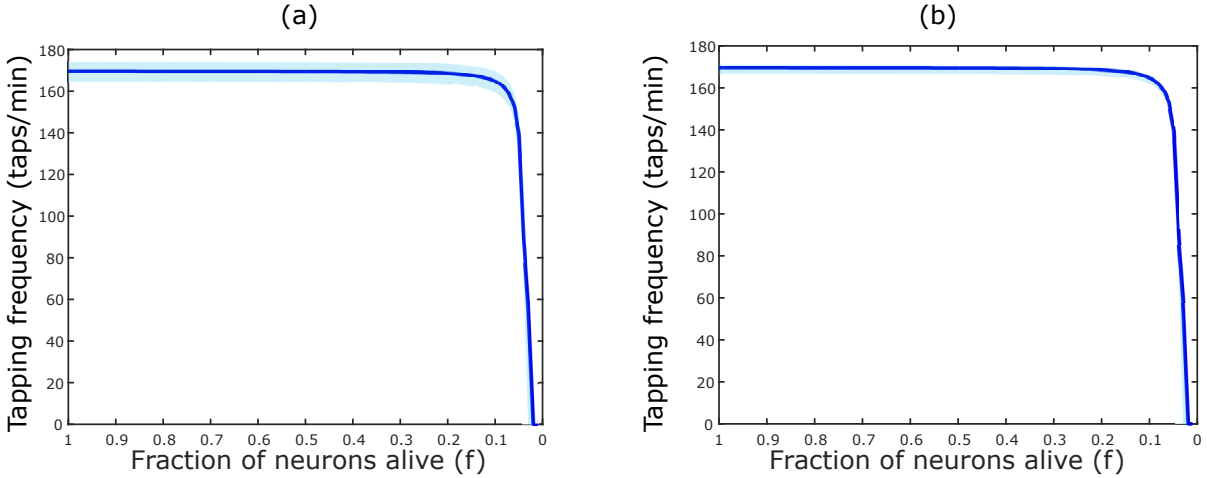

Figure 16. Tapping frequency without levodopa, hence considering only endogenous dopamine, as a function of the fraction of neurons alive when for receptor D1 (a) B_{max}^{D1} ±40% and (b) k_D^{D1} ±40%.

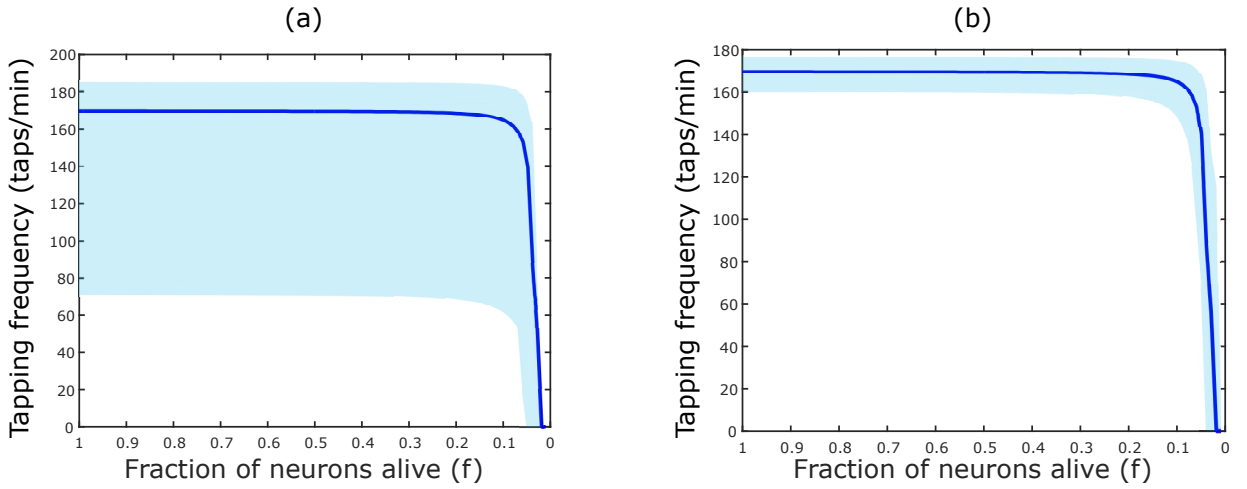

Figure 17. Tapping frequency without levodopa, hence considering only endogenous dopamine, as a function of the fraction of neurons alive when for receptor D2 (a) B_{max}^{D2} ±40% and (b) k_D^{D2} ±40%.

The model predicts a better effectiveness of D2 agonists over D1 agonists, which confirms the current clinical use.

4. Discussion

The main objective of this study was to develop a mechanistic model that integrates neurodynamics of basal ganglia, dopamine kinetics and levodopa kinetics in order to understand the different mechanisms involved in the modification of levodopa's effect as Parkinson's disease progresses. The relationship between denervation and the more rapid onset and the shorter effect duration of levodopa was investigated.

Three models were combined to represent the important underlying processes. First, a two compartment pharmacokinetic model of levodopa, connected to a third compartment of levodopa's brain concentration was adapted. Then, dopamine kinetics in the striatum was modeled by the inclusion of the main components, namely, release, recapture by DATs and removal. Finally, a neurocomputational model of basal ganglia was used to represent the three neurotransmission pathways and the impact of dopamine on these pathways and on cholinergic interneurons. These models were then connected through scaling or units modification. The involved parameters were derived from animal or human data or fitted

to data in previously published studies. Validation was performed with the output of each model to ensure consistency with clinical observations.

We used the full model to produce levodopa's plasma and brain concentrations, dopamine concentrations, fraction of bound receptors and motor activity (finger tapping frequency) as a function of time, Figure 14. Disease progression was also investigated by simulating the tapping frequency in time for a same dose of levodopa with different fractions of neurons alive, as shown in Figure 15. We also used the model to illustrate the pulsatile patterns of dopamine, induced by the therapy throughout the disease progression, Figure 13. Disease severity is here given by the fraction f of neurons alive in the substantia nigra. It was shown to be related in a linear way to UPDRS3 score [**33**]. Few studies analyzed the relation between Hoehn and Yahr scale (H&Y) in Parkinson's disease with UPDRS. In a previous study [**70**], it was concluded that UPDRS scores for all 4 parts increase significantly with every H&Y stage and also with 5-years increaments of disease duration in the first 15 years of the disease. The fraction f is then somehow also related to H&Y scale. Distribution and elimination from the brain compartment as well as dopamine release, recapture by DATs and removal are the processes affected by the progression of the disease.

The neurocomputational model used in the current study was previously built to simulate the finger tapping task with levodopa administration [**6**]. We here expanded this model through the addition of dopamine kinetics description. To investigate the impact of the disease progression, expressed here in terms of neurons loss, on the different mechanisms, it was important to detail the dopamine kinetics since nonlinear relationships are involved with denervation.

Additional action channels could be used to represent more complex motor tasks, which can still be addressed with the modeling structure developed here. The neurocomputational model of basal ganglia was previously used with four action channels [**7**]. The present model can be applied to study bradykinesia using toe tapping or pronation/supination movements for both hands as a measure of slowness of movements [**31**]. It could also be used in future

studies to investigate different action selection patterns representing dyskinesias and motor fluctuations as in [**76**].

Previous studies have focused their efforts on understanding Parkinson's disease by developing neurocomputational models of basal ganglia [**5, 7, 6, 14, 21, 28, 37, 29, 35, 51, 66, 76, 79**]. Several neurocomputational models of basal ganglia explicitly include the basal ganglia subregions where one to three of the neurotransmission pathways are represented [**7, 6, 14, 21, 28, 37, 29, 35, 51, 66, 79**]. Additional to finger tapping, bradykinesia was evaluated through arm movement [**21**]. Other symptoms such as handwriting [**29**], tremor [**37**] or the impact of learning [**5, 7, 28**], reward, punishment [**35**] and synaptic plasticity [**66, 76, 79**] were also considered in several neurocomputational models. As opposed to our model, dopamine kinetics was not explicitly considered in these studies.

The disease progression was also investigated through modeling of dopamine kinetics as an isolated phenomenon per se with [**25, 61, 62**] and without [**9, 26**] considering the impact of neuronal death and levodopa intake. The importance of the compensation mechanisms in signaling through dopamine receptors D1 and D2 [**26, 25**], the release and recapture of dopamine [**9, 61**] and the serotoninergic system [**62**] in dopamine kinetics were previously highlighted. However, the implication of the different processes of dopamine kinetics in the basal ganglia intrinsic function was not part of these studies. It is important to investigate the relation of dopamine and neuronal activity in the basal ganglia for a better understanding of the disease and its medication.

The model developed here is intended to represent a more holistic approach of Parkinson's disease and its therapy, with an attempt to reach a good balance between simplicity and accuracy. We were also concerned by the physiological interpretation of the involved parameters and an appropriate comparison with existing data. The model can be used in the context of two different time scales, one on a scale of hours in order to monitor the effect of the drug following its administration; the other is on a much longer scale with the objective of investigating the progression of the disease. The novelty of this work lies in its mechanistic approach of the drug to clinical effect during the progression of Parkinson's disease.

The model would benefit from the addition of the effect of tonic versus phasic dopamine [**26**], as well as dopamine release by serotoninergic neurons [**62**]. A better estimation of the individual weights parameters of the neurocomputational model would help individualize therapeutic predictions by using a customized model to assess the patient's motor activity. A limitation of the model is the non-identifiability of parameters Q_{12} and Q_{21} in the pharmacokinetic model. Since we did not have pharmacokinetic data, we used the parameters values reported in [**6**]. However, as formulated and with the accessible data, the model of [**6**] presents a fundamental issue of identifiability (parameters Q_{12} and Q_{21} are not uniquely defined). Scaling was used to connect the dopamine kinetics model to the neurocomputational model of basal ganglia in order to maintain the value of synaptic weights originally fitted to patients data. Refitting data with this new model would prevent the need for scaling. We are confident this scaling does not significantly change the output of the model. The ultimate purpose of this modeling exercise is to optimize levodopa's regimen. As dyskinesia is reported as the main side effect of the chronic use of levodopa [**76**], extension of our model to integrate this motor complication would inform on the evolution towards the thin line that separates levodopa benefits from harm effects throughout the disease.

Indeed, dyskinesias could possibly be delayed by reducing the dose while maintaining the beneficial effect. Different routes of administration of levodopa are tested due to the occurrence of side effects and due to the progression of the disease [**4**]. In future studies, other pharmacokinetic models (duodenal infusion, oral,..) could be added to the present model to determine not only optimized regimens but also optimized route of administration of levodopa for each patient.

The present model assumes a homogeneous death of neurons in the substantia nigra. However, recent studies [**25**] showed heterogenous loss of neurons, with the existence of completely void regions. The link between reduction in dopamine and the lost of spatial coherence in innervation is however beyond the scope of our present work. In the present study, the conditions for well-mixed levodopa pharmacokinetics and dopamine kinetics models hold, and

this assumption is commonly used in the literature on levodopa pharmacokinetics. Synaptic space with tonic firing has also been shown to be well-mixed [**78**].

Finally, a sensitivity analysis could be carried out for the herein proposed model with dopamine kinetics in order to determine the most important mechanisms in the onset of symptoms and loss of effect of levodopa. For this, we can draw on a recent work by Ursino et al. [**76**] which performed a sensitivity analysis of the Go/NoGo pathways, the STN and the cholinergic interneurons.

To conclude, the integrative model developed here was able to reproduce the behaviour of levodopa's effect by representing its most important mechanisms, especially the fact that the therapeutic effect of levodopa start to mimic plasma concentration with the progression of the disease. This quantitative systems approach is a promising step towards the understanding of important mechanisms involved in Parkinson's disease and designing optimal drug regimens.

Acknowledgements

F.V.-V. received a scholarship from the Natural Sciences and Engineering Research Council (NSERC), Canada through the PGS-D program. Support was also provided by NSERC -Industrial Chair in Pharmacometrics funded by Novartis, Pfizer and Syneos, as well as FRQNT Projet d'équipe (F.N.).

Conflict of interest

The authors declare that they have no conflict of interest.

Author Contributions

This work makes up a portion of the doctoral thesis of FVV. Construction of the model: FVV PR MU FN. Numerical simulations: FVV. Writing of the paper: FVV PR MU FN.

References

[1] Urszula Adamiak, Maria Kaldonska, Gabriela Klodowska-Duda, Elzbieta Wyska, Krzysztof Safranow, Monika Bialecka et Barbara Gawronska-Szklarz : Pharmacokinetic-pharmacodynamic modeling of levodopa in patients with advanced parkinson disease. *Clinical neuropharmacology*, 33:135–141, mai 2010.

[2] Y Agid : Parkinson's disease: pathophysiology. *Lancet (London, England)*, 337:1321–1324, juin 1991.

[3] R L Albin, A B Young et J B Penney : The functional anatomy of basal ganglia disorders. *Trends in neurosciences*, 12:366–375, octobre 1989.

[4] Sten-Magnus Aquilonius et Dag Nyholm : Development of new levodopa treatment strategies in parkinson's disease-from bedside to bench to bedside. *Upsala journal of medical sciences*, 122:71–77, juin 2017.

[5] F. Gregory Ashby et Matthew J. Crossley : A computational model of how cholinergic interneurons protect striatal-dependent learning. *Journal of Cognitive Neuroscience*, 23(6):1549–1566, jun 2011.

[6] Chiara Baston, Manuela Contin, Giovanna Calandra Buonaura, Pietro Cortelli et Mauro Ursino : A mathematical model of levodopa medication effect on basal ganglia in parkinson's disease: An application to the alternate finger tapping task. *Frontiers in Human Neuroscience*, 10, jun 2016.

[7] Chiara Baston et Mauro Ursino : A biologically inspired computational model of basal ganglia in action selection. *Computational Intelligence and Neuroscience*, 2015:1–24, 2015.

[8] Brian P Bergstrom et Paul A Garris : "passive stabilization" of striatal extracellular dopamine across the lesion spectrum encompassing the presymptomatic phase of parkinson's disease: a voltammetric study in the 6-ohda-lesioned rat. *Journal of neurochemistry*, 87:1224–1236, décembre 2003.

[9] Janet A Best, H Frederik Nijhout et Michael C Reed : Homeostatic mechanisms in dopamine synthesis and release: a mathematical model. *Theoretical Biology and Medical Modelling*, 6(1), sep 2009.

[10] E Bezard, S Dovero, C Prunier, P Ravenscroft, S Chalon, D Guilloteau, A R Crossman, B Bioulac, J M Brotchie et C E Gross : Relationship between the appearance of symptoms and the level of nigrostriatal degeneration in a progressive 1-methyl-4-phenyl-1,2,3,6-tetrahydropyridine-lesioned macaque model of parkinson's disease. *The Journal of neuroscience : the official journal of the Society for Neuroscience*, 21:6853–6861, septembre 2001.

[11] Kevin J. Black, Haley K. Acevedo et Jonathan M. Koller : Dopamine buffering capacity imaging: A pharmacodynamic fmri method for staging parkinson disease. *Frontiers in Neurology*, 11:370, 2020.

[12] Isabelle Boileau, Mark Guttman, Pablo Rusjan, John R Adams, Sylvain Houle, Junchao Tong, Oleh Hornykiewicz, Yoshiaki Furukawa, Alan A Wilson, Shitij Kapur et Stephen J Kish : Decreased binding of the d3 dopamine receptor-preferring ligand [11c]-(+)-phno in drug-naive parkinson's disease. *Brain : a journal of neurology*, 132:1366–1375, mai 2009.

[13] Evgeny A Budygin, Carrie E John, Yolanda Mateo et Sara R Jones : Lack of cocaine effect on dopamine clearance in the core and shell of the nucleus accumbens of dopamine transporter knock-out mice. *The Journal of neuroscience : the official journal of the Society for Neuroscience*, 22:RC222, mai 2002.

[14] James F Cavanagh, Thomas V Wiecki, Michael X Cohen, Christina M Figueroa, Johan Samanta, Scott J Sherman et Michael J Frank : Subthalamic nucleus stimulation reverses mediofrontal influence over decision threshold. *Nature Neuroscience*, 14(11):1462–1467, sep 2011.

[15] Phylinda L S Chan, John G Nutt et Nicholas H G Holford : Modeling the short- and long-duration responses to exogenous levodopa and to endogenous levodopa production in parkinson's disease. *Journal of pharmacokinetics and pharmacodynamics*, 31:243–268, juin 2004.

[16] Phylinda L S Chan, John G Nutt et Nicholas H G Holford : Pharmacokinetic and pharmacodynamic changes during the first four years of levodopa treatment in parkinson's disease. *Journal of pharmacokinetics and pharmacodynamics*, 32:459–484, août 2005.

[17] Y H Chou, P Karlsson, C Halldin, H Olsson et L Farde : A pet study of d(1)-like dopamine receptor ligand binding during altered endogenous dopamine levels in the primate brain. *Psychopharmacology*, 146:220–227, septembre 1999.

[18] M Contin, R Riva, P Martinelli, F Albani, P Avoni et A Baruzzi : Levodopa therapy monitoring in patients with parkinson disease: a kinetic-dynamic approach. *Therapeutic drug monitoring*, 23:621–629, décembre 2001.

[19] G C Cotzias, M H Van Woert et L M Schiffer : Aromatic amino acids and modification of parkinsonism. *The New England journal of medicine*, 276:374–379, février 1967.

[20] A R Crossman, C E Clarke, S Boyce, R G Robertson et M A Sambrook : Mptp-induced parkinsonism in the monkey: neurochemical pathology, complications of treatment and pathophysiological mechanisms. *The Canadian journal of neurological sciences. Le journal canadien des sciences neurologiques*, 14:428–435, août 1987.

[21] Vassilis Cutsuridis et Stavros Perantonis : A neural network model of parkinson's disease bradykinesia. *Neural networks : the official journal of the International Neural Network Society*, 19:354–374, mai 2006.

[22] M R DeLong : Primate models of movement disorders of basal ganglia origin. *Trends in neurosciences*, 13:281–285, juillet 1990.

[23] C Dentresangle, M Le Cavorsin, M Savasta et V Leviel : Increased extracellular da and normal evoked da release in the rat striatum after a partial lesion of the substantia nigra. *Brain research*, 893:178–185, mars 2001.

[24] M Dietz, S Harder, J Graff, G Künig, P Vontobel, K L Leenders et H Baas : Levodopa pharmacokinetic-pharmacodynamic modeling and 6-[18f]levodopa positron emission tomography in patients with parkinson's disease. *Clinical pharmacology and therapeutics*, 70:33–41, juillet 2001.

[25] J. K. Dreyer : Three mechanisms by which striatal denervation causes breakdown of dopamine signaling. *Journal of Neuroscience*, 34(37):12444–12456, sep 2014.

[26] Jakob K. Dreyer, Kjartan F. Herrik, Rune W. Berg et Jørn D. Hounsgaard : Influence of phasic and tonic dopamine release on receptor activation. *Journal of Neuroscience*, 30(42):14273–14283, 2010.

[27] G Fabbrini, J Juncos, M M Mouradian, C Serrati et T N Chase : Levodopa pharmacokinetic mechanisms and motor fluctuations in parkinson's disease. *Annals of neurology*, 21:370–376, avril 1987.

[28] Michael J. Frank : Dynamic dopamine modulation in the basal ganglia: A neurocomputational account of cognitive deficits in medicated and nonmedicated parkinsonism. *Journal of Cognitive Neuroscience*, 17(1):51–72, 2005.

[29] G Gangadhar, D Joseph, A V Srinivasan, D Subramanian, R G Shivakeshavan, N Shobana et V S Chakravarthy : A computational model of parkinsonian handwriting that highlights the role of the indirect pathway in the basal ganglia. *Human movement science*, 28:602–618, octobre 2009.

[30] C R Gerfen, T M Engber, L C Mahan, Z Susel, T N Chase, F J Monsma et D R Sibley : D1 and d2 dopamine receptor-regulated gene expression of striatonigral and striatopallidal neurons. *Science (New York, N.Y.)*, 250:1429–1432, décembre 1990.

[31] Christopher G Goetz, Barbara C Tilley, Stephanie R Shaftman, Glenn T Stebbins, Stanley Fahn, Pablo Martinez-Martin, Werner Poewe, Cristina Sampaio, Matthew B Stern, Richard Dodel, Bruno Dubois, Robert Holloway, Joseph Jankovic, Jaime Kulisevsky, Anthony E Lang, Andrew Lees, Sue Leurgans, Peter A LeWitt, David Nyenhuis, C Warren Olanow, Olivier Rascol, Anette Schrag, Jeanne A Teresi, Jacobus J van Hilten, Nancy LaPelle et Movement Disorder Society UPDRS Revision Task Force : Movement disorder society-sponsored revision of the unified parkinson's disease rating scale (mds-updrs): scale presentation and clinimetric testing results. *Movement disorders : official journal of the Movement Disorder Society*, 23:2129–2170, novembre 2008.

[32] G Gomez, M V Escande, L M Suarez, L Rela, J E Belforte, R Moratalla, M G Murer, O S Gershanik et I R E Taravini : Changes in dendritic spine density and inhibitory perisomatic connectivity onto medium spiny neurons in l-dopa-induced dyskinesia. *Molecular neurobiology*, 56:6261–6275, septembre 2019.

[33] Sandrine Greffard, Marc Verny, Anne-Marie Bonnet, Jean-Yves Beinis, Claude Gallinari, Sylvie Meaume, François Piette, Jean-Jacques Hauw et Charles Duyckaerts : Motor score of the unified parkinson disease rating scale as a good predictor of lewy body–associated neuronal loss in the substantia nigra. *Archives of Neurology*, 63(4):584, apr 2006.

[34] Parkinson Study Group : Dopamine transporter brain imaging to assess the effects of pramipexole vs levodopa on parkinson disease progression. *JAMA*, 287:1653–1661, avril 2002.

[35] M Guthrie, C E Myers et M A Gluck : A neurocomputational model of tonic and phasic dopamine in action selection: a comparison with cognitive deficits in parkinson's disease. *Behavioural brain research*, 200:48–59, juin 2009.

[36] M Guttman et P Seeman : L-dopa reverses the elevated density of d2 dopamine receptors in parkinson's diseased striatum. *Journal of neural transmission*, 64:93–103, 1985.

[37] Mohammad Haeri, Yashar Sarbaz et Shahriar Gharibzadeh : Modeling the parkinson's tremor and its treatments. *Journal of Theoretical Biology*, 236(3):311–322, oct 2005.

[38] S Harder et H Baas : Concentration-response relationship of levodopa in patients at different stages of parkinson's disease. *Clinical pharmacology and therapeutics*, 64:183–191, août 1998.

[39] Bertil Hille : G protein-coupled mechanisms and nervous signaling. *Neuron*, 9(2):187–195, aug 1992.

[40] Shin Hisahara et Shun Shimohama : Dopamine receptors and parkinson's disease. *International journal of medicinal chemistry*, 2011:403039, 2011.

[41] Nicholas H G Holford, Phylinda L S Chan, John G Nutt, Karl Kieburtz, Ira Shoulson et Parkinson Study Group : Disease progression and pharmacodynamics in parkinson disease - evidence for functional protection with levodopa and other treatments. *Journal of pharmacokinetics and pharmacodynamics*, 33:281–311, juin 2006.

[42] Nick Holford et John G Nutt : Disease progression, drug action and parkinson's disease: why time cannot be ignored. *European journal of clinical pharmacology*, 64:207–216, février 2008.

[43] C N Homann, K Suppan, K Wenzel, G Giovannoni, G Ivanic, S Horner, E Ott et H P Hartung : The bradykinesia akinesia incoordination test (brain test), an objective and user-friendly means to evaluate patients with parkinsonism. *Movement disorders : official journal of the Movement Disorder Society*, 15:641–647, juillet 2000.

[44] Lars Hunger, Arvind Kumar et Robert Schmidt : Abundance compensates kinetics: Similar effect of dopamine signals on d1 and d2 receptor populations. *Journal of Neuroscience*, 40(14):2868–2881, 2020.

[45] Lisa Kuramoto, Jacquelyn Cragg, Ramachandiran Nandhagopal, Edwin Mak, Vesna Sossi, Raul de la Fuente-Fernández, A Jon Stoessl et Michael Schulzer : The nature of progression in parkinson's disease: an application of non-linear, multivariate, longitudinal random effects modelling. *PloS one*, 8:e76595, 2013.

[46] Hiroto Kuwabara, Mary E McCaul, Gary S Wand, Christopher J Earley, Richard P Allen, Elise M Weerts, Robert F Dannals et Dean F Wong : Dissociative changes in the bmax and kd of dopamine d2/d3 receptors with aging observed in functional subdivisions of the striatum: a revisit with an improved data analysis method. *Journal of nuclear medicine : official publication, Society of Nuclear Medicine*, 53:805–812, mai 2012.

[47] T Lee, P Seeman, A Rajput, I J Farley et O Hornykiewicz : Receptor basis for dopaminergic supersensitivity in parkinson's disease. *Nature*, 273:59–61, mai 1978.

[48] A Lopez, A Muñoz, M J Guerra et J L Labandeira-Garcia : Mechanisms of the effects of exogenous levodopa on the dopamine-denervated striatum. *Neuroscience*, 103:639–651, 2001.

[49] Torsten May : Striatal dopamine d1-like receptors have higher affinity for dopamine in ethanol-treated rats. *European Journal of Pharmacology*, 215(2-3):313–316, may 1992.

[50] Jonathan W Mink : The basal ganglia: Focused selection and inhibition of competing motor programs. *Progress in Neurobiology*, 50(4):381 – 425, 1996.

[51] Ahmed A. Moustafa et Mark A. Gluck : A neurocomputational model of dopamine and prefrontal–striatal interactions during multicue category learning by parkinson patients. *Journal of Cognitive Neuroscience*, 23(1):151–167, jan 2011.

[52] Kim A. Neve et Rachael L. Neve : *Molecular Biology of Dopamine Receptors*, pages 27–76. Humana Press, Totowa, NJ, 1997.

[53] Maria Nord, Peter Zsigmond, Anita Kullman et Nil Dizdar : Levodopa pharmacokinetics in brain after both oral and intravenous levodopa in one patient with advanced parkinson's disease. *Advances in Parkinson's Disease*, 06(02):52–66, 2017.

[54] J G Nutt et N H Holford : The response to levodopa in parkinson's disease: imposing pharmacological law and order. *Annals of neurology*, 39:561–573, mai 1996.

[55] J G Nutt, W R Woodward, J H Carter et S T Gancher : Effect of long-term therapy on the pharmacodynamics of levodopa. relation to on-off phenomenon. *Archives of neurology*, 49:1123–1130, novembre 1992.

[56] C Warren Olanow, Yves Agid, Yoshi Mizuno, Alberto Albanese, Ubaldo Bonuccelli, U Bonuccelli, Philip Damier, Justo De Yebenes, Oscar Gershanik, Mark Guttman, F Grandas, Mark Hallett, Ole Hornykiewicz, Peter Jenner, R Katzenschlager, William J Langston, Peter LeWitt, Eldad Melamed, M A Mena, P P Michel, Catherine Mytilineou, Jose A Obeso, Werner Poewe, Niall Quinn, R Raisman-Vozari, Ali H Rajput, Olivier Rascol, Christina Sampaio et Fabrizio Stocchi : Levodopa in the treatment of parkinson's disease: current controversies. *Movement disorders : official journal of the Movement Disorder Society*, 19:997–1005, septembre 2004.

[57] W Olanow, A H Schapira et O Rascol : Continuous dopamine-receptor stimulation in early parkinson's disease. *Trends in neurosciences*, 23:S117–S126, octobre 2000.

[58] P K. Pal, C S. Lee, A Samii, M Schulzer, A J. Stoessl, E K. Mak, J Wudel, T Dobko et J K.C. Tsui : Alternating two finger tapping with contralateral activation is an objective measure of clinical severity in parkinson's disease and correlates with pet. *Parkinsonism & related disorders*, 7:305–309, octobre 2001.

[59] Doris E Payer, Mark Guttman, Stephen J Kish, Junchao Tong, John R Adams, Pablo Rusjan, Sylvain Houle, Yoshiaki Furukawa, Alan A Wilson et Isabelle Boileau : D3 dopamine receptor-preferring [11c]phno pet imaging in parkinson patients with dyskinesia. *Neurology*, 86:224–230, janvier 2016.

[60] Werner Poewe, Angelo Antonini, Jan Cm Zijlmans, Pierre R Burkhard et François Vingerhoets : Levodopa in the treatment of parkinson's disease: an old drug still going strong. *Clinical interventions in aging*, 5:229–238, septembre 2010.

[61] Michael C. Reed, Janet Best et H. Frederik Nijhout : Passive and active stabilization of dopamine in the striatum. *Bioscience Hypotheses*, 2(4):240 – 244, 2009.

[62] Michael C Reed, H Frederik Nijhout et Janet A Best : Mathematical insights into the effects of levodopa. *Frontiers in integrative neuroscience*, 6:21, 2012.

[63] E.K. Richfield, J.B. Penney et A.B. Young : Anatomical and affinity state comparisons between dopamine d1 and d2 receptors in the rat central nervous system. *Neuroscience*, 30(3):767–777, jan 1989.

[64] J O Rinne, A Laihinen, H Ruottinen, U Ruotsalainen, K Någren, P Lehikoinen, V Oikonen et U K Rinne : Increased density of dopamine d2 receptors in the putamen, but not in the caudate nucleus in early parkinson's disease: a pet study with [11c]raclopride. *Journal of the neurological sciences*, 132:156–161, octobre 1995.

[65] András Salamon, Dénes Zádori, László Szpisjak, Péter Klivényi et László Vécsei : Neuroprotection in parkinson's disease: facts and hopes. *Journal of Neural Transmission*, 127(5):821–829, dec 2019.

[66] Henning Schroll, Julien Vitay et Fred H Hamker : Working memory and response selection: a computational account of interactions among cortico-basalganglio-thalamic loops. *Neural networks : the official journal of the International Neural Network Society*, 26:59–74, février 2012.

[67] P Seeman et H B Niznik : Dopamine receptors and transporters in parkinson's disease and schizophrenia. *FASEB journal : official publication of the Federation of American Societies for Experimental Biology*, 4:2737–2744, juillet 1990.

[68] Marina Senek, Dag Nyholm et Elisabet I Nielsen : Population pharmacokinetics of levodopa/carbidopa microtablets in healthy subjects and parkinson's disease patients. *European journal of clinical pharmacology*, 74:1299–1307, octobre 2018.

[69] Sushil Sharma, Carolyn Seungyoun Moon, Azza Khogali, Ali Haidous, Anthony Chabenne, Comfort Ojo, Miriana Jelebinkov, Yousef Kurdi et Manuchair Ebadi : Biomarkers in parkinson's disease (recent update). *Neurochemistry international*, 63:201–229, septembre 2013.

[70] Matej Skorvanek, Pablo Martinez-Martin, Norbert Kovacs, Mayela Rodriguez-Violante, Jean-Christophe Corvol, Pille Taba, Klaus Seppi, Oleg Levin, Anette Schrag, Thomas Foltynie, Mario Alvarez-Sanchez, Tomoko Arakaki, Zsuzsanna Aschermann, Iciar Aviles-Olmos, Eve Benchetrit, Charline Benoit, Alberto Bergareche-Yarza, Amin Cervantes-Arriaga, Anabel Chade, Florence Cormier, Veronika Datieva, David A Gallagher, Nelida Garretto, Zuzana Gdovinova, Oscar Gershanik, Milan Grofik, Vladimir Han, Jing Huang, Liis Kadastik-Eerme, Monica M Kurtis, Graziella Mangone, Juan Carlos Martinez-Castrillo, Amelia Mendoza-Rodriguez, Michal Minar, Henry P Moore, Mari Muldmaa, Christoph Mueller, Bernadette Pinter, Werner Poewe, Karin Rallmann, Eva Reiter, Carmen Rodriguez-Blazquez, Carlos Singer, Barbara C Tilley, Peter Valkovic, Christopher G Goetz et Glenn T Stebbins : Differences in mds-updrs scores based on hoehn and yahr stage and disease duration. *Movement disorders clinical practice*, 4:536–544, 2017.

[71] Lance A Smith, Michael J Jackson, Matthew J Hansard, Eleni Maratos et Peter Jenner : Effect of pulsatile administration of levodopa on dyskinesia induction in drug-naïve mptp-treated common marmosets: effect of dose, frequency of administration, and brain exposure. *Movement disorders : official journal of the Movement Disorder Society*, 18:487–495, mai 2003.

[72] David Sulzer, Stephanie J. Cragg et Margaret E. Rice : Striatal dopamine neurotransmission: Regulation of release and uptake. *Basal Ganglia*, 6(3):123–148, aug 2016.

[73] Ana Lisa Taylor Tavares, Gregory S X E Jefferis, Mandy Koop, Bruce C Hill, Trevor Hastie, Gary Heit et Helen M Bronte-Stewart : Quantitative measurements of alternating finger tapping in parkinson's disease correlate with updrs motor disability and reveal the improvement in fine motor control from medication and deep brain stimulation. *Movement disorders : official journal of the Movement Disorder Society*, 20:1286–1298, octobre 2005.

[74] B R Thanvi et T C N Lo : Long term motor complications of levodopa: clinical features, mechanisms, and management strategies. *Postgraduate Medical Journal*, 80(946):452–458, 2004.

[75] E J Triggs, B G Charles, M Contin, P Martinelli, P Cortelli, R Riva, F Albani et A Baruzzi : Population pharmacokinetics and pharmacodynamics of oral levodopa in parkinsonian patients. *European journal of clinical pharmacology*, 51:59–67, 1996.

[76] Mauro Ursino et Chiara Baston : Aberrant learning in parkinson's disease: A neurocomputational study on bradykinesia. *The European journal of neuroscience*, 47:1563–1582, juin 2018.

[77] Mauro Ursino, Elisa Magosso, Giovanna Lopane, Giovanna Calandra-Buonaura, Pietro Cortelli et Manuela Contin : Mathematical modeling and parameter estimation of levodopa motor response in patients with parkinson disease. *PLOS ONE*, 15(3):1–20, 03 2020.

[78] B Jill Venton, Hui Zhang, Paul A Garris, Paul E M Phillips, David Sulzer et R Mark Wightman : Real-time decoding of dopamine concentration changes in the caudate-putamen during tonic and phasic firing. *Journal of neurochemistry*, 87:1284–1295, décembre 2003.

[79] Thomas V Wiecki et Michael J Frank : Neurocomputational models of motor and cognitive deficits in parkinson's disease. *Progress in brain research*, 183:275–297, 2010.

[80] M J Zigmond, E D Abercrombie, T W Berger, A A Grace et E M Stricker : Compensations after lesions of central dopaminergic neurons: some clinical and basic implications. *Trends in neurosciences*, 13:290–296, juillet 1990.

Deuxième chapitre.

Nonlinear pharmacodynamics of Levodopa through Parkinson's disease progression

par

Florence Véronneau-Veilleux[1], Mauro Ursino[2],
Philippe Robaey[3], Daniel Lévesque[4] et Fahima Nekka[5]

([1]) Faculté de Pharmacie, Université de Montréal, Montréal, Québec, Canada

([2]) Department of Electrical, Electronic and Information Engineering "Guglielmo Marconi", University of Bologna, 40136 Bologna, Italy

([3]) Faculty of Medicine, University of Ottawa, Ottawa, Ontario, Canada

([4]) Faculté de Pharmacie, Université de Montréal, Montréal, Québec, Canada

([5]) Faculté de Pharmacie, Université de Montréal
Centre de recherches mathématiques, Université de Montréal,
Centre for Applied Mathematics in Bioscience and Medicine (CAMBAM), McGill University, Montréal, Québec, Canada

Cet article a été publié dans *Chaos* vol. 30,9 (2020): 093146. Le matériel supplémentaire associé à cet article se trouve à l'annexe B de la présente thèse .

Dans ce deuxième chapitre, l'objectif est d'étudier les modifications non-linéaires de la pharmacodynamique de la lévodopa avec la progression de la maladie de Parkinson puisqu'elles compliquent l'optimisation des régimes posologiques. À cette fin, le modèle développé au Chapitre 1, comprenant un modèle de la pharmacocinétique de la lévodopa, de la dynamique de la dopamine et de la neurotransmission dans les ganglions de la base, est utilisé pour effectuer différentes simulations. En particulier, les relations, pour différentes doses de lévodopa, entre la concentration plasmatique, la concentration cérébrale de dopamine et la réponse à une tâche motrice avec la dénervation sont étudiées et mises en parallèle avec le rétrécissement de l'index thérapeutique.

Abstract. The effect of levodopa on the alleviation of Parkinson's disease symptoms is altered in a highly nonlinear manner as the disease progresses. This can be attributed to different compensation mechanisms taking place in the basal ganglia where the dopaminergic neurons are progressively lost. This alteration in the effect of levodopa complicates the optimization of drug regimen. The present work aims at investigating the nonlinear dynamics of Parkinson's disease and its therapy through mechanistic mathematical modeling. Using a holistic approach, a pharmacokinetic model of levodopa was combined to a dopamine dynamics and a neurocomputational model of basal ganglia. The influence of neuronal death on these different mechanisms was also integrated. Using this model, we were able to investigate the nonlinear relationships between levodopa plasma concentration, dopamine brain concentration and response to a motor task. Variations in dopamine concentrations in the brain for different levodopa doses were also studied. Finally, we investigated the narrowing of levodopa therapeutic index with the progression of the disease as a result of these nonlinearities. In conclusion, various consequences of nonlinear dynamics in Parkinson's disease treatment were studied by developing an integrative model. This model paves the way towards individualization of dosing regimen. Using sensor based information, the parameters of the model could be fitted to individual data to propose optimal individual regimens.
Keywords: Parkinson's disease, levodopa, pharmacodynamics, denervation, basal ganglia

1. Introduction

Parkinson's disease is a neurodegenerative disorder associated with the loss of dopaminergic neurons in the basal ganglia. Motor symptoms such as bradykinesia, rigidity, tremor and postural instability are related to this depletion of dopamine [**37**]. Bradykinesia, defined as the slowing of movements, is a disabling symptom on which the current paper focuses.

To alleviate Parkinson disease's symptoms, levodopa is used as the gold standard drug treatment. Levodopa is the synthesis precursor of dopamine, it is decarboxylated into dopamine by dopaminergic neurons. It does not cure the disease but helps in reducing the symptoms [**24**]. During the first years of therapy, levodopa effect lasts even when levodopa plasma concentration fades because the central nervous system can store dopamine into intracellular vesicles due to the activity of various transporters [**39**]. Indeed, at the onset of disease, dopamine can be stored and released as needed. With the loss of neurons,

this buffering capacity is lost and dopamine is rapidly released in the synaptic cleft. At this stage, levodopa becomes more and more dependent on plasma concentration and available neurons are not able to buffer the fluctuations in dopamine coming from the treatment (with each pills) [**39**]. Levodopa's effect varies with the level of denervation in a nonlinear manner, leading to serious challenges for optimization of its regimen. Compensation processes that occur at the level of brain dopamine also behave in a nonlinear manner. These compensation processes keep the level of dopamine well balanced until the level of denervation reaches a critical threshold that results in a drop of dopamine concentration. It accounts for the appearance of symptoms when 60% to 90% of dopaminergic neurons are already lost [**1, 41**]. Furthermore, the effect of dopamine on the basal ganglia is regulated by nonlinear dynamics.

The presence of these nonlinearities and the complexity of the disease and its therapy call for a better understanding of the involved mechanisms, for which in vivo studies cannot always be easily undertaken. The main objective of the current paper is to study the nonlinear effect of denervation on levodopa pharmacodynamics. Using a holistic approach, this work combines basal ganglia structure modeling and dopamine dynamics with a pharmacokinetics model of levodopa.

Previous studies focused on modeling the dynamics of basal ganglia without levodopa and dopamine dynamics. These models include one to three neurotransmission pathways and targeted different symptoms. Tremor was investigated through velocity response modeled with block diagram of basal ganglia [**20**]. Velocity in the x and y axis were considered with a network of oscillators of basal ganglia to investigate micrographia patterns, i.e. reduced handwriting, in parkinsonian patients [**18**]. A neural network model of basal ganglia [**13**] and a firing rate model [**3**] were applied to bradykinesia through arm movements and finger tapping respectively. Conductance-based model of basal ganglia [**25, 35**] and double-oscillator [**26**] of basal ganglia model were also used to study the appearance of oscillations in basal ganglia neural activity.

Parallel studies solely focused on modeling dopamine dynamics. Homeostasis in dopamine synthesis, release and reuptake were previously modeled [**33**]. Consequences of levodopa

therapy on serotoninergic and dopaminergic systems with detailed description of enzymes and transporters dynamics have also been considered [**34**], as well as compensation mechanisms in signaling through dopaminergic receptors [**16**]. Although more physiologically detailed than the model presented here, none of the former studies include dopamine dynamics effect on neurotransmission in the basal ganglia.

With the objective to provide a more thorough appreciation of all the nonlinear dynamics of dopamine and levodopa effect with disease progression, a complete model is here developed through a quantitative systems pharmacology approach. The novelty of our model is to combine both nonlinear dynamics of dopamine and basal ganglia. Up-to-date knowledge of the pathophysiology and pharmacology was used to build and validate the model with the additional objective to represent relevant clinical motor task.

The current paper is organized as follows: the details of the three parts constituting the model are given in section 2. Results of the relation between motor task and dopamine with levodopa plasma concentration are detailed in section 3.1. Finally, relations of doses and therapeutic index with denervation levels are given in section 3.2.

2. Methods

Various nonlinear mechanisms modify action selection in Parkinson's disease, including dopamine dynamics and neurotransmission in basal ganglia. All these aspects are significantly altered by denervation in the substantia nigra, which reflects the disease progression. To analyze these mechanisms and their nonlinear effects, the present model includes three parts: levodopa pharmacokinetics, dopamine dynamics, and action selection in the basal ganglia.

Levodopa pharmacokinetics is expressed by a two-compartment pharmacokinetic model. Dopamine dynamics account for the changes in dopamine concentration in the brain and its binding with D1 and D2 dopamine receptors. Finally, a neurocomputational model accounts for activity in each basal ganglia nucleus, and computes action selection as a function of concentrations of bound receptors. The overall model is used to simulate finger tapping,

which is a clinically relevant output to assess bradykinesia. Disease progression is represented by the degree of nigrostriatal denervation given here by the fraction of neurons alive in the substantia nigra and noted f. Figure 18 illustrates the three parts of the model and its output.

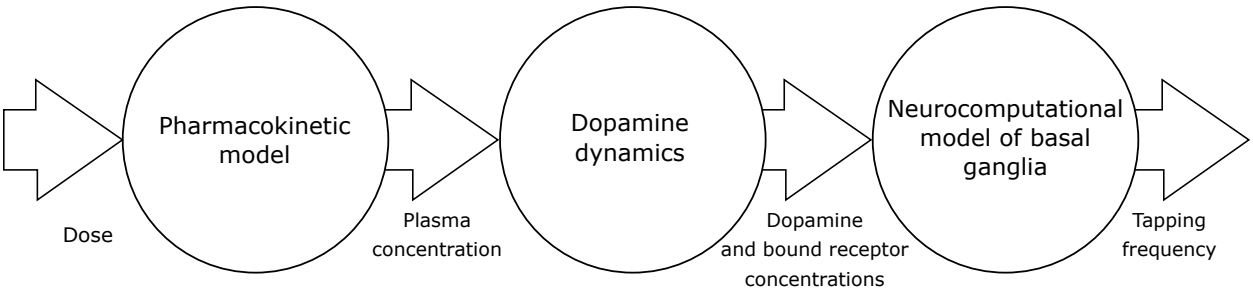

Figure 18. Representation of the three parts of the model.

2.1. Levodopa Pharmacokinetics

Compartmental models are used in pharmacokinetics to represent the body as a chain of compartments. Two compartment models have shown to be well suited for fitting levodopa plasma concentrations [**3, 8, 36**]. In the present work, a third compartment is added for brain concentrations. The present pharmacokinetic model was adapted from [**3**] and is illustrated in Figure 19.

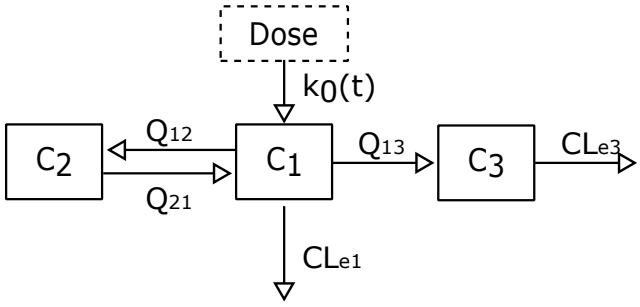

Figure 19. Representation of the two compartment pharmacokinetic model with a third compartment for brain concentration.

Concentrations in the central (C_1) and peripheral (C_2) compartment with an intravenous infusion of levodopa are respectively given by the following equations:

$$V_1 \frac{dC_1}{dt} = k_0(t) + Q_{21}C_2 - (Q_{12} + CL_{etot})C_1, \tag{2.1}$$

$$V_2 \frac{dC_2}{dt} = Q_{12}C_1 - Q_{21}C_2, \tag{2.2}$$

where Q_{ij} are inter-compartment clearance from the ith to the jth compartment and V_i the volume of compartment i. The total elimination is given by $CL_{etot} = CL_{e1} + Q_{13}$. The rate $k_0(t)$ is the infusion rate, estimated to 3.33 mg/min for 30 min and 0 the rest of the time for a total dose of 100 mg [**3**]. These equations are independant of the fraction f of neurons alive since it is reported that denervation does not affect the pharmacokinetic of levodopa [**10**].

Levodopa is able to cross the blood brain barrier to reach the brain. Nonlinear dynamics with disease progression appear at the level of levodopa brain concentration, which is given here by the concentration C_3 in the third compartment. Dopaminergic neurons have the ability to transform levodopa into dopamine, store dopamine and release it when needed. As disease progresses, this buffering capacity is lost due to neuronal degeneration. Concentration in the brain is therefore dependent in a nonlinear manner to the fraction f of neurons alive and can be expressed by the following equation:

$$V_3 \frac{dC_3}{dt} = \frac{1}{f} \cdot Q_{13}C_1 - \frac{1}{f} \cdot CL_{e3}C_3. \tag{2.3}$$

Previous studies have shown that parameter CL_{e3} is correlated with denervation [**12, 15**]. CL_{e3} is here inversely proportional to the fraction f. The parameter Q_{13} is also inversely proportional to f since levodopa storage is decreased with denervation [**39**]. Parameters Q_{13} and CL_{e3}, previously represented with one parameter k_e, were shown to increase with disease progression [**5, 10, 21**]. It is as if levodopa fills a leaky reservoir that becomes leakier with denervation. It is called the buffering capacity. In order to represent the buffering capacity in detail, disruptions to the L-Tyrosine $\rightarrow$ L-DOPA $\rightarrow$ Dopamine pathway with vesicular

dopamine should be modeled [**4, 34**]. For simplicity purposes, these mechanisms were represented here by this increase in parameter Q_{13} and CL_{e3} with denervation. The dependence of CL_{etot} on f in equation 2.1 was neglected since parameter Q_{13} is small compared with CL_{e1}.

The value of the parameters are taken from [**3**] and are given in the Supplementary material B.

2.2. Dopamine dynamics

Once in the brain, levodopa is decarboxylated into dopamine by the aromatic amino acid decarboxylase enzyme. It results in an increased capacity of dopamine release in the synaptic cleft. Dopamine terminals are in the striatum. After dopamine is released in the synaptic space, it can be recaptured into presynaptic terminals by the dopamine transporter (DAT) or removed from the synaptic cleft (by enzymes, glial cells, diffusion, etc). With denervation, these processes are modified in a nonlinear manner. Figure 20 gives a schematic representation of these processes.

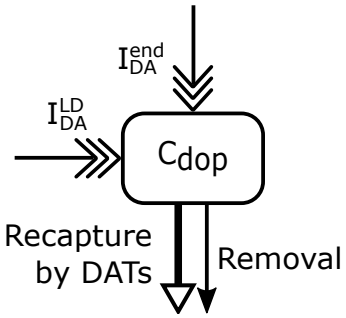

Figure 20. Representation of dopamine release, recapture by transporters DATs and removal. The triple-headed arrows represent dopamine release, the arrow with empty head represents recapture by DATs (saturable) and the arrow with solid head represent the linear removal. I_{DA}^{end}, I_{DA}^{LD} and C_{dop} are explained below.

For the sake of simplicity, only relevant and measurable mechanisms are incorporated in the model, namely, release, recapture and removal of dopamine in the synaptic cleft. The equation for dopamine concentrations C_{dop} in μmol/L in the synaptic cleft, adapted from [**4, 33**], is :

$$\underbrace{\frac{dC_{dop}(t)}{dt}}_{\text{Dopamine concentration}} = \underbrace{f \cdot (I_{DA}^{end} + I_{DA}^{LD}(t))}_{\text{Dopamine Release}} - \underbrace{\frac{f \cdot V_{max} C_{dop}(t)}{(k_m + C_{dop}(t))}}_{\text{Recapture by DATs}} - \underbrace{\frac{1}{f} \cdot k_{rem} C_{dop}(t)}_{\text{Removal}}, \tag{2.4}$$

where I_{DA}^{end} is the endogenous dopamine release term, $I_{DA}^{LD}(t)$ is the levodopa related release term, V_{max} is the maximum binding rate to the transporters DATs, k_m is the Michaelis-Menten constant and k_{rem} is the removal constant. It is assumed that dopamine release and reuptake by DATs decrease linearly with f since dopaminergic neurons are dying. Removal of dopamine is assumed to be inversely proportionnal to f [**33**] since it is easier for dopamine to be removed when terminals become more sparse. Dopamine release uniquely due to levodopa is related to levodopa brain concentrations through the following equation:

$$I_{DA}^{LD}(t) = k_{3dop} C_3(t). \tag{2.5}$$

Finally, the postsynaptic effect of dopamine on the neurons of the striatum are considered here to be equal to the concentrations of bound receptors [**22**]. Dopamine D1 and D2 receptor subtypes are included in the model and their respective concentrations are given by the following function:

$$\text{Bound receptor}_i = \frac{B_{max}^i C_{dop}}{k_D^i + C_{dop}}, \tag{2.6}$$

where $i \in \{D1, D2\}$, k_D^i and B_{max}^i are respectively the dissociation constant and the receptor's maximal concentration, which have a different value for each type of receptor.

In dopamine dynamics, there are two main nonlinearities, both related to Michaelis-Menten relationship. The first holds in the recapture by DATs in equation 2.4, the second is represented by the equation 2.6 of the bound receptors. Both involve an upper saturation, which will saturate motor response at high levels of dopamine concentration.

2.3. Neurocomputational model of basal ganglia

The basal ganglia are the center for movement selection and initiation [**27**]. They are composed of subcortical nuclei such as the striatum, the globus pallidus, the substantia nigra and the subthalamic nucleus, connected through three main neurotransmission pathways. The direct pathway (Go) promotes the movement, the indirect pathway (NoGo) inhibits it and the hyperdirect pathway suppresses erroneous movement. Cholinergic interneurons represent another important component that integrate direct and indirect striatal output pathways activities [**7**]. Figure 21 depicts the different nuclei and their connections.

Dopamine, both endogenous and exogenous, has an excitatory effect on the Go part of the striatum (D1 receptors), an inhibitory effect on the NoGo part of the striatum (D2 receptors) and an inhibitory effect on the cholinergic interneurons as seen in Figure 21.

The current neurocomputational model was adapted from [**3**]. It details the neural activity for neurons in each nucleus of the basal ganglia. In order to model the finger tapping task, each nucleus is composed of two neurons: one for the raising of the finger and the other for its lowering. The general equation of the neuronal activity of a neuron located in the nuclei k receiving current from nuclei m is:

$$\tau \frac{du_i^k}{dt} = -u_i^k + \sum_{j=1}^{2} w_{ij}^{km} y_j^m. \tag{2.7}$$

where i is the number of the neuron, either 1 or 2 for each action. w^{km} is the weight of the connection between nuclei k and m. The nature of the connections, inhibitory or excitatory, stems from the knowledge of the three neurotransmission pathways. The post-synaptic variable u_i^k is then scaled between zero and one to provide the neuron's activity by the following sigmoidal function:

$$\begin{aligned} y_i^k &= \zeta(u_i^k) \\ &= \frac{1}{1 + e^{-a(u_i^k - u_0)}}, \end{aligned} \tag{2.8}$$

where a is affecting the central slope and u_0 the central position. More details about this model can be found in [**3**]. Parameters values are given in the Supplementary material B. The

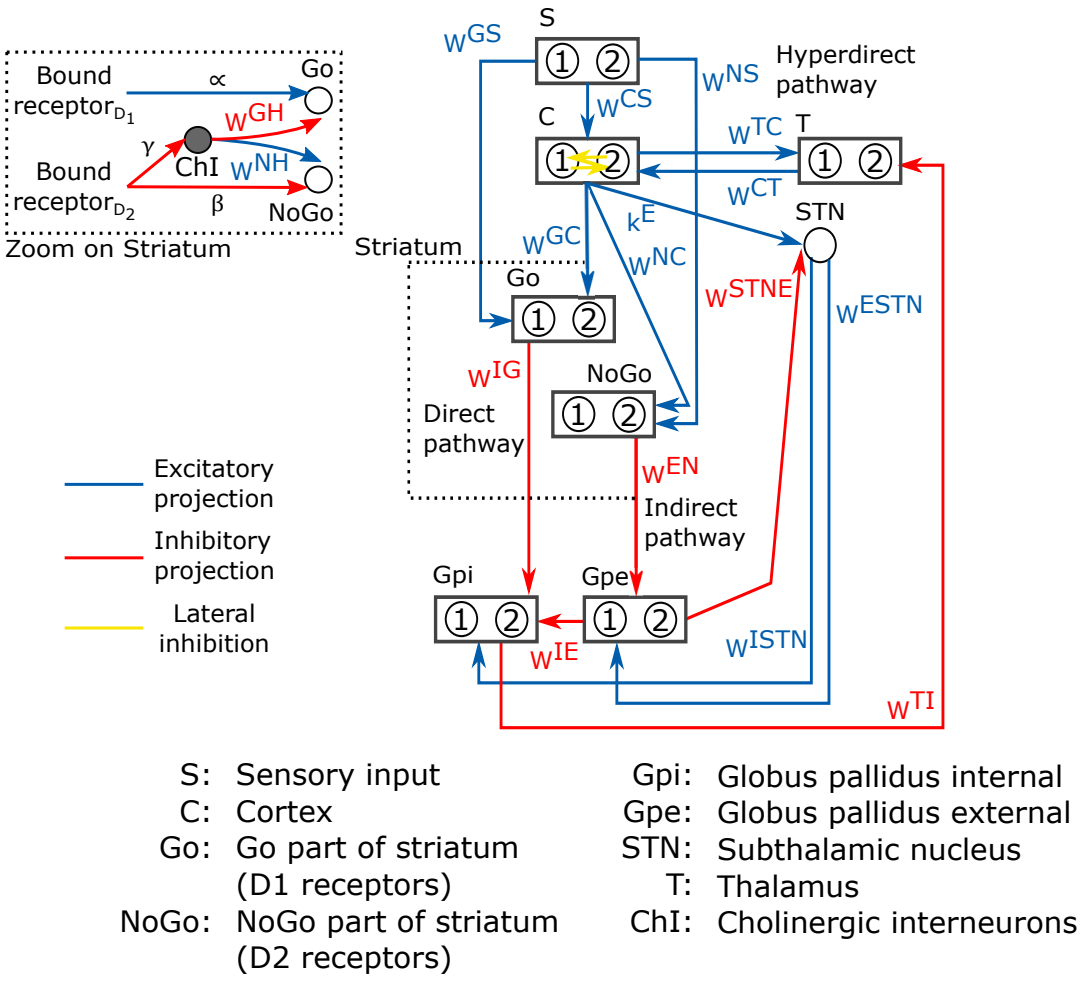

Figure 21. Schematic representation of the basal ganglia neurocomputational model with the three neurotransmission pathways adapted from[**3**]. The boxes represent different brain regions, the circles represent neurons, the numbers in the circle represent the number of the action channel, the yellow arrows represent lateral inhibition in the cortex, the blue arrows represent excitatory connections and the red arrows represent inhibitory connections.

model developed in [**3**] was extended to include dopamine dynamics and receptor binding. Dopamine dynamics model was added to represent modification in these dynamics through disease progression and their impact on levodopa's effect. Bound receptors (D1 and D2) concentrations were added because they can be modified by dopamine agonists sometimes used in Parkinson's disease [**23**]. Hypersensitivity can also be induced in D2 receptors by denervation [**31**].

3. Results

The outputs of the model and its qualitative behavior were compared to available data. Parameters of the pharmacokinetic model were fit to patients data. Maximal levodopa concentration in the brain obtained with our model ($\sim 0.8\mu mol/L$ for $f = 0.3$) was close to the one measured in humans [**28**]. The values of dopamine concentration without medication are typically around $0.01 - 0.03\mu mol/L$ [**38**], in agreement with those obtained with our model. Qualitative behavior such as the loss of neurons capacity to buffer dopamine fluctuations with denervation [**32**] and the loss in levodopa duration's effect with denervation [**17, 30, 32**] were reproduced with the model.

Using the three parts of the model presented above, several simulations can be performed to highlight the nonlinear dynamics underlying Parkinson's disease and its treatment. In the following sections, some exemplary results are illustrated to uncover the different relations between levodopa dose, levodopa plasma concentrations, dopamine concentrations and motor response.

3.1. Nonlinear dynamics of plasma concentrations, dopamine concentrations and motor task

For a given dose, levodopa response exhibits nonlinear dynamics with the progression of neuronal loss. To elucidate these dynamics, brain dopamine concentrations and finger tapping frequencies are investigated as a function of levodopa plasma concentrations. Since, after dose administration, levodopa plasma concentration changes in time, the curves in Figures 22 and 23 are dynamical, they represent temporal trajectories, the direction of which is given by the colored arrows.

For the sake of clarity, dopamine dynamics with levodopa intake was divided into two different conditions, reflecting different Parkinson's disease severity. The mild condition (early stage) is represented in Figure 22 (b) and the severe condition (late stage) in Figure 22 (c). In pharmacokinetics and pharmacodynamics studies the loop curve like the ones in Figure 22 are called hysteresis. These hysteresis curves, which reflect all the processes

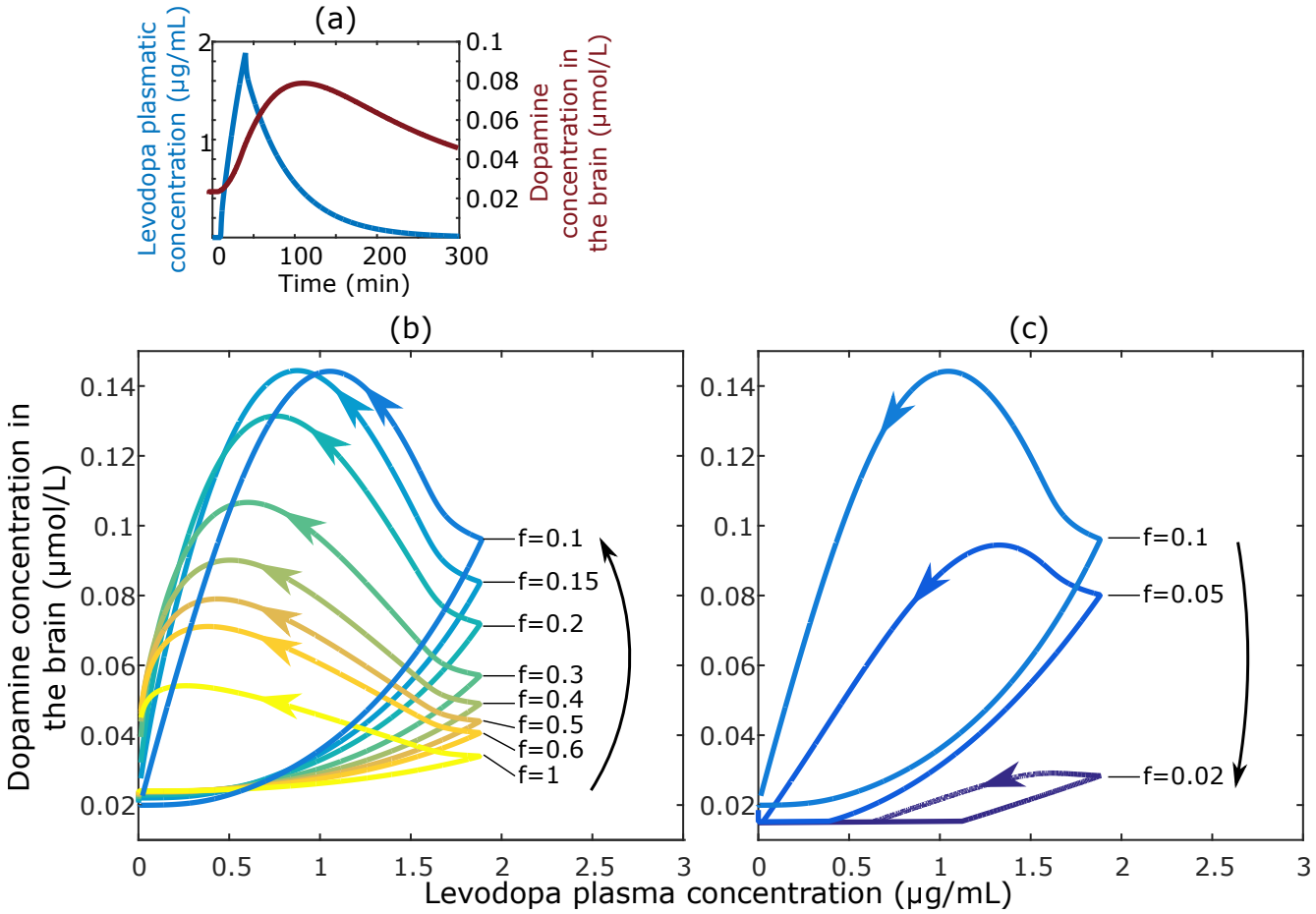

Figure 22. (a) Levodopa plasma concentration in time and its related dopamine concentration in the brain for $f = 0.5$. Dopamine concentrations in the brain as a function of levodopa plasma concentrations for different degrees of denervation in early (b) and late (c) stages of the disease for a single levodopa dose of 100 mg. The values of the parameters used can be found in the Appendix, except for the value of the fraction f, indicated directly in the figure.

associated with dopamine storage and on demand release by dopamine neurons, suggest the presence of a delay between plasma and brain concentrations. Indeed, peak plasma and brain concentration do not coincide. An example of this delay is shown in Figure 22(a) for a fraction $f = 0.5$. With denervation, this delay shortens due to the loss of buffering capacity of the dopaminergic neurons. This is shown by the rightward shift of dopamine peak concentration in Figure 22(b)(c). The peak of brain dopamine concentration is observed for higher concentration of plasma levodopa, the peaks are getting closer so the delay is decreasing. Also, in a healthy (normal) situation, brain dopamine levels continue to increase even during the decline of levodopa plasma concentration. This will be lost with denervation.

The hysteresis loops appearing in Figure 22 (b) and (c) are a consequence of the dynamics in equations 2.1 to 2.6. As the disease progresses, this dynamics change in a complex way due to the change in f. In the mild condition ($f = 1 \longrightarrow 0.1$), maximal dopamine brain concentrations increases with denervation. This is due to compensation mechanisms, such as a reduction in recapture by DATs and a quicker release from levodopa. The dopamine concentration rises more rapidly as seen by the increase in the steepness of the curve with the progression of the disease, Figure 22(b).

In the severe phase ($f = 0.1 \longrightarrow 0$), Figure 22 (c), the loss of neurons is too significant for compensation mechanisms to be effective. This results in a reduction of the delay and in the variation between maximal and minimal dopamine concentrations. The value of dopamine brain concentration when plasma levodopa concentration is zero (that is the basal brain dopamine level) also decreases with denervation.

From a clinical point of view, it is interesting to study the effect of these nonlinear dynamics on the response to a motor task. The model was used here to simulate finger tapping frequency during a few hours after levodopa administration, in order to inform the effect of levodopa in alleviating bradykinesia. As shown in Figure 23(b) and (c), a pharmacokinetic-pharmacodynamic hysteresis is observed at the beginning of the disease with values of f close to 1. The black arrows represent the trend direction of the change of curves as the disease progresses. The curves are again dynamical and their direction is given by the colored arrows. For values of f close to one, the tappping frequency remains high even with variation in levodopa plasmatic concentration. For low values of f, the peak level of levodopa does not produce enough brain dopamine and the tapping frequency drops. For a tapping frequency below approximately 55 taps/min the model stops to reach the threshold to activate the action, and there is almost no movement. Examples of temporal profiles of tapping frequency are shown in Figure 23(a). In early state of disease ($f = 1 \longrightarrow 0.1$), finger tapping remains high for a long period, even when levodopa plasma concentration is returning close to zero as seen in Figure 23(b). Conversely, in late state of disease ($f = 0.1 \longrightarrow 0$),

finger tapping first increases, then exhibits a dramatic fall, meaning that the efficacy of levodopa is rapidly wearing off as seen in Figure 23(c).

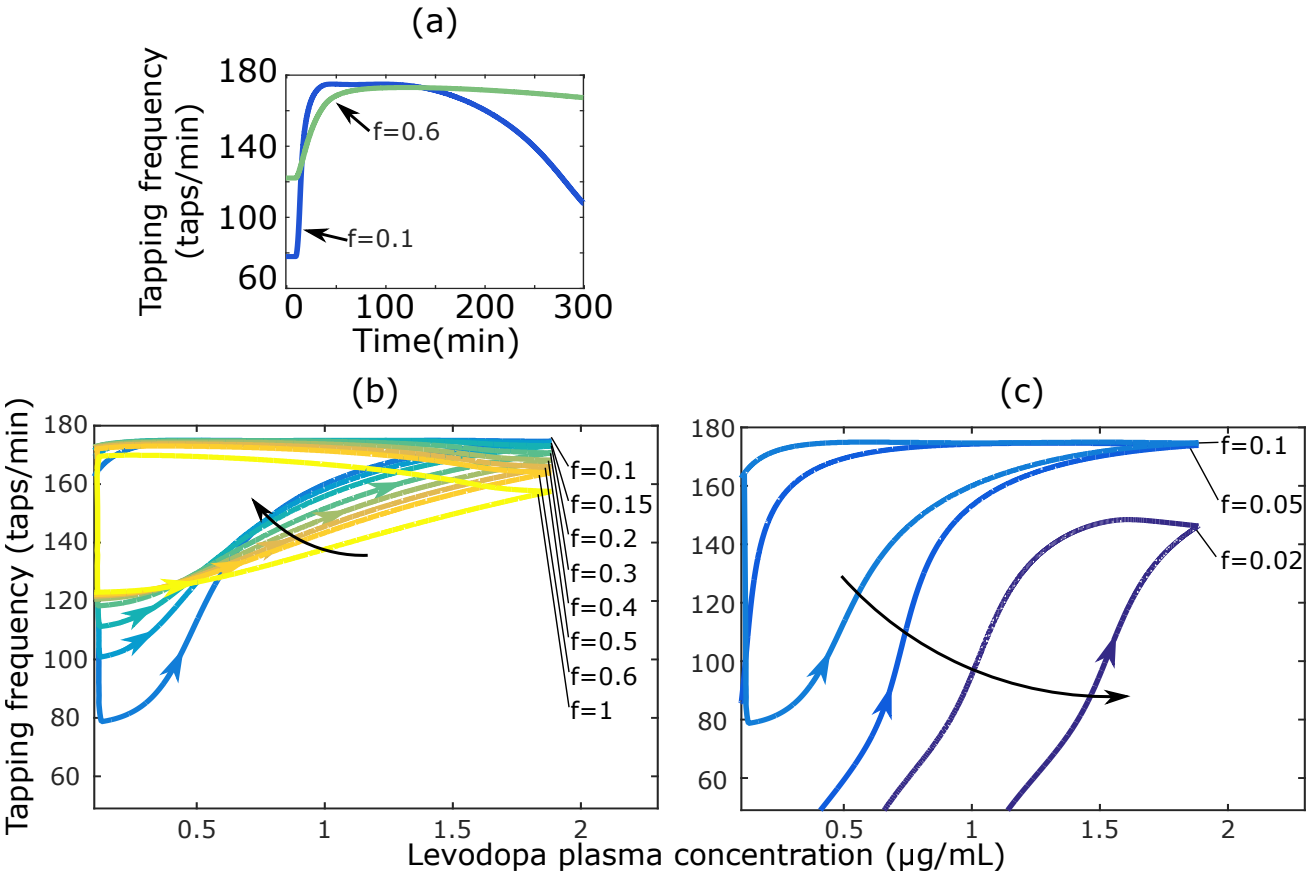

Figure 23. (a) Example of temporal pattern of finger tapping in time for $f = 0.10$ and $f = 0.6$ (b) Tapping frequency as a function of levodopa plasma concentration for different degrees of denervation in early (b) and late (c) stages of the disease for a single levodopa dose of 100 mg. The values of the parameters used can be found in the Appendix, except for the value of the fraction f, indicated directly in the figure.

This pharmacokinetic-pharmacodynamic hysteresis underlies the presence of a delay in the effect. It indicates the persistance of the effect once the systemic concentration of levodopa is waned. The presence of such an hysteresis was previously reported in humans [**2, 11, 14**]. The upward shift shows that the peak tapping frequency is observed for higher concentration of plasma levodopa with disease progression. For mild cases, an increase in levodopa effect is observed, which is in line with the literature [**9, 21, 29**]. For the most severe cases, the curve collapses and a subsequent motor impairment occurs. As disease progresses and f decreases, the curve flattens out. This suggests that the delay is reduced.

This shortening of delay with disease progression is a well documented effect of levodopa [**17, 30, 32**]. It is thought to be caused by the loss of buffering effect of dopaminergic neurons. When $f \approx 0.02$, the tapping frequency is drastically reduced. The quantity of remaining neurons is too small for compensation mechanisms to be possible.

3.2. Nonlinear relations in doses and therapeutic index

Levodopa is very effective in the early stages of the disease. However, as the disease progresses, shortening of its effect duration and wearing off periods make dosing difficult. A standard approach is to increase the dose of levodopa and its frequency [**6**]. Unfortunately, these adjustments can lead to motor complications attributed to the nonlinear dynamics governing denervation.

Using the model with different levels of denervation, the maximal dopamine concentrations in the brain as a function of levodopa dose are shown in Figure 24. Again, the black arrows represent the direction of the curves as the disease progresses. The maximal dopamine concentrations shown in Figure 24 occur at different moments for the different doses and fraction f.

In the healthy brain ($f = 1$), a slight increase in maximal concentration is seen with increasing dose. The increase is almost linear. As the disease progresses ($f = 1 \longrightarrow 0.2$), the maximal concentration increases significantly as the dose is escalated. The increase becomes almost exponential, Figure 24 (a). Indeed, dopamine release is decreased with denervation but so its recapture by DATs. This compensatory mechanisms leads to higher maximal dopamine concentrations until denervation is too high (late stages of disease). At this stage ($f < 0.2$), as shown in Figure 24 (b), compensation is no longer possible and the maximal concentration drops. The increase in maximum concentration with dose goes back to being linear. This suggest the impossibility to restore dopamine concentrations even with increasing doses when denervation is too advanced.

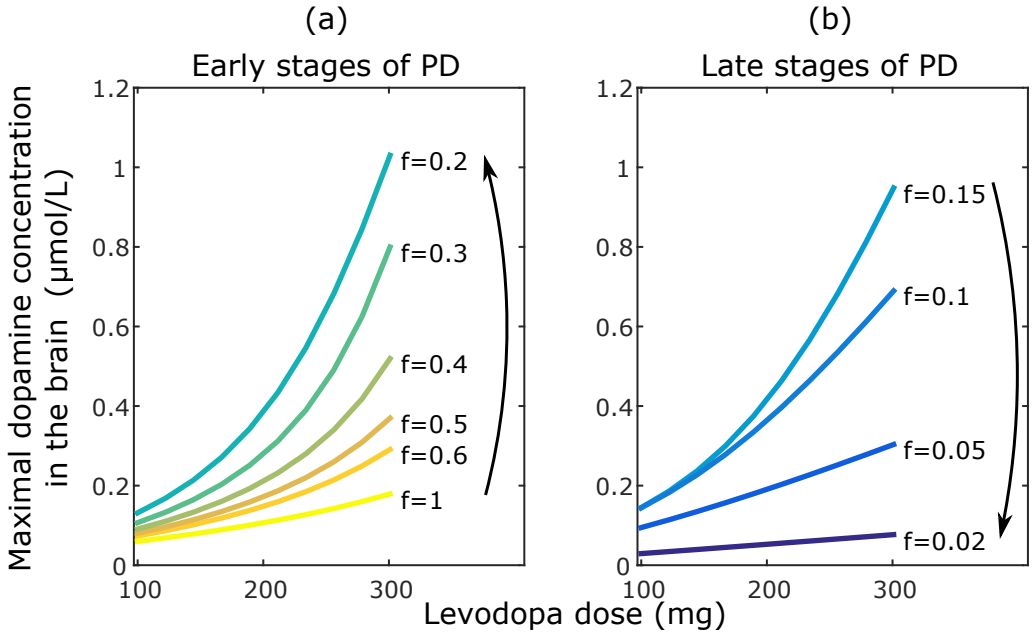

Figure 24. Maximal dopamine concentration in the brain as a function of levodopa dose for different fraction of neurons alive. The values of the parameters used can be found in the Appendix, except for the value of the fraction f, indicated directly in the figure.

At advanced stages of denervation, high doses of levodopa are required to restore dopamine concentrations, creating high dopamine peak which may lead to involuntary movements called dyskinesias. As a result, it becomes difficult to treat the patient by properly preventing bradykinesia and avoiding dyskinesias. This difficulty in treating patients is reflected in the narrowing of levodopa therapeutic index. We studied the narrowing of therapeutic index through the maximal dopamine concentration in the brain, and the mean dopamine concentration computed during ten hours after dose administration. High maximal concentrations can be associated with dyskinesias and motor fluctuations. Low mean levels signify insufficient capacity to prevent bradykinesia for a long period. Accordingly, in Figure 25, a therapeutic index was fixed in terms of dopamine concentration. The exact index is not known but is illustrated through an example. As disease progresses, we can see that high doses (> 200 mg) give rise to concentrations that are no longer in the therapeutic window, causing excessive peaks which could induce dyskinesias. At high denervation ($f < 0.1$) however, a lower dose (100 mg or even 200 mg) produces a low mean dopamine

level and could be insufficient to prevent bradykinesia. Information in Figure 25 and Figure 26 are complementary.

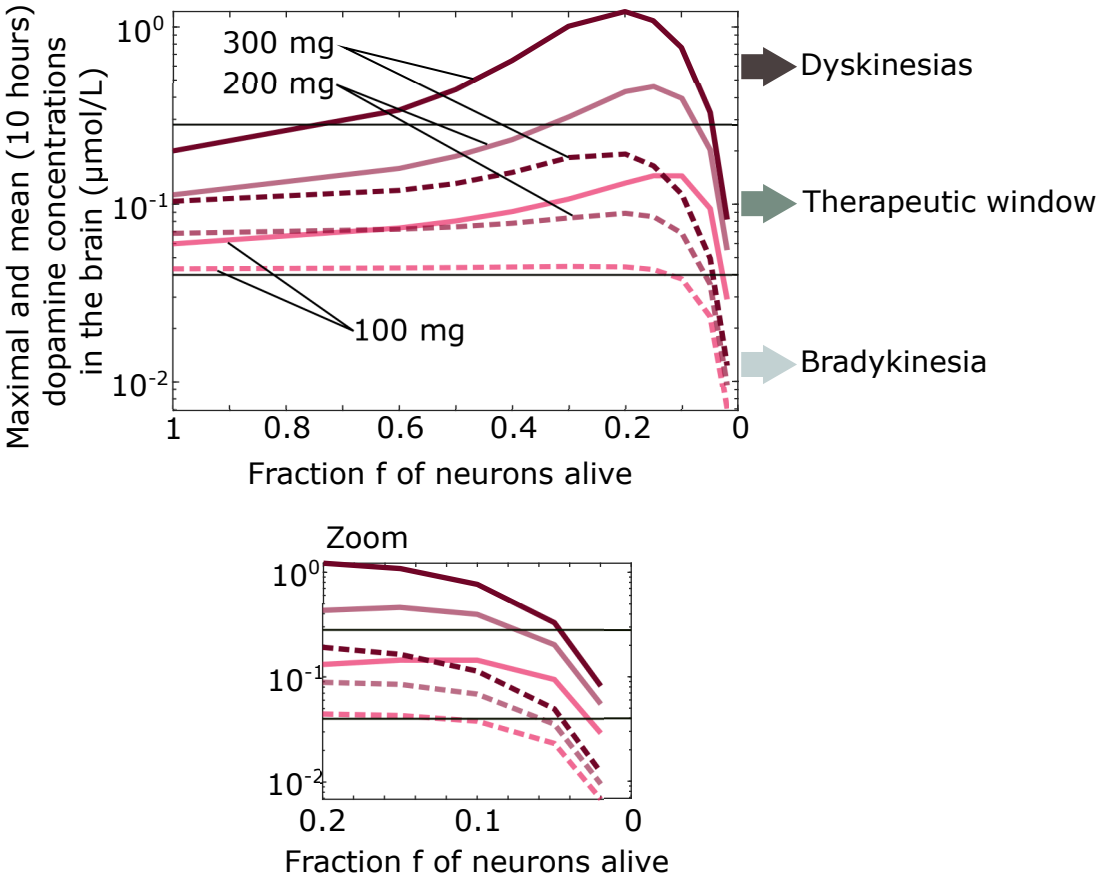

Figure 25. Maximal (solid line) and mean for 10 hours (dashed line) concentrations as a function of fraction f for 3 different doses, 100m mg, 200 mg and 300 mg (shades of pink).

Figure 26 illustrates the percentage of time spent in the therapeutic window for a single 100 mg dose of levodopa for different f values. Concentrations leading to a tapping frequency of over 122 taps/min were defined to be in the therapeutic window. Many scales are used to assess the degree of severity of Parkinson's disease. The most common is the the Unified Parkinson's Disease Rating Scale (UPDRS), which is divided into different parts that are individually scored (symptom scale system). Its different parts are evaluated by interviews and clinical observations. The third part (UPDRS3) is used to assess motor function, with the score 0 being attributed to a healthy patient. In order to present the results in a clinically relevant way and to highlight its relation with the therapeutic window, UPDRS3 score is

represented in Figure 26 by different shades of blue. We used a previously published linear regression of UPDRS3 score with denervation [**19**] to estimate the scores.

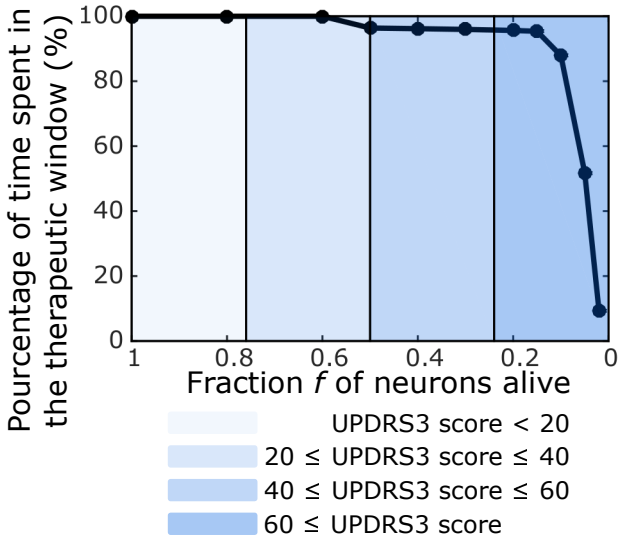

Figure 26. Percentage of time spent in the therapeutic window as a function of the fraction of neurons alive and its relation to UPDRS3 score for a levodopa dose of 100 mg. The values of the parameters used can be found in the Appendix.

Parkinson's symptoms do not appear until 60% to 90% of dopaminergic neurons are lost [**1, 41**] ($f = 0.4 - 0.1$). This explains the sudden fall in the time spent in the therapeutic window when $f = 0.2 \longrightarrow 0$. For values of f lower than 0.2, the percentage decreases in a nonlinear manner.

4. Discussion

Understanding the nonlinear dynamics that underly Parkinson's disease therapy is critical to optimize the current treatment, to fit individualized needs and to find information about alternative therapies. To this aim, we developed a mechanistic model integrating altogether levodopa pharmacokinetics, dopamine dynamics and basal ganglia neurotransmission. The impact of neuronal degeneration was included throughout the model in order to mimic the progression of Parkinson's disease. The response to the finger tapping task was included for different levels of denervation in relation to bradykinesia. The link between dopamine brain

concentration and tapping frequency with levodopa plasma concentrations was investigated. We were able to highlight the influence of the compensation mechanisms on levodopa's duration and delay in effect as denervation progresses. In particular, we were able to show two important phenomena, both of clinical relevance. At high levels of denervation, therapeutic doses of levodopa may have no-effect, or their effect may vanish quite rapidly within a few hours, leading to the well-known wear off phenomena often observed in severe parkinsonian patients. Conversely, larger doses of levodopa may produce high transient peaks in brain dopamine concentration, which may be associated with dyskinesias. These two aspects explain the nonlinear decrease in therapeutic index, highlighting how the therapeutic effect may be proximal to side effects as the disease progresses.

This work combines in a mechanistic way three dynamical models. It provides a broader description of Parkinson's disease and its therapy, while keeping a good balance between simplicity and accuracy. The model can be useful to monitor levodopa treatment on a scale of hours or to look at the impact of denervation on a yearly level.

In addition, this model has the advantage of reproducing the response to a motor task, making it clinically meaningful.

However, accurately monitoring symptoms in Parkinson's patients remains a challenge on a day-to-day basis. In the recent years, mobile Health services based on continuous monitoring sensors of patients movements were developed. Our model could be fitted to data collected with these devices, to estimate individual paramaters and health conditions that can inform the dosing adaptation. Indeed, with the progression of the disease and the apperance of side effects, individualization of the therapy is recommended. A proof of concept has just been released in the work of Thomas and al. [**40**], where a dosing adjustment algorithm has been proposed to tailor levodopa therapy to individual needs using sensor based information. For the present model to be used in tailoring dosing schedules, individual rating measured by wearable sensors would be required to estimate the physiological and pharmacokinetic parameters of the model. These parameter values can then serve in the

process of individualized drug regimen optimization. Moreover, a sensitivity analysis can help identify the mechanisms that primarly drive the sudden waning in levodopa's effect.

In conclusion, important nonlinearities were highlighted with the integrative model of levodopa, dopamine and basal ganglia dynamics developed here, which additionally accounts for Parkinson's disease progression. This system pharmacology approach is a promising step towards optimization of levodopa therapy, clinical trial designs and translation of the finding into a mobile health decision tool.

Availability of data

The data that supports the findings of this study are available within the article.

Acknowledgements

F.V.-V. received a scholarship from the Natural Sciences and Engineering Research Council (NSERC), Canada through the PGS-D program. Support was also provided by NSERC -Industrial Chair in Pharmacometrics funded by Novartis, Pfizer and Syneos, as well as FRQNT Projet d'équipe (F.N.).

Author Contributions

This work makes up a portion of the doctoral thesis of FVV. Construction of the model: FVV MU PR DL FN. Numerical simulations: FVV. Writing of the paper: FVV MU PR DL FN.

References

[1] Y Agid : Parkinson's disease: pathophysiology. *Lancet (London, England)*, 337:1321–1324, juin 1991.

[2] Horst Baas, Frank Zehrden, Roland Selzer, Ralf Kohnen, Joern Loetsch et Sebastian Harder : Pharmacokinetic-pharmacodynamic relationship of levodopa with and without tolcapone in patients with parkinson's disease. *Clinical Pharmacokinetics*, 40(5):383–393, May 2001.

[3] Chiara Baston, Manuela Contin, Giovanna Calandra Buonaura, Pietro Cortelli et Mauro Ursino : A mathematical model of levodopa medication effect on basal ganglia in parkinson's disease: An application to the alternate finger tapping task. *Frontiers in Human Neuroscience*, 10, jun 2016.

[4] Janet A Best, H Frederik Nijhout et Michael C Reed : Homeostatic mechanisms in dopamine synthesis and release: a mathematical model. *Theoretical Biology and Medical Modelling*, 6(1), sep 2009.

[5] Kevin J Black, Haley K Acevedo et Jonathan M Koller : Dopamine buffering capacity imaging: A pharmacodynamic fmri method for staging parkinson disease. *Frontiers in neurology*, 11:370, 2020.

[6] David J Brooks : Optimizing levodopa therapy for parkinson's disease with levodopa/carbidopa/entacapone: implications from a clinical and patient perspective. *Neuropsychiatric disease and treatment*, 4:39–47, février 2008.

[7] Roger Cachope et Joseph F Cheer : Local control of striatal dopamine release. *Frontiers in behavioral neuroscience*, 8:188, 2014.

[8] Phylinda L S Chan, John G Nutt et Nicholas H G Holford : Modeling the short- and long-duration responses to exogenous levodopa and to endogenous levodopa production in parkinson's disease. *Journal of pharmacokinetics and pharmacodynamics*, 31:243–268, juin 2004.

[9] Phylinda L S Chan, John G Nutt et Nicholas H G Holford : Pharmacokinetic and pharmacodynamic changes during the first four years of levodopa treatment in parkinson's disease. *Journal of pharmacokinetics and pharmacodynamics*, 32:459–484, août 2005.

[10] M Contin, R Riva, P Martinelli, F Albani, P Avoni et A Baruzzi : Levodopa therapy monitoring in patients with parkinson disease: a kinetic-dynamic approach. *Therapeutic drug monitoring*, 23:621–629, décembre 2001.

[11] M. Contin, R. Riva, P. Martinelli, P. Cortelli, F. Albani et A. Baruzzi : A levodopa kinetic-dynamic study of the rate of progression in parkinson's disease. *Neurology*, 51(4):1075–1080, 1998.

[12] Manuela Contin, Paolo Martinelli, Roberto Riva, Maurizio Dondi, Stefano Fanti, Cinzia Pettinato, Cesa Scaglione, Fiorenzo Albani et Agostino Baruzzi : Assessing dopaminergic function in parkinson's disease: levodopa kinetic-dynamic modeling and spect. *Journal of neurology*, 250:1475–1481, décembre 2003.

[13] Vassilis Cutsuridis et Stavros Perantonis : A neural network model of parkinson's disease bradykinesia. *Neural networks : the official journal of the International Neural Network Society*, 19:354–374, mai 2006.

[14] Dirk Deleu, Margaret G. Northway et Yolande Hanssens : Clinical pharmacokinetic and pharmacodynamic properties of drugs used in the treatment of parkinson's disease. *Clinical Pharmacokinetics*, 41(4):261–309, Apr 2002.

[15] M Dietz, S Harder, J Graff, G Künig, P Vontobel, K L Leenders et H Baas : Levodopa pharmacokinetic-pharmacodynamic modeling and 6-[18f]levodopa positron emission tomography in patients with parkinson's disease. *Clinical pharmacology and therapeutics*, 70:33–41, juillet 2001.

[16] J. K. Dreyer : Three mechanisms by which striatal denervation causes breakdown of dopamine signaling. *Journal of Neuroscience*, 34(37):12444–12456, sep 2014.

[17] G Fabbrini, J Juncos, M M Mouradian, C Serrati et T N Chase : Levodopa pharmacokinetic mechanisms and motor fluctuations in parkinson's disease. *Annals of neurology*, 21:370–376, avril 1987.

[18] G Gangadhar, D Joseph, A V Srinivasan, D Subramanian, R G Shivakeshavan, N Shobana et V S Chakravarthy : A computational model of parkinsonian handwriting that highlights the role of the indirect pathway in the basal ganglia. *Human movement science*, 28:602–618, octobre 2009.

[19] Sandrine Greffard, Marc Verny, Anne-Marie Bonnet, Jean-Yves Beinis, Claude Gallinari, Sylvie Meaume, François Piette, Jean-Jacques Hauw et Charles Duyckaerts : Motor score of the unified parkinson disease rating scale as a good predictor of lewy body associated neuronal loss in the substantia nigra. *Archives of Neurology*, 63(4):584, apr 2006.

[20] Mohammad Haeri, Yashar Sarbaz et Shahriar Gharibzadeh : Modeling the parkinson's tremor and its treatments. *Journal of Theoretical Biology*, 236(3):311–322, oct 2005.

[21] S Harder et H Baas : Concentration-response relationship of levodopa in patients at different stages of parkinson's disease. *Clinical pharmacology and therapeutics*, 64:183–191, août 1998.

[22] Bertil Hille : G protein-coupled mechanisms and nervous signaling. *Neuron*, 9(2):187–195, aug 1992.

[23] Shin Hisahara et Shun Shimohama : Dopamine receptors and parkinson's disease. *International Journal of Medicinal Chemistry*, 2011:1–16, 2011.

[24] Nick Holford et John G Nutt : Disease progression, drug action and parkinson's disease: why time cannot be ignored. *European journal of clinical pharmacology*, 64:207–216, février 2008.

[25] Lucas A Koelman et Madeleine M Lowery : Beta-band resonance and intrinsic oscillations in a biophysically detailed model of the subthalamic nucleus-globus pallidus network. *Frontiers in computational neuroscience*, 13:77, 2019.

[26] Chen Liu, Changsong Zhou, Jiang Wang, Chris Fietkiewicz et Kenneth A Loparo : The role of coupling connections in a model of the cortico-basal ganglia-thalamocortical neural loop for the

generation of beta oscillations. *Neural networks : the official journal of the International Neural Network Society*, 123:381–392, décembre 2019.

[27] Jonathan W Mink : The basal ganglia: Focused selection and inhibition of competing motor programs. *Progress in Neurobiology*, 50(4):381 – 425, 1996.

[28] Maria Nord, Peter Zsigmond, Anita Kullman et Nil Dizdar : Levodopa pharmacokinetics in brain after both oral and intravenous levodopa in one patient with advanced parkinson's disease. *Advances in Parkinson's Disease*, 06(02):52–66, 2017.

[29] J G Nutt, W R Woodward, J H Carter et S T Gancher : Effect of long-term therapy on the pharmacodynamics of levodopa. relation to on-off phenomenon. *Archives of neurology*, 49:1123–1130, novembre 1992.

[30] W Olanow, A H Schapira et O Rascol : Continuous dopamine-receptor stimulation in early parkinson's disease. *Trends in neurosciences*, 23:S117–S126, octobre 2000.

[31] B. Picconi, D. Centonze, S. Rossi, G. Bernardi et P. Calabresi : Therapeutic doses of l-dopa reverse hypersensitivity of corticostriatal d2-dopamine receptors and glutamatergic overactivity in experimental parkinsonism. *Brain*, 127(7):1661–1669, may 2004.

[32] Werner Poewe, Angelo Antonini, Jan Cm Zijlmans, Pierre R Burkhard et François Vingerhoets : Levodopa in the treatment of parkinson's disease: an old drug still going strong. *Clinical interventions in aging*, 5:229–238, septembre 2010.

[33] Michael C. Reed, Janet Best et H. Frederik Nijhout : Passive and active stabilization of dopamine in the striatum. *Bioscience Hypotheses*, 2(4):240 – 244, 2009.

[34] Michael C Reed, H Frederik Nijhout et Janet A Best : Mathematical insights into the effects of levodopa. *Frontiers in integrative neuroscience*, 6:21, 2012.

[35] Jonathan E. Rubin et David Terman : High frequency stimulation of the subthalamic nucleus eliminates pathological thalamic rhythmicity in a computational model. *Journal of Computational Neuroscience*, 16(3):211–235, may 2004.

[36] Marina Senek, Dag Nyholm et Elisabet I Nielsen : Population pharmacokinetics of levodopa/carbidopa microtablets in healthy subjects and parkinson's disease patients. *European journal of clinical pharmacology*, 74:1299–1307, octobre 2018.

[37] Sushil Sharma, Carolyn Seungyoun Moon, Azza Khogali, Ali Haidous, Anthony Chabenne, Comfort Ojo, Miriana Jelebinkov, Yousef Kurdi et Manuchair Ebadi : Biomarkers in parkinson's disease (recent update). *Neurochemistry international*, 63:201–229, septembre 2013.

[38] David Sulzer, Stephanie J. Cragg et Margaret E. Rice : Striatal dopamine neurotransmission: Regulation of release and uptake. *Basal Ganglia*, 6(3):123–148, aug 2016.

[39] B R Thanvi et T C N Lo : Long term motor complications of levodopa: clinical features, mechanisms, and management strategies. *Postgraduate Medical Journal*, 80(946):452–458, 2004.

[40] Ilias Thomas, Moudud Alam, Filip Bergquist, Dongni Johansson, Mevludin Memedi, Dag Nyholm et Jerker Westin : Sensor-based algorithmic dosing suggestions for oral administration of levodopa/carbidopa microtablets for parkinson's disease: a first experience. *Journal of neurology*, 266:651–658, mars 2019.

[41] M J Zigmond, E D Abercrombie, T W Berger, A A Grace et E M Stricker : Compensations after lesions of central dopaminergic neurons: some clinical and basic implications. *Trends in neurosciences*, 13:290–296, juillet 1990.

Troisième chapitre.

A web application for individualized optimization of levodopa dosing regimens in Parkinson's disease

par

Florence Véronneau-Veilleux[1] et Fahima Nekka[2]

([1]) Faculté de Pharmacie, Université de Montréal, Montréal, Québec, Canada

([2]) Faculté de Pharmacie, Université de Montréal
Centre de recherches mathématiques, Université de Montréal,
Centre for Applied Mathematics in Bioscience and Medicine (CAMBAM), McGill University, Montréal, Québec, Canada

Cet article est en préparation.

Avec la progression de la maladie de Parkinson, l'index thérapeutique de la lévodopa se réduit, complexifiant ainsi la recherche de régimes posologiques adéquats pour chaque patient. Ainsi, au premier et deuxième chapitre de la présente thèse, un modèle intégratif de l'effet de la lévodopa sur le système dopaminergique des ganglions de la base a été développé et analysé dans la perspective d'être utilisé pour optimiser les régimes posologiques. L'objectif de ce troisième chapitre est donc de développer, en tant que preuve de concept, une application Web pour aider les cliniciens à identifier les régimes posologiques individualisés optimaux de la lévodopa. Dans cette application, les données de fréquence de tapotement des doigts du patient sont utilisées pour estimer la valeur de certains paramètres du modèle précédemment développé. Le modèle ainsi personnalisé peut ensuite être utilisé pour déterminer le régime optimal en minimisant trois critères : le temps pendant lequel la fréquence de tape du patient est inférieure à un seuil, la dose totale et la fréquence de dosage.

Abstract.

As Parkinson's disease progresses, the optimisation of its therapy, where levodopa is the most potent and prescribed drug, becomes increasingly difficult. The important loss of dopaminergic neurons that becomes prominent at advanced stages of the disease, gives rise to more rapid onset and shorter effect duration of levodopa. This challenge is amplified by the fact that almost the same dose that produces effect is also responsible for side effects. To address this challenging dosing regimen issue, we developed a Web-based application to assist clinicians in the determination of patient-specific optimal dosing regimen of levodopa. The use of such applications in clinical settings has been popularized over the last few years, largely driven by the development of sensors that can closely monitor Parkinson's disease symptoms. The data collected with these sensors can be used as input to the application to individualize patients' parameters. This is accomplished through a fitting procedure of a mechanistic mathematical model of Parkinson Disease that we previously developed. This model simulates the finger tapping frequency, as a measure of bradykinesia, in time for a specific dose of levodopa. Some parameters of the model are individualized by fitting finger tapping frequencies data. Then, the model is used to determine the optimal regimen by minimising three criteria: the time during which the patient's tapping frequency is below a desired minimum tapping frequency, the total dose, and the dosing frequency. A tab in the application is specifically dedicated to the simulations of different regimens by the clinician.
Keywords: Parkinson's disease, levodopa, optimization of regimens, mHealth, Web application

1. Introduction

Parkinson's disease is the second most common neurodegenerative disease after Alzheimer's [**7, 16**]. It is characterized by the degeneration of dopaminergic neurons in the basal ganglia, leading to various symptoms such as tremor at rest, postural disabilities, rigidity, and bradykinesia, the latter referring to the slowing of movements. At the moment, there is no available cure. However, alleviation of symptoms is possible by using levodopa, considered the gold standard treatment. Levodopa is in fact very effective at the beginning of the disease, a period referred to as the honeymoon, where a generic dosing schedule can be used. With the worsening of the disease, the duration of effect is reduced, necessitating

either increased doses or more frequent administrations. Side effects such as dyskinesias (involuntary movements), judged by some patients as more distressing than the disease symptoms themselves, can then appear when larger and more frequent doses become routine. Indeed, it was estimated that 45-50% [**1, 10**] of patients experience dyskinesias after five years of levodopa use. As disease progresses, the therapeutic index is reduced [**9**], which complicates further the determination of appropriate dosing regimen for clinicians [**12**]. These complications call for more informed individualization of dosing regimen along the disease progression.

The objective of the current work is thus to develop, as a proof of concept, a Web application to help clinicians in their daily practice in identifying patient-specific optimal dosing regimen. Our previously developed mechanistic model of levodopa's effect [**15**] is implemented in the application. Values of some parameters are first individualized through fitting to the patient's data, namely tapping frequencies after a dose intake of levodopa, and then the optimal dosing regimen for this patient can be found using an optimization algorithm. The motor task of tapping frequency was chosen because of its simplicity, non-invasiveness, and its high correlation with the subscore of bradykinesia in the Unified Parkinson's Disease Rating Scale (UPDRS) [**6, 11**], an international scale for Parkinson's disease.

The progress achieved over the past few years in wearable devices that can continuously monitor Parkinson's disease symptoms in patients medicated with levodopa has opened the possibility for the development of web and mobile tools for the optimization of therapy. For example, a recent paper by Daneault et al. [**4**] reported that accelerometer data of 28 parkinsonian patients were recorded using a GeneActiv wristwatch on the most affected side of patients, and a Pebble smartwatch on their least affected side, added to a smartphone at the patient's waist. The three devices were used to collect data at home while the patients continue performing their usual daily activities for two days. Moreover, the Shimmer3 sensor was used in [**13**] and [**12**] to measure accelerometer data at the pronation-supination task for both wrists. The data collected with such wearable devices can be used to individualize the parameters values of predictive models using fitting procedures. In [**12**], different parameters

of a PKPD model were fitted to accelerometer data. The individualized model was then used to optimize the dosing regimen of levodopa/carbidopa microtablets.

Using the mechanistic model of Parkinson and its therapy [**15, 14**], a similar approach was used here. Different model parameters related to the dopaminergic system of basal ganglia were individualized by fitting finger tapping frequency data. The model was then used to find the optimal regimen of levodopa intravenous infusion according to the minimization of three criteria: the time during which the patient's tapping frequency is below a desired minimum target value, the total dose, and the dosing frequency. This procedure was implemented in a Web application using Matlab software to provide a user-friendly interface to be used by clinicians.

The originality of our work lies in the use of a mechanistic model that includes parameters that can be individualized according to patients' needs. This proof-of-principle platform is generic enough to be expanded to the optimization of other treatments regimen (dopamine agonists...) and different routes of administration (oral, duodenal infusion, ...).

The different parts of the Web application are described in the Methods section. An example of the use of the Web application with data extracted from [**2**] is provided in the Results section.

2. Methods

In our previous work [**15, 14**], a mechanistic model of Parkinson's Disease and its medication was developed. This model was used to simulate the levodopa plasma concentration and effect curve for a given dose of levodopa at different stages of the disease. The model is divided into three parts: a pharmacokinetic model of levodopa to simulate the plasma concentration-time curve; a dopamine dynamics model to represent the dopamine concentration-time curve in the brain; and finally a neurocomputational model of basal ganglia for the neuronal activity in all subregions of basal ganglia. From the neuronal activity, the finger tapping frequency is deduced and used to evaluate levodopa's effect on bradykinesia. The different stages of disease are implemented in the model through a parameter

f representing the fraction of dopaminergic neurons alive in the basal ganglia, previously shown to be linearly related to UPDRS3 score [**5**]. UPDRS is an international measure used to quantify the progression of Parkinson's disease and the response to treatment. Its third component (UPDRS3) assesses the patient's motor function.

The current Web application was developed with MATLAB App designer.

2.1. Parameter fitting procedure

The Web App was developed to provide a patient-specific optimization of dosing regimen. To this end, some model parameters [**15**] must be individualized. The model represents the patient' motor data after levodopa intake. The input to this App is comprised of the levodopa intake dose and finger-tapping frequency recorded at different time points post dose. The model is fitted by finding the parameters values that minimize the distance between the simulated tapping frequency and the recorded data using the dosing information. The MATLAB function fminsearch was used for the fitting procedure. This function used the simplex algorithm. Around the initial estimate of the parameters, a simplexe is created by adding 5% to their value. Then the algorithm walks through the different "vertices" and chooses the one that optimises the most the objective function. Then from this vertex, a new simplex is created and the process is repeated until the difference in the value of the objective function between two iterations has reached the threshold. The fitted parameters of the model are: the fraction of neurons alive f, Q_{13} and CL_{e3} , representing respectively the inter-compartmental clearance and clearance of levodopa from the brain compartment and α, β, γ the dopamine weights for the different neurotransmission pathways, as shown in green in Figure 27.

In the clinical practice, the UPDRS score of the patient is entered as an input to the Web App. This score is used to estimate the initial value of f for the fitting procedure. Indeed, a linear relation was reported by Greffard et al between the UPDRS score and denervation [**5**] of patients. The denervation was estimated post mortem. The linear relation between denervation and UPDRS score with the parameters estimated with the data is the following:

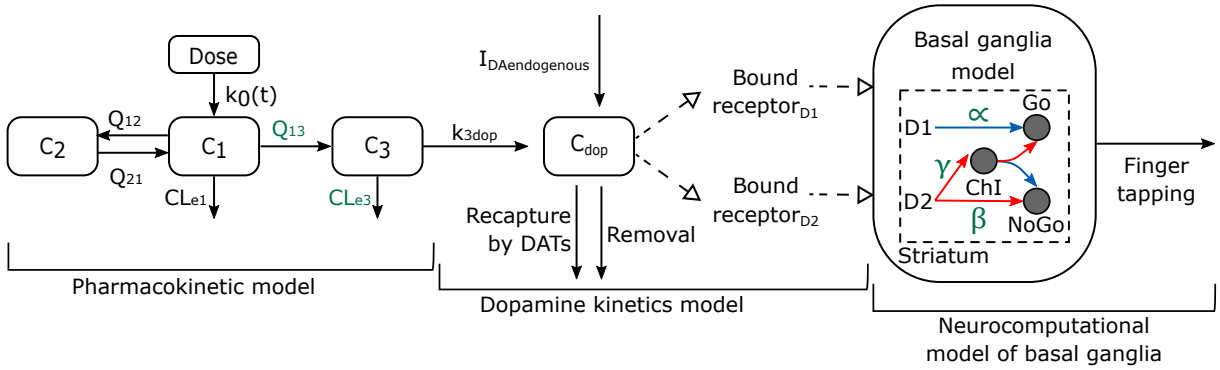

Figure 27. Model representation with its three parts, individualized parameters are in green

$$f_0 = \frac{updrs3 - 77.9}{-120}, \tag{2.1}$$

where f_0 is the initial estimate of f in the fitting procedure and UPDRS3 is the patient UPDRS-part III subscore. At the end of the fitting procedure, the model carries individualized parameters values and can thus be used to simulate different dosing regimens for each specific patient.

2.2. Regimen simulation

Let us give a typical example to illustrate the functioning of the App. In the regimen simulation page, the clinician must enter the desired minimal tapping frequency for the patient, as well as the levodopa dose for a period of 30 min infusion at 8am, 12h, 4pm and 8pm. These are the same times used in the optimization procedure described in the next section. With this dosing information, the previously individualized model is used to simulate the evolution of the tapping frequency with time. The tapping frequency and the minimal desired tapping frequency are shown in a Figure on this tab for visualization purposes. The time spent in the therapeutic window, defined as the time for which the tapping frequency is above the minimal desired tapping frequency previously entered by the clinician, the total daily dose and the frequency of dosing are given in the inserted table.

2.3. Optimization of regimen

The Web App also offers the possibility to optimize the dosing regimen for a specific patient (inverse problem compared to the above). In the current version of the app, used to illustrate its application, 30 minutes infusion of 0, 50 and 100mg given at 8am, 12h, 4pm and 8pm were considered. All possible regimens are simulated with the individualized model and the optimal regimen is then identified. To this end, the clinician needs to enter the desired minimum tapping frequency and the weights (w) of each of the involved criteria of the objective function (OF) defined as the following:

$$OF = w_1 \frac{TimeOFF}{24h} + w_2 \frac{TotalDose}{600mg} + w_3 \frac{DosingFrequency}{4}. \tag{2.2}$$

OF represents a score of the simulated regimen, which is the sum of the value to three criteria. The best regimen should have the lowest OF value possible. For a given regimen, the component Time OFF corresponds to the time during which the patient's tapping frequency is less than the desired minimum tapping frequency. Its division by 24h is meant to express the result in percentage. The Total Dose is the total daily dose that would be given to the patient; it is divided by 600 mg, which corresponds to the maximal recommended daily dose. Dosing frequency is the total number of daily doses and can be 4 at a maximum here. The minimization of the Time OFF is intended to maximize the time in which bradykinesia is decreased by levodopa. Minimization of the Total Dose and the Dosing frequency is used to minimize side effects. Each component of the objective function is multiplied by a weight, w_1, w_2 and w_3 which can be defined by the clinician according to his experience and to the patient's clinical concern. These weights represent the importance the clinician or patient wants to attribute to each criterion for optimization. For example, a patient more concerned about reducing the symptoms than the side effects could use $w_1 = 1, w_2 = 0, w_3 = 0$, so the optimization is performed only to reduce the time off. A similar vision involving weights in the regimen optimization involved in an objective function within an Web App was previously

used to individualize ADHD medication [**3**]. All possible dosing regimens are then tested to identify the one with the minimal value of objective function (OF).

3. Results

Data of finger tapping frequencies were extracted from [**2**]. They were used with the corresponding dosing information to showcase the applicability of the Web App. Four tabs are included in the App: Drug concentration, Fitting, Simulation of regimen and Optimisation. The first two tabs are mainly used to enter the patient's data and to fit the model's parameters. The other two are used to evaluate the performance of the dosing regimen either in a direct way through the choice of a specific regimen, or in an inverse way, by fixing the performance criteria and finding the corresponding optimal drug regimen.

In the following sections, a typical example will serve to illustrate the Web App functioning.

3.1. Patient's information and data

The Concentration tab of the App comprises three types of information that the clinician needs to enter: 1) the patient's UPDRS part III subscore, 2) the infusion time and 3) the dose received prior to the recording of finger tapping frequencies. Once this information is entered, the Plot concentrations button allows to simulate the pharmacokinetic curve. Parameters from [**2**] were used herein to simulate the plasma concentration in time. Alternatively, mean values taken from population pharmacokinetic models can be used to simulate the plasma concentration to prevent having to measure plasma concentration at the patient bedside.

Figure 28 shows the first tab of the App with the simulation of the patient's dosing information prior to data recording.

The tapping frequency data are entered in the Fitting tab, as shown in Figure 29. The clinician must enter the data himself in the current version of the App. Eventually, it would be possible to collect these data directly from sensors. Visualisation of the data (black dots) is possible using the Plot data button. The Fitting button allows to fit the model parameters

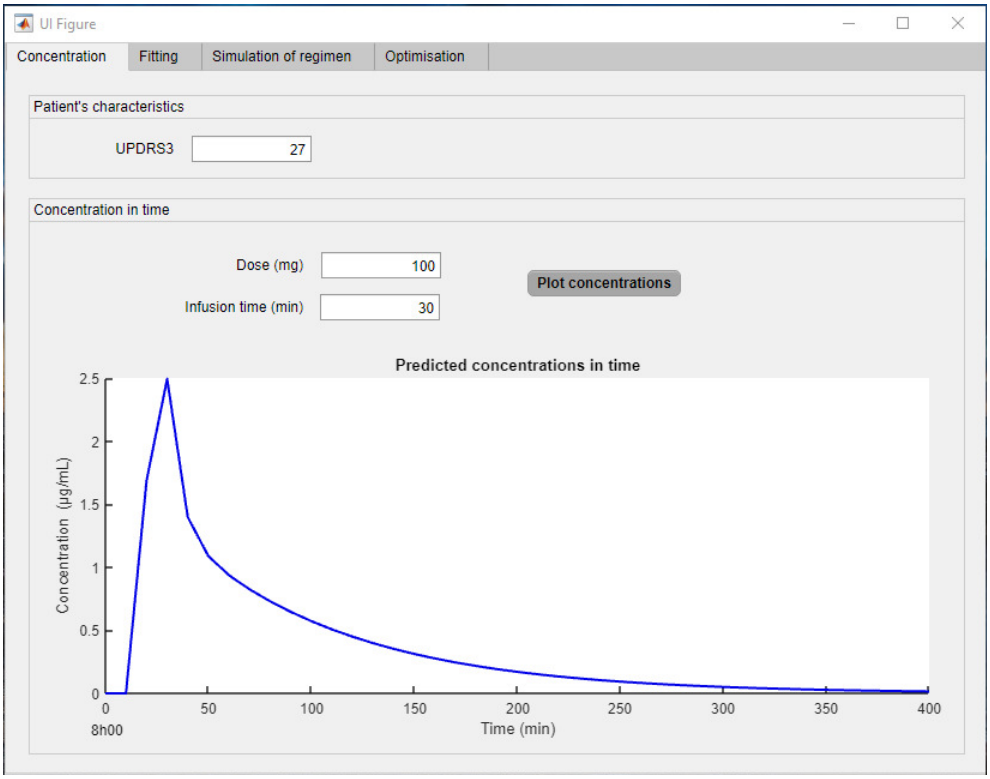

Figure 28. First tab of the Web application

as described in section 2.1. Once the fitting procedure is over, the estimated parameters are given in a table and the simulated finger tapping curve is plotted (blue line) to be compared with the patient's data.

3.2. Regime's simulation

The Simulation of regimen tab is shown in Figure 30. This part of the App is dedicated to the to assessment of the dosing regimen in a direct way, allowing the clinician to test a specific regimen and compute its different components.

As observed in Figure 30, five boxes are dedicated to input different information: the minimal desired tapping frequency along with the doses at 8am, noon, 4pm and 8 pm for the example considered here. The mechanistic model with the specified dosing regimen will be simulated by pressing the Simulate regimen button. The simulated finger tapping curve with the minimal desired tapping frequency will be generated in the figure. The time spent above the minimal desired frequency, the total daily dose and the dosing frequency will be

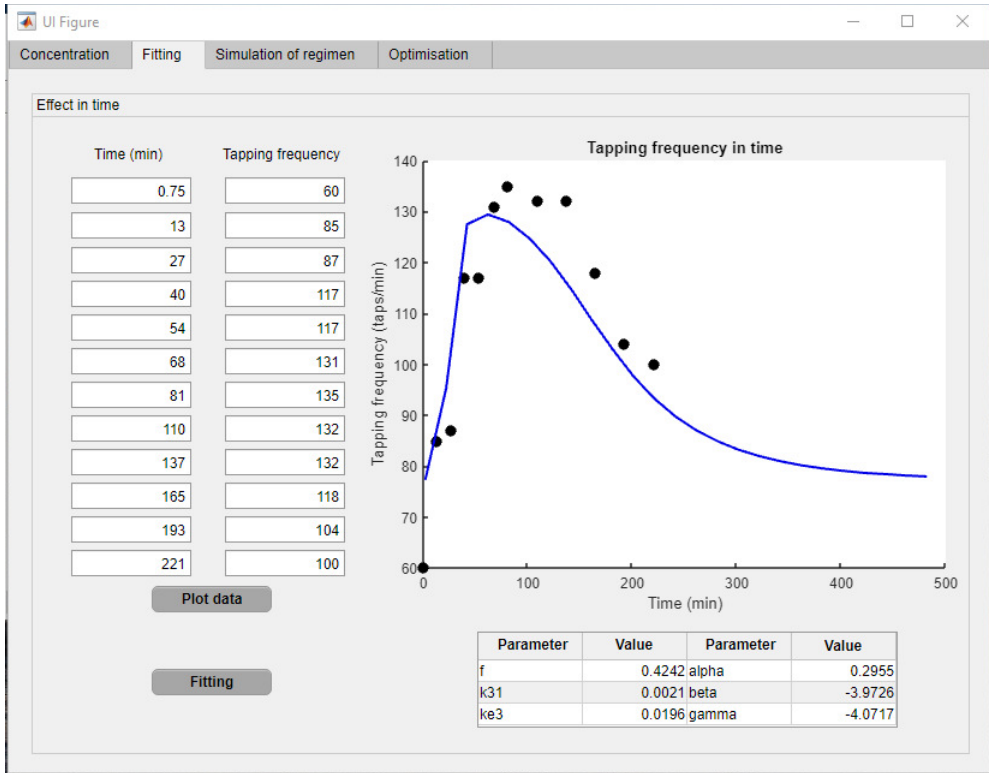

Figure 29. Second tab of the Web application

computed and displayed in the table. The clinician can therefore visualize the regimen and have the value of its different performance features.

3.3. Regimen's optimization

The Optimisation tab of the App is shown in Figure 31.

Here, the investigation of the drug regimen is performed in an indirect way, i.e. once the different information and criteria are entered, the algorithm is used to find the best regimen according to these criteria. To this end, all the considered dosing regimen are simulated and the one minimizing the objective function defined by equation 2.2 is selected as the optimal one. As previously mentioned, the doses considered for the current example of 30 minutes infusion are 0 mg (no dose), 50 mg and 100mg, with the corresponding dosing times of 8am, noon, 4 pm and 8 pm. The first input in this tab of the application is the minimal desired tapping frequency, used to compute the Time OFF in equation 2.2. The three other inputs are the weights w_1, w_2 and w_3, used in the objective function of equation

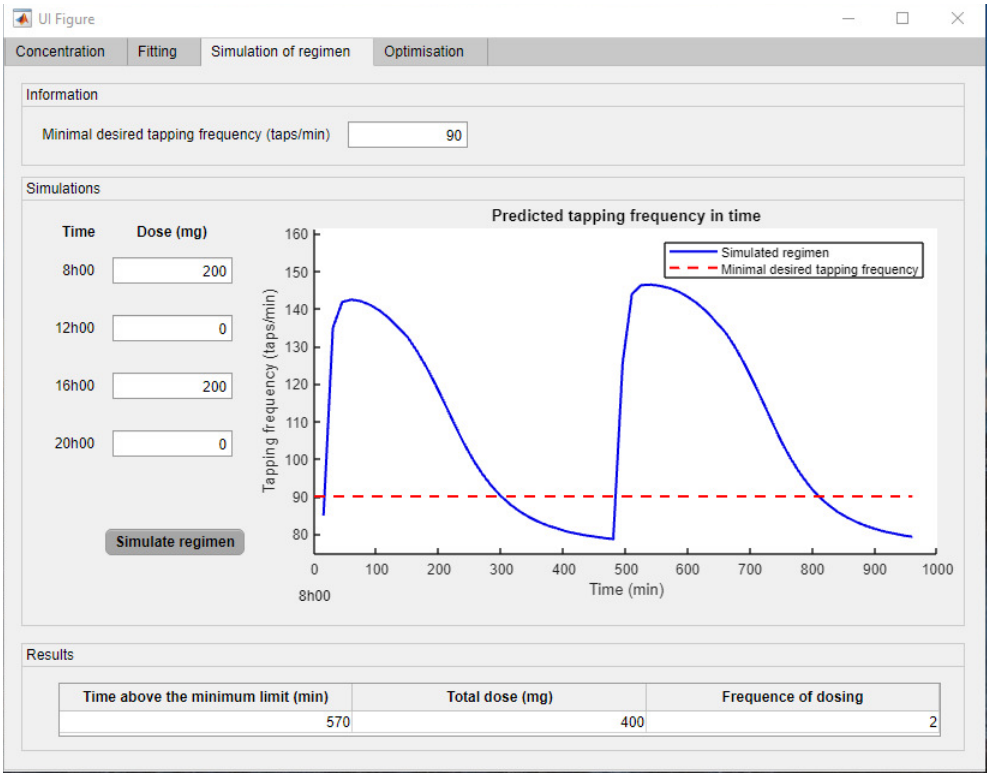

Figure 30. Third tab of the Web application

2.2. The clinician can choose the weights according to the importance he wishes to give to each of the three components: the Time OFF, the total daily dose and the dosing frequency. The optimization starts by pressing the Optimize regimen button. Once the optimization process is over, the optimal dose to be given at 8am, noon, 4pm and 9 pm are indicated in the table. The tapping frequency curve with the individualized parameters values and the optimized regimen is plotted in blue in the figure. The minimal desired tapping frequency is also plotted in dashed red. The clinician can therefore visualize the effect of the obtained optimal regimen.

4. Discussion

Levodopa, the gold-standard treatment to alleviate Parkinson's disease symptoms, is very effective at the onset of disease. Unfortunately, as disease progresses, the duration of its effect decreases, and the optimization of the regimen becomes difficult due to the appearance of side effects. The main objective of this work was therefore to develop, as a proof of concept,

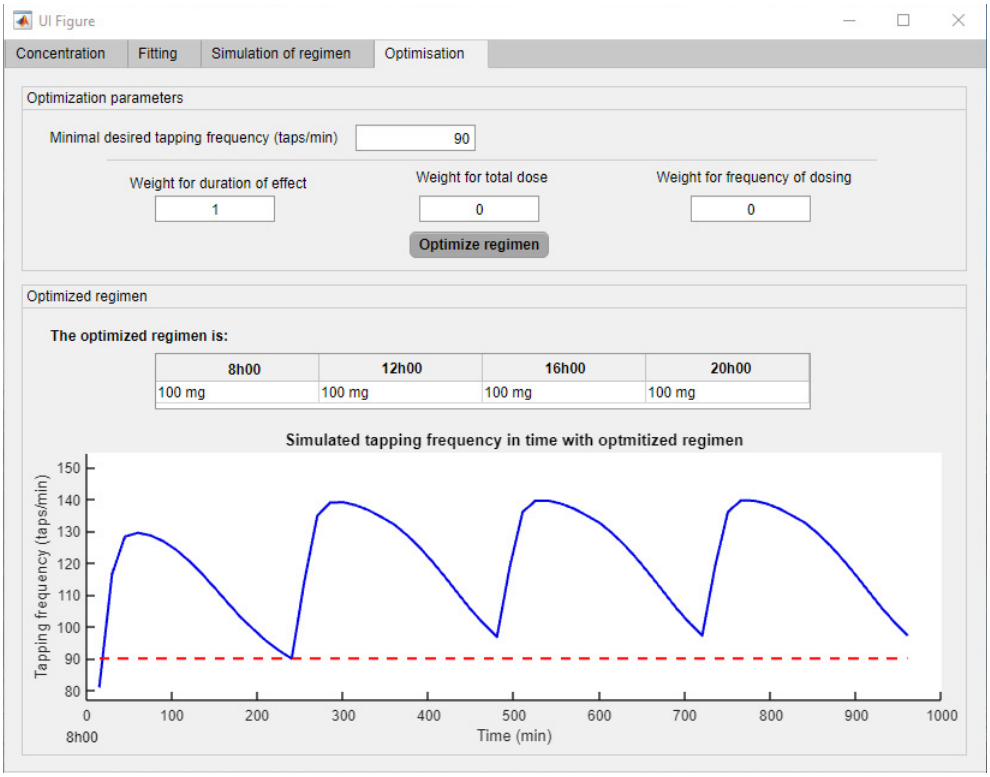

Figure 31. Fourth tab of the Web application

a Web Application that could, in the future, assist clinicians in their search for an optimal and individualized levodopa dosing regimen. This App was developed in MATLAB and based on a mechanistic model previously developed by our team [**15**]. Prior to the use of the App, the finger tapping frequency of the patient at a specific dose of levodopa needs to be recorded. This can be obtained through the use of sensors [**8**]. The first tab of the App interface then simulates plasma concentration curve for the dose given at the moment of the tapping frequencies recording. In the second tab, the frequency data are entered, and model's parameters are fitted to obtain patient's personalized values. The clinician can simulate and visualize different dosing regimens in the third tab and obtain the time above a minimal desired tapping frequency, the total daily dose, and the frequency of dosing. Finally, using the last tab, all possible dosing regimens of 0, 50 or 100 mg given at either 8am, noon, 4pm and 8pm are simulated to determine the optimal one. This regimen is obtained by minimizing an objective function that is the weighted sum of the time under the minimal desired tapping frequency, the total dose, and the dosing frequency.

In a recent work [**12**], an algorithm was developed to optimize the dosing of levodopa microtablets. An empiric pharmacokinetic-pharmacodynamic Emax model was used to fit data obtained from the Parkinson's KinetiGraph™ (PKG) and to be transposed in a treatment response scale (TRS). Our work here differs by its mechanistic modeling approach involved in the dopamine as well as in the neurocomputational submodels. To optimize different route of administration of levodopa, only modification of the pharmacokinetic part of the whole model could be here modified.

This Web app harnesses tapping frequencies data to personalize the model in a non-invasive and simple way for the patients. The data could even be recorded by the patient at home. The use of a mechanistic model in the App would allow to optimize levodopa regimens for different administration routes (oral, duodenal infusion, ...) and with its evolution with denervation. The Web app not only performs an optimization of regimen but also allows the clinician to simulate the regimens to be evaluated, adding further flexibility. Some limitations do however exist. The parameters included in the model/App that have to be estimated with the data were chosen based on our general knowledge of the model. A more thorough sensitivity analysis should be performed to identify the more sensitive parameters in order to improve model individualization. Moreover, this first version of the App only considers three doses given four times a day. More possibilities can be added to allow a wider exploration of the optimization process. More sophisticated optimization algorithms can also be used to accelerate the simulation exercise. Finally, the Web app needs to be approved in clinical settings before its use with patients.

Nevertheless, this application is a first proof of concept of the use of a mechanistic model for personalized optimization of levodopa dosing regimens and is a promising step towards improved management of Parkinson's disease symptoms with pharmacotherapy.

Author Contributions

This work makes up a portion of the doctoral thesis of FVV. Construction of the application: FVV FN. Numerical simulations: FVV. Writing of the paper: FVV FN.

References

[1] J E Ahlskog et M D Muenter : Frequency of levodopa-related dyskinesias and motor fluctuations as estimated from the cumulative literature. *Movement disorders : official journal of the Movement Disorder Society*, 16:448–458, mai 2001.

[2] Chiara Baston, Manuela Contin, Giovanna Calandra Buonaura, Pietro Cortelli et Mauro Ursino : A mathematical model of levodopa medication effect on basal ganglia in parkinson's disease: An application to the alternate finger tapping task. *Frontiers in human neuroscience*, 10:280, 2016.

[3] Guillaume Bonnefois, Philippe Robaey, Olivier Barrière, Jun Li et Fahima Nekka : An evaluation approach for the performance of dosing regimens in attention-deficit/hyperactivity disorder treatment. *Journal of child and adolescent psychopharmacology*, 27:320–331, mai 2017.

[4] Jean-Francois Daneault, Gloria Vergara-Diaz, Federico Parisi, Chen Admati, Christina Alfonso, Matilde Bertoli, Edoardo Bonizzoni, Gabriela Ferreira Carvalho, Gianluca Costante, Eric Eduardo Fabara, Naama Fixler, Fatemah Noushin Golabchi, John Growdon, Stefano Sapienza, Phil Snyder, Shahar Shpigelman, Lewis Sudarsky, Margaret Daeschler, Lauren Bataille, Solveig K Sieberts, Larsson Omberg, Steven Moore et Paolo Bonato : Accelerometer data collected with a minimum set of wearable sensors from subjects with parkinson's disease. *Scientific data*, 8:48, février 2021.

[5] Sandrine Greffard, Marc Verny, Anne-Marie Bonnet, Jean-Yves Beinis, Claude Gallinari, Sylvie Meaume, François Piette, Jean-Jacques Hauw et Charles Duyckaerts : Motor score of the unified parkinson disease rating scale as a good predictor of lewy body-associated neuronal loss in the substantia nigra. *Archives of neurology*, 63:584–588, avril 2006.

[6] C N Homann, K Suppan, K Wenzel, G Giovannoni, G Ivanic, S Horner, E Ott et H P Hartung : The bradykinesia akinesia incoordination test (brain test), an objective and user-friendly means to evaluate patients with parkinsonism. *Movement disorders : official journal of the Movement Disorder Society*, 15:641–647, juillet 2000.

[7] Andrea Lee et Rebecca M Gilbert : Epidemiology of parkinson disease. *Neurologic clinics*, 34:955–965, novembre 2016.

[8] Luca Lonini, Andrew Dai, Nicholas Shawen, Tanya Simuni, Cynthia Poon, Leo Shimanovich, Margaret Daeschler, Roozbeh Ghaffari, John A Rogers et Arun Jayaraman : Wearable sensors for parkinson's disease: which data are worth collecting for training symptom detection models. *NPJ digital medicine*, 1:64, 2018.

[9] Christofer Lundqvist : Continuous levodopa for advanced parkinson's disease. *Neuropsychiatric disease and treatment*, 3:335–348, juin 2007.

[10] O Rascol, D J Brooks, A D Korczyn, P P De Deyn, C E Clarke et A E Lang : A five-year study of the incidence of dyskinesia in patients with early parkinson's disease who were treated with ropinirole or levodopa. *The New England journal of medicine*, 342:1484–1491, mai 2000.

[11] Ana Lisa Taylor Tavares, Gregory S X E Jefferis, Mandy Koop, Bruce C Hill, Trevor Hastie, Gary Heit et Helen M Bronte-Stewart : Quantitative measurements of alternating finger tapping in parkinson's disease correlate with updrs motor disability and reveal the improvement in fine motor control from medication and deep brain stimulation. *Movement disorders : official journal of the Movement Disorder Society*, 20:1286–1298, octobre 2005.

[12] Ilias Thomas, Moudud Alam, Filip Bergquist, Dongni Johansson, Mevludin Memedi, Dag Nyholm et Jerker Westin : Sensor-based algorithmic dosing suggestions for oral administration of levodopa/carbidopa microtablets for parkinson's disease: a first experience. *Journal of neurology*, 266:651–658, mars 2019.

[13] Ilias Thomas, Jerker Westin, Moudud Alam, Filip Bergquist, Dag Nyholm, Marina Senek et Mevludin Memedi : A treatment-response index from wearable sensors for quantifying parkinson's disease motor states. *IEEE journal of biomedical and health informatics*, 22:1341–1349, septembre 2018.

[14] Florence Véronneau-Veilleux, Philippe Robaey, Mauro Ursino et Fahima Nekka : An integrative model of parkinson's disease treatment including levodopa pharmacokinetics, dopamine kinetics, basal ganglia neurotransmission and motor action throughout disease progression. *Journal of pharmacokinetics and pharmacodynamics*, 48:133–148, février 2021.

[15] Florence Véronneau-Veilleux, Mauro Ursino, Philippe Robaey, Daniel Lévesque et Fahima Nekka : Nonlinear pharmacodynamics of levodopa through parkinson's disease progression. *Chaos (Woodbury, N.Y.)*, 30:093146, septembre 2020.

[16] Yuncheng Wu, Weidong Le et Joseph Jankovic : Preclinical biomarkers of parkinson disease. *Archives of neurology*, 68:22–30, janvier 2011.

Quatrième chapitre.

A mechanistic model of ADHD as resulting from dopamine phasic/tonic imbalance during reinforcement learning

par

Florence Véronneau-Veilleux [1], Philippe Robaey[2], Mauro Ursino[3] et Fahima Nekka[4]

([1]) Faculté de Pharmacie, Université de Montréal, Montréal, Québec, Canada

([2]) Faculty of Medicine, University of Ottawa, Ottawa, Ontario, Canada

([3]) Department of Electrical, Electronic and Information Engineering "Guglielmo Marconi", University of Bologna, 40136 Bologna, Italy

([4]) Faculté de Pharmacie, Université de Montréal
Centre de recherches mathématiques, Université de Montréal,
Centre for Applied Mathematics in Bioscience and Medicine (CAMBAM), McGill University, Montréal, Québec, Canada

Cet article a été soumis à *Frontiers in Computational Neuroscience*.

Diverses hypothèses ont été avancées concernant l'étiologie du TDAH. L'une d'elles suggère qu'un déséquilibret entre la dopamine tonique, concentration de base, et la dopamine phasique, impliquée dans l'apprentissage par renforcement, serait à l'origine des symptômes. L'objectif de ce quatrième chapitre est d'évaluer, à l'aide d'un modèle QSP, les impacts possibles d'un tel déséquilibre sur les ganglions de la base et sur la réponse à un stimulus dans le cadre du TDAH. Le modèle développé au Chapitre 1 est adapté pour inclure la dopamine tonique et phasique. Deux groupes de patients virtuels, avec ou sans déséquilibre de la dopamine, sont créés pour étudier leurs réponses à une série de stimuli. Les patients présentant un tel déséquilibre ont des temps de réaction plus longs et commettent plus d'erreurs, tel qu'observé chez les patients souffrant de TDAH. Une métrique est aussi développée pour différencier la performance des patients.

Abstract. Attention deficit hyperactivity disorder (ADHD) is the most common neurodevelopmental disorder in children. Although the involvement of dopamine in this disorder seems to be established, the nature of dopaminergic dysfunction remains controversial. The purpose of this study was to test whether the key response characteristics of ADHD could be simulated by a mechanistic model that combines a decrease in tonic dopaminergic activity with an increase in phasic responses in cortical-striatal loops during learning reinforcement. To this end, we combined a dynamic model of dopamine with a neurocomputational model of the basal ganglia with multiple action channels. We also included a dynamic model of tonic and phasic dopamine release and control, and a learning procedure driven by tonic and phasic dopamine levels. In the model, the dopamine imbalance is the result of impaired presynaptic regulation of dopamine at the terminal level. Using this model, virtual individuals from a dopamine imbalance group and a control group were trained to associate four stimuli with four actions with fully informative reinforcement feedback. In a second phase, they were tested without feedback. Subjects in the dopamine imbalance group showed poorer performance with more variable reaction times due to the presence of fast and very slow responses, difficulty in choosing between stimuli even when they were of high intensity, and greater sensitivity to noise. Learning history was also significantly more variable in the dopamine imbalance group, explaining 75% of the variability in reaction time using quadratic regression. The response profile of the virtual subjects varied as a function of the learning history variability index to produce increasingly severe impairment, beginning with an increase in response variability alone, then accumulating a decrease in performance and finally a learning deficit. Although ADHD is certainly a heterogeneous disorder, these results suggest that typical features of ADHD can be explained by a phasic/tonic imbalance in dopaminergic activity alone.

Keywords: Attention deficit hyperactivity disorder, tonic and phasic dopamine, neurocomputational model, basal ganglia, reinforcement learning

1. Introduction

Attention Deficit Hyperactivity Disorder (ADHD) is a complex neurodevelopmental disorder characterized by pervasive inattention, impulsivity, and restlessness that is inconsistent with the patient's age [**3**]. The origin of ADHD is largely genetic, and for a smaller part environmental, mostly specific to each individual [**15, 106**]. The first genome-genome wide

meta-analysis identified twelve loci in regions containing enhancers and promoters of expression in central nervous system tissues [**21**]. None of these loci were linked to the dopamine system, despite the fact that dopamine genes have been associated with ADHD in candidate gene approaches [**63, 30**]. Other converging evidence supports a role for dopaminergic dysfunction in ADHD. To briefly list them, most animal models used in ADHD research show some type of dopamine dysfunction [**98**]. Stimulants such as methylphenidate, which are the first line of treatment, block more than 50% of dopamine transporters (DAT) in the striatum when given in therapeutic doses [**100**]. ADHD patients are vulnerable to drug dependence, which may be explained by an overlap of ADHD with the dopamine deficiency syndrome [**13**]. In functional brain imaging, the most consistent findings are deficits in activity in fronto-striatal circuits where dopamine supports reinforcement learning [**23, 70**]. The clearest and most reproducible structural abnormalities in ADHD are located in the basal ganglia and can be normalized by the use of stimulant medications [**68**]. There appears to be a 5- to 10-year lag in the pruning of fronto-striatal circuits in ADHD patients compared to their typically developing peers [**22**]. Functional magnetic resonance and diffusion tensor imaging modalities consistently indicate disrupted connectivity in regions and tracts involving fronto-striatal-thalamic loops in ADHD [**79**].

Different models have been proposed to account for a dopaminergic dysfunction. In the basal ganglia, dopamine release may be sustained (tonic) and regulated by prefrontal cortical afferents, or transient (phasic), caused by bursts of firing of dopaminergic neurons [**44**]. The dynamic developmental theory (DDT) of ADHD proposed a hypo-dopaminergic cause. Blunted phasic dopamine bursts impair reinforcement learning [**101, 80**], while a hypoactive tonic firing rate results in impaired extinction of previously reinforced behaviors [**80**]. A neural network developed by Frank et al. [**34, 35**] instantiated key properties of cortico-striatal-thalamocortical loops, including direct and indirect basal ganglia pathways. These authors used this basal ganglia model to test the plausibility of the DDT of ADHD with reduced tonic and phasic dopamine levels in the striatum [**36**]. While they showed that dopamine modulates the Go and NoGo pathways in the striatum, as well as average reaction

time, they were unable to reproduce the increased variability in reaction time, a key feature of ADHD [**59**], with this hypodopaminergic model alone.

As an alternative we here tested the plausibility of a model that combines a decrease in tonic dopamine activity with an increase in phasic responses [**45**]. In Grace's model, this imbalance is the result of impaired presynaptic regulation of dopamine at the terminal level, and not a central decrease in DA tonic activity that is associated with other conditions, such as chronic stress [**11, 25**]. This imbalance produces abnormally large reward reinforcements, which explains impulsivity, as well as the preference for smaller immediate rewards over larger delayed rewards [**57, 72**]. This model received some support in a PET study showing reduced tonic release and increased phasic release of dopamine in the right caudate in adults with ADHD [**6**].

In the present study, we used a mechanistic model of the basal ganglia dopaminergic system that we previously developed to help rationally improve pharmacological interventions in Parkinson's disease [**99**]. The model is a combination of a neurocomputational model of the basal ganglia [**9, 8**] and a model of dopamine dynamics [**26**] that includes dopamine release and reuptake by DAT. In addition, we included the tonic and phasic release of dopamine as well as the negative regulation of dopaminergic neuron activity by autoreceptors. We used phasic dopamine release as a reward prediction error signal for a correct response and a phasic decrease in tonic dopamine activity as a punishment prediction error signal for a false response [**83**]. Considering that ADHD results from transactions between at-risk individuals and their specific environment [**16, 17**], we used this computational model to test the hypothesis that the phasic/tonic imbalance of DA release would lead, during reinforcement learning, to the development in some individuals of ADHD characteristics, in particular response variability.

As dopamine in basal ganglia is primarily involved in learning reinforcement, we considered dopamine phasic vs. tonic release imbalance as a risk factor, and created two groups of virtual participants: one with a phasic/tonic imbalance and the other with the normal balance. We trained all of them to learn responses to 4 stimuli presented in a random sequence,

using a forced-choice probabilistic task with a fixed reinforcement learning schedule and fully informative reinforcement feedback. Next, we assessed the outcome of learning reinforcement process in a test phase to determine whether or not ADHD characteristics would be present more frequently in the dopamine imbalance group than in the control group. Finally, we identified the characteristics of the learning phase that were associated with the development of these ADHD features in the dopamine imbalance group.

2. Methods

The mechanistic model herein developed can be divided into two parts: the dopamine dynamics model and the neurocomputational model of basal ganglia. Synaptic learning in the basal ganglia is modeled with the Hebb's rule, which states that two neurons having both high activity will strengthen their connections, whereas connections will weaken in case of neurons with opposite activity. This rule allows the value of synaptic weights to be modified according to tonic and phasic dopamine concentrations. The simulations comprise a learning and a test phase.

2.1. Dopamine dynamics model

The dopamine dynamics model describes the temporal dopamine concentration, both tonic and phasic, autoreceptors occupancy and dopaminergic receptors occupancy. It was adapted from previously published models [**27, 28, 26, 40**].

The main mechanisms of dopamine regulation are outlined in the equations of the model and are represented in Figure 32. Dopamine is synthesized in the dopaminergic neurons and then released in the synaptic cleft. Sustained dopamine release refers to tonic dopamine, while transient dopamine release generated by bursts refers to phasic dopamine. The release of phasic dopamine is a reward prediction error signal [**66, 102**], whereas a drop in dopamine levels is a punishment prediction error signal. In the synaptic cleft, dopamine can be recaptured by DATs into the presynaptic neuron or be removed from the synaptic cleft by different mechanisms such as diffusion or inactivation by the Catechol-O-methyltransferase.

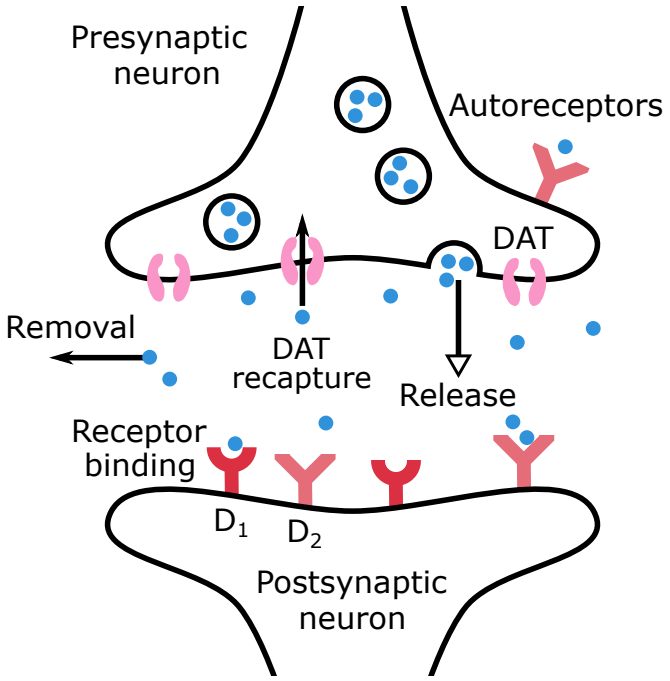

Figure 32. Schematic representation of dopamine release, recapture, removal and binding to receptors in the synaptic cleft

The remaining dopamine molecules can bind to dopaminergic autoreceptors located on the presynaptic neurons or to receptors on the postsynaptic neurons. In the present work, only dopaminergic receptors D_1 and D_2 are considered. All the above mentioned mechanisms are accounted for by the dopamine dynamics model, formulated in equations 2.1 and 2.2, where $C_{DA}(t)$ is the dopamine concentration ($\mu M/L$) in the synaptic cleft and $AR(t)$ the autoreceptors occupancy. Some terms were highlighted to provide a clearer connection between the different equations.

$$\underbrace{\frac{dC_{DA}(t)}{dt}}_{\text{Dopamine concentration}} = \underbrace{(I_{DA}^{tonic} + I_{DA}^{phasic}(t))}_{\text{Dopamine Release}} - \underbrace{\frac{V_{max}C_{DA}(t)}{(k_m + C_{DA}(t))}}_{\text{Recapture by DATs}} - \underbrace{k_{rem}C_{DA}(t)}_{\text{Removal}}, \tag{2.1}$$

$$\underbrace{\frac{dAR(t)}{dt}}_{\text{Autoreceptor occupancy}} = \underbrace{C_{DA}(t)k_{on}(1 - AR(t))}_{\text{Binding to autoreceptors}} - \underbrace{k_{off}AR(t)}_{\text{Unbinding to autoreceptors}} . \tag{2.2}$$

As indicated in equation 2.1, the release of dopamine is divided into two terms to account for both tonic and phasic release. The recapture by DATs is a saturable process described by a Michaelis-Menten equation. All other mechanisms contributing to dopamine removal are assumed to be linear [**14, 26**] and are schematized through the last term in the right-hand member of equation 2.1. The binding to autoreceptors is proportional to dopamine concentration and free autoreceptors, while unbinding is proportional only to bound autoreceptors.

Autoreceptors have a regulatory effect on dopamine concentration. Indeed, they provide a negative feedback to adjust dopamine concentration through firing rate, synthesis, and release [**10, 12**]. Prolonged dopamine agonist exposure desensitizes autoreceptors in dopamine neurons [**78**]. Loss of inhibition influence facilitates further dopamine release and has been linked to drug abuse. Desensitization was not included in the model which is focused on the short-term effect of dopamine on autoreceptors. If tonic dopamine level decreases (in our ADHD model through increased dopamine reuptake), the temporary decrease in autoreceptor-mediated inhibition would mainly increase phasic dopamine release following the model developed by Grace [**44, 46**]. Autoinhibition of the presynaptic neurons is included in the model through the phasic release term only which is associated with the reward prediction error, while the tonic term is not here modified by autoreceptors occupancy [**44**].

The tonic dopamine release term is given by:

$$I_{DA}^{tonic} = \rho \frac{P_r^{tonic} n_0}{\alpha_{vf} N_A} \upsilon_{tonic}, \tag{2.3}$$

where ρ is the terminal density, P_r^{tonic} the tonic release probability, n_0 the number of molecules released per vesicles fusion, α_{vf} the extracellular volume fraction, N_A the Avogadros constant and υ_{tonic} the tonic firing rate. The tonic release is independent of autoreceptors occupancy, as explained above.

The phasic release term at time t is given by:

— when there is no response yet, and no prediction error signal:

$$I_{DA}^{phasic}(t) = 0, \tag{2.4}$$

— when there is a reward prediction error signal at time t_{reward}:

$$I_{DA}^{phasic}(t) = \rho \frac{\left(P_r^{phasic} \cdot \frac{0.334}{AR(t)}\right) n_0 |RPE|}{\alpha_{vf} N_A} \left(\upsilon_{phasic} \cdot \frac{0.334}{AR(t)}\right), \tag{2.5}$$

$$\text{for } t_{reward} + 0.1 \leq t \leq t_{reward} + 0.1 + 0.05, \tag{2.6}$$

— when there is a punishment prediction error at time $t_{punishment}$:

$$C_{DA}(t) = 0, \tag{2.7}$$

$$\text{for } t_{punishment} + 0.1 \leq t \leq t_{punishment} + 0.1 + 0.05. \tag{2.8}$$

The terminal density (ρ), the number of molecules released per vesicles fusion (n_0), the extracellular volume fraction (α_{vf}) and the Avogadros constant (N_A) parameters are not modified by autoreceptors occupancy. Since vesicular release probability (P_r^{phasic}) and phasic firing rate (υ_{phasic}) are decreased by autoreceptors [**44**], they are assumed to be inversely proportional to autoreceptors occupancy [**10, 28**]. The exact relationship is not known but assumed here as inversely proportional for simplicity. The value 0.334, used to normalize the equation for the control case, corresponds to autoreceptors occupancy. Therefore, equation 2.10 indicates that the activation of autoreceptors reduces phasic dopamine release. The values $0.1s$ [**7**] and $0.05s$ represent the latency and duration of the reward or punishment error prediction signal, respectively. Phasic dopamine release is also proportional to the reward prediction signal. This issue will be discussed in more details in section 2.3.

In the occurrence of a punishment, the activity of the dopamine neuron is temporarily suppressed (both tonic and phasic firing rate fall to zero). According to equations 2.1 and 2.8, this can be simulated in the model assuming $\upsilon_{tonic} = 0$ which corresponds to the following differential equation:

$$\frac{dC_{DA}(t)}{dt} = -\frac{V_{max} C_{DA}(t)}{k_m + C_{DA}(t)} - k_{rem} C_{DA}(t). \tag{2.9}$$

With the parameters we used, this equation requires about 500 ms to reach the new equilibrium with $C_{DA} = 0$, which is close to the duration of dopamine neuron activity suppression

after the absence of an expected reward [**82**]. However, the time to reach this equilibrium may vary as a function of the previous discharge rate, tonic dopamine level, or reuptake. To simplify the model, the value $C_{DA} = 0$ was directly applied at the same time as for the phasic dopamine discharge associated with a reward, as shown in equations 2.12 and 2.13.

In the model, autoreceptors occupancy depends on the overall dopamine concentration (tonic and phasic). It could be argued that, due to diffusion, only a fraction of phasic dopamine reaches autoreceptors and thus alters the release. Simulations were performed to integrate this concentration gradient on phasic dopamine reaching autoreceptors, but the results were not significantly different (not shown here), therefore the version presented here was chosen for simplicity.

Finally, dopamine molecules can bind to dopaminergic receptors, corresponding to D_1 and D_2 receptors in the current work. The occupancy of receptors of type $i \in \{1,2\}$ in time is given by the following function:

$$D_i(t) = \frac{B_{max}^{D_i} C_{DA}(t)}{k_D^{D_i} + C_{DA}(t)} \tag{2.10}$$

where $B_{max}^{D_i}$ and $k_D^{D_i}$ are the maximal concentration and dissociation constant of type i receptors, respectively. Receptors occupancy will be used in the neurocomputational model of basal ganglia as the postsynaptic effect of dopamine on the neurons in the different neurotransmission pathways [**53**].

The parameter values for the dopamine dynamics model are given in Table 3.

Using the developed model, two groups of virtual individuals were created: control and dopamine imbalance individuals. The difference between the two groups lies in the modification of the V_{max} parameter of equation 2.1. From a mathematical standpoint, the parameter k_m could also have been decreased to obtain similar results.

2.2. Neurocomputational model of basal ganglia

Tonic and phasic dopamine are coding prediction error signals in the basal ganglia [**85**]. ADHD is associated with dopamine dysfunctions in the cortex and the basal ganglia [**20,**

Table 3. Parameter values in the dopamine dynamic model

Parameters	Description	Value	Literature value	Reference
V_{max}	Maximal reuptake rate by DATs	Control : 1.2 $\mu M/Ls$ Dopamine imbalance : 1.8 $\mu M/Ls$	[0.2 4.3]	[**40, 67, 69, 87**]
k_m	apparent Michaelis–Menten constant	0.15 $\mu M/L$	[0.1, 0.2]	[**40, 54, 58, 67**]
k_{rem}	Removal rate	0.04 s^{-1}	0.04	[**28**]
k_{on}	On-rate for DA binding to presynaptic autoreceptors	10 $\mu M^{-1}s^{-1}$	10	[**28**]
k_{off}	Off-rate for DA binding to presynaptic autoreceptors	0.4 s^{-1}	0.4	[**28**]
ρ	Density of dopamine terminals in striatum	$0.025 \cdot 10^{15}$ terminals/L	adapted	
α_{vf}	Volume fraction of extracellular space	0.21	[0.19, 0.22]	[**91**]
n_0	Number of dopamine molecules released during vesicle fusion	3000 molecules/terminal	3000	[**26, 74**]
N_A	Avogadros constant	$6.02214076 \cdot 10^{23}\ M^{-1}$	$6.02214076 \cdot 10^{23}$	
P_r^{phasic}	Vesicle release probability	0.06	[0.025, 0.15]	[**28**]
P_r^{tonic}	Vesicle release probability	0.06	[0.025, 0.15]	[**28**]
υ_{tonic}	Average tonic firing rate	4 s^{-1}	[4,5]	[**31**]
υ_{phasic}	Average phasic firing rate	40 s^{-1}	[20,100]	[**31**]
B_{max}^{D1}	D_1 receptor maximal density	1.6 $\mu M/L$	1.6	[**56**]
k_D^{D1}	D_1 receptor dissociation constant	1 $\mu M/L$	1	[**77**]
B_{max}^{D2}	D_2 receptor maximal density	0.08 $\mu M/L$	0.08	[**56**]
k_D^{D2}	D_2 receptor dissociation constant	0.01 $\mu M/L$	0.01	[**77**]

38, 42, 68, 71, 88]. Hence, a neurocomputational model of basal ganglia with a learning procedure was added to the dopamine dynamics model.

The neurocomputational model presented here is an adaptation from the model developed in [**8**]. It involves the temporal neural activity in the cortex, the thalamus and the different regions of the basal ganglia (striatum, globus pallidus intern and extern, and subthalamic nucleus), with a representation of the external stimulus S. The neuronal activities are normalized to obtain a value between 0 and 1. The connections between each region follow three neurotransmission pathways: direct, indirect and hyperdirect. The direct pathway promotes movement, the indirect inhibits it, and the hyperdirect pathway suppresses erroneous movements. D_1 and D_2 receptors occupancy have an excitatory effect in the direct pathway and an inhibitory effect in the indirect pathway, respectively. Both pathways are potentiated by the effect of cholinergic interneurons, also included in the model.

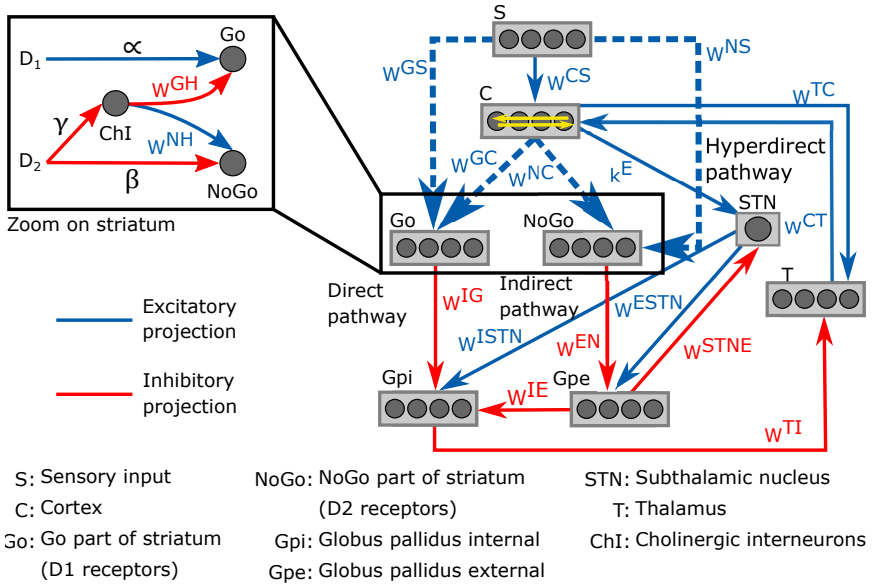

Figure 33. Schematic representation of the neurocomputational model of basal and its four action channels.

A representation of the neurocomputational model of basal ganglia is given in Figure 33. Each region of the model is divided into four action channels, representing different alternative choices. This division allow investigating the response of basal ganglia to various target stimuli. Neural activity in each action channel is computed through an ordinary differential equation, simulating neural dynamics, and a sigmoidal relationship, which mimics the typical non-linear phenomena of the neurons (lower threshold and upper saturation).

The input to each differential equation is calculated by summing all the upstream activities converging to that neuron, weighted by the synaptic strength. The synaptic weight matrices correspond to the weight of connections between the regions for all four action channels. Equations and parameter values of the model can be found in the Supplementary material C.

2.3. Learning in the basal ganglia

Impairments in reinforcement learning are thought to be involved in ADHD [**1, 80, 95**]. Therefore, we included a reinforcement learning process with reward and punishment prediction error signals in the model. The strength of connections between each region of basal ganglia is given by synaptic weight matrices noted w^{ij}, where i and j are the postsynaptic and presynaptic regions, respectively . The values of these weights can be modified by the learning process. For simplicity, only matrices related to striatum, w^{GS}, w^{NS}, w^{GC} , w^{NC}, were considered to be plastic; these connections are represented by dashed lines in Figure 33. The matrices w^{GC} and w^{NC} are diagonal while w^{GS} and w^{NS} are full matrices. At the beginning of the learning process, these weight matrices are in a naive state, with no differentiation between the actions channels. Here are the initial value of the matrices:

$$w^{GC} = w^{NC} = \begin{bmatrix} 0.5 & 0 & 0 & 0 \\ 0 & 0.5 & 0 & 0 \\ 0 & 0 & 0.5 & 0 \\ 0 & 0 & 0 & 0.5 \end{bmatrix}, \tag{2.11}$$

$$w^{GS} = w^{NS} = \begin{bmatrix} 0.5 & 0.5 & 0.5 & 0.5 \\ 0.5 & 0.5 & 0.5 & 0.5 \\ 0.5 & 0.5 & 0.5 & 0.5 \\ 0.5 & 0.5 & 0.5 & 0.5 \end{bmatrix}. \tag{2.12}$$

We here give the details of a typical trial of the learning process. A stimulus representation S is sent for 800 ms to each action channel. One channel will receive a strong stimulus

of value 1, another one receives a weaker stimulus of value 0.2, while the two others receive even weaker stimuli with a value of 0.1 each. In the present work, we used an input vector with the same dimension as the number of possible actions, with a higher value (close to 1) at the same position of the rewarded action, and a smaller value at the positions of the punished actions, just to simplify the final analysis of the synapses. An input vector with different dimensions and with different values could be used as well, resulting in a more complex pattern of synapses. The idea here is to simply associate an input vector to a "winner takes all" output vector, considered as the selected response. The possible considered vectors for S are $S = \begin{bmatrix} 1 & 0.2 & 0.1 & 0.1 \end{bmatrix}$, $S = \begin{bmatrix} 0.2 & 1 & 0.1 & 0.1 \end{bmatrix}$, $S = \begin{bmatrix} 0.1 & 0.1 & 0.2 & 1 \end{bmatrix}$ and $S = \begin{bmatrix} 0.1 & 0.1 & 1 & 0.2 \end{bmatrix}$. Neuronal activity in all regions of basal ganglia are computed for 800 ms. An action is considered to have been performed or chosen if the activity in its related action channel in the cortex is above 0.9, while the activity in all other channels is close to zero, using the winner-takes-all dynamics implemented in the cortex.

We used a fixed scale of prediction error values throughout learning. The prediction error is the discrepancy between observed and expected outcome, and a naive subject cannot predict whether the response would be correct or not. If the chosen action is in the action channel with the highest value of S, a reward prediction error of 1 is attributed. If however the second highest value (0.2) is chosen, a smaller reward prediction error of 0.1 is attributed. A punishment prediction error is given when the the lowest value (0.1) is chosen. Rewards prediction errors are signaled by phasic dopamine peaks governed by equation 2.11. When a punishment prediction error occurs, dopamine concentration drops to zero. This is equivalent to providing the virtual subjects with rewards and punishments, but we delivered directly the reward/punishment prediction error dopamine signals. These prediction errors are the differences between received and predicted rewards [**84**], where here the virtual patient predicts a reward when an action is chosen. This process is repeated over 1000 trials (epochs). Once the learning procedure is complete, the model is expected to effectively differentiate between weak and strong stimuli, so that responses occur only when strong stimuli are applied.

The resulting rewards/punishments prediction error signal will lead to a modification of the synaptic weights contained in the matrices. These weights modifications during the learning process are dictated by the Hebb Rule, which states two neurons having both high activity will strengthen their connections, whereas connections will weaken in case of neurons with opposite activity. The Hebb rule describes how much the weights are increased or decreased at each step of the training procedure. In particular, the following equation holds at each step to assign a new synaptic value, [**9**]:

$$w^{AB} \leftarrow w^{AB} + \Delta w^{AB}, \tag{2.13}$$

where w^{AB} represents the matrix containing the weights from the presynaptic region B to the postsynaptic region A, with A being either S or C in Figure 33 and B being either G (Go) or N (NoGo) in the same figure, and Δw^{AB} is the synaptic change computed at this step. Each row in these matrices represent the synapses entering the postsynaptic neuron, and each column those emerging from the presynaptic one. Hence, all matrices have 4×4 dimensions in the work presented here. This modification of the synaptic weights happens once every epoch between a latency period of $0.1s$ and for a duration of $0.05s$ once an action is chosen. The latency and duration are the same as the ones for the reward/punishment error prediction signal. The individual elements at position ij in the array Δw^{AB} are computed through the following equation (Hebb rule):

$$\Delta w_{ij}^{AB} = \phi \cdot (y_j^B - \vartheta_{presynaptic})^+ (y_i^A - \vartheta_{postsynaptic}), \tag{2.14}$$

where y_j^B is the activity of the presynaptic neuron in the action channel j of the region B, y_i^A is the activity of the postsynaptic neuron in the action channel i of the region A and $\vartheta_{presynaptic}$, $\vartheta_{postsynaptic}$ the pre- and postsynaptic thresholds . The positive part function ($[]^+$) ensures that learning occurs only if the presynaptic neurons are excited and their activity is above the threshold. Of course, in case of diagonal matrices (w^{GC} and w^{NC}), only the

elements with $i = j$ are trained, compared to non-diagonal matrices w^{GS} and w^{NS} where all elements are trained. Dopamine is thought to have the ability to modulate synaptic plasticity, although the exact relationship does not seem to be established [**39, ?, 76**]. From previous work, it seemed reasonable to assume a proportionnal relationship with dopamine ratio and RPE. The gain parameter ϕ is proportional to the reward prediction error since, for example, a large reward prediction error will lead to a larger variation in the synaptic value than a small reward prediction error. The gain parameter is also proportional to the ratio of phasic peak and tonic dopamine. It is calculated beforehand and considered as a constant. The equation is the following:

$$\phi = 0.0013 \cdot \mid RPE \mid \cdot \text{DA ratio}, \tag{2.15}$$

$$\text{DA ratio} = \left(\frac{C_{DA}^{phasic} - C_{DA}^{tonic}}{C_{DA}^{tonic}} \right). \tag{2.16}$$

The dopamine ratio is higher in the dopamine imbalance group (with a value of ~ 8.3) compared to the control one (with a value of ~ 3), so the gain parameter ϕ is higher.

2.4. Simulation of virtual patients groups

The control and dopamine imbalance groups, with 10 virtual subjects each, were created with the model. The only difference between the two groups is in the value of V_{max}. A higher rate of dopamine recapture is expected to lower the dopamine tonic concentration which in turn is expected to increase the phasic dopamine concentration, and thus the tonic phasic dopamine ratio, through a lower occupancy of autoreceptors. The steps of the learning procedure of a subject are summarized below.

(1) The synaptic weight matrices w^{GS}, w^{NS}, w^{GC}, w^{NC} start in a naive state, meaning no differentiation between the actions channels.

(2) Out of the four choices ($S = \begin{bmatrix} 1 & 0.2 & 0.1 & 0.1 \end{bmatrix}$, $S = \begin{bmatrix} 0.2 & 1 & 0.1 & 0.1 \end{bmatrix}$, $S = \begin{bmatrix} 0.1 & 0.1 & 0.2 & 1 \end{bmatrix}$ and $S = \begin{bmatrix} 0.1 & 0.1 & 1 & 0.2 \end{bmatrix}$), a stimulus S in sent to the cortex

for 800 ms. The process will be repeated for the other 3 stimuli in a random order. Noise was added in the cortex, derived from a uniform distribution and ranging from 0 to 0.2. The seed of the noise differentiates the individuals within a group but not between groups, while the V_{max} value differentiates the two groups. For example, the control individual #1 has the same noise's seed as dopamine imbalance individual #1, but a different value of V_{max}. At the end of the 800 ms, the subject receives either a large or a small reward prediction error signal according to his choice of the action that corresponds to the highest or the second strongest stimulus, respectively. Otherwise, the patient receives a punishment prediction error signal. Transient peaks of phasic dopamine are given accordingly and the Hebb rule is applied to modify the value of synapses. This process is repeated with the three other choices of S.

(3) Step 2 is repeated 250 times for a total of $250 \times 4 = 1000$ epochs.

(4) Once the training phase is over, the performance of the virtual subjects in each group was assessed in a testing phase. For each individual, the weight matrices were fixed to the values found at the end of the training process to assess their performance.

During the test phase, we also used a four-choice reaction time task. A series of stimuli are presented to the virtual individuals in the different action channels through a signal S to the cortex. The stimulus in the targeted action channel has a value of 1 with the addition of noise. Noise is also added in the other action channels directly in the cortex. Each stimulus is presented for 1800 ms with a 500 ms pause in between each stimulus.The criterion for a response is an activity in one of the four action channels in the cortex greater than 0.9. Due to the winner-takes-all dynamics, the other three channels will then have activity close to zero. For simplicity purposes, a response in the same action channel as the target stimulus is considered as a success. Otherwise it constitutes a failure. Or course successes and failures could have been defined in different ways. The idea here is simply to associate to an input vector, an output vector considered as the correct response.

During the test phase, there is always a response after a stimulus, being a success or a failure. Each individual is presented 100 stimuli. The mean and standard deviation of the

percentage of successes and of the reaction times are computed in each simulated group. Stimulus of different amplitudes were also sent in the first action channel and the responses were recorded to study the differentiation between weak and strong signals. In order to compare the ability of differentiating between weak and strong signals, we repeated the task and computed the cortex activity for different values of noise added to the input signal (S).

3. Results

3.1. Tonic and phasic dopamine release

Using the model, dopamine concentrations were simulated for the two groups as shown in Figure 34. Phasic peaks were created by a burst lasting 0.05 s.

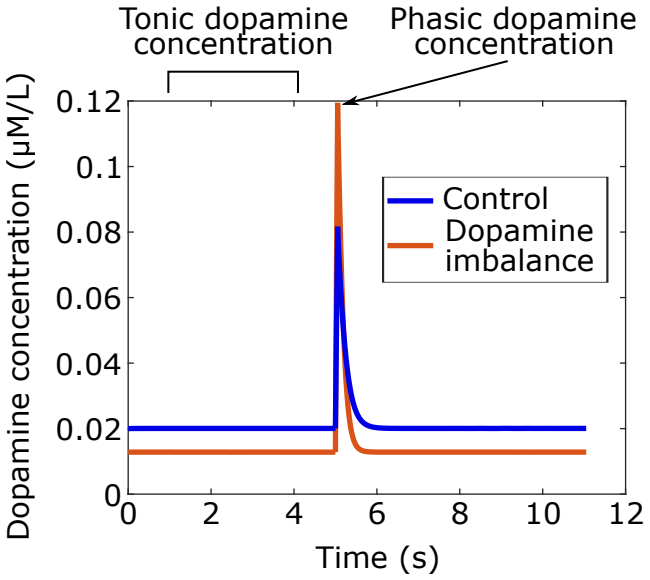

Figure 34. Tonic and phasic dopamine concentrations in time simulated with the model for the dopamine imbalance and the control group. In the dopamine imbalance group, tonic dopamine levels are lower due to increased recapture, which leads to decreased autoreceptor occupancy. Reduced autoreceptor occupancy causes higher peak of phasic dopamine because of autoregulation.

As seen in Figure 34, dopamine imbalance individuals have lower tonic dopamine concentration due to higher dopamine recapture. In turn, autoreceptors regulation causes higher phasic dopamine concentration. This dopamine imbalance will have different impact on the learning process in the basal ganglia.

3.2. Performance during the test phase

In the first task, the mean and standard deviation of the percentage of successes to a serie of 100 stimuli and of reaction times are computed in each simulated group and shown in the following figure.

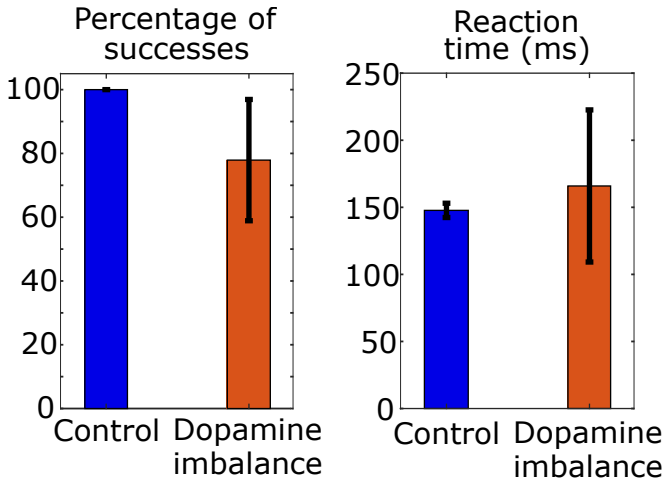

Figure 35. Mean and standard deviation of reaction time and percentage of success of choices in a serie of 100 stimuli in each group

As shown in Figure 35, the rate of successes was lower and more variable in the dopamine imbalance group, as compared to the control group. Moreover, the simulated mean reaction times was slower in the dopamine imbalance group than in the control group. In our simulations, the mean and standard deviation of reaction times are respectively 1.12 and 9.20 times larger in the dopamine imbalance group than in the control group.We used the ex-Gaussian distribution to estimate the reaction time distribution by combining a normal and an exponential distribution. Three parameters characterized the ex-Gaussian distribution: the mean μ and standard deviation σ of the normal distribution, and τ representing the mean and standard deviation of the exponential part. An ex-Gaussian distribution was fitted to the simulated reaction times of the virtual individuals as seen in Figure 36.

The τ parameter was 12 times larger in the dopamine imbalance group than in the control group (47 vs. 3.8) while the μ parameter was 0.8 times smaller (118 vs. 144).

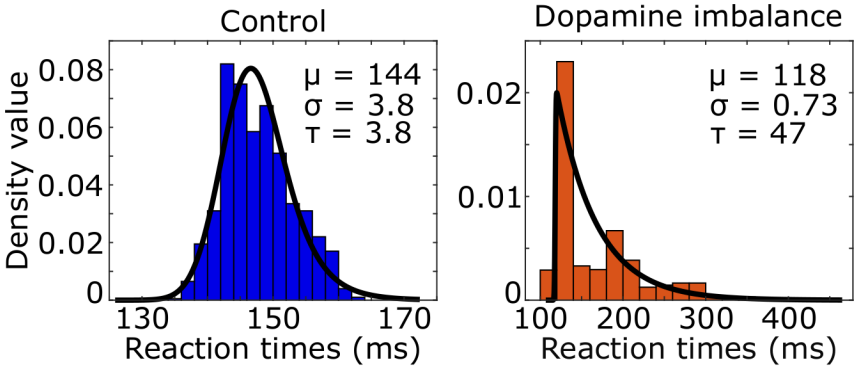

Figure 36. Histogram (colored boxes) and fitted density function (black line) of simulated reaction times of the virtual individuals in the control and dopamine imbalance groups

3.3. Performance with increasing noise

We assessed the performance of the individuals in each group described in the above section by increasing the standard deviation of the noise added to the input signal S. A series of 100 stimuli was again presented with a noise directly added to the stimulus representation in the cortex S, with a mean of 1 and a standard deviation ranging from 0 to 1. A larger standard deviation increased the proportion of trial contaminated by higher intensity noise. Figure 37 shows that in the dopamine imbalance group the mean percentage of successes (orange solid line) quickly dropped while the variability (orange shaded area) increased with increasing noise variability. By contrast, in the control group, the performance remained optimal, with no variability, until the noise variability was greater than 0.6

3.4. Input and output of basal ganglia

During the test phase, we also computed the output activity in the cortex related to the response as a function of the input value of the stimulus. A stimulus of different amplitudes, ranging from 0.1 to 1, is sent in the first action channel while all three other channels receive noise of small amplitude. The mean, the 5th and the 95th output curves of the cortex neuronal activity in the first action channel as a function of the input signal value for each group are shown in Figure 38.

By comparing neural activity of basal ganglia input and output, it is clear that in control subjects, the basal ganglia have a high neural gain. Response-related activity is suppressed

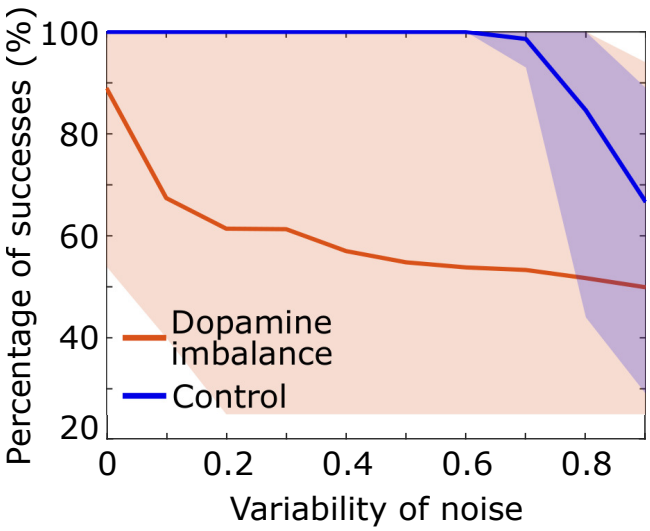

Figure 37. Percentage of success as a function of noise standard deviation for the individuals in each group.The curve of each individual are contained in the shaded area.

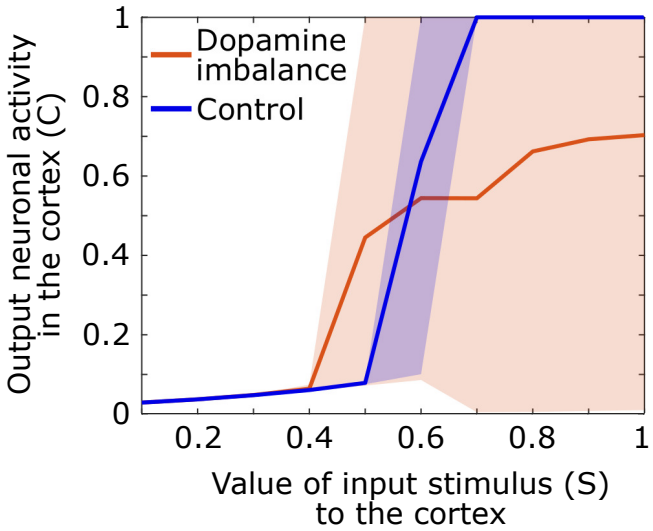

Figure 38. Output neuronal activity in the cortex as a function of different input stimuli. Solid line: mean neuronal activity of the individuals in each group, shaded area: 5th and 95th percentiles of neuronal activity of the individuals in the group

until stimulus-related cortical activity reaches 0.5 in the control group. Output activity then increases rapidly for an input between 0.5 and 0.7 at which point it remains maximal. In contrast, in the dopamine imbalance group, activity is suppressed up to an input of 0.4, after which the gain increases rapidly but only for stimulus-related activity between 0.4 and 0.5. For stimulus-related activity values between 0.5 and 1, the gain is strongly attenuated as response-related activity increases from 4.5 to 7. However, the most striking aspect of

the gain is the extreme variability of the output in the dopamine imbalance group, which ranges from 0 to 1 in response to stimulus-related activity values between 0.7 and 1. In this group, some individuals respond correctly and others have wrong responses which will lead to an output activity close to zero due to the winner-takes-all dynamic, thus inducing high variability. In contrast, in the controls, the variability is almost zero, except for the amplification phase, especially around the inflection point.

3.5. Performance during the training phase

During the training phase, we computed the number of trials to obtain 5 successful responses over 10 successive trials. All participants in the normal group reached the learning criterion, but 2 participants in the dopamine imbalance group failed to do so even after 1000 trials. The number of trials to reach criterion was on average 65.1 (SD = 52.6) in the control group, but 20% higher in the dopamine imbalance group, with an average of 85.5 (SD=67.8), excluding those who never reached the criterion.

3.6. Evolution of synaptic weights

Four synaptic weights matrices were modified during training: w^{GS}, w^{NS} (stimulus-related synaptic weights) and w^{GC}, w^{NC} (response-related synaptic weights). These matrices start in a naive configuration, with no differentiation between the four action channels. They are modified during the training by the Hebb Rule, with a gain parameter that is proportional to the phasic vs. tonic dopamine ratio.

Over the course of the 1000 trials in the training phase, the matrix weights changed differently between the two groups, and between individuals within each group. Figures 49 to 56 of Supplementary material C show the matrix values across trials for the 10 subjects in each of the control and dopamine imbalance groups. In the direct pathway, for control subjects, all stimulus-related synaptic weights first decreased, then increased slightly for successes (diagonal), but continued to decrease for errors. Response-related synaptic weights increased slightly. Inter-individual differences remained small, with a slight increase at the

end of learning. In the indirect pathway, all stimulus- and response-related synaptic weights decreased, again with a slight increase in interindividual differences.

In comparison, the trends were the same for the group with dopamine imbalance, but inter-individual differences in synaptic weights and their evolution during learning were much larger. In the direct pathway, stimulus-related synaptic weights strongly increased for successes at different times during learning until they reached a maximum in some individuals, whereas they decreased slightly in others. Synaptic weights off the diagonal (errors) decreased for all individuals but diverged at different times. Synaptic weights related to the response showed the same changes as stimulus-related weights. In the indirect pathway, synaptic weights decreased for both the response and stimulus channels, but this decrease began at different times during learning across individuals. Hence, inter-individual differences were much larger at the end of the learning phase in the dopamine imbalance than in the control group.

3.7. History of rewards and punishments prediction errors during training

In the present section, a metric is developed to differentiate the performance in the test phase of the dopamine imbalance group from the control one based on their history during the training phase. During the training process, the history of rewards and punishments is stored in a vector with value 1 for a large reward, 0.1 for a small reward, -1 for a punishment and 0 for no response. It is therefore possible to study the history of each individual and to relate it to his performance in the test phase.

Figure 39 shows the cumulative sum of the history vector for each action channel of the first 5 individuals in each group. A negative cumulative sum results from a series of failures overcoming successes, while a positive cumulative sum would indicate the opposite.

There seems to be an initial phase in which there is an excess of errors, followed by a second phase (> 500 epoch) in which rewards prediction errors dominate over punishments for all actions.

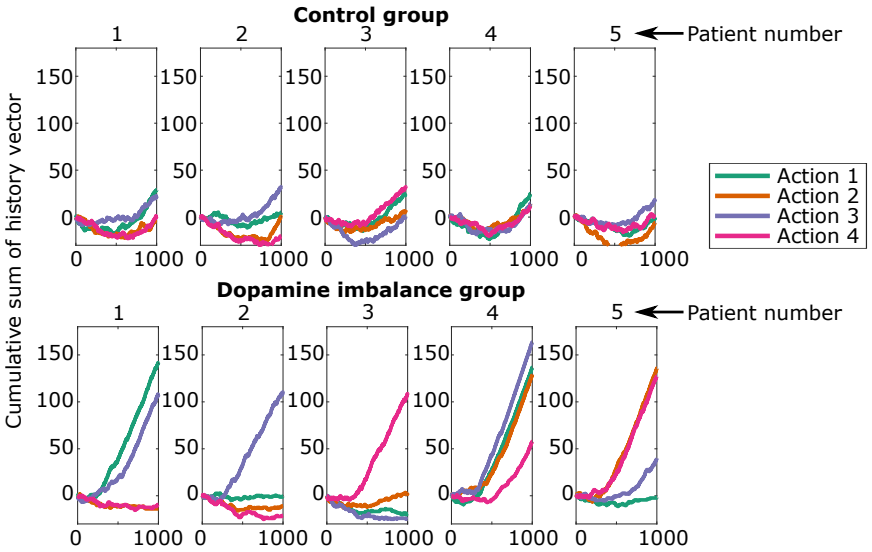

Figure 39. Cumulative sum of history vector at each epoch for the first five individuals in each group

Individuals from the control group seem to learn each action in a proportional way for all action channels. The individuals in the dopamine imbalance group had a higher number of rewards for some action channels at the expense of the others. In order to quantify the inter-individual differences in learning, a weighted standard deviation (*weighted std*) for the cumulative sum of history was computed for each individual, and expressed by the following equations:

$$ratio = \frac{1}{1000} \frac{\sum_{i=1}^{1000} \sum_{j=1}^{4} \#\text{negative } cumsum_{action_j}(i)}{\sum_{i=1}^{1000} \sum_{j=1}^{4} \#\text{positive } cumsum_{action_j}(i)}, \tag{3.1}$$

$$std_{history} = \frac{1}{1000} \sqrt{\sum_{i=1}^{1000} \left(\sum_{j=1}^{4} (cumsum_{action_j}(i) - mean(i))^2 \right)}, \tag{3.2}$$

$$weighted\ std_{history} = ratio \cdot std_{history} \tag{3.3}$$

where i is the epoch number, j the action number, $cumsum_{action_j}(i)$ the cumulative sum of history vector for action j at epoch i and $mean(i)$ is the the mean of cumulative history at epoch i for all action channels. The standard deviation of the history ($std_{history}$) is weighted by a ratio to take into account the fact that the cumulative sum of history is either positive or negative. The ratio is the sum of negative cumulative sum of history divided by the sum of

positive cumulative sum of history, leading to a larger ratio when the negative cumulative sum exceeds the positive one. Division by 1000 is for scaling. The $weighted\ std_{history}$ was larger in the dopamine imbalance group than the control one. In order to assess the relationship between the training and test phase, a plot of the standard deviation of the reaction times as a function of the $weighted\ std_{history}$ value is depicted in Figure 40. A linear regression (dashed line) and a quadratic function (dashed curve) between the $weighted\ std_{history}$ and the standard deviation of reaction times were applied to the control group and the imbalance group, respectively. The individuals in the dopamine imbalance group could be divided into three subgroups (a,b and c) along the quadratic regression as seen in Figure 40. Group a contained the individuals with a perfect performance, low μ, low σ and low τ. which explains their proximity to the individuals in the control group. The individuals with a less than perfect performance were divided into groups b and c. The distribution of reaction times in the group b is closer to an exponential distribution than to a normal one with low μ and σ but very high τ due to an excess of slow responses as reported in the literature [**59**]. These individuals have both fast and very slow reaction times, driving thus the mean to a high value. As the $weighted\ std_{history}$ increases for individuals in group c, the performance further decreased with fewer correct responses, the μ parameters increased, and the σ and τ had intermediate values and were quite similar.

4. Discussion

Comparison between simulated and reported dopamine concentration

In the current work, we investigated the effect of phasic vs. tonic dopamine imbalance during reinforcement learning on overt responses and on synaptic weights in the basal ganglia. We altered the phasic vs. tonic ratio by increasing the rate of maximal dopamine reuptake by DATs. As the rate of dopamine reuptake increases, the tonic level of dopamine decreases, which results in a decrease in autoreceptor binding, and in turn in an increase in the phasic response [**33**]. This modification increased the phasic response by about 40%. The values of simulated dopamine concentrations that we found are consistent with

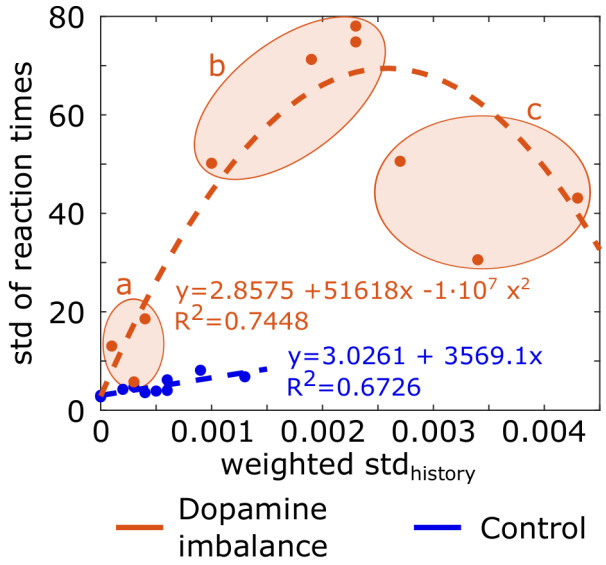

Figure 40. Standard deviation (std) of reaction times for each individual in each group as a function of the *weighted* $std_{history}$. Equation of the linear regression and quadratic regression performed respectively in the control group and dopamine imbalance group are shown. Individuals in the dopamine imbalance group are divided into three sub-groups, a, b and c.

those reported in the literature, with a tonic concentration between 0.005 and $0.02\mu M/L$ [**56, 103**], and a phasic concentration ranges between 0.01 and 1 $\mu M/L$ [**105**]. More precisely, phasic dopamine concentrations were estimated to be ~ 0.1 $\mu M/L$ in [**7**].

Evidence for the role of DATs in ADHD

Although increased reuptake by DAT did change the DA phasic/tonic ratio as expected, one may question whether it is a plausible mechanism in Grace's ADHD model. DAT function is regulated by changes in endocytic trafficking that are governed by binding interactions of its N- and C-terminal domain structures. DAT is thus a key player within an interactome that includes other components, in particular dopamine autoreceptors, that control the balance of dopaminergic discharge. There is also a body of evidence on the role of DATs in ADHD. In a meta-analysis, DAT striatal density was increased by 14% in ADHD. However, DAT density was higher in patients previously medicated with stimulant [**41**]. This conclusion was disputed as some patients may have been misclassified [**89**], but the fact that long-term treatment with stimulant increased DAT density has been demonstrated [**104**]. Genetic

variants could also affect DAT function. There are different genetic variants of DAT [**48**] but the most studied is a variable number tandem repeat (VNTR) in the 3' regulatory regions of the gene, which results in two main forms (long 10R, and short 9R). The 10R has been found to be associated with ADHD, at least in children and youth [**47**], and is associated with a small increase in DAT binding [**96**]. Even if this effect is small, this polymorphism has been associated with activation changes in the striatum and other brain regions [**32, 81, 29, 5**], and varies with the clinical expression of ADHD [**61**]. Moreover, different genetic variants can combine to produce haplotypes such as the association of the 10-repeat allele with the 6-repeat allele of a VNTR located in intron 8 [**37, 43**], or be modulated by epigenetic factors [**94, 60, 107**] that could affect DAT function. DAT function can thus be described in a continuum and modifying DAT reuptake appears to be a credible mechanism for shifting the phasic/tonic ratio of dopamine release in Grace's model. However, other ways are possible, such as changing the properties of the autoreceptors, or combining both.

Comparison of simulated with clinically observed reaction times

Clinically, subjects with ADHD consistently show a typical response pattern on a variety of tasks. They generally make more errors than controls and their reaction times are paradoxically both faster and slower, and more variable overall, as compared with healthy controls [**52, 55**]. This variability is primarily due to an excess of slow responses that can be detected by the τ component of an ex-Gaussian distribution [**59**]. This τ parameter best discriminates ADHD subjects [**62**] from controls and appears to be a reliable endophenotype, as unaffected siblings showed intermediate values between ADHD subjects and healthy controls [**64**]. In the present simulations, the group with dopamine imbalance also showed more variable reaction times, including an excess of very slow responses, as compared with the control group. Specifically, the μ parameter was smaller, reflecting impulsive responses, but the τ was much larger, due to a greater proportion of very slow responses, with a decrease of the σ parameter overall, which reflects the Gaussian variance. Thus, shifting

the phasic/tonic dopamine ratio reproduced a response pattern typically seen in ADHD subjects, whereas a model incorporating only a decrease in both phasic and tonic dopamine release did not [**36**]. We observed this response pattern in a simple reinforcement learning task while it has been observed in a wide variety of experimental tasks with ADHD subjects. Future studies will need to test whether this response pattern generalizes to other tasks, but it is a possibility insofar as any experimental task has a learning component. Indeed, data are typically collected after participants have reached a performance threshold during a training phase.

Comparison of the simulated response in the dopamine imbalance group and the clinical response of ADHD patients

The change in reaction time distribution, although most typical of ADHD, is not the only difference we observed. The subjects with a dopamine imbalance also showed a lower and more variable success rate on average. Within the signal detection theory [**90**], the sensory discrimination ability is termed d'. In our simulation, the test phase used a force choice task in which d' is the percentage of successes [**90**]. The control group obtained perfect results, but the success rate was decreased by 22% in the dopamine imbalance group. Subjects with ADHD also showed decreased d' in a meta-analysis of continuous performance test (CPT) performance [**55**]. Furthermore, we tested the effect of noise, matching each individual in the dopamine imbalance group with one individual in the control group for the seed of noise. In both groups, the success rate degraded and became more variable with increasing noise, but the dopamine imbalance group was more sensitive and showed a drop in success and a large variability for low noise levels that did not affect the performance of control subjects. Similarly, children with ADHD have been shown to have lower auditory discrimination ability than controls in the presence of background noise [**93**].

Neural gain description In order to further characterize the response pattern to stimuli of varying intensity we computed the neural gain between the input and the output of the system. A strong gain is associated with a stable attractor [**50**] in which the system

quickly converges to a stable activity pattern since it is less susceptible to noise. In contrast, a weak gain is characterized by variable attractors that can lead to different unstable and shallow activity patterns. In the present simulation, for stimulus-related input values that always produced a stable response in controls (≥ 0.7), response-related output activity was much more variable in the group with dopamine imbalance. In this group, the more random responses reflected a more exploratory approach where different responses could be produced even for high stimulus-related inputs in the cortex. In experimental situations, subjects with ADHD demonstrated the same type of exploratory approach. In a probabilistic reversal learning task [**51**], ADHD subjects did not choose their response strictly on the basis of their belief in the value of the stimulus, but more often took an exploratory approach. When the neural gain was estimated by a sigmoidal function, this exploratory approach also resulted in a less steep decision function. The phasic response may reinforce the response to low-intensity sensory events, which could lead to a more prolonged phase of discovery of new actions in a learning situation [**75**].

Learning history to differentiate the individuals

But the most significant result of the simulation, consistent with our original hypothesis, is that while all at-risk subjects had the same dopamine release imbalance, the ADHD response pattern developed to different degrees depending on the individual learning experience. On average, during this probabilistic learning task with 100% valid feedback, subjects in the dopaminergic imbalance group required more learning trials than controls to reach a success criterion. Again, this replicates a result obtained with ADHD children [**65**]. However, the sequence of stimuli was random with a unique seed of noise for each individual within a group, which ultimately resulted in a unique learning environment for each individual within each group. This unique environment was shared with the matched individual in the other group. When we examined separately for each individual the cumulative changes in synaptic weights between cortex and basal ganglia over the course of learning, we found that individuals in the control group showed a similar history

regardless of response. In contrast, in the dopamine imbalance group, individuals showed a larger increase in synaptic weight for one or more actions, with onset at different times in the first half of the training phase. As a consequence, the intraindividual differences were much larger in the dopamine imbalance group than in the control group. We computed the weighted standard deviation of the cumulative sum of history to estimate the intraindividual differences during learning. In the control group, using a linear model, we could explain 67% of the variability of individual reaction times during the test phase with the weighted cumulative sum of history. In the control group, however, we had to use a quadratic model to explain the variability between these two measures. Three subgroups of individuals could be distinguished in the dopamine imbalance group (Figure 40). Within a similar range of weighted history variability as the controls, individuals in this subgroup a showed the same perfect performance as the controls. However, the initial slope of the parabola was much steeper than in controls, reflecting the excessive reinforcement for some responses, and the variability of their reaction time was much higher than in controls, but still lower than in the rest of the dopamine imbalance group. This combination of perfect accuracy but high variability in response could define a subthreshold ADHD subgroup, where features of ADHD are already present but do not affect overt accuracy. Closer to the vertex of the parabola, we distinguish a second subgroup b of individuals with weighted history variability larger than the controls (with some negative cumulative weights), and whose accuracy was impaired though not dramatically. The distribution of reaction times contained both fast and very slow responses. Their performance most closely resembled that observed in most of the subjects diagnosed with ADHD as their functioning is clearly impaired. Individuals with extreme weighted history variability (with mostly negative cumulative weights) were hardly learned the stimulus-response association and their performance was even poorer. Their reaction time distribution looked more gaussian with a large variability and very slow mean reaction time. Individuals in this subgroup c could be compared to subjects with a severe ADHD leading to a learning disability. In conclusion, variability in response history is much greater in subjects with dopamine imbalance, although they were exposed

on average to the same learning environment as controls. Intraindividual variability in response times is related to intraindividual variability in experience with the learning environment. It increases when certain responses are reinforced at the expense of other responses during learning, making response selection more difficult in a test phase. But this variability in experience, and therefore also in response times, is much more pronounced in subjects with an imbalance in dopamine release. For subjects in subgroups a and b, the increase in response time variability as a function of weighted learning history variability is approximately linear, but the slope is much steeper than for controls. In these subjects, the increase in phasic dopamine release at the expense of tonic release can excessively strengthen or weaken cortico-striatal synapses associated with different responses and strengthen some responses at the expense of others. These imbalances lead first to an increase in response time variability with a mixture of fast and slow responses, and as these imbalances increase during learning to a decrease in performance in the test phase. In contrast, healthy controls show little variation in the history vector during learning. Consequently, they exhibited a small normal variation in reaction time that was also predicted by the weighted variability of the history with a linear function, but with a smaller slope that reflects a more balanced reinforcement of responses. To the extent that functional connectivity between the striatum and cortex reflects changes in their synaptic connections, our model is consistent with the observed correlation between inattention and hyperactivity/impulsivity scores in networks involving the striatum [**71**]. As these changes are marked by the strengthening of some connections at the expense of others, this also explains the contradictory results in studies comparing an ADHD group with a control group that report either hypoconnectivity [**18, 73**] or hyperconnectivity [**92, 19**] within the cortico-striato-thalamo-cortical loops in ADHD.

Comparison with published work

This qualitative agreement we observed between simulations and experimental findings is remarkable because it is achieved by altering a single parameter of dopaminergic terminal

functioning, which results in phasic-tonic imbalance in dopamine release. Frank's model [**36**], which implemented a reduction in both phasic and tonic dopamine levels, needed to incorporate a noradrenergic component with an increased tonic vs. phasic ratio in order to mimic the increase in reaction time variability observed in ADHD subjects.These authors did not further analyze the distribution of reaction time as a function of noradrenaline release imbalance, so we do not know whether this model reproduces the typical ex-gaussian distribution that we found. Obviously, our results do not rule out noradrenergic dysfunction in ADHD. There is strong evidence of it. Drugs modulating norepinephrine transmission by blocking the NET such as atomoxetine [**86**] or the alpha2-adrenergic agonists such as clonidine or guanfacine [**2**] are effective treatments for ADHD. Methylphenidate significantly occupies NET at clinically relevant doses in humans [**49**] and atomoxetine showed a dose-dependent occupancy of NET in monkeys [**24**]. NET availability was decreased in a group of adult ADHD subjects in attention-relevant regions (frontal, parietal, thalamic, cerebellar), especially in the right hemisphere [**97**]. The shift from exploitation to exploration behavior has been proposed to be mediated by the firing mode of norepinephrine neurons in the locus coeruleus [**4**]. However, the results of our model suggest that norepinephrine is not necessary to reproduce the typical ADHD response pattern observed in experimental reaction time tasks, which may be accounted for by a phasic/tonic imbalance in dopaminergic activity alone. This reinforces the concept of ADHD as a heterogeneous disorder, in which the same response patterns may be produced by different dysfunctions, whether or not interacting.

Limitations

The present model has limitations. Some parameters in the model might not be identifiable and the exact value of some others is not known. The values assigned to parameters is the same for all the subjects within each group and does not reflect the interindividual variability found in control and clinical groups, but support the proof-of-concept approach. The task we used does not require inhibitory processes, which will have to be tested in further studies. Also, in further studies the dysfunctions in the noradrenergic system should also be included

to better simulate the pathophysiology of ADHD. Nevertheless, our model is a first step to investigate the implication of the dopaminergic system in ADHD with a mechanistic approach.

Conclusion

To conclude, our model opens perspectives to be used as a platform to generate and test hypothesis regarding the dopaminergic system in ADHD. The effect of medication on performance, the impact of different patterns of noise, the difference in commission and omission errors and the continuum in the severity of ADHD symptoms could be explored with this model. The model could also be used to simulate a no-response task where the patient is asked to withhold the response when a certain stimulus is sent like in the go/no-go task performed in clinical practice. This modeling approach is a promising step towards the development of an integrative model of the dopaminergic system in basal ganglia for the elucidation of its associated pathologies.

Conflict of Interest Statement

The authors declare that the research was conducted in the absence of any commercial or financial relationships that could be construed as a potential conflict of interest.

Author Contributions

This work makes up a portion of the doctoral thesis of FVV. Construction of the model: FVV PR MU FN. Numerical simulations: FVV. Writing of the paper: FVV PR MU FN.

Funding

F.V.-V. received a scholarship from the Natural Sciences and Engineering Research Council (NSERC), Canada through the PGS-D program. Support was also provided by NSERC - Industrial Chair in Pharmacometrics funded by Novartis, Pfizer and Syneos, as well as FRQNT Projet d'équipe (F.N.).

References

[1] L Alexander et N Farrelly : Attending to adult adhd: a review of the neurobiology behind adult adhd. *Irish journal of psychological medicine*, 35:237–244, septembre 2018.

[2] Amy F Arnsten, Lawrence Scahill et Robert L Findling : alpha2-adrenergic receptor agonists for the treatment of attention-deficit/hyperactivity disorder: emerging concepts from new data. *Journal of child and adolescent psychopharmacology*, 17:393–406, août 2007.

[3] American Psychiatric Association : *Diagnostic and Statistical Manual of Mental Disorders*. American Psychiatric Association, 2013.

[4] Gary Aston-Jones et Jonathan D Cohen : Adaptive gain and the role of the locus coeruleus-norepinephrine system in optimal performance. *The Journal of comparative neurology*, 493:99–110, décembre 2005.

[5] Ali Bacanli, Gul Unsel-Bolat, Serkan Suren, Kemal Utku Yazici, Cem Calli, Duygu Aygunes Jafari, Buket Kosova, Luis Augusto Rohde et Eyup Sabri Ercan : Effects of the dopamine transporter gene on neuroimaging findings in different attention deficit hyperactivity disorder presentations. *Brain imaging and behavior*, 15:1103–1114, avril 2021.

[6] Rajendra D Badgaiyan, Sampada Sinha, Munawwar Sajjad et David S Wack : Attenuated tonic and enhanced phasic release of dopamine in attention deficit hyperactivity disorder. *PloS one*, 10: e0137326, 2015.

[7] Nigel S Bamford, R Mark Wightman et David Sulzer : Dopamine's effects on corticostriatal synapses during reward-based behaviors. *Neuron*, 97:494–510, février 2018.

[8] Chiara Baston, Manuela Contin, Giovanna Calandra Buonaura, Pietro Cortelli et Mauro Ursino : A mathematical model of levodopa medication effect on basal ganglia in parkinson's disease: An application to the alternate finger tapping task. *Frontiers in human neuroscience*, 10:280, 2016.

[9] Chiara Baston et Mauro Ursino : A biologically inspired computational model of basal ganglia in action selection. *Computational intelligence and neuroscience*, 2015:187417, 2015.

[10] Jean-Martin Beaulieu et Raul R Gainetdinov : The physiology, signaling, and pharmacology of dopamine receptors. *Pharmacological reviews*, 63:182–217, mars 2011.

[11] Pauline Belujon et Anthony A Grace : Regulation of dopamine system responsivity and its adaptive and pathological response to stress. *Proceedings. Biological sciences*, 282, avril 2015.

[12] M Benoit-Marand, E Borrelli et F Gonon : Inhibition of dopamine release via presynaptic d2 receptors: time course and functional characteristics in vivo. *The Journal of neuroscience : the official journal of the Society for Neuroscience*, 21:9134–9141, décembre 2001.

[13] Kenneth Blum, Amanda Lih-Chuan Chen, Eric R Braverman, David E Comings, Thomas J H Chen, Vanessa Arcuri, Seth H Blum, Bernard W Downs, Roger L Waite, Alison Notaro, Joel Lubar, Lonna Williams, Thomas J Prihoda, Tomas Palomo et Marlene Oscar-Berman : Attention-deficit-hyperactivity disorder and reward deficiency syndrome. *Neuropsychiatric disease and treatment*, 4:893–918, octobre 2008.

[14] Evgeny A Budygin, Carrie E John, Yolanda Mateo et Sara R Jones : Lack of cocaine effect on dopamine clearance in the core and shell of the nucleus accumbens of dopamine transporter knock-out mice. *The Journal of neuroscience : the official journal of the Society for Neuroscience*, 22:RC222, mai 2002.

[15] S Alexandra Burt : Rethinking environmental contributions to child and adolescent psychopathology: a meta-analysis of shared environmental influences. *Psychological bulletin*, 135:608–637, juillet 2009.

[16] S Alexandra Burt : Are there shared environmental influences on attention-deficit/hyperactivity disorder? reply to wood, buitelaar, rijsdijk, asherson, and kuntsi [corrected] (2010). *Psychological bulletin*, 136:341–343, mai 2010.

[17] S Alexandra Burt, Henrik Larsson, Paul Lichtenstein et Kelly L Klump : Additional evidence against shared environmental contributions to attention-deficit/hyperactivity problems. *Behavior genetics*, 42:711–721, septembre 2012.

[18] Xiaohua Cao, Qingjiu Cao, Xiangyu Long, Li Sun, Manqiu Sui, Chaozhe Zhu, Xinian Zuo, Yufeng Zang et Yufeng Wang : Abnormal resting-state functional connectivity patterns of the putamen in medication-naïve children with attention deficit hyperactivity disorder. *Brain research*, 1303:195–206, décembre 2009.

[19] Taciana G Costa Dias, Vanessa B Wilson, Deepti R Bathula, Swathi P Iyer, Kathryn L Mills, Bria L Thurlow, Corinne A Stevens, Erica D Musser, Samuel D Carpenter, David S Grayson, Suzanne H Mitchell, Joel T Nigg et Damien A Fair : Reward circuit connectivity relates to delay discounting in children with attention-deficit/hyperactivity disorder. *European neuropsychopharmacology : the journal of the European College of Neuropsychopharmacology*, 23:33–45, janvier 2013.

[20] Ana Cubillo, Rozmin Halari, Anna Smith, Eric Taylor et Katya Rubia : A review of fronto-striatal and fronto-cortical brain abnormalities in children and adults with attention deficit hyperactivity disorder (adhd) and new evidence for dysfunction in adults with adhd during motivation and attention. *Cortex; a journal devoted to the study of the nervous system and behavior*, 48:194–215, février 2012.

[21] Ditte Demontis, Raymond K Walters, Joanna Martin, Manuel Mattheisen, Thomas D Als, Esben Agerbo, Gísli Baldursson, Rich Belliveau, Jonas Bybjerg-Grauholm, Marie Bækvad-Hansen, Felecia Cerrato, Kimberly Chambert, Claire Churchhouse, Ashley Dumont, Nicholas Eriksson, Michael Gandal, Jacqueline I Goldstein, Katrina L Grasby, Jakob Grove, Olafur O Gudmundsson, Christine S Hansen, Mads Engel Hauberg, Mads V Hollegaard, Daniel P Howrigan, Hailiang Huang, Julian B Maller, Alicia R Martin, Nicholas G Martin, Jennifer Moran, Jonatan Pallesen, Duncan S Palmer, Carsten Bøcker Pedersen, Marianne Giørtz Pedersen, Timothy Poterba, Jesper Buchhave Poulsen, Stephan Ripke, Elise B Robinson, F Kyle Satterstrom, Hreinn Stefansson, Christine Stevens, Patrick Turley, G Bragi Walters, Hyejung Won, Margaret J Wright, ADHD Working Group of the Psychiatric Genomics Consortium (PGC), Early Lifecourse & Genetic Epidemiology (EAGLE) Consortium, 23andMe Research Team, Ole A Andreassen, Philip Asherson, Christie L Burton, Dorret I Boomsma, Bru Cormand, Søren Dalsgaard, Barbara Franke, Joel Gelernter, Daniel Geschwind, Hakon Hakonarson, Jan Haavik, Henry R Kranzler, Jonna Kuntsi, Kate Langley, Klaus-Peter Lesch, Christel Middeldorp, Andreas Reif, Luis Augusto Rohde, Panos Roussos, Russell Schachar, Pamela Sklar, Edmund J S Sonuga-Barke, Patrick F Sullivan, Anita Thapar, Joyce Y Tung, Irwin D Waldman, Sarah E Medland, Kari Stefansson, Merete Nordentoft, David M Hougaard, Thomas Werge, Ole Mors, Preben Bo Mortensen, Mark J Daly, Stephen V Faraone, Anders D Børglum et Benjamin M Neale : Discovery of the first genome-wide significant risk loci for attention deficit/hyperactivity disorder. *Nature genetics*, 51:63–75, janvier 2019.

[22] Daniel P Dickstein : Paying attention to attention-deficit/hyperactivity disorder. *JAMA network open*, 1:e181504, août 2018.

[23] Steven G Dickstein, Katie Bannon, F Xavier Castellanos et Michael P Milham : The neural correlates of attention deficit hyperactivity disorder: an ale meta-analysis. *Journal of child psychology and psychiatry, and allied disciplines*, 47:1051–1062, octobre 2006.

[24] Y-S Ding, M Naganawa, J-D Gallezot, N Nabulsi, S-F Lin, J Ropchan, D Weinzimmer, T J McCarthy, R E Carson, Y Huang et M Laruelle : Clinical doses of atomoxetine significantly occupy both norepinephrine and serotonin transports: Implications on treatment of depression and adhd. *NeuroImage*, 86:164–171, février 2014.

[25] Erik H Douma et E Ronald de Kloet : Stress-induced plasticity and functioning of ventral tegmental dopamine neurons. *Neuroscience and biobehavioral reviews*, 108:48–77, janvier 2020.

[26] Jakob K Dreyer : Three mechanisms by which striatal denervation causes breakdown of dopamine signaling. *The Journal of neuroscience : the official journal of the Society for Neuroscience*, 34:12444–12456, septembre 2014.

[27] Jakob K Dreyer, Kjartan F Herrik, Rune W Berg et Jørn D Hounsgaard : Influence of phasic and tonic dopamine release on receptor activation. *The Journal of neuroscience : the official journal of the Society for Neuroscience*, 30:14273–14283, octobre 2010.

[28] Jakob Kisbye Dreyer et Jørn Hounsgaard : Mathematical model of dopamine autoreceptors and uptake inhibitors and their influence on tonic and phasic dopamine signaling. *Journal of neurophysiology*, 109:171–182, janvier 2013.

[29] Sarah Durston, John A Fossella, Martijn J Mulder, B J Casey, Tim B Ziermans, M Nathalie Vessaz et Herman VAN Engeland : Dopamine transporter genotype conveys familial risk of attention-deficit/hyperactivity disorder through striatal activation. *Journal of the American Academy of Child and Adolescent Psychiatry*, 47:61–67, janvier 2008.

[30] Stephen V Faraone et Henrik Larsson : Genetics of attention deficit hyperactivity disorder. *Molecular psychiatry*, 24:562–575, avril 2019.

[31] Ashley M Fennell, Elizabeth G Pitts, Lacey L Sexton et Mark J Ferris : Phasic dopamine release magnitude tracks individual differences in sensitization of locomotor response following a history of nicotine exposure. *Scientific reports*, 10:173, janvier 2020.

[32] E E Forbes, S M Brown, M Kimak, R E Ferrell, S B Manuck et A R Hariri : Genetic variation in components of dopamine neurotransmission impacts ventral striatal reactivity associated with impulsivity. *Molecular psychiatry*, 14:60–70, janvier 2009.

[33] C P Ford : The role of d2-autoreceptors in regulating dopamine neuron activity and transmission. *Neuroscience*, 282:13–22, décembre 2014.

[34] Michael J Frank : Dynamic dopamine modulation in the basal ganglia: a neurocomputational account of cognitive deficits in medicated and nonmedicated parkinsonism. *Journal of cognitive neuroscience*, 17:51–72, janvier 2005.

[35] Michael J Frank et Eric D Claus : Anatomy of a decision: striato-orbitofrontal interactions in reinforcement learning, decision making, and reversal. *Psychological review*, 113:300–326, avril 2006.

[36] Michael J Frank, Amy Santamaria, Randall C O'Reilly et Erik Willcutt : Testing computational models of dopamine and noradrenaline dysfunction in attention deficit/hyperactivity disorder. *Neuropsychopharmacology : official publication of the American College of Neuropsychopharmacology*, 32:1583–1599, juillet 2007.

[37] Barbara Franke, Alejandro Arias Vasquez, Stefan Johansson, Martine Hoogman, Jasmin Romanos, Andrea Boreatti-Hümmer, Monika Heine, Christian P Jacob, Klaus-Peter Lesch, Miguel Casas, Marta Ribasés, Rosa Bosch, Cristina Sánchez-Mora, Núria Gómez-Barros, Noèlia Fernàndez-Castillo, Mònica Bayés, Anne Halmøy, Helene Halleland, Elisabeth T Landaas, Ole B Fasmer, Per M Knappskog, Angelien J G A M Heister, Lambertus A Kiemeney, J J Sandra Kooij, A Marije Boonstra, Cees C Kan, Philip Asherson, Stephen V Faraone, Jan K Buitelaar, Jan Haavik, Bru Cormand, Josep Antoni Ramos-Quiroga et Andreas Reif : Multicenter analysis of the slc6a3/dat1 vntr haplotype in persistent adhd suggests differential involvement of the gene in childhood and persistent adhd. *Neuropsychopharmacology : official publication of the American College of Neuropsychopharmacology*, 35:656–664, février 2010.

[38] T Frodl et N Skokauskas : Meta-analysis of structural mri studies in children and adults with attention deficit hyperactivity disorder indicates treatment effects. *Acta psychiatrica Scandinavica*, 125:114–126, février 2012.

[39] Nicolas Frémaux et Wulfram Gerstner : Neuromodulated spike-timing-dependent plasticity, and theory of three-factor learning rules. *Frontiers in neural circuits*, 9:85, 2015.

[40] Justine A Fuller, Mark H Burrell, Andrew G Yee, Kavinda Liyanagama, Janusz Lipski, Jeffery R Wickens et Brian I Hyland : Role of homeostatic feedback mechanisms in modulating methylphenidate actions on phasic dopamine signaling in the striatum of awake behaving rats. *Progress in neurobiology*, 182:101681, novembre 2019.

[41] Paolo Fusar-Poli, Katya Rubia, Giorgio Rossi, Giuseppe Sartori et Umberto Balottin : Striatal dopamine transporter alterations in adhd: pathophysiology or adaptation to psychostimulants? a meta-analysis. *The American journal of psychiatry*, 169:264–272, mars 2012.

[42] J N Giedd, J Blumenthal, E Molloy et F X Castellanos : Brain imaging of attention deficit/hyperactivity disorder. *Annals of the New York Academy of Sciences*, 931:33–49, juin 2001.

[43] Ian R Gizer, Courtney Ficks et Irwin D Waldman : Candidate gene studies of adhd: a meta-analytic review. *Human genetics*, 126:51–90, juillet 2009.

[44] A A Grace : Phasic versus tonic dopamine release and the modulation of dopamine system responsivity: a hypothesis for the etiology of schizophrenia. *Neuroscience*, 41:1–24, 1991.

[45] Anthony A. Grace : Psychostimulant actions on dopamine and limbic system function: Relevance to the pathophysiology and treatment of adhd. *Stimulant drugs and ADHD: Basic and clinical neuroscience.*, pages 134–157, 2001.

[46] Anthony A Grace : Dysregulation of the dopamine system in the pathophysiology of schizophrenia and depression. *Nature reviews. Neuroscience*, 17:524–532, août 2016.

[47] Edna Grünblatt, Anna Maria Werling, Alexander Roth, Marcel Romanos et Susanne Walitza : Association study and a systematic meta-analysis of the vntr polymorphism in the 3'-utr of dopamine transporter gene and attention-deficit hyperactivity disorder. *Journal of neural transmission (Vienna, Austria : 1996)*, 126:517–529, avril 2019.

[48] F Grünhage, T G Schulze, D J Müller, M Lanczik, E Franzek, M Albus, M Borrmann-Hassenbach, M Knapp, S Cichon, W Maier, M Rietschel, P Propping et M M Nöthen : Systematic screening for dna sequence variation in the coding region of the human dopamine transporter gene (dat1). *Molecular psychiatry*, 5:275–282, mai 2000.

[49] Jonas Hannestad, Jean-Dominique Gallezot, Beata Planeta-Wilson, Shu-Fei Lin, Wendol A Williams, Christopher H van Dyck, Robert T Malison, Richard E Carson et Yu-Shin Ding : Clinically relevant doses of methylphenidate significantly occupy norepinephrine transporters in humans in vivo. *Biological psychiatry*, 68:854–860, novembre 2010.

[50] Tobias U Hauser, Vincenzo G Fiore, Michael Moutoussis et Raymond J Dolan : Computational psychiatry of adhd: Neural gain impairments across marrian levels of analysis. *Trends in neurosciences*, 39:63–73, février 2016.

[51] Tobias U Hauser, Reto Iannaccone, Juliane Ball, Christoph Mathys, Daniel Brandeis, Susanne Walitza et Silvia Brem : Role of the medial prefrontal cortex in impaired decision making in juvenile attention-deficit/hyperactivity disorder. *JAMA psychiatry*, 71:1165–1173, octobre 2014.

[52] Aaron S Hervey, Jeffery N Epstein, John F Curry, Simon Tonev, L Eugene Arnold, C Keith Conners, Stephen P Hinshaw, James M Swanson et Lily Hechtman : Reaction time distribution analysis of neuropsychological performance in an adhd sample. *Child neuropsychology : a journal on normal and abnormal development in childhood and adolescence*, 12:125–140, avril 2006.

[53] B Hille : G protein-coupled mechanisms and nervous signaling. *Neuron*, 9:187–195, août 1992.

[54] A S Horn : Dopamine uptake: a review of progress in the last decade. *Progress in neurobiology*, 34:387–400, 1990.

[55] Cynthia L Huang-Pollock, Sarah L Karalunas, Helen Tam et Amy N Moore : Evaluating vigilance deficits in adhd: a meta-analysis of cpt performance. *Journal of abnormal psychology*, 121:360–371, mai 2012.

[56] Lars Hunger, Arvind Kumar et Robert Schmidt : Abundance compensates kinetics: Similar effect of dopamine signals on d1 and d2 receptor populations. *The Journal of neuroscience : the official journal of the Society for Neuroscience*, 40:2868–2881, avril 2020.

[57] Jacob N S Jackson et James MacKillop : Attention-deficit/hyperactivity disorder and monetary delay discounting: A meta-analysis of case-control studies. *Biological psychiatry. Cognitive neuroscience and neuroimaging*, 1:316–325, juillet 2016.

[58] Carrie E John, Evgeny A Budygin, Yolanda Mateo et Sara R Jones : Neurochemical characterization of the release and uptake of dopamine in ventral tegmental area and serotonin in substantia nigra of the mouse. *Journal of neurochemistry*, 96:267–282, janvier 2006.

[59] Michael J Kofler, Mark D Rapport, Dustin E Sarver, Joseph S Raiker, Sarah A Orban, Lauren M Friedman et Ellen G Kolomeyer : Reaction time variability in adhd: a meta-analytic review of 319 studies. *Clinical psychology review*, 33:795–811, août 2013.

[60] Gabriella Lambacher, Esterina Pascale, Mariangela Pucci, Silvia Mangiapelo, Claudio D'Addario et Walter Adriani : Search for an epigenetic biomarker in adhd diagnosis, based on the dat1 gene 5'-utr methylation: a new possible approach. *Psychiatry research*, 291:113154, septembre 2020.

[61] Steve S Lee, Benjamin B Lahey, Irwin Waldman, Carol A Van Hulle, Paul Rathouz, William E Pelham, Jan Loney et Edwin H Cook : Association of dopamine transporter genotype with disruptive behavior disorders in an eight-year longitudinal study of children and adolescents. *American journal of medical genetics. Part B, Neuropsychiatric genetics : the official publication of the International Society of Psychiatric Genetics*, 144B:310–317, avril 2007.

[62] C Leth-Steensen, Z K Elbaz et V I Douglas : Mean response times, variability, and skew in the responding of adhd children: a response time distributional approach. *Acta psychologica*, 104:167–190, mai 2000.

[63] Dawei Li, Pak C Sham, Michael J Owen et Lin He : Meta-analysis shows significant association between dopamine system genes and attention deficit hyperactivity disorder (adhd). *Human molecular genetics*, 15:2276–2284, juillet 2006.

[64] H-Y Lin, S-L Hwang-Gu et S S-F Gau : Intra-individual reaction time variability based on ex-gaussian distribution as a potential endophenotype for attention-deficit/hyperactivity disorder. *Acta psychiatrica Scandinavica*, 132:39–50, juillet 2015.

[65] Marjolein Luman, Tieme W P Janssen, Marleen Bink, Rosa van Mourik, Athanasios Maras et Jaap Oosterlaan : Probabilistic learning in children with attention-deficit/hyperactivity disorder. *Journal of attention disorders*, page 1087054720905094, février 2020.

[66] M Marinelli et J E McCutcheon : Heterogeneity of dopamine neuron activity across traits and states. *Neuroscience*, 282:176–197, décembre 2014.

[67] L J May, W G Kuhr et R M Wightman : Differentiation of dopamine overflow and uptake processes in the extracellular fluid of the rat caudate nucleus with fast-scan in vivo voltammetry. *Journal of neurochemistry*, 51:1060–1069, octobre 1988.

[68] Tomohiro Nakao, Joaquim Radua, Katya Rubia et David Mataix-Cols : Gray matter volume abnormalities in adhd: voxel-based meta-analysis exploring the effects of age and stimulant medication. *The American journal of psychiatry*, 168:1154–1163, novembre 2011.

[69] C Nicholson : Interaction between diffusion and michaelis-menten uptake of dopamine after iontophoresis in striatum. *Biophysical journal*, 68:1699–1715, mai 1995.

[70] Luke J Norman, Christina Carlisi, Steve Lukito, Heledd Hart, David Mataix-Cols, Joaquim Radua et Katya Rubia : Structural and functional brain abnormalities in attention-deficit/hyperactivity disorder and obsessive-compulsive disorder: A comparative meta-analysis. *JAMA psychiatry*, 73:815–825, août 2016.

[71] Marianne Oldehinkel, Christian F Beckmann, Raimon H R Pruim, Erik S B van Oort, Barbara Franke, Catharina A Hartman, Pieter J Hoekstra, Jaap Oosterlaan, Dirk Heslenfeld, Jan K Buitelaar et Maarten Mennes : Attention-deficit/hyperactivity disorder symptoms coincide with altered striatal connectivity. *Biological psychiatry. Cognitive neuroscience and neuroimaging*, 1:353–363, juillet 2016.

[72] Connor H G Patros, R Matt Alderson, Lisa J Kasper, Stephanie J Tarle, Sarah E Lea et Kristen L Hudec : Choice-impulsivity in children and adolescents with attention-deficit/hyperactivity disorder (adhd): A meta-analytic review. *Clinical psychology review*, 43:162–174, février 2016.

[73] Jonathan Posner, Virginia Rauh, Allison Gruber, Inbal Gat, Zhishun Wang et Bradley S Peterson : Dissociable attentional and affective circuits in medication-naïve children with attention-deficit/hyperactivity disorder. *Psychiatry research*, 213:24–30, juillet 2013.

[74] E N Pothos, V Davila et D Sulzer : Presynaptic recording of quanta from midbrain dopamine neurons and modulation of the quantal size. *The Journal of neuroscience : the official journal of the Society for Neuroscience*, 18:4106–4118, juin 1998.

[75] Peter Redgrave, Kevin Gurney et John Reynolds : What is reinforced by phasic dopamine signals? *Brain research reviews*, 58:322–339, août 2008.

[76] John N J Reynolds et Jeffery R Wickens : Dopamine-dependent plasticity of corticostriatal synapses. *Neural networks : the official journal of the International Neural Network Society*, 15:507–521, 2002.

[77] Margaret E Rice et Stephanie J Cragg : Dopamine spillover after quantal release: rethinking dopamine transmission in the nigrostriatal pathway. *Brain research reviews*, 58:303–313, août 2008.

[78] Brooks G Robinson, James R Bunzow, Jonathan B Grimm, Luke D Lavis, Joshua T Dudman, Jennifer Brown, Kim A Neve et John T Williams : Desensitized d2 autoreceptors are resistant to trafficking. *Scientific reports*, 7:4379, juin 2017.

[79] Jacqueline Fifi Saad, Kristi R Griffiths et Mayuresh S Korgaonkar : A systematic review of imaging studies in the combined and inattentive subtypes of attention deficit hyperactivity disorder. *Frontiers in integrative neuroscience*, 14:31, 2020.

[80] Terje Sagvolden, Espen Borgå Johansen, Heidi Aase et Vivienne Ann Russell : A dynamic developmental theory of attention-deficit/hyperactivity disorder (adhd) predominantly hyperactive/impulsive and combined subtypes. *The Behavioral and brain sciences*, 28:397–419; discussion 419–68, juin 2005.

[81] Björn H Schott, Constanze I Seidenbecher, Daniela B Fenker, Corinna J Lauer, Nico Bunzeck, Hans-Gert Bernstein, Wolfgang Tischmeyer, Eckart D Gundelfinger, Hans-Jochen Heinze et Emrah Düzel : The dopaminergic midbrain participates in human episodic memory formation: evidence from genetic imaging. *The Journal of neuroscience : the official journal of the Society for Neuroscience*, 26:1407–1417, février 2006.

[82] W Schultz, P Dayan et P R Montague : A neural substrate of prediction and reward. *Science (New York, N.Y.)*, 275:1593–1599, mars 1997.

[83] Wolfram Schultz : Getting formal with dopamine and reward. *Neuron*, 36:241–263, octobre 2002.

[84] Wolfram Schultz : Dopamine reward prediction error coding. *Dialogues in clinical neuroscience*, 18:23–32, mars 2016.

[85] Wolfram Schultz : Reward prediction error. *Current Biology*, 27(10):R369 – R371, 2017.

[86] Shimon Schwartz et Christoph U Correll : Efficacy and safety of atomoxetine in children and adolescents with attention-deficit/hyperactivity disorder: results from a comprehensive meta-analysis and metaregression. *Journal of the American Academy of Child and Adolescent Psychiatry*, 53:174–187, février 2014.

[87] D Schönfuss, T Reum, P Olshausen, T Fischer et R Morgenstern : Modelling constant potential amperometry for investigations of dopaminergic neurotransmission kinetics in vivo. *Journal of neuroscience methods*, 112:163–172, décembre 2001.

[88] Larry J Seidman, Eve M Valera et Nikos Makris : Structural brain imaging of attention-deficit/hyperactivity disorder. *Biological psychiatry*, 57:1263–1272, juin 2005.

[89] Neivo Silva, Claudia M Szobot, Ming C Shih, Marcelo Q Hoexter, Carlos Eduardo Anselmi, Flavio Pechansky, Rodrigo A Bressan et Luis Augusto Rohde : Searching for a neurobiological basis for self-medication theory in adhd comorbid with substance use disorders: an in vivo study of dopamine transporters using (99m)tc-trodat-1 spect. *Clinical nuclear medicine*, 39:e129–e134, février 2014.

[90] H Stanislaw et N Todorov : Calculation of signal detection theory measures. *Behavior research methods, instruments, & computers : a journal of the Psychonomic Society, Inc*, 31:137–149, février 1999.

[91] Eva Syková et Charles Nicholson : Diffusion in brain extracellular space. *Physiological reviews*, 88:1277–1340, octobre 2008.

[92] Lixia Tian, Tianzi Jiang, Yufeng Wang, Yufeng Zang, Yong He, Meng Liang, Manqiu Sui, Qingjiu Cao, Siyuan Hu, Miao Peng et Yan Zhuo : Altered resting-state functional connectivity patterns of anterior cingulate cortex in adolescents with attention deficit hyperactivity disorder. *Neuroscience letters*, 400:39–43, mai 2006.

[93] Yi-Min Tien, Vincent Chin-Hung Chen, Tun-Shin Lo, Chia-Fen Hsu, Michael Gossop et Kuo-You Huang : Deficits in auditory sensory discrimination among children with attention-deficit/hyperactivity disorder. *European child & adolescent psychiatry*, 28:645–653, mai 2019.

[94] Erika Tonelli, Esterina Pascale, Miriam Troianiello, Claudio D'Addario et Walter Adriani : Dat1 gene methylation as an epigenetic biomarker in attention deficit hyperactivity disorder: A commentary. *Frontiers in genetics*, 11:444, 2020.

[95] Gail Tripp et Jeff R Wickens : Research review: dopamine transfer deficit: a neurobiological theory of altered reinforcement mechanisms in adhd. *Journal of child psychology and psychiatry, and allied disciplines*, 49:691–704, juillet 2008.

[96] Elizabeth M Tunbridge, Marco Narajos, Charlotte H Harrison, Charles Beresford, Andrea Cipriani et Paul J Harrison : Which dopamine polymorphisms are functional? systematic review and meta-analysis of comt, dat, dbh, ddc, drd1-5, maoa, maob, th, vmat1, and vmat2. *Biological psychiatry*, 86:608–620, octobre 2019.

[97] Christine Ulke, Michael Rullmann, Jue Huang, Julia Luthardt, Georg-Alexander Becker, Marianne Patt, Philipp M Meyer, Solveig Tiepolt, Swen Hesse, Osama Sabri et Maria Strauss : Adult attention-deficit/hyperactivity disorder is associated with reduced norepinephrine transporter availability in right attention networks: a (s,s)-o-[, javax.xml.bind.jaxbelement@32a363f0, c]methylreboxetine positron emission tomography study. *Translational psychiatry*, 9:301, novembre 2019.

[98] Michael A van der Kooij et Jeffrey C Glennon : Animal models concerning the role of dopamine in attention-deficit hyperactivity disorder. *Neuroscience and biobehavioral reviews*, 31:597–618, 2007.

[99] Florence Véronneau-Veilleux, Philippe Robaey, Mauro Ursino et Fahima Nekka : An integrative model of parkinson's disease treatment including levodopa pharmacokinetics, dopamine kinetics, basal ganglia neurotransmission and motor action throughout disease progression. *Journal of pharmacokinetics and pharmacodynamics*, octobre 2020.

[100] N D Volkow, G J Wang, J S Fowler, S J Gatley, J Logan, Y S Ding, R Hitzemann et N Pappas : Dopamine transporter occupancies in the human brain induced by therapeutic doses of oral methylphenidate. *The American journal of psychiatry*, 155:1325–1331, octobre 1998.

[101] Nora D Volkow, Gene-Jack Wang, Joanna S Fowler et Yu-Shin Ding : Imaging the effects of methylphenidate on brain dopamine: new model on its therapeutic actions for attention-deficit/hyperactivity disorder. *Biological psychiatry*, 57:1410–1415, juin 2005.

[102] P Waelti, A Dickinson et W Schultz : Dopamine responses comply with basic assumptions of formal learning theory. *Nature*, 412:43–48, juillet 2001.

[103] Matthew J Wanat, Ingo Willuhn, Jeremy J Clark et Paul E M Phillips : Phasic dopamine release in appetitive behaviors and drug addiction. *Current drug abuse reviews*, 2:195–213, mai 2009.

[104] Gene-Jack Wang, Nora D Volkow, Timothy Wigal, Scott H Kollins, Jeffrey H Newcorn, Frank Telang, Jean Logan, Millard Jayne, Christopher T Wong, Hao Han, Joanna S Fowler, Wei Zhu et James M Swanson : Long-term stimulant treatment affects brain dopamine transporter level in patients with attention deficit hyperactive disorder. *PloS one*, 8:e63023, 2013.

[105] Robert J Wickham, Wojciech Solecki, Liza R Rathbun, Nichole M Neugebauer, Robert Mark Wightman et Nii A Addy : Advances in studying phasic dopamine signaling in brain reward mechanisms. *Frontiers in bioscience (Elite edition)*, 5:982–999, juin 2013.

[106] Alexis C Wood, Jan Buitelaar, Fruhling Rijsdijk, Philip Asherson et Jonna Kuntsi : Rethinking shared environment as a source of variance underlying attention-deficit/hyperactivity disorder symptoms: comment on burt (2009). *Psychological bulletin*, 136:331–340, mai 2010.

[107] Yi Xu, Xiang-Tao Chen, Man Luo, Yuqing Tang, Guangxiang Zhang, De Wu, Bin Yang, Di-Yun Ruan et Hui-Li Wang : Multiple epigenetic factors predict the attention deficit/hyperactivity disorder among the chinese han children. *Journal of psychiatric research*, 64:40–50, mai 2015.

Cinquième chapitre.

Mathematical simulation of methylphenidate response in a model of dopamine release imbalance: insights for ADHD treatment

par

Florence Véronneau-Veilleux[1], Philippe Robaey[2], Mauro Ursino[3] et Fahima Nekka[4]

([1]) Faculté de Pharmacie, Université de Montréal, Montréal, QC, Canada

([2]) Children's Hospital of Eastern Ontario, University of Ottawa, Ottawa, Ontario, Canada

([3]) Department of Electrical, Electronic and Information Engineering "Guglielmo Marconi", University of Bologna, Bologna 40136, Italy

([4]) Faculté de Pharmacie, Université de Montréal
Centre de recherches mathématiques, Université de Montréal,
Centre for Applied Mathematics in Bioscience and Medicine (CAMBAM), McGill University, Montréal, Québec, Canada

Cet article est en préparation.

Le méthylphénidate est fréquemment utilisé pour réduire les symptômes du TDAH. Pourtant, jusqu'à 30% des patients n'y répondent pas et les causes sont mal connues. L'ojectif de ce dernier chapitre est d'évaluer les différentes réponses au méthylphénidate engendrées par l'inhibition de la recapture de la dopamine durant l'apprentissage par renforcement dans les ganglions de la base. Pour ce faire, un modèle pharmacocinétique du méthylphénidate est intégré au modèle des ganglions de la base présenté au Chapitre 4 de la présente thèse. Une cohorte de patients virtuels présentant des symptômes typiques du TDAH est créée et leurs réponses au méthylphénidate à travers différents schémas d'apprentissage par renforcement sont analysées. Une métrique précédemment développée est utilisée pour différencier les répondants des non-répondants et met en évidence l'implication potentielle d'un apprentissage excessif de certaines réponses chez les non-répondants.

Abstract. Methylphenidate (MPH) is widely used to reduce the symptoms of hyperactivity, inattention and impulsivity in attention-deficit hyperactivity disorder (ADHD). However, up to 30% of patients are considered non-responders because they do not have beneficial effects or have adverse effects with MPH. MPH acts by blocking the recapture of noradrenaline and dopamine, which is involved in reinforcement learning. This study aims to investigate the effect of dopamine recapture inhibition by MPH on reinforcement learning in the dopaminergic system of basal ganglia on the different responses to MPH using mechanistic modeling. To this aim, we combined a pharmacokinetic model of MPH with a brain compartment to a previously developed model of the dopaminergic system of basal ganglia. A cohort of 30 virtual patients with ADHD-like symptoms were created and their responses to MPH during a choice reaction task with different reinforcement learning patterns were analyzed. A metric was developed to differentiate the responders from the non-responders, highlighting the excessive learning of some responses among non-responders. The dose response relationship was also simulated.

Keywords: ADHD, methylphenidate, responders, mechanistic modeling, reinforcement learning

1. Introduction

Stimulant medications (methylphenidate - MPH, salt of amphetamines) are the first-line pharmacological treatment for attention deficit hyperactivity disorder (ADHD). ADHD is a complex neurodevelopmental disorder characterized by pervasive inattention, impulsivity, and restlessness that is inconsistent with the patient's age [**3**]. MPH inhibits both dopamine (DA) and norepinephrine (NE) reuptake by blocking their respective transporters (DAT and NET), thereby increasing the availability of DA and NE at the synaptic level. Positron emission tomography (PET) studies in humans have shown that MPH bound to DAT in basal ganglia (ED50 = 0.25 mg/kg) [**58**] but also to NET (ED50 = 0.14 mg/kg) [**28**], especially in the thalamus, with a higher affinity than for DAT. In the basal ganglia, MPH increases synaptic dopamine by blocking DAT. However, in the prefrontal cortex, where NET mediates both DA and NE reuptake, MPH increases synaptic availability of both DA and NE [**7**]. It

is therefore unclear whether the effects of MPH are primarily related to its binding to DAT, NET, or both.

Determining whether the mechanisms of action of MPH is primarily dopaminergic, noradrenergic or mixed is of therapeutic importance because ADHD is a complex disorder for which imbalances in both NE and DA firing patterns have been proposed. The question is also relevant in a therapeutic perspective as about 20-30% of ADHD patients show poor response to MPH [**24**]. Alternative medications more specific to the NE system can then be proposed, such as alpha-2 adrenergic agonists (clonidine, guanfacine) or selective NE reuptake inhibitors (atomoxetine). Predictors of the response to MPH could give insights about the system involved in the therapeutic effect.

Over the past decade, pharmacogenetic studies have most often taken a candidate gene approach to test whether the genetic variants that influence response to MPH are more relevant to the dopaminergic or noradrenergic system. However, they have not yielded consistent results [**18**]. A recent meta-analysis concluded a small but significant impact on MPH efficacy of genetic variants affecting the dopaminergic system (dopamine transporter), dopamine (D4 receptor), but also the NE system (adrenergic receptor(α2A), NET), or both systems (catechol-O-methyltransferase).

Another line of research was to determine whether certain brain structures more related to the DA or NE system could predict the response to MPH. Patients who respond poorly to MPH have reduced striatal volume [**37**] and increased fronto-striatal connectivity [**30**], compared with good responders. Long-term treatment was also associated with normalization of gray matter volume in the right caudate nucleus [**38**]. These observations are consistent with the normalizing effect of a single dose of MPH on basal ganglia activity and their functional connectivity with the frontal cortex and cerebellum [**45, 46**]. These studies suggest that DA plays a key role in MPH therapeutic effect, as it is the most abundant neuromodulator in the basal ganglia (striatum and caudate nuclei).

However, the question of the preferential mode of action of MPH remains elusive, especially because of the heterogeneity of the patients themselves who may associate to varying

degrees abnormalities in both systems that are functionally linked. We have therefore turned to computational models where it is possible to model one component only and test whether this particular component can reproduce the effects of treatment as observed in the clinic.

The objective of the present study is therefore to investigate therapeutic responses to MPH and identify potential indicators that differentiate responders through mathematical mechanistic modeling of basal ganglia's dopaminergic system. We here adapt to the context of ADHD and MPH a basal ganglia model that we previously developed for the study of Parkinson's disease and levodopa [**60**]. We use this model to simulate the therapeutic response to MPH while a learning pattern is applied to virtual individuals with ADHD-like characteristics having a tonic and phasic dopamine imbalance. Although both noradrenaline and dopamine are involved in ADHD, only the latter neurotransmitter is modeled in this study.

Our previously developed model of ADHD is characterized by a DA release imbalance (increased phasic and decreased tonic release) in the basal ganglia [**59**]. Lower tonic activity, in addition to its own sustained effect, increases the phasic reward prediction error (DA phasic increase) through DA binding with autoreceptors [**1**]. By modeling one component of ADHD (DA in basal ganglia) and using a task (reinforcement learning) which is known to engage the DA striatal-cortical loop [**21**], we tested the effects of a DA release imbalance. In this paper, we test the normalizing effect of MPH. We showed that virtual subjects with DA imbalance exhibited a distinct ADHD trait: an increased variability in response times that was produced by a mixture of fast and slow responses, which ultimately impaired performance. Furthermore, we showed that the proportion of slow and fast responses, as well as the degraded performance, depended on individual learning histories in which some responses are reinforced to the expense of other responses.

Using this model, in the present study, we simulated the therapeutic response to MPH and specifically tested the effect of the stimulant on the DA system in the basal ganglia. Specifically, we addressed three research questions about MPH responders: (1) Can increased variability and decreased accuracy in response be improved by modeling the effect of MPH

on DAT reuptake once this ADHD trait has developed during learning in subjects with DA release imbalance? (2) Is the proportion of responders vs. non-responders a function not only of their response variability but also of their learning history? (3) Given that in Grace's model, both tonic and phasic components of DA release are affected [**1**], what are the most critical components to consider in distinguishing responders from non-responders? In the present model, responders are defined as those whose performance increases with methylphenidate as in [**11**].

The model and parameters estimation are first introduced in the Methods Section. Next, therapeutic response to MPH with different learning patterns are analyzed in the Results Section, where a metric differentiating responders from non-responders is also introduced, along with the dose-response relationship.

2. Methods

The mechanistic model of basal ganglia's dopaminergic system used here consists of three parts. The first part is a pharmacokinetic model of MPH immediate release, where a brain compartment is included. The MPH brain concentration modifies the recapture of dopamine described in the second part of the model. Indeed, the second part is the dopamine dynamic model, describing the release, recapture, affected by the MPH concentration in the brain compartment, and elimination of dopamine. Dopamine concentration then modifies the neuronal activity in the basal ganglia model. Finally, the third part is the neurocomputational model of basal ganglia relating neuronal activity with dopamine. The three parts of the model are represented in Figure 41.

In addition to this model, the following section describes the creation of a cohort of 30 virtual individuals with tonic and phasic dopamine imbalance, presenting ADHD-like symptoms (as described in [**59**]), as well as the procedure used to account for reinforcement learning.

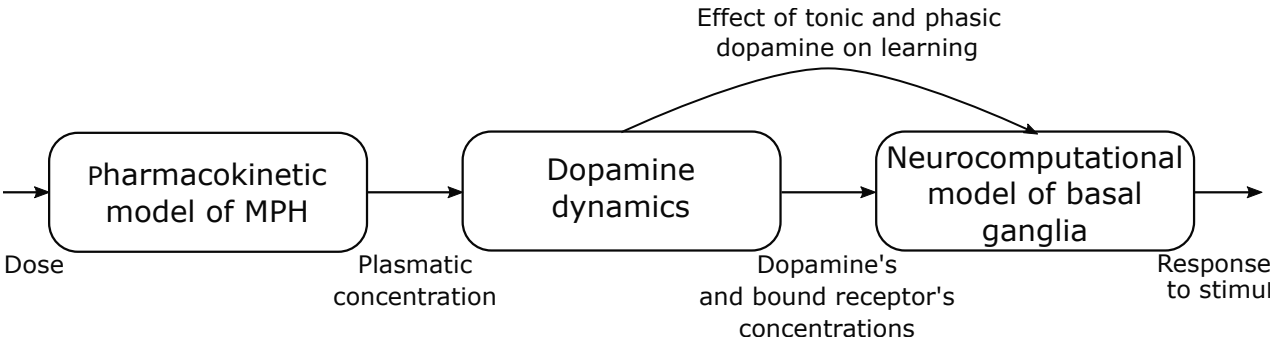

Figure 41. Representation of the three parts of the model and their relation.

2.1. Pharmacokinetic model of MPH with brain compartment

MPH is a first-choice stimulant treatment to alleviate ADHD symptoms. MPH is available in different formulations, including immediate and extended release. MPH can cross the blood-brain barrier and works primarily by blocking dopamine and noradrenaline transporters, respectively DATs and NETs [**12**]. In this work, we consider the immediate release MPH and its effect on blocking DATs.

This pharmacokinetic (PK) model of oral MPH, depicted in Figure 42, was adapted from a population PK model of MPH immediate release developed with data of 44 males [**8**]. It is a one compartment model with first order absorption and elimination. A compartment was added to account for the kinetics of MPH in the brain since we wanted to model MPH effect on blocking DATs in the basal ganglia.

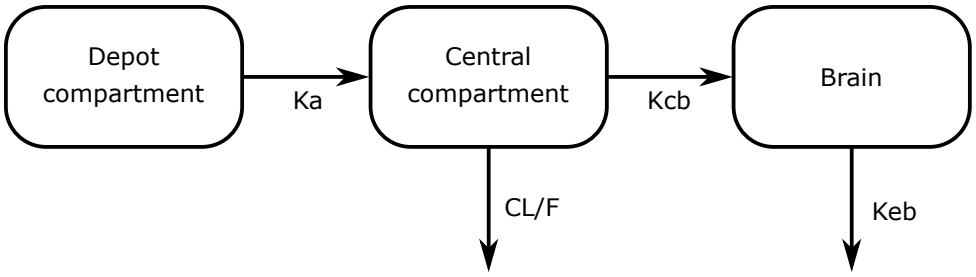

Figure 42. Representation of the PK model of MPH.

As a first approximation, the variability of the PK parameters was omitted, and only the typical values were used here. The inter and intra-individual variabilities should be added in future studies.

The equations of the PK model are the following:

$$\frac{dA_{depot}}{dt} = -K_a A_{depot}, \tag{2.1}$$

$$\frac{dA_{central}}{dt} = K_a A_{depot} - \left(\frac{CL/F}{V/F} + K_{cb}\right) A_{central}, \tag{2.2}$$

$$C_{MPH_{plasma}} = \frac{A_{central}}{V/F}, \tag{2.3}$$

where A_{depot} and $A_{central}$ are respectively the quantity of MPH in the depot and central compartments. The parameters K_{cb}, K_{eb} representing the transfer rate from the central to the brain compartment, and the elimination rate from the brain compartment, respectively, are added to the initial PK model by Bonnefois et al. [**8**]. In order to reproduce the results described in [**8**] for plasma kinetics, the term $\left(\frac{CL/F}{V/F} + K_{cb}\right)$ is fixed as the typical value of $\frac{CL/F}{V/F}$ in [**8**], with K_{cb} estimated from data as described in the following sections. Given $K_e = \frac{CL/F}{V/F} + K_{cb}$, the explicit expression for $A_{central}$ is $A_{central} = \frac{DoseK_a}{K_a - K_e}(e^{-K_e t} - e^{-K_a t})$.

The brain compartment kinetics is decribed by the following equations:

$$\frac{dA_{brain}}{dt} = K_{cb} A_{central} - K_{eb} A_{brain}, \tag{2.4}$$

$$C_{MPH_{brain}} = \frac{A_{brain}}{V_{brain}}, \tag{2.5}$$

where A_{brain} and $C_{MPH_{brain}}$ are respectively the quantity and the concentration of MPH in the brain compartment.

2.2. Dopamine dynamics model

The blocking effect of MPH on DATs decreases dopamine recapture, resulting in an increase in its concentration in the synaptic cleft.

The dopamine dynamic model described in [**59**] was adapted here to integrate the blocking of DATs by MPH. The equations of the dopamine dynamic model are the following:

$$\underbrace{\frac{dC_{DA}(t)}{dt}}_{\text{Dopamine concentration}} = \underbrace{(I_{DA}^{tonic} + I_{DA}^{phasic}(t))}_{\text{Dopamine Release}} - \underbrace{\frac{V_{max}C_{DA}(t)}{(k_{mDA}(t) + C_{DA}(t))}}_{\text{Recapture by DATs}} - \underbrace{k_{rem}C_{DA}(t)}_{\text{Removal}}, \tag{2.6}$$

$$\underbrace{\frac{dAR(t)}{dt}}_{\text{Autoreceptor occupancy}} = \underbrace{C_{DA}(t)k_{on}(1 - AR(t))}_{\text{Binding to autoreceptors}} - \underbrace{k_{off}AR(t)}_{\text{Unbinding to autoreceptors}}, \tag{2.7}$$

where C_{DA} is the concentration of dopamine in $\mu mol/L$, and AR represents the autoreceptors occupancy [**16, 17, 15, 20**]. Tonic and phasic dopamine denote the sustained concentrations and the burst release, respectively, with the latter being related to rewards in learning [**48, 62**].

The tonic dopamine release rate is given by:

$$I_{DA}^{tonic} = \rho\frac{P_r^{tonic}n_0}{\alpha_{vf}N_A}\upsilon_{tonic}, \tag{2.8}$$

The description and values of all parameters are given in Table 5.

Autoreceptors have a regulatory effect on dopamine concentrations and can modulate firing rate, synthesis, and release [**5, 6**]. In accordance with Grace's model [**22, 23**], a decrease of tonic dopamine will decrease autoreceptor occupancy, which in turn will increase phasic dopamine release in the model herein developed. The phasic release term at time t ($I_{DA}^{phasic}(t)$) depends on the presence of rewards or punishments during the learning task as follows:

— when there is no response yet, and no prediction error signal:

$$I_{DA}^{phasic}(t) = 0, \tag{2.9}$$

— when there is a reward at time t_{reward}:

$$I_{DA}^{phasic}(t) = \rho \frac{\left(P_r^{phasic} \cdot \frac{0.334}{AR(t)}\right) n_0 |reward|}{\alpha_{vf} N_A} \left(\upsilon_{phasic} \cdot \frac{0.334}{AR(t)}\right), \tag{2.10}$$

$$\text{for } t_{reward} + 0.1 \leq t \leq t_{reward} + 0.15, \tag{2.11}$$

— when there is a punishment at time $t_{punishment}$:

$$C_{DA}(t) = 0, \tag{2.12}$$

$$\text{for } t_{punishment} + 0.1 \leq t \leq t_{punishment} + 0.15. \tag{2.13}$$

The blocking of DATs is modeled as a binding competition between dopamine and MPH. With MPH intake, the dissociation constant for the recapture by DATs (k_m in equation 2.14) becomes the apparent dissociation constant with MPH, noted $k_{m_{DA}}(t)$ [**32**], which depends on MPH concentration in the brain and is the following function:

$$k_{m_{DA}}(t) = k_m + \frac{k_m}{0.21} \cdot C_{MPH_{brain}}(t), \tag{2.14}$$

where k_m is the dissociation constant for dopamine and DATs without MPH, and $C_{MPH_{brain}}$ is the concentration of MPH in the brain compartment. As $C_{MPH_{brain}}$ increases, $k_{m_{DA}}$ will increase, therefore recapture will decrease and the concentration of dopamine in the synaptic cleft will increase. The same type of equation was used in [**20**].

Finally, dopamine will bind to dopaminergic receptors, herein D1 and D2. Receptors occupancy is used as the postsynaptic effect of dopamine on the neurons in the neurocomputational model of basal ganglia [**29**]. The occupancy with time of receptors of type $i \in \{1,2\}$ is given by the following equation:

$$D_i(t) = \frac{B_{max}^{D_i} C_{DA}(t)}{k_D^{D_i} + C_{DA}(t)}, \tag{2.15}$$

where C_{DA} is the concentration of dopamine. The dopamine dynamic model is described in more details in [**59**].

2.3. Estimation of parameters

The PK parameters were directly set as the typical values described in [**8**]. The two added parameters related to the brain compartment, K_{cb} and K_{eb}, were estimated by fitting data of dopamine concentrations as described below. The dopamine model parameters were taken from the literature.

An optimisation algorithm implemented in Matlab was used to estimate parameters K_{cb} and K_{eb} by minimizing the distance between simulations of the model and experimental data of dopamine levels, with the intake of MPH collected on squirrel monkeys, [**13**]. Comparison of the squirrel monkeys data with the model simulations using the estimated parameters values is shown in Figure 43.

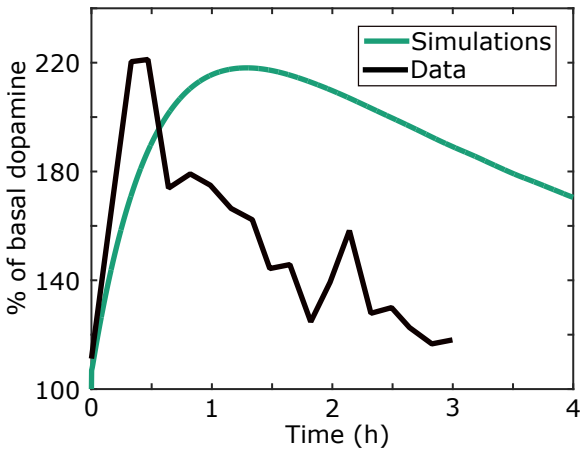

Figure 43. Comparison of increase in dopamine levels in squirrel monkeys [**13**] with a simulation of the model with the estimated value of parameters K_{cb} and K_{eb}.

Only the maximum concentration in dopamine is used in the current work, which simulated value is in adequate agreement with the data. The remaining curve features are not well reproduced, probably owing to the lack of data for this elimination part [**13**].

The estimated K_{cb} value is higher than that of $\frac{CL/F}{V/F}$, as observed in Table 4, which is in line with the literature since a significant amount of MPH crosses the blood brain barrier [**9, 61**].

Once K_{cb} and K_{eb} were estimated, simulations were performed to compare the model response with available data. Using our model, the DATs occupancy can be simulated with

the following equations:

$$DATS_{occupancyMPH} = \frac{C_{MPH_{brain}}(t)}{C_{MPH_{brain}}(t) + k_{m_{MPH}}(t)}, \tag{2.16}$$

$$k_{m_{MPH}}(t) = 0.21 + \frac{0.21}{0.15} \cdot C_{dop}(t), \tag{2.17}$$

where, $DATS_{occupancyMPH}$ is the occupancy of DATs by MPH, $C_{MPH_{brain}}$ is the MPH concentration in the brain compartment and $k_{m_{MPH}}$ is the apparent dissociation constant of MPH with DATs. DATs occupancy data were taken and combined from different sources [**51, 52, 53, 58, 57**]. The comparison of model simulated DATs occupancy with data is shown in Figure 44.

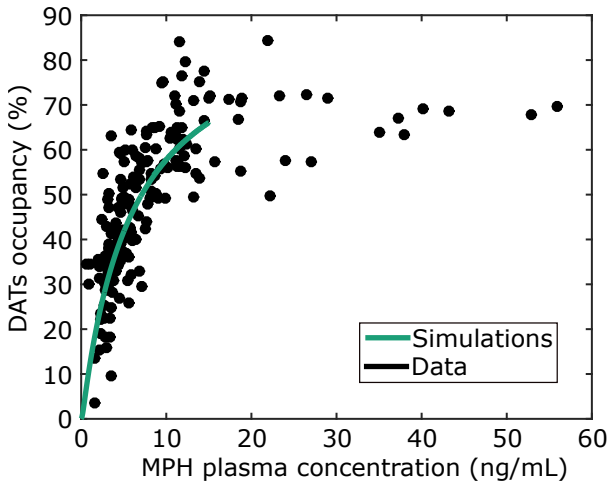

Figure 44. Comparison of DATs occupancy simulated with the model with data taken from literature [**51, 52, 53, 58, 57**].

Although the values of K_{cb} and K_{eb} were not estimated with the DATs occupancy data, the obtained model simulations are in line with these data.

Finally, the model simulation was compared to data of MPH brain concentration [**54**], as shown in Figure 45.

Again, model predictions of a variable which was not used for parameters estimation are close enough to the data.

Tables 4 and 5 report the pharmacokinetics and dopamine models' parameters value and descriptions.

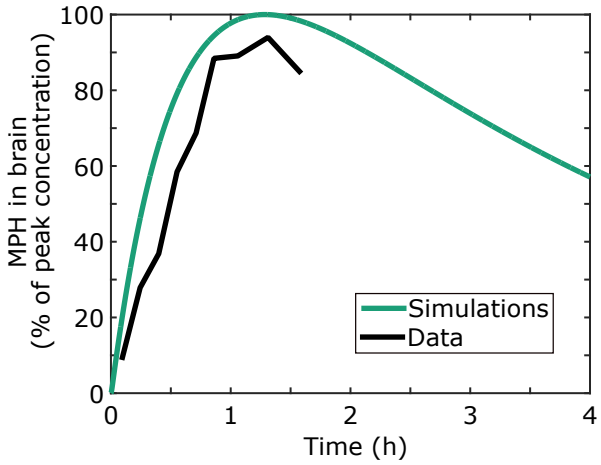

Figure 45. Percentage increase from baseline in brain MPH concentration: data [**54**] versus model simulations.

Parameters	Description	Value	Reference
CL/L	Apparent clearance	9.0920×10^{-4} L/h	[**8**]
V/F	Apparent volume of distribution	949 L	[**8**]
K_a	Absorption rate constant	1.72 h^{-1}	[**8**]
K_{cb}	Distribution rate constant from central to brain compartment	0.2676 h^{-1}	Estimated
K_{eb}	Elimination rate constant from the brain compartment	281 h^{-1}	Estimated
V_{brain}	Volume of the brain	0.1096 L	Estimated

Table 4. Parameter values of the MPH Pharmacokinetics model including the brain compartment.

2.4. Neurocomputational model of BG

To simulate the responses to a choice reaction tasks, a neurocomputational model adapted from [**4, 59**] is used. In this model, the neuronal activity in the cortex, the thalamus and in each nucleus of basal ganglia (striatum, globus pallidus intern and extern, subthalamic nucleus) is described. All sub-regions are connected through three neurotransmission pathways: direct, indirect and hyperdirect. The direct pathway promotes the movement, the indirect inhibits it and the hyperdirect pathway suppresses erroneous movements. The occupancy of the dopaminergic receptors D1 and D2 as described by equation 2.15 will modify the neuronal activity of the striatum (Go and NoGo) and that of cholinergic interneurons

Parameters	Description	Value	Reference
V_{max}	Maximal reuptake rate by DATs	1.8 $\mu M/Ls$	[**20, 36, 39, 49**]
k_m	apparent Michaelis–Menten constant	0.15 $\mu M/L$	[**20, 31, 34, 36**]
k_{rem}	Removal rate	0.04 s^{-1}	[**17**]
k_{on}	On-rate for DA binding to presynaptic autoreceptors	10 $\mu M^{-1}s^{-1}$	[**17**]
k_{off}	Off-rate for DA binding to presynaptic autoreceptors	0.4 s^{-1}	[**17**]
ρ	Density of dopamine terminals in striatum	$0.025 \cdot 10^{15}$ terminals/L	adapted
α_{vf}	Volume fraction of extracellular space	0.21	[**55**]
n_0	Number of dopamine molecules released during vesicle fusion	3000 molecules/terminal	[**15, 42**]
N_A	Avogadros constant	$6.02214076 \cdot 10^{23}$ M^{-1}	
P_r^{phasic}	Vesicle release probability	0.06	[**17**]
P_r^{tonic}	Vesicle release probability	0.06	[**17**]
υ_{tonic}	Average tonic firing rate	4 s^{-1}	[**19**]
υ_{phasic}	Average phasic firing rate	40 s^{-1}	[**19**]
B_{max}^{D1}	D_1 receptor maximal density	1.6 $\mu M/L$	[**33**]
k_D^{D1}	D_1 receptor dissociation constant	1 $\mu M/L$	[**44**]
B_{max}^{D2}	D_2 receptor maximal density	0.08 $\mu M/L$	[**33**]
k_D^{D2}	D_2 receptor dissociation constant	0.01 $\mu M/L$	[**44**]

Table 5. Parameter values of the dopamine dynamic model.

(ChI). The subregions are divided into 4 action channels in order to simulate the response of the basal ganglia to 4 different stimuli.

A representation of the neurocomputational model of basal ganglia is given in Figure 46.

The neuronal activity in each action channel is described by an ordinary differential equation, simulating neuronal dynamics, and a sigmoidal relationship that mimics the typical non-linear lower threshold and upper saturation behavior of neurons. In the equations of neuronal activity, the input is the weighted sum of the projecting neurons activities. The synaptic weight matrices w_{ij} shown in Figure 46 correspond to the weights of the connections

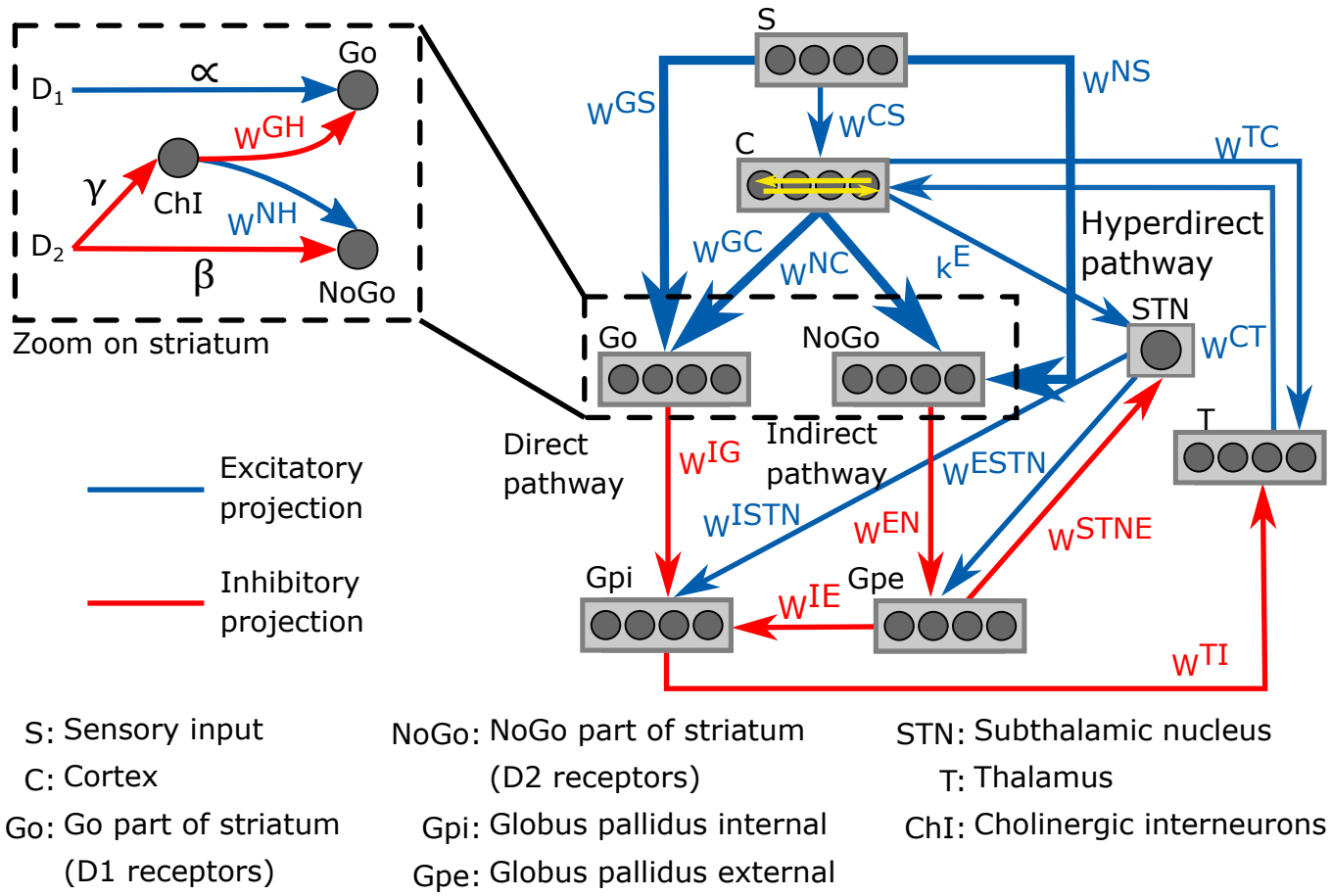

Figure 46. Representation of the neurocomputational model of BG with the three neurotransmission pathways.

between regions j and i. More details of the neurocomputational model of BG are given in [**59**].

2.5. Learning procedure

As in our previous paper [**59**], a reinforcement learning process was included in the model because it is thought to be involved in ADHD [**2, 47, 56**].

In the learning procedure, the relation between the stimuli and the response is learned through modification of some synaptic weight matrices. Most studies converge towards an implication of the striatum in the response to MPH. Therefore, only the synaptic weight matrices related to striatum, w^{GS}, w^{NS}, w^{GC} , w^{NC} were modified with the learning process;

all other weight matrices remained constant. The modification of the weight matrices is dictated by the Hebb rule, stating that two neurons having both high neuronal activity will strengthen their connection, and weaken if they have opposite activity.

A cohort of 30 virtual patients were trained with the Hebb rule, in two training phases, without and with MPH, as described below:

First phase of training without MPH:

(1) The virtual individuals are trained as described in [**59**]. Compared to control subjects, the individuals with ADHD-like symptoms have lower tonic dopamine and higher phasic dopamine levels. We hypothesized that this dopamine imbalance may be important in the onset of ADHD symptoms. This phase yields 30 individuals with differing synaptic weights, but identical physiological parameters and therefore tonic/phasic dopamine ratio [**59**].

Second phase of training with MPH:

(1) For each dose of MPH, the plasma MPH, brain MPH and dopamine concentrations are simulated. The ratio of tonic and phasic dopamine at peak plasma concentration is simulated with the model and is used as the new ratio in the second training phase.

(2) The patients receive a series of stimulus. Each entry in the stimulus vector is either 1 or 0, with the addition of noise. The expected (correct) response is an action in the same channel as the stimulus. All other responses are considered as incorrect.

The Hebb rule is described in [**59**].

In order to evaluate the effect of the rewards and punishments in training with medication, four scenarios of learning were tested and described in Table 6.

3. Results

The effect of different doses of MPH immediate release with four scenarios of reinforcement learning are simulated. The different responses, a measure to differentiate responders from non-responders, and the dose-response relationship are presented below.

Scenario	A	B	C	D
Description	-No reward -No punishment -No modification of synaptic weights -Only tonic dopamine is considered	-Rewards -Punishments -Modification of synaptic weights -Tonic and phasic dopamine considered	- No reward -Punishments -Modification of synaptic weights -Tonic and phasic dopamine considered	-Rewards -No punishment -Modification of synaptic weights -Tonic and phasic dopamine considered

Table 6. Description of the four learning scenarios

3.1. Comparison of scenarios

The 30 virtual patients were trained when medicated with MPH and using different scenarios for the learning procedure in order to compare their performances. In each scenario, the patients had to perform a choice reaction task. In this task, a series of 100 stimuli are presented to the patients through a signal S to the cortex. Each stimulus is associated with one action channel. When the patient responds to a stimulus is in the same action channel as the targeted stimulus, it is considered a correct response, otherwise it is considered as a mistake. Therefore, for each patient, it is possible to calculate the number of correct answers out of 100. Each patient performed the task before and while taking MPH. The virtual patients whose number of correct answers increased with MPH are considered responders, otherwise they are considered non-responders.

For each scenario and each dose, either 5mg or 10mg, the number of responders is computed. As an example, the number of correct responses out of 100 with 10 mg of MPH as a function of the performance without MPH in Scenario C is shown in Figure 47.

In Figure 47, individuals below and above the line represent respectively non-responders and responders. Some individuals, shown in green, had a perfect performance even before taking the medication.

For each responder, the difference in the number of correct responses with and without MPH is calculated as an indicator of the effect of MPH. The mean increase in performance of the responders was then computed to compare the impact of scenarios and doses. The results are presented in Table 7.

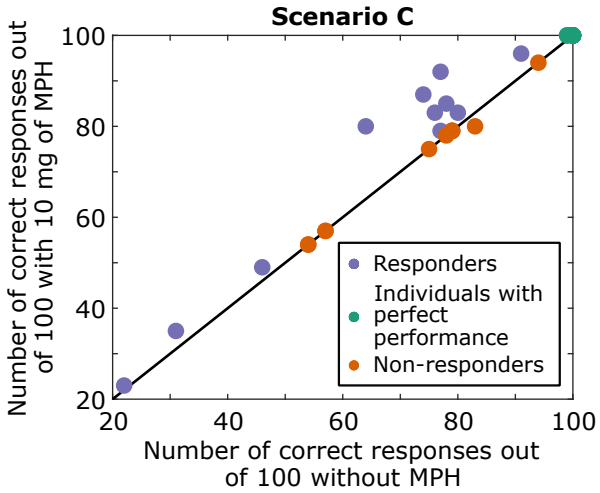

Figure 47. Performance (number of correct responses out of 100) with 10 mg MPH as a function of the performance without MPH in Scenario C.

Results	Dose: 5 mg				Dose: 10 mg			
	A	B	C	D	A	B	C	D
Number of responders	9	6	11	5	10	9	12	8
Mean increase in performance of responders	6	3.5	5.9	3.6	9.7	4.2	6.4	4.6

Table 7. Number of responders and their increase in performance for the different scenarios and doses

As observed in Table 7, the number of responders is higher in scenarios A and C, regardless of the dose administred. Since only the increase in tonic dopamine is present for scenario A, its effectiveness could mean that a significant part of the short term MPH's effect in this model is due to the increase in tonic dopamine.

In scenario C, only punishments are considered in the learning procedure. Since scenario C is one of the most performing ones, it could be interpreted that too much erroneous stimulus-response learning had occurred in the learning of patients without medication. Therefore the learning with MPH in Scenario C allows to correct these previously acquired wrong connections between stimulus and response.

Scenarios B and D do not stand out as better learning scenarios and both consider rewards in their learning procedure. This is in alignment with the assumption that too many rewards had occured in the training of these patients without medication, because the learning with more rewards cannot properly correct the wrong connections acquired previously.

In each scenario, the number of responders increase with dose. This could be interpreted by the fact that some patients do not respond to a 5 mg dose, but they do respond to a 10 mg dose.

As expected, the mean increase in performance in each scenario is higher with 10mg than with 5mg. The dose response curve will be described in more details in Section 3.3.

From this model, it can be concluded that scenarios A and C are the two best scenarios regarding the number of responders and the increase in performance. Increased tonic dopamine has an important impact on enhancing performance of MPH medicated patients. Also, punishments are more effective in improving patient's performance, probably due to the fact that these patients received too many rewards in the previous learning procedure without medication. Therefore the punishments can correct the previously acquired wrong connections.

3.2. Responders and non-responders

As shown in Table 7, the maximum percentage of responders in the four scenarios is 12/30, i.e. 40%. However, ten virtual patients had a perfect performance before taking medication, hence would not have needed to take MPH. Out of the patients without a perfect performance, 12/20, i.e. 60%, are responders, thus a bit lower than the 70% responders clinically observed [**43, 50**]. However, the objective of the present study was not to reproduce the settings of clinical studies but rather to investigate the differences between responders and non-responders. In this model, all the virtual patients have the same value of physiological parameters. Only the seed of the noise added to the stimulus used to create the patients is different. In order to create more realistic clinical settings, more inter-individual variability should be added.

In a previous paper [**59**], we developed a metric that was able to differentiate three subgroups of patients. As mentionned, these groups were trained without medication, assuming an imbalance in their tonic and phasic dopamine. In this learning process, the patients started in a naive setting, meaning that there were no differentiation between the action

channels in the synaptic weights of the striatum. A series of stimuli were sent to the patients for a total of 1000 epochs. At each epoch, a stimulus of value 1 was sent in the targeted action channel, while another stimulus of value 0.2 was sent in a different action channel; noise was sent in the two others. When the patient's response occured in the targeted action channel, he received a big reward and therefore a burst of phasic dopamine. When the patient's response was in the action channel associated with the stimulus of value 0.2, he received a small reward and a smaller burst of phasic dopamine. The patient received a punishment when the response was in the two other action channels. The synaptic weights were modified according to the Hebb rule as a consequence of these rewards and punishments.

The same procedure is used here to train the 30 patients without medication. The history of rewards and punishments is stored in a vector, with the entry at each epoch being set to 1 for a big reward, 0.1 for a small reward, -1 for a punishment, and 0 for an absence of response. The patients with dopamine imbalance had an uneven learning in the action channels, meaning that the individuals received more rewards in some action channels than others.

As is [**59**], the cumulative sum of history vector is computed to quantify the inter-individual differences in learning and is expressed by the following equations:

$$std_{history} = \frac{\sqrt{\sum_{i=1}^{1000}\left(\sum_{j=1}^{4}(cumsum_{action_j}(i) - mean(i))^2\right)}}{1000}, \tag{3.1}$$

$$ratio = \frac{1}{1000}\frac{\sum_{i=1}^{1000}\sum_{j=1}^{4}\#\text{negative } cumsum_{action_j}(i)}{\sum_{i=1}^{1000}\sum_{j=1}^{4}\#\text{positive } cumsum_{action_j}(i)}, \tag{3.2}$$

$$weighted\ std_{history} = ratio \cdot std_{history}, \tag{3.3}$$

where i is the epoch number, j the action number, $cumsum_{action_j}(i)$ the cumulative sum of history vector for action j at epoch i and $mean(i)$ is the the mean of cumulative history at epoch i for all action channels. The standard deviation of the history vector ($std_{history}$) computes the distance between the cumulative sum of history vector for each action channel, and the mean cumulative history vector for all action channels. The standard deviation of

history is weighted by a ratio in order to take into account the fact that the cumulative sum of history can be either positive or negative. Indeed, when more punishments than rewards occur during the learning process, the cumulative sum of history is negative. The ratio is the number of epochs at which the cumulative sum of history is negative divided by the the number of epochs at which the cumulative sum of history is positive, leading to a larger ratio when the negative cumulative sum exceeds the positive one. Division by 1000 is for scaling.

This weighted standard deviation of history was used previously to divide the patients in three subgroups and analyse their performance and reaction times. The subgroup a contained the individuals who had a perfect performance on a choice reaction task despite the fact that they had an imbalance in tonic and phasic dopamine. The subgroups b and c contained the individuals who did not have a perfect performance on the task. The individuals in group b had a few very slow reaction times and some faster. The distribution of the reaction times of these individuals was closer to an exponential rather than normal one. The individuals in subgroup c had an higher value of weighted standard deviation of history. Their mean reaction time was also higher, because it was not driven by few very slow responses.

The weighted standard deviation of history ($weighted\ std_{history}$) is used here again to classify the responders vs non-responders to MPH. Again, the individuals in group a are the ones with a perfect performance on the choice reaction times. The responders are found to be mostly in the subgroup b and the non-responders in subgroup c. In the present model, responders are defined as those whose performance on the choice reaction task increases either with 5 or 10 mg of methylphenidate as in [**11**]. As in [**59**], the weighted standard deviation of history ($weighted\ std_{history}$) was plotted as a function of the standard deviation of reaction times. Figure 48 shows the three subgroups with the responders and non-responders for all four scenarios.

As shown in Figure 48, while the three subgroups are not completely differentiated, it is still possible to identify characteristics of responders and non-responders to MPH. Individuals in subgroup a are non-responders by default because their performance is already perfect and therefore cannot be increased. We hypothesize that individuals in subgroup c

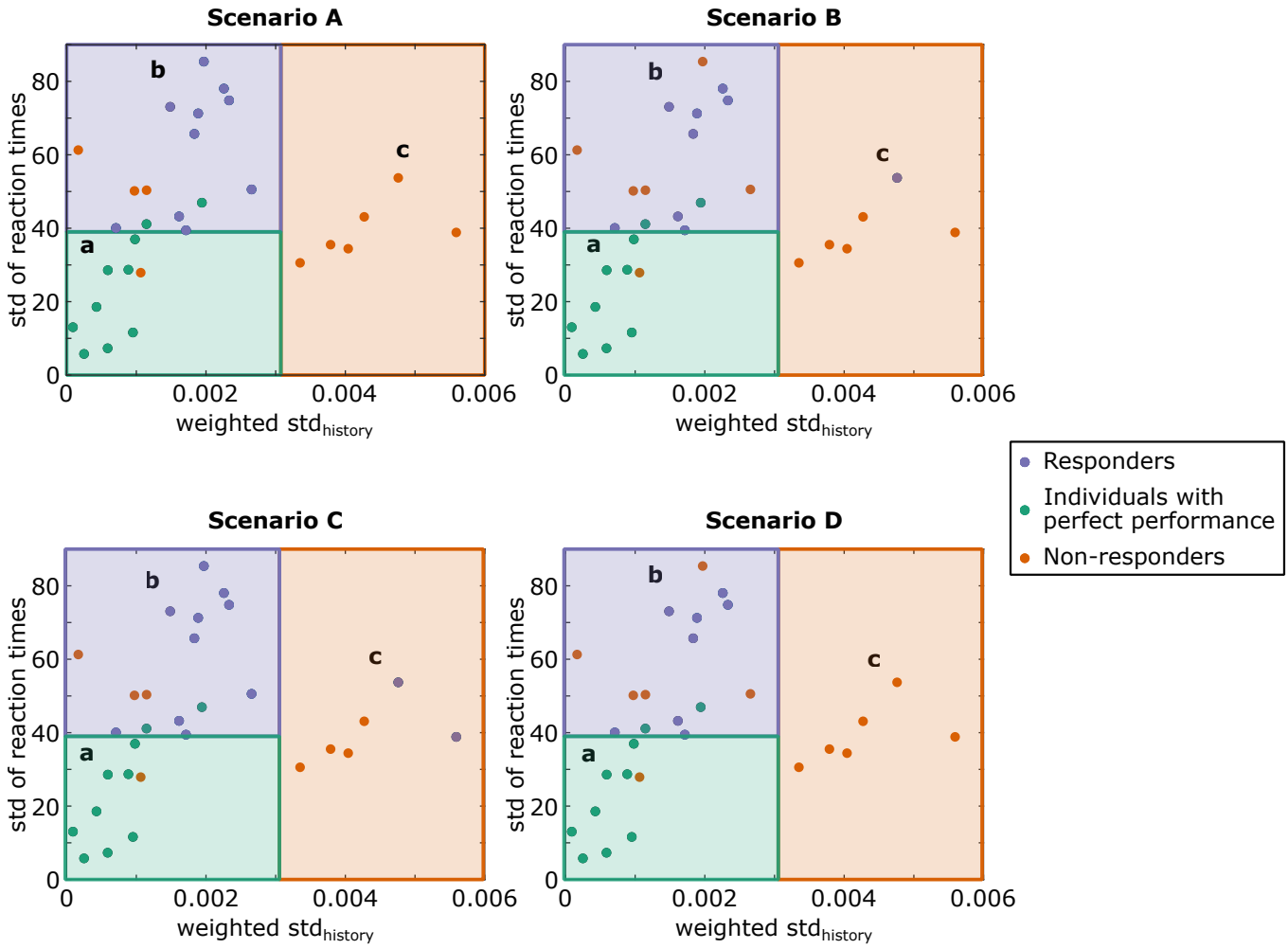

Figure 48. Standard deviation and weighted standard deviation of history for all 30 virtual patients in the four learning scenarios.

are non-responders due to excessive learning in some action channels. Indeeed, in subgroup c, the *weighted* $std_{history}$ is higher than in subgroup b, due to either a higher ratio (which would imply lower number of rewards or higher number of punishments during the learning process), or a higher standard deviation of history (indicating excessive learning in some action channels in comparison with the others).

This excessive learning in some action channels, resulting in punishments or fewer rewards for the other channels, could probably lead to wrong connections between stimulus and response. This excessive learning could not be corrected with medication. This hypothesis is in line with the fact that scenarios A and C were shown in Section 3.1 to be better than scenarios B and D at increasing the performance of medicated patients. Scenarios B and

D both contained reward in their learning procedure. Since we hypothesized that excessive learning in some action channels could impair the effect of MPH, it is consistent to obtain that the scenarios involving more learning with rewards are not as efficient as the others.

3.3. Dose-response relationship

The effect of 5 and 10 mg doses was simulated with the present model. The dose-response curves of responders for all four scenarios are shown in Figure 49, with each line representing a responder patient. The performances with a 0 mg dose are the baseline performances (without medication).

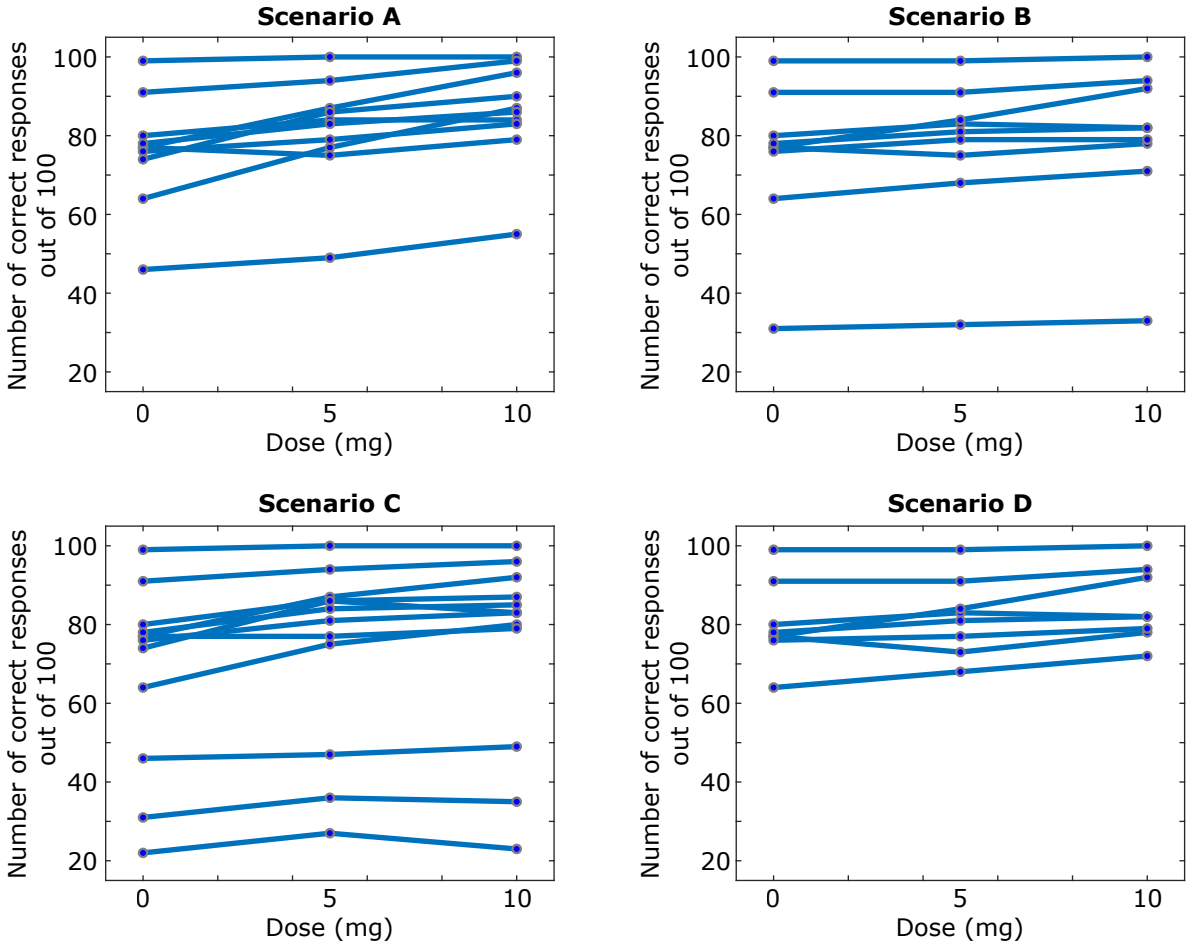

Figure 49. Dose-response curves of the responders to methylphenidate in each scenarios.

As seen in Figure 49, the performance of most patients increases with increasing doses. Some patients had a better performance with 5mg than with 10 mg. Not enough doses

were simulated to describe the shape of the dose-response relationship (linear, sigmoïd, U-shaped,...).

Figure 49 also highlights the presence of more responders in scenarios A and C. Patients with lower baseline performance respond to MPH when trained in scenario C but do not in the other ones. In scenario C, only punishments are used during the learning procedure, which again might allow the patients with poorer performance to correct their previously learned wrong stimulus-responses connections. Only rewards are considered in the learning procedure of scenario D, which is the scenario with the least responders. Indeed, responders to MPH in the scenario D are the ones with an already high baseline performance.

4. Discussion

MPH is one of the most common psychostimulant used to reduce the symptoms of ADHD. However, up to 30% of the patients are non-responders to MPH which means that they are either not experiencing benefits or have adverse effects [**43, 50**]. The exact mechanisms underlying MPH response are not fully understood [**10**]. The aim of this study was therefore to investigate the response of MPH from the perspective of the dopaminergic system of basal ganglia with a mecanistic mathematical model.

A pharmacokinetic model of MPH immediate release with an added compartment for the brain was joined to a previously developed model of the dopaminergic system of basal ganglia. A cohort of 30 virtual patients with dopamine imbalance was created. These virtual individuals were shown to have common caracteristics with ADHD patients [**59**]. The developed model allowed to investigate the dose-response curve and the effect of different scenarios of learning with medication on virtual patients. Non-responders to MPH were differentiated from responders by excessive learning in some action channels.

By modeling the response to MPH, we observed that MPH was improving the performance in the second phase of training. By defining a responder by an increase in correct responses with MPH, we observed on average across all scenarios 7.75 responders with 5 mg

of MPH, and 9.75 responders with 10 mg, hence an increase with dose of about 31%. In addition, the proportion of perfect performers, responders and non-responders, clearly depended on their position in the plane defined by the variability of reaction time and the weighted standard deviation of history. When we divided this plan into three sections, one type of subject was predominant in each (see Figure 48). Considering only the scenario A (tonic DA only is included in the simulation, without any Hebbian change in synaptic weight), the section a comprised a majority of perfect performers (N=9), and much fewer responders (N=2) and non-responder (N=1). The section b was occupied mainly by responders (N=8), 3 and much fewer non-responders (N=3) and perfect responders (N=1). Finally, the section c included only non-responders (N=6), with no response or perfect response. This difference in distribution was highly statistically significant. The proportions changed slightly in the other scenarios which introduced part or whole Hebbian synaptic modifications, but without affecting the dominant type in each section.

We already showed that the variability of reaction time could reflect quite different ex-gaussian distributions when taking in account the variability of learning history, weighted by the fact that the cumulative sum of history is either positive or negative. With a similar range of weighted history variability as the controls, individuals with a DA release imbalance but with a low reaction time variability (albeit still higher than the controls) often showed a perfect performance. Their larger reaction time variability was due to a combination of a small μ parameter (in ex-gaussian distribution), reflecting impulsive responses, but a large τ parameter due to a high proportion of very slow responses. Because of a ceiling effect due to the perfect performance of many subjects, the proportion of responders (2/12) and non-responders (1/12) was very small in this section.

Within the same range of weighted history variability but with a larger reaction time variability, the subjects with a DA imbalance showed a moderately impaired performance. Our previous study [**59**] showed that these subjects were characterized by a higher proportion of very slow responses. This reaction time distribution was typical of that observed in patients diagnosed clinically with ADHD, who also exhibit a moderate decrease in performance. The

subject in this section were also characterized by a high proportion of MPH responders. Finally, when the learning history variability further increased, the subjects with a DA imbalance showed a somewhat lower reaction time variability, although still much higher than the normal controls. In this study [**59**], the ex-gaussian analysis showed that the μ parameter increased in this subgroup, reflecting a slowing of most responses, while the τ parameter decreased but still remained higher than in the subgroup *b*. This subgroup *c* showed a further deterioration of the performance which became quite poor (about 60% of hits). We compared this poor overall performance with that of subjects with both ADHD and a learning disability.

The proportion of responders to MPH in these 3 subgroups partly defined by difference in reaction time variability can be compared with previous clinical data assessing the relationship between reaction time variability and response to methylphenidate in children with ADHD. Within a group of 88 ADHD subjects enrolled in a prospective 12-week, open-labeled, multicenter study to examine optimal dosage of OROS methylphenidate, MPH responders showed smaller response time variability at baseline. Baseline response time variability was a significant predictor of the response to MPH: it predicted 94.9% of responder, 17.2% of non-responder and 69.3% of overall group [**35**]. In another post-hoc analysis of data from a multicenter, open-label, 12-week trial of OROS-MPH in 109 Korean children with ADHD, lower response time variability scores on a continuous performance task were associated with a significantly higher probability of both objective and subjective responses to MPH, compared with both types of nonresponses to MPH [**41**]. The severity of ADHD has been showed to moderate the response to MPH [**40**], but the two latter studies suggest that the reaction time variability, a typical ADHD trait, is a valid biomarker of the response to MPH, with the limitation that both studies did not use a control group.

In the present simulation, taking in account only the 20 subjects with a less than perfect performance, we found 2 responders versus 5 non-responders among subjects with low standard deviation of reaction time, but 8 responders versus 5 non-responders among those

with high standard deviation of reaction time. This result apparently contradicts the previous clinical studies, since the proportion of responders is higher in subjects with a higher standard deviation of reaction times. But this difference in responders must be put into the perspective of differences in variability in learning history. In the ex-gaussian analysis, we showed that the response time variability of subjects in group b (with a smaller weighted history variability) was higher than that of group c (with a larger weighted history variability), because they had on the one hand a much lower value of the σ parameter (reflecting a smaller Gaussian component), but on the other hand a much larger value of the τ parameter (reflecting a larger exponential component). The two previous clinical studies [**35, 41**] have not decomposed the response time variance into ex-gaussian components. However, if we consider only the gaussian components of the variance, our simulation results are consistent with the previous clinical data: the group with a smaller gaussian component has a higher proportion of responders. A simulation should not be considered as a faithful reproduction of the reality it simulates, but more as a useful graph to understand it. For example, our simulation seeks to establish the consequences of an imbalance in DA release during reinforcement learning on the response time distribution, specifically on the impulsive and slow responses. However, the simulation is not meant to reproduce their exact proportion of impulsive and slow responses, which depends on many parameters that we cannot estimate. Moreover, the simulation allows us to make a testable prediction. The exponential τ component may be a better predictor of MPH response and be associated with a higher proportion of MPH responders. At this time, no clinical study has yet used the ex-gaussian distribution to predict response to MPH in ADHD.

Our DA imbalance model clearly links an ADHD trait (i.e., increase variability, especially due to slow responses) to the learning history of motor responses. This link may explain why in a retrospective study of 73 children aged 5-17 years diagnosed with ADHD and treated with MPH, motor problems were more severe among responders that among non-responders. Motor problems were assessed by testing reciprocal coordination of hand movements, control of walking, presence of synkinesis (unwanted contractions of the muscles of the face during

attempted movement), difficulty in dynamic balance (sideway jump and stops) and diadochokinesis (rapid pronation-supination movement on both hands). Success at these tests require a precise reinforcement of discrete synaptic connections between the motor cortex and the basal ganglia to avoid motor contamination. Excessive reinforcement linked to a DA release imbalance could reinforce unwanted movements, lead to motor problems and also affect the response to MPH.

To better understand the effects of MPH on the functional integration of different parts of the brain (functional connectivity), the effects of a single 20 mg dose were compared to placebo in healthy subjects [**14**]. The effects of MPH on functional connectivity at rest covaried with the known distribution of DAT in the brain. Connectivity within the DAT-related network was only increased in somato-motor areas, such as the precentral and postcentral gyri and the anterior division of the supramarginal gyrus. Furthermore, these changes in functional connectivity in DAT-enriched regions after a single dose of MPH correlated with the ability to choose new options during a novelty reinforcement learning task. This study showed that when dopaminergic discharge is balanced, MPH enhanced the functional connectivity in sensory-motor regions so that new responses can be learned more readily when they are reinforced.

In this perspective, we created four scenarios to identify which components of DA discharge are most critical to account for the therapeutic effects of MPH. We compared the proportion of responders for a dose of 5 and 10 mg of MPH in four different scenarios: (A) tonic DA release component only, (B) both tonic and phasic release component, (C) tonic and phasic (but only for the positive reward prediction error) release component, and (D) tonic and phasic (but only for the negative punishment prediction error) release component. The proportion of responder was higher with the tonic component only (scenario A) and with the tonic/ negative prediction error (scenario C). When the positive reward prediction of the model was active (scenarios B and D), the number of MPH responders was lower, although the difference between conditions seemed to decrease for the higher 10 mg dose. The tonic component of DA allowed for some learning, by either a primarily excitatory effect for the

Go part or an inhibitory effect for the NoGo part of the striatum. When a phasic component related to feedback was included, only the effect of MPH on the negative punishment increased the number of responders. This suggests that the mechanism of action of MPH on the phasic component was primarily by reinforcing unlearning of incorrect stimulus-response associations. The additional responders in the scenario C appeared to be subjects with an overall poor performance (see Figure 49).

ADHD patients seem indeed less sensitive to negative feedback. In a feedback-based learning task, an ADHD group without medication showed a decrease in error-related negativity (ERN) and error-related positivity (Pe), compared with typically developing children (TD), particularly as learning progressed throughout the task. Compared to the drug-free group, an ADHD group treated with MPH showed normalized Pe [**27**]. In addition, when the ADHD children performed a selective attention task with three feedback conditions (reward, punishment, and no feedback), they did not show the evoked heart rate (EHR) slowdowns on error trials observed in TD children, regardless of the feedback condition. However, MPH normalized the EHR decelerations to errors and error feedback in the no-feedback condition and the punishment condition, respectively [**25**] . Subjects with ADHD are therefore characterized by a decrease in negative feedback sensitivity after an error, a deficit that is corrected by MPH. The error- and feedback-related deceleration of EHR could reflect the same error monitoring system that is responsible for the emergence of error-related negativity (ERN)[**26**]. The locus coeruleus, which is the primary source nucleus of norepinephrine in the brain, can be hypothesized to be involved in this cardiac response. However, the dopaminergic system may also be involved in the error detection deficit. Specifically, a low tonic level of DA diminishes the effect of a temporary cessation of DA discharge following negative feedback for an error. The signal could be restored by MPH which increases the tonic DA level and would allow a better correction of stimulus-response association errors at the striatum level.

In conclusion, our simulation of the effect of MPH on the DA system in the basal ganglia showed (1) that MPH improved performance in virtual subjects who developed an ADHD

response profile, (2) that being an MPH responder could be predicted by different components of response time variance and weighted learning history variability, and (3) that tonic discharge and phasic drop of DA after negative feedback was critical for MPH response. These results strongly support a dopaminergic model to explain the therapeutic effects of MPH in ADHD and allows to propose some simple biomarkers of MPH response to be tested clinically. This study has however some limitations. We focused on the concept of responders and used relatively low MPH doses of 5 and 10 mg to detect the threshold of the response. The next steps will be to test the effect of higher doses (15 and 20 mg) and compute the corresponding DAT occupancy. Continuous behavioral variables will also need to be considered (such as reaction times, components of the reaction time distribution, different types of errors, etc.) as well as other continuous variables in our model (DA discharge, gain function, noise sensitivity, etc.) to further explore moderators of the MPH response. This will be the subject of future studies.

Author Contributions

This work makes up a portion of the doctoral thesis of FVV. Construction of the model: FVV PR MU FN. Numerical simulations: FVV. Writing of the paper: FVV PR MU FN.

References

[1] *Stimulant Drugs and ADHD: Basic and Clinical Neuroscience*. OXFORD UNIV PR, 2000.

[2] L Alexander et N Farrelly : Attending to adult adhd: a review of the neurobiology behind adult adhd. *Irish journal of psychological medicine*, 35:237–244, septembre 2018.

[3] American Psychiatric Association : *Diagnostic and Statistical Manual of Mental Disorders*. American Psychiatric Association, may 2013.

[4] Chiara Baston et Mauro Ursino : A biologically inspired computational model of basal ganglia in action selection. *Computational intelligence and neuroscience*, 2015:187417, 2015.

[5] Jean-Martin Beaulieu et Raul R Gainetdinov : The physiology, signaling, and pharmacology of dopamine receptors. *Pharmacological reviews*, 63:182–217, mars 2011.

[6] M Benoit-Marand, E Borrelli et F Gonon : Inhibition of dopamine release via presynaptic d2 receptors: time course and functional characteristics in vivo. *The Journal of neuroscience : the official journal of the Society for Neuroscience*, 21:9134–9141, décembre 2001.

[7] Craig W Berridge, David M Devilbiss, Matthew E Andrzejewski, Amy F T Arnsten, Ann E Kelley, Brooke Schmeichel, Christina Hamilton et Robert C Spencer : Methylphenidate preferentially increases catecholamine neurotransmission within the prefrontal cortex at low doses that enhance cognitive function. *Biological psychiatry*, 60:1111–1120, novembre 2006.

[8] Guillaume Bonnefois, Philippe Robaey, Olivier Barrière, Jun Li et Fahima Nekka : An evaluation approach for the performance of dosing regimens in attention-deficit/hyperactivity disorder treatment. *Journal of child and adolescent psychopharmacology*, 27:320–331, mai 2017.

[9] Ann C Childress, Marina Komolova et F Randy Sallee : An update on the pharmacokinetic considerations in the treatment of adhd with long-acting methylphenidate and amphetamine formulations. *Expert opinion on drug metabolism & toxicology*, 15:937–974, novembre 2019.

[10] Soo-Churl Cho, Jun-Won Hwang, Boong-Nyun Kim, Ho-Young Lee, Hyo-Won Kim, Jae-Sung Lee, Min-Sup Shin et Dong-Soo Lee : The relationship between regional cerebral blood flow and response to methylphenidate in children with attention-deficit hyperactivity disorder: comparison between non-responders to methylphenidate and responders. *Journal of psychiatric research*, 41:459–465, septembre 2007.

[11] Adam R Clarke, Robert J Barry, Rory McCarthy et Mark Selikowitz : Eeg differences between good and poor responders to methylphenidate and dexamphetamine in children with attention-deficit/hyperactivity disorder. *Clinical neurophysiology : official journal of the International Federation of Clinical Neurophysiology*, 113:194–205, février 2002.

[12] Vanessa Coelho-Santos, Filipa L Cardoso, Ricardo A Leitão, Carlos A Fontes-Ribeiro et Ana Paula Silva : Impact of developmental exposure to methylphenidate on rat brain's immune privilege and behavior: Control versus adhd model. *Brain, behavior, and immunity*, 68:169–182, février 2018.

[13] Paul W Czoty, Alexandros Makriyannis et Jack Bergman : Methamphetamine discrimination and in vivo microdialysis in squirrel monkeys. *Psychopharmacology*, 175:170–178, septembre 2004.

[14] Ottavia Dipasquale, Daniel Martins, Arjun Sethi, Mattia Veronese, Swen Hesse, Michael Rullmann, Osama Sabri, Federico Turkheimer, Neil A Harrison, Mitul A Mehta et Mara Cercignani : Unravelling the effects of methylphenidate on the dopaminergic and noradrenergic functional circuits.

Neuropsychopharmacology : official publication of the American College of Neuropsychopharmacology, 45:1482–1489, août 2020.

[15] Jakob K Dreyer : Three mechanisms by which striatal denervation causes breakdown of dopamine signaling. *The Journal of neuroscience : the official journal of the Society for Neuroscience*, 34:12444–12456, septembre 2014.

[16] Jakob K Dreyer, Kjartan F Herrik, Rune W Berg et Jørn D Hounsgaard : Influence of phasic and tonic dopamine release on receptor activation. *The Journal of neuroscience : the official journal of the Society for Neuroscience*, 30:14273–14283, octobre 2010.

[17] Jakob Kisbye Dreyer et Jørn Hounsgaard : Mathematical model of dopamine autoreceptors and uptake inhibitors and their influence on tonic and phasic dopamine signaling. *Journal of neurophysiology*, 109:171–182, janvier 2013.

[18] Nada A Elsayed, Kaila M Yamamoto et Tanya E Froehlich : Genetic influence on efficacy of pharmacotherapy for pediatric attention-deficit/hyperactivity disorder: Overview and current status of research. *CNS drugs*, 34:389–414, avril 2020.

[19] Ashley M Fennell, Elizabeth G Pitts, Lacey L Sexton et Mark J Ferris : Phasic dopamine release magnitude tracks individual differences in sensitization of locomotor response following a history of nicotine exposure. *Scientific reports*, 10:173, janvier 2020.

[20] Justine A Fuller, Mark H Burrell, Andrew G Yee, Kavinda Liyanagama, Janusz Lipski, Jeffery R Wickens et Brian I Hyland : Role of homeostatic feedback mechanisms in modulating methylphenidate actions on phasic dopamine signaling in the striatum of awake behaving rats. *Progress in neurobiology*, 182:101681, novembre 2019.

[21] Paul W Glimcher : Understanding dopamine and reinforcement learning: the dopamine reward prediction error hypothesis. *Proceedings of the National Academy of Sciences of the United States of America*, 108 Suppl 3:15647–15654, septembre 2011.

[22] A A Grace : Phasic versus tonic dopamine release and the modulation of dopamine system responsivity: a hypothesis for the etiology of schizophrenia. *Neuroscience*, 41:1–24, 1991.

[23] Anthony A Grace : Dysregulation of the dopamine system in the pathophysiology of schizophrenia and depression. *Nature reviews. Neuroscience*, 17:524–532, août 2016.

[24] L L Greenhill, J M Swanson, B Vitiello, M Davies, W Clevenger, M Wu, L E Arnold, H B Abikoff, O G Bukstein, C K Conners, G R Elliott, L Hechtman, S P Hinshaw, B Hoza, P S Jensen, H C Kraemer, J S March, J H Newcorn, J B Severe, K Wells et T Wigal : Impairment

and deportment responses to different methylphenidate doses in children with adhd: the mta titration trial. *Journal of the American Academy of Child and Adolescent Psychiatry*, 40:180–187, février 2001.

[25] Yvonne Groen, Lambertus J M Mulder, Albertus A Wijers, Ruud B Minderaa et Monika Althaus : Methylphenidate improves diminished error and feedback sensitivity in adhd: An evoked heart rate analysis. *Biological psychology*, 82:45–53, septembre 2009.

[26] Yvonne Groen, Albertus A Wijers, Lambertus J M Mulder, Ruud B Minderaa et Monika Althaus : Physiological correlates of learning by performance feedback in children: a study of eeg event-related potentials and evoked heart rate. *Biological psychology*, 76:174–187, octobre 2007.

[27] Yvonne Groen, Albertus A Wijers, Lambertus J M Mulder, Brenda Waggeveld, Ruud B Minderaa et Monika Althaus : Error and feedback processing in children with adhd and children with autistic spectrum disorder: an eeg event-related potential study. *Clinical neurophysiology : official journal of the International Federation of Clinical Neurophysiology*, 119:2476–2493, novembre 2008.

[28] Jonas Hannestad, Jean-Dominique Gallezot, Beata Planeta-Wilson, Shu-Fei Lin, Wendol A Williams, Christopher H van Dyck, Robert T Malison, Richard E Carson et Yu-Shin Ding : Clinically relevant doses of methylphenidate significantly occupy norepinephrine transporters in humans in vivo. *Biological psychiatry*, 68:854–860, novembre 2010.

[29] B Hille : G protein-coupled mechanisms and nervous signaling. *Neuron*, 9:187–195, août 1992.

[30] Soon-Beom Hong, Ben J Harrison, Alex Fornito, Chul-Ho Sohn, In-Chan Song et Jae-Won Kim : Functional dysconnectivity of corticostriatal circuitry and differential response to methylphenidate in youth with attention-deficit/hyperactivity disorder. *Journal of psychiatry & neuroscience : JPN*, 40:46–57, janvier 2015.

[31] A S Horn : Dopamine uptake: a review of progress in the last decade. *Progress in neurobiology*, 34:387–400, 1990.

[32] Edward C Hulme et Mike A Trevethick : Ligand binding assays at equilibrium: validation and interpretation. *British journal of pharmacology*, 161:1219–1237, novembre 2010.

[33] Lars Hunger, Arvind Kumar et Robert Schmidt : Abundance compensates kinetics: Similar effect of dopamine signals on d1 and d2 receptor populations. *The Journal of neuroscience : the official journal of the Society for Neuroscience*, 40:2868–2881, avril 2020.

[34] Carrie E John, Evgeny A Budygin, Yolanda Mateo et Sara R Jones : Neurochemical characterization of the release and uptake of dopamine in ventral tegmental area and serotonin in substantia nigra of the mouse. *Journal of neurochemistry*, 96:267–282, janvier 2006.

[35] Seung-Hye Lee, Dong-Ho Song, Bung-Nyun Kim, Yoo Sook Joung, Eun Hye Ha, Keun-Ah Cheon, Yee-Jin Shin, Hee Jeong Yoo et Dong-Won Shin : Variability of response time as a predictor of methylphenidate treatment response in korean children with attention deficit hyperactivity disorder. *Yonsei medical journal*, 50:650–655, octobre 2009.

[36] L J May, W G Kuhr et R M Wightman : Differentiation of dopamine overflow and uptake processes in the extracellular fluid of the rat caudate nucleus with fast-scan in vivo voltammetry. *Journal of neurochemistry*, 51:1060–1069, octobre 1988.

[37] A Moreno, L Duñó, E Hoekzema, M Picado, L M Martín, J Fauquet, Y Vives-Gilabert, A Bulbena et O Vilarroya : Striatal volume deficits in children with adhd who present a poor response to methylphenidate. *European child & adolescent psychiatry*, 23:805–812, septembre 2014.

[38] Tomohiro Nakao, Joaquim Radua, Katya Rubia et David Mataix-Cols : Gray matter volume abnormalities in adhd: voxel-based meta-analysis exploring the effects of age and stimulant medication. *The American journal of psychiatry*, 168:1154–1163, novembre 2011.

[39] C Nicholson : Interaction between diffusion and michaelis-menten uptake of dopamine after iontophoresis in striatum. *Biophysical journal*, 68:1699–1715, mai 1995.

[40] Elizabeth B Owens, Stephen P Hinshaw, Helen C Kraemer, L Eugene Arnold, Howard B Abikoff, Dennis P Cantwell, C Keith Conners, Glen Elliott, Laurence L Greenhill, Lily Hechtman, Betsy Hoza, Peter S Jensen, John S March, Jeffrey H Newcorn, William E Pelham, Joanne B Severe, James M Swanson, Benedetto Vitiello, Karen C Wells et Timothy Wigal : Which treatment for whom for adhd? moderators of treatment response in the mta. *Journal of consulting and clinical psychology*, 71:540–552, juin 2003.

[41] Subin Park, Bung-Nyun Kim, Soo-Churl Cho, Jae-Won Kim, Min-Sup Shin, Hee-Jeong Yoo, Doug Hyun Han et Jae Hoon Cheong : Baseline severity of parent-perceived inattentiveness is predictive of the difference between subjective and objective methylphenidate responses in children with attention-deficit/hyperactivity disorder. *Journal of child and adolescent psychopharmacology*, 23:410–414, août 2013.

[42] E N Pothos, V Davila et D Sulzer : Presynaptic recording of quanta from midbrain dopamine neurons and modulation of the quantal size. *The Journal of neuroscience : the official journal of the Society for Neuroscience*, 18:4106–4118, juin 1998.

[43] M D Rapport, C Denney, G J DuPaul et M J Gardner : Attention deficit disorder and methylphenidate: normalization rates, clinical effectiveness, and response prediction in 76 children. *Journal of the American Academy of Child and Adolescent Psychiatry*, 33:882–893, 1994.

[44] Margaret E Rice et Stephanie J Cragg : Dopamine spillover after quantal release: rethinking dopamine transmission in the nigrostriatal pathway. *Brain research reviews*, 58:303–313, août 2008.

[45] Katya Rubia, Rozmin Halari, Ana Cubillo, Abdul-Majeed Mohammad, Mick Brammer et Eric Taylor : Methylphenidate normalises activation and functional connectivity deficits in attention and motivation networks in medication-naïve children with adhd during a rewarded continuous performance task. *Neuropharmacology*, 57:640–652, décembre 2009.

[46] Katya Rubia, Rozmin Halari, Abdul-Majeed Mohammad, Eric Taylor et Michael Brammer : Methylphenidate normalizes frontocingulate underactivation during error processing in attention-deficit/hyperactivity disorder. *Biological psychiatry*, 70:255–262, août 2011.

[47] Terje Sagvolden, Espen Borgå Johansen, Heidi Aase et Vivienne Ann Russell : A dynamic developmental theory of attention-deficit/hyperactivity disorder (adhd) predominantly hyperactive/impulsive and combined subtypes. *The Behavioral and brain sciences*, 28:397–419; discussion 419–68, juin 2005.

[48] Wolfram Schultz : Dopamine reward prediction error coding. *Dialogues in clinical neuroscience*, 18:23–32, mars 2016.

[49] D Schönfuss, T Reum, P Olshausen, T Fischer et R Morgenstern : Modelling constant potential amperometry for investigations of dopaminergic neurotransmission kinetics in vivo. *Journal of neuroscience methods*, 112:163–172, décembre 2001.

[50] T Spencer, J Biederman, T Wilens, M Harding, D O'Donnell et S Griffin : Pharmacotherapy of attention-deficit hyperactivity disorder across the life cycle. *Journal of the American Academy of Child and Adolescent Psychiatry*, 35:409–432, avril 1996.

[51] Thomas J Spencer, Joseph Biederman, Patrick E Ciccone, Bertha K Madras, Darin D Dougherty, Ali A Bonab, Elijahu Livni, Dolly A Parasrampuria et Alan J Fischman : Pet study examining pharmacokinetics, detection and likeability, and dopamine transporter receptor occupancy of short- and long-acting oral methylphenidate. *The American journal of psychiatry*, 163:387–395, mars 2006.

[52] Thomas J Spencer, Ali A Bonab, Darin D Dougherty, Jessica Martin, Tara McDonnell et Alan J Fischman : A pet study examining pharmacokinetics and dopamine transporter occupancy of two long-acting formulations of methylphenidate in adults. *International journal of molecular medicine*, 25:261–265, février 2010.

[53] Thomas J Spencer, Ali A Bonab, Darin D Dougherty, Tara Mirto, Jessica Martin, Allison Clarke et Alan J Fischman : Understanding the central pharmacokinetics of spheroidal oral drug absorption system (sodas) dexmethylphenidate: a positron emission tomography study of dopamine

transporter receptor occupancy measured with c-11 altropane. *The Journal of clinical psychiatry*, 73: 346–352, mars 2012.

[54] J M Swanson et N D Volkow : Serum and brain concentrations of methylphenidate: implications for use and abuse. *Neuroscience and biobehavioral reviews*, 27:615–621, novembre 2003.

[55] Eva Syková et Charles Nicholson : Diffusion in brain extracellular space. *Physiological reviews*, 88:1277–1340, octobre 2008.

[56] Gail Tripp et Jeff R Wickens : Research review: dopamine transfer deficit: a neurobiological theory of altered reinforcement mechanisms in adhd. *Journal of child psychology and psychiatry, and allied disciplines*, 49:691–704, juillet 2008.

[57] N D Volkow, G J Wang, J S Fowler, S J Gatley, J Logan, Y S Ding, S L Dewey, R Hitzemann, A N Gifford et N R Pappas : Blockade of striatal dopamine transporters by intravenous methylphenidate is not sufficient to induce self-reports of "high". *The Journal of pharmacology and experimental therapeutics*, 288:14–20, janvier 1999.

[58] N D Volkow, G J Wang, J S Fowler, S J Gatley, J Logan, Y S Ding, R Hitzemann et N Pappas : Dopamine transporter occupancies in the human brain induced by therapeutic doses of oral methylphenidate. *The American journal of psychiatry*, 155:1325–1331, octobre 1998.

[59] Florence Véronneau-Veilleux, Philippe Robaey, Mauro Ursino et Fahima Nekka : A mechanistic model of adhd as resulting from dopamine phasic-tonic imbalance during reinforcement learning. *Submitted.*

[60] Florence Véronneau-Veilleux, Philippe Robaey, Mauro Ursino et Fahima Nekka : An integrative model of parkinson's disease treatment including levodopa pharmacokinetics, dopamine kinetics, basal ganglia neurotransmission and motor action throughout disease progression. *Journal of pharmacokinetics and pharmacodynamics*, 48:133–148, février 2021.

[61] Mark L Wolraich et Melissa A Doffing : Pharmacokinetic considerations in the treatment of attention-deficit hyperactivity disorder with methylphenidate. *CNS drugs*, 18:243–250, 2004.

[62] Kareem A Zaghloul, Justin A Blanco, Christoph T Weidemann, Kathryn McGill, Jurg L Jaggi, Gordon H Baltuch et Michael J Kahana : Human substantia nigra neurons encode unexpected financial rewards. *Science (New York, N.Y.)*, 323:1496–1499, mars 2009.

Discussion

L'objectif principal de la présente thèse était d'élucider les mécanismes physiologiques liés à deux pathologies affectant le système dopaminergique des ganglions de la base ainsi que leurs réponses aux thérapies associées, tout en visant une optimisation des régimes thérapeutiques. Les traitements couramment utilisés ont été considérés, soient la lévodopa et le méthylphénidate, dans le cadre de la maladie de Parkinson et du TDAH, respectivement. À cette fin, un modèle de pharmacologie quantitative des systèmes (QSP), intégrant la dynamique de la dopamine et la neurotransmission dans les ganglions de la base, a été développé. Pour l'étude de la maladie de Parkinson, la perte des neurones dopaminergiques, caractéristique de cette pathologie, a été représentée pour ainsi évaluer l'évolution de la réponse thérapeutique en fonction du degré de dénervation, c'est-à-dire, en fonction de la progression de la maladie. Pour l'étude du TDAH, l'impact de la plasticité synaptique durant une tâche d'apprentissage par renforcement a été implémentée dans le modèle, en y associant aussi un modèle PK du méthylphénidate. Le modèle fut élaboré en ayant comme double objectif d'être intégratif et modulable afin qu'il puisse être utilisé dans le cadre d'études portant sur des pathologies diverses du système dopaminergique des ganglions de la base.

Au Chapitre 1, l'analyse de l'effet de la lévodopa avec la progression de la maladie de Parkinson, mesuré par une tâche motrice (tapotement des doigts), ainsi qu'une comparaison des simulations aux données disponibles ont été effectuées à l'aide du modèle développé. La fréquence de tapotement des doigts a servi comme indicateur clinique de l'effet de la lévodopa sur la bradykinésie. Les processus de régulation pour le maintien de l'homéostasie de la dopamine ont alors été investigués. Au Chapitre 2, les relations non-linéaires entre la

concentration plasmatique de lévodopa, la concentration cérébrale de dopamine ainsi que la fréquence de tapotement des doigts avec la progression de la maladie ont été investiguées. De plus, des analyses portant sur la concentration en dopamine dans le cerveau, selon différentes doses de lévodopa, et l'implication des relations non-linéaires sur le rétrécissement de l'index thérapeutique avec la dénervation ont été réalisées. Au Chapitre 3, dans un soucis d'applicabilité de notre approche, nous avons développé, comme preuve de concept, une application pour optimiser et personnaliser le régime posologique de la lévodopa. Dans cette application, la valeur de certains paramètres du modèle précédemment développé était personnalisée en fonction des données motrices du patient. Des régimes posologiques variés ont ensuite été testés afin d'identifier le régime optimal spécifique au patient et ce, en utilisant différents critères.

Au Chapitre 4, l'hypothèse de l'implication, dans le TDAH, d'un débalancement entre la dopamine tonique et phasique, durant l'apprentissage par renforcement, a été testée. Le groupe de patients virtuels créés avec le modèle et présentant un tel débalancement manisfestait des symptômes typiques du TDAH, tels qu'un plus grand nombre de réponses incorrectes à une tâche de réponses à des stimuli, et des temps de réaction plus grands. Finalement, au Chapitre 5, l'effet du rétablissement de la balance entre dopamine tonique et phasique par le MPH sur le nombre de bonne réponses des patients à cette même tâche fut analysé. Divers scénarios d'apprentisage ont alors été testés ainsi que différentes doses de MPH, pour en comparer la proportion de répondants vs non-répondants au MPH. Une métrique développée dans ce travail a permis de mettre de l'avant l'apprentissage excessif de certaines tâches comme facteur potentiellement impliqué dans la non-réponse au MPH.

La modélisation computationnelle en neuroscience s'apparentant à celle utilisée dans cette thèse a débuté dans les années 1950, avec l'introduction du modèle de neurones d'Hodgkin et Huxley. Pourtant, l'utilisation de l'approche QSP adoptée ici pour l'étude de la pharmacothérapie associée aux pathologies du système nerveux central (CNS) a pris du temps à voir le jour [**4**]. La complexité des pathologies du CNS a probablement dissuadé la communauté de pharmacométrie, souvent habituée à une formulation plus macroscopique des systèmes

impliqués, d'utiliser cette approche au profit d'une approche compartimentale. Toutefois, étant donné le faible taux de succès des essais cliniques dans la découverte de nouveaux médicaments pour traiter les maladies neurodégénératives ainsi que les coûts élevés qui y sont rattachés, la nécessité d'utiliser de nouvelles approches est devenue évidente [**4**]. La modélisation QSP combinée à la modélisation PK/PD s'est donc alors imposée. L'avantage de l'approche QSP est son caractère non invasive, sa capacité à intégrer des données et des connaissances provenant de différentes sources, et sa faculté d'extrapoler des prédictions au-delà de la portée des données disponibles [**1**]. De plus, cette approche à saveur mécanistique peut être formulée de façon assez générique afin de s'adapter à divers contextes thérapeutiques. C'est ainsi qu'en identifiant les composantes communes de la maladie de Parkinson et du TDAH, nous avons réussi, dans le cadre de cette thèse, à étudier ces deux pathologies et leurs thérapies.

Toutefois, il reste encore beaucoup à faire dans l'étude de la pharmacothérapie associée aux pathologies du système dopaminergique. En effet, en plus de la bradykinésie, le présent modèle pourrait être adapté afin d'incorporer la plasticité synaptique ainsi que l'utilisation de la lévodopa par les neurones sérotoninergiques, phénomènes qui seraient impliqués dans l'apparition des dyskinésies (mouvements involontaires). Une meilleure compréhension des effets secondaires pourrait conduire à l'identification de stratégies pour les retarder. De plus, le modèle développé dans cette thèse impliquait des valeurs moyennes de paramètres. Afin d'évaluer l'impact de la variabilité sur l'index thérapeutique et l'optimisation du régime posologique, considérant que certains patients ne répondent pas de façon satisfaisante à la lévodopa et ce, même aux premiers stades de la maladie, la variabilité inter et intra-individuelle pourrait donc être considérées au niveau des paramètres PK de la lévodopa [**2**]. Le processus de sélection des paramètres à personnaliser dans l'application Web pourrait également être affiné par une analyse de sensibilité du modèle de la dopamine et du modèle des ganglions de la base, à l'aide de données cliniques. Des algorithmes d'optimisation plus sophistiqués, tels que des algorithmes génétiques ou de contrôle optimal, pourraient également être implémentés dans l'application Web. Ceci permettrait de considérer une variété de régimes

posologiques plus complexes qui ne pourraient être testés dans leur intégralité autrement. Il serait aussi envisageable d'implémenter, en plus du modèle PK d'infusion intraveineuse considéré ici, des modèles PK correspondant aux autres voies d'administration (orale et infusion duodénale). Ainsi, cette application pourrait guider les cliniciens non seulement dans le choix du régime posologique optimal mais aussi dans le choix de la voie d'administration à préconiser. Avant son implantation, cette application devra aussi être validée de façon rigoureuse avec des cliniciens. Enfin, dans le futur, des capteurs permettant aux patients de mesurer et collecter leur fréquence de tapotement des doigts, à différents moments, pourraient être reliés à l'application Web pour permettre l'individualisation ainsi que l'optimisation des régimes posologiques. La faisabilité d'une telle approche a déjà été établie par l'utilisation de capteurs pour le suivi de divers symptômes de la maladie de Parkinson [**3**] et même par la personnalisation des régimes de lévodopa sous forme de microcomprimés à l'aide des données motrices recueillies par de tels capteurs [**5**].

De plus, le TDAH est un trouble multifactoriel. Ainsi, en plus de l'impact d'un dysfonctionnement du système dopaminergique tel que considéré dans cette thèse, celui se produisant au niveau du système noradrénergique devrait être ajouté au modèle. Les mêmes considérations de variabilité mentionnées pour la lévodopa s'appliquerait au MPH, les modèles PK de population du MPH ne manquent pas dans la littérature. D'autres modes de libération, telle que la libération prolongée, peuvent faire partie des thérapies considérées dans une optique d'optimisation des doses et des temps d'administration, mais aussi de combinaisons possibles des formulations existantes et pourraient ainsi être ajoutés au modèle.

Pour conclure, l'approche par modélisation QSP adoptée tout au long de cette thèse démontre une grande polyvalence et adaptabilité aux différents aspects impliqués dans le processus de recherche et de développement du médicament [**1**]. Ces modèles peuvent permettre d'appréhender la complexité de différentes pathologies en créant un cadre théorique pour les étudier. Alors que l'on entre dans l'ère de la médecine personnalisée, les modèles QSP représentent aussi des outils de choix pour la personnalisation et l'optimisation des traitements. Cette approche trouve son apogée lorsqu'elle est développée en étroite collaboration

avec des cliniciens et des scientifiques de plusieurs disciplines. Ainsi, c'est en transcendant les frontières des différentes disciplines, qu'il sera possible de développer des outils pour faire face aux défis multidimensionnels du système de la santé en gardant toujours comme première préoccupation, le bien-être des patients.

Références

[1] Erica L Bradshaw, Mary E Spilker, Richard Zang, Loveleena Bansal, Handan He, Rhys D O Jones, Kha Le, Mark Penney, Edgar Schuck, Brian Topp, Alice Tsai, Christine Xu, Marjoleen J M A Nijsen et Jason R Chan : Applications of quantitative systems pharmacology in model-informed drug discovery : Perspective on impact and opportunities. *CPT : pharmacometrics & systems pharmacology*, 8:777–791, novembre 2019.

[2] Phylinda L S Chan, John G Nutt et Nicholas H G Holford : Importance of within subject variation in levodopa pharmacokinetics : a 4 year cohort study in parkinson's disease. *Journal of pharmacokinetics and pharmacodynamics*, 32:307–331, août 2005.

[3] Jean-Francois Daneault, Gloria Vergara-Diaz, Federico Parisi, Chen Admati, Christina Alfonso, Matilde Bertoli, Edoardo Bonizzoni, Gabriela Ferreira Carvalho, Gianluca Costante, Eric Eduardo Fabara, Naama Fixler, Fatemah Noushin Golabchi, John Growdon, Stefano Sapienza, Phil Snyder, Shahar Shpigelman, Lewis Sudarsky, Margaret Daeschler, Lauren Bataille, Solveig K Sieberts, Larsson Omberg, Steven Moore et Paolo Bonato : Accelerometer data collected with a minimum set of wearable sensors from subjects with parkinson's disease. *Scientific data*, 8:48, février 2021.

[4] Hugo Geerts, John Wikswo, Piet H van der Graaf, Jane P F Bai, Chris Gaiteri, David Bennett, Susanne E Swalley, Edgar Schuck, Rima Kaddurah-Daouk, Katya Tsaioun et Mary Pelleymounter : Quantitative systems pharmacology for neuroscience drug discovery and development : Current status, opportunities, and challenges. *CPT : pharmacometrics & systems pharmacology*, 9:5–20, janvier 2020.

[5] Ilias Thomas, Moudud Alam, Filip Bergquist, Dongni Johansson, Mevludin Memedi, Dag Nyholm et Jerker Westin : Sensor-based algorithmic dosing suggestions for oral administration of levodopa/carbidopa microtablets for parkinson's disease : a first experience. *Journal of neurology*, 266:651–658, mars 2019.

Annexe A

Cette annexe contient le matériel supplémentaire associé à l'article *An Integrative Model of Parkinson's Disease Treatment Including Levodopa Pharmacokinetics, Dopamine Kinetics, Basal Ganglia Neurotransmission and Motor Action throughout Disease Progression* présenté au Chapitre 1.

A.1 Scaling

The use of pre-existing models (levodopa PK model, dopamine kinetics model and neurocomputational model of basal ganglia) requires some scaling between the output and input of each model. The transformation of levodopa brain concentration into its related release of dopamine molecules per terminal and the scaling of the fraction of bound dopaminergic receptors are presented here.

A.1.1 Levodopa brain concentration into dopamine molecules per terminal

Once levodopa has reached the brain, it is decarboxylated into dopamine by the neurons of the substantia nigra. It will then increase the dopamine relase term I_{DA}. In order to combine the pharmacokinetic model of levodopa to the dopamine kinetics model, the levodopa brain concentration given by $C_3(t)$ of equation 2.3 needs to be transformed into its related dopamine release. The number of dopamine molecules per terminal that will be produced by

decarboxylation of levodopa is given by the following equation :

$$n_{Levodopa}(t) = C_3(t)\frac{N_A c_L}{\rho M_{Levodopa}} \tag{.0.1}$$

where $n_{Levodopa}(t)$ is the number of molecules per terminal produced by levodopa, $C_3(t)$ is the levodopa brain concentration, N_A is the Avogadro's constant, c_L is a conversion factor of milliliters into liters, ρ is the terminal density in the intact substantia nigra and $M_{Levodopa}$ is the molar mass of levodopa. The value of each parameter of equation .0.1 is given in Table 8.

Tableau 8. Parameter values for the conversion of levodopa brain concentration into its related release of dopamine molecules per terminal

Parameter	Description	Value	Reference
N_A	Avogadro's constant	$6.02 \cdot 10^{23}\ \frac{molecules}{mol}$	
C_L	Conversion factor	$1000\ \frac{mL}{L}$	
ρ	Terminal density	$0.1 \cdot 10^{15}\ \frac{\text{terminals}}{L}$	[**4**]
$M_{Levodopa}$	Molar mass	$197.1879 \cdot 10^{6}\ \frac{\mu g}{mol}$	

A.1.2 Scaling of the concentration of bound receptors

Once the dopamine concentration is found, the concentration of bound D1 and D2 receptors can be estimated with equation 2.11. These values will respectively affect the neurons in the direct and indirect pathways of the neurocomputational model. In order to keep the same parameter values for the neurocomputational model as the ones presented in [**2**], the fraction of bound receptors must be of the same magnitude as the dopamine effect defined in [**2**]. In order to have the same basal value of dopamine effect, the parameters have been scaled this way :

$$\text{Bound receptor}D_1{}^{scaled} = \text{Bound receptor}D_1 + 5.5650 \times 10^{-04} \tag{.0.2}$$

$$\text{Bound receptor}D_2{}^{scaled} = \text{Bound receptor}D_2 - 0.0060. \tag{.0.3}$$

With the aim to have the same amplitude of dopamine effect, the parameters α, β and γ of the neurocomputational model were also modified to $\alpha = 2.8323/B_{max}^{D_1}$, $\beta = -0.9750/B_{max}^{D_2}$ and $\gamma = -0.9750/B_{max}^{D_2}$. These values are also given in Table 15. This scaling is a drawback of the model. In the future, the parameters of the neurocomputational model of basal ganglia should be reassess to fit individual data presented in [**2**] in order to prevent this scaling.

A.2 Dopamine release term

An equation was developed [**4**] to estimate the release term $I_{DA}(t)$ used in equation 2.7. The same estimation was used here. In the present model, the release term $I_{DA}(t)$ is the sum of the endogenous and exogenous release of dopamine. The release of dopamine is then given by the following equations :

$$I_{DA} = \rho \frac{P(n_0 + n_{Levodopa}(t))}{\alpha_{vf} N_A} v_0 \tag{.0.4}$$

$$= \rho \frac{P n_0}{\alpha_{vf} N_A} v_0 + \rho \frac{P n_{Levodopa}(t)}{\alpha_{vf} N_A} v_0 \tag{.0.5}$$

$$= I_{DAendogenous} + I_{DAlevodopa}(t) \tag{.0.6}$$

were ρ is the terminal density, P is the vesicular release probability, n_0 is the number of molecules released per vesicule fusion, α is the extracellular volume fraction, N_A is the Avogadro's constant and v_0 is the average firing rate of dopaminergic neurons. Equation .0.6 is the same as equation 2.8 presented in the paper. The parameters for this equation are given in Table 9. The exogenous release of dopamine by decarboxylation of levodopa is given

by the following equation :

$$I_{DAlevodopa}(t) = \rho \frac{Pn_{Levodopa}(t)}{\alpha_{vf} N_A} v_0 \tag{.0.7}$$

$$= \rho \frac{PC_3(t) \dfrac{N_A c_L}{\rho M_{Levodopa}}}{\alpha_{vf} N_A} v_0 \tag{.0.8}$$

$$= \frac{Pc_L v_0}{\alpha_{vf} M_{Levodopa}} C_3(t) \tag{.0.9}$$

$$= k_{3dop} C_3(t) \tag{.0.10}$$

and the parameters for this equation are given in Table 10.

Tableau 9. Parameters value for the dopamine release term in absence of levodopa therapy

Parameter	Description	Value	Reference
ρ	Terminal density	$0.1 \cdot 10^{15}$ $\frac{\text{terminals}}{L}$	[**4**]
P	Vesicular release probability	0.1	[**4**]
n_0	Number of molecules released per vesicule fusion	3000 $\frac{\text{molecules}}{\text{terminal}}$	[**4, 5**]
α_{vf}	Extracellular volume fraction	0.2	[**4, 7**]
N_A	Avogadro's constant	$6.02 \cdot 10^{23} \cdot 10^{-6}$ $\frac{\text{molecules}}{\mu mol}$	
v_0	Average firing rate	4 s^{-1}	[**4**]

Tableau 10. Parameters value for the dopamine release term with levodopa therapy

Parameter	Description	Value	Reference
ρ	Terminal density	$0.1 \cdot 10^{15}$ $\frac{\text{terminals}}{L}$	[**4**]
P	Vesicular release probability	0.07	[**4**]
n_0	Number of molecules released per vesicule fusion	$(3000 + n_{Levodopa}(t))$ $\frac{\text{molecules}}{\text{terminal}}$	[**4, 5**]
α_{vf}	Extracellular volume fraction	0.2	[**4, 7**]
N_A	Avogadro's constant	$6.02 \cdot 10^{23} \cdot 10^{-6}$ $\frac{\text{molecules}}{\mu M}$	
v_0	Average firing rate	3 s^{-1}	[**4**]

The value for the terminal density given in Tables 9 and 10 is the one for the intact substantia nigra. As the disease progresses, this density will decrease. This model considers an homogenous neuronal death in space and a density proportional to the fraction of neurons alive (f). The release term will then become :

$$(f \cdot \rho)\frac{Pn_0}{\alpha_{vf} N_A} v_0 = f \cdot I_{DA}. \tag{.0.11}$$

The relation given by equation .0.11 leads to the first term in equation 2.10 in the paper.

A.3 Neurocomputational model of basal ganglia

The neurocomputational model of basal ganglia was previously developed to simulate the neuronal activity in each subregion of the basal ganglia [**2, 3**]. The same model was used here.

The activity of the neurons in the cortex, the striatum, the globus pallidus internal and external, the subthalamic nucleus and the thalamus in addition to neurons representing the sensory input from the cortex are developped in this model. The abbreviation used in the equations are listed in Table 21.

Tableau 11. Abbreviations for the subregions of the basal ganglia

Subregion's name	Abbreviation
Sensory input	S
Cortex	C
Cortex's lateral inhibition	L
Go part of striatum (D1 receptors)	G
NoGo part of striatum (D2) receptors	N
Globus pallidus internal	I
Globus pallidus external	E
Subthalamic nucleus	STN
Thalamus	T
Cholinergic interneurons	H

In order to keep the model as simple as possible, the equations for the neuronal activity are of type firing rate neurons. There are two neurons in each subregion to represent the two possible actions (raising or lowering the finger) except in the subthalamic nucleus and

for the cholinergic interneuron. Let i be the number of the postsynaptic neuron (1 or 2) in the subregion k receiving current from the presynaptic neuron number j in the subregion m with a weight of w^{km}. The general form of the equations are the following :

$$\tau \frac{u_i^k}{dt} = -u_i^k + \sum_{j=1}^{2} w_{ij}^{km} y_j^m. \tag{.0.12}$$

The post synaptic variable u_i^k is transformed into the activity of the neuron (scaled between zero and one) by the following sigmoidal function :

$$\begin{aligned} y_i^k &= \zeta(u_i^k) \\ &= \frac{1}{1 + e^{-a(u_i^k - u_0)}}. \end{aligned} \tag{.0.13}$$

The value of the parameters of the sigmoïdal function are presented in Table 12.

Tableau 12. Values of the parameters of the sigmoïdal function

Parameter	Description	Value	Reference
a	Parameter affecting the central slope	4	[**2**]
u_0	Value to obtain a y_i^k of 0.5	1	

The parameter a is a parameter affecting the central slope and u_0 is the value of u_i^k to obtain a y_i^k of 0.5. The subregions are connected through the three neurotransmission pathways described in section 2.3 and are represented in Figure **??** of the paper. Knowing the connections between each subregion and their nature (excitatory or inhibitory) enables us to write the equation of the neuronal activity of each subregion. With all the u and y beeing 2×1 vectors except for u^{STN}, y^{STN}, u^H and y^H which are 1×1 vectors, the equations are the following :

Cortical neurons :

$$\tau_L \frac{du^L}{dt} = -u^L + Ly^C, \tag{.0.14}$$

$$\tau \frac{du^C}{dt} = -u^C + w^{CS} S + u^L + w^{CT} y^T, \tag{.0.15}$$

$$y_i^C = \zeta(u_i^C) \; i \in \{1,2\}, \tag{.0.16}$$

Go neurons :

$$\tau\frac{u^G}{dt} = -u^G + w^{GS}S + w^{GC}y^C + \alpha \cdot \text{Bound receptor}_{D1}(y^G - \upsilon^G) + w^{GH}y^H \begin{bmatrix}1\\1\end{bmatrix}, \quad (.0.17)$$

$$y_i^G = \zeta(u_i^G)\ i \in \{1,2\}, \quad (.0.18)$$

NoGo neurons :

$$\tau\frac{du^N}{dt} = -u^N + w^{NS}S + w^{NC}y^C + \beta \cdot \text{Bound receptor}_{D2} + w^{NH}y^H \begin{bmatrix}1\\1\end{bmatrix}, \quad (.0.19)$$

$$y_i^N = \zeta(u_i^N)\ i \in \{1,2\}, \quad (.0.20)$$

GPe neurons :

$$\tau\frac{du^E}{dt} = -u^E + w^{EN}y^N + w^{ESTN}y^{STN} + I^E, \quad (.0.21)$$

$$y_i^E = \zeta(u_i^E)\ i \in \{1,2\}, \quad (.0.22)$$

GPi neurons :

$$\tau\frac{du^I}{dt} = -u^I + w^{IG}y^G + w^{IE}y^E + w^{ISTN}y^{STN} \begin{bmatrix}1\\1\end{bmatrix} + I^I, \quad (.0.23)$$

$$y_i^I = \zeta(u_i^I)\ i \in \{1,2\}, \quad (.0.24)$$

STN neuron :

$$\tau\frac{du^{STN}}{dt} = -u^{STN} + k_E E + \sum_{i=1}^{2} w_i^{STNE}y_i^E, \quad (.0.25)$$

$$\text{with } E = y_1^C y_1^C + 2y_1^C y_2^C + y_2^C y_2^C, \quad (.0.26)$$

$$y^{STN} = \zeta(u^{STN}), \quad (.0.27)$$

Thalamus neurons :

$$\tau \frac{du^T}{dt} = -u^T + w^{TI} y^I + w^{TC} y^C, \tag{.0.28}$$

$$y_i^T = \zeta(u_i^T)\ i \in \{1,2\}, \tag{.0.29}$$

Cholinergic interneuron :

$$\tau \frac{du^H}{dt} = -u^H + I^H + \gamma \cdot \text{Bound receptor}_{D2}, \tag{.0.30}$$

$$y^H = \zeta(u^H). \tag{.0.31}$$

See [**2, 3**] for more details concerning this model. The weights of the connections between each subregion are matrices presented in Table 13. The membrane time constants (τ) are also presented in Table 13. These values were found to fit the data of the finger tapping task [**2**].

Both parts of the globus pallidus (intern and extern) [**6**] and the cholinergic interneurons [**1**] are tonically active. This implies the presence of an external input to those neurons. The value of these external inputs are presented in Table 14.

The value of the weight of dopamine impact of the Go, NoGo and cholinergic interneurons are defined in Table 15.

The parameters value of α, β and γ were modified from the original values presented in [**2**] for scaling as discussed in section A.1.

Tableau 13. Values of the synaptic weights and of the membrane time constant (τ) in the neurocomputational model of basal ganglia

Parameter	Description	Value	Reference
w^{CS}	Weight between S and C	$\begin{bmatrix} 1.1 & 0.2 \\ 0.2 & 1.1 \end{bmatrix}$	[**2**]
L	Lateral inhibition weight	$\begin{bmatrix} 0 & -1.2 \\ -1.2 & 0 \end{bmatrix}$	
w^{CT}	Weight between T and C	$\begin{bmatrix} 4 & 0 \\ 0 & 4 \end{bmatrix}$	
w^{GC}	Weight between C and Go	$\begin{bmatrix} 0.48 & 0 \\ 0 & 0.48 \end{bmatrix}$	
w^{GS}	Weight between S and Go	$\begin{bmatrix} 0.9 & 0 \\ 0 & 0.9 \end{bmatrix}$	
w^{NC}	Weight between C and NoGo	$\begin{bmatrix} 1.08 & 0 \\ 0 & 1.08 \end{bmatrix}$	
w^{NS}	Weight between S and NoGo	$\begin{bmatrix} 0.1 & 0 \\ 0 & 0.1 \end{bmatrix}$	
w^{EN}	Weight between NoGo and GPe	$\begin{bmatrix} -2.2 & 0 \\ 0 & -2.2 \end{bmatrix}$	
w^{IE}	Weight between GPe and GPi	$\begin{bmatrix} -3 & 0 \\ 0 & -3 \end{bmatrix}$	
w^{IG}	Weight between Go and GPi	$\begin{bmatrix} -12 & 0 \\ 0 & -12 \end{bmatrix}$	
w^{TC}	Weight between C and T	$\begin{bmatrix} 3 & 0 \\ 0 & 3 \end{bmatrix}$	
w^{TI}	Weight between GPi and T	$\begin{bmatrix} -3 & 0 \\ 0 & -3 \end{bmatrix}$	
k_E	Energy weight in STN	7	
w^{STNE}	Weight between GPe and STN	-1	
w^{ESTN}	Weight between STN and GPe	1	
w^{ISTN}	Weight between STN and GPi	14	
w^{GH}	Weight between ChI and Go	-1	
w^{NH}	Weight between ChI and NoGo	1	
τ	Time constant	24 ms	
τ_L	Time constant for lateral inhibition	120 ms	

Tableau 14. Values of the external input to the neurons

Parameter	Description	Value	Reference
I^E	External input to GPe	$\begin{bmatrix}1\\1\end{bmatrix}$	[**2**]
I^I	External input to GPi	$\begin{bmatrix}3\\3\end{bmatrix}$	
I^H	External input to ChI	1.25	

Tableau 15. Parameter values related to dopamine effect in the basal ganglia

Parameter	Description	Value	Reference
υ^G	Threshold of Go neurons	0.3	[**2**]
α	Dopamine weight to Go neurons	404.6143	
β	Dopamine weight to NoGo neurons	-65	Modified for scaling
γ	Dopamine weight to ChI	-65	

Références

[1] Teemu Aitta-Aho, Benjamin U Phillips, Elpiniki Pappa, Y Audrey Hay, Fiona Harnischfeger, Christopher J Heath, Lisa M Saksida, Tim J Bussey et John Apergis-Schoute : Accumbal cholinergic interneurons differentially influence motivation related to satiety signaling. *eNeuro*, 4, 2017.

[2] Chiara Baston, Manuela Contin, Giovanna Calandra Buonaura, Pietro Cortelli et Mauro Ursino : A mathematical model of levodopa medication effect on basal ganglia in parkinson's disease : An application to the alternate finger tapping task. *Frontiers in Human Neuroscience*, 10, jun 2016.

[3] Chiara Baston et Mauro Ursino : A biologically inspired computational model of basal ganglia in action selection. *Computational Intelligence and Neuroscience*, 2015:1–24, 2015.

[4] J. K. Dreyer : Three mechanisms by which striatal denervation causes breakdown of dopamine signaling. *Journal of Neuroscience*, 34(37):12444–12456, sep 2014.

[5] E N Pothos, V Davila et D Sulzer : Presynaptic recording of quanta from midbrain dopamine neurons and modulation of the quantal size. *The Journal of neuroscience : the official journal of the Society for Neuroscience*, 18:4106–4118, juin 1998.

[6] R Mark Richardson, Curt R Freed, Shoichi A Shimamoto et Philip A Starr : Pallidal neuronal discharge in parkinson's disease following intraputamenal fetal mesencephalic allograft. *Journal of neurology, neurosurgery, and psychiatry*, 82:266–271, mars 2011.

[7] Eva Syková et Charles Nicholson : Diffusion in brain extracellular space. *Physiological reviews*, 88: 1277–1340, octobre 2008.

Annexe B

Cette annexe contient le matériel supplémentaire associé à l'article *Nonlinear pharmacodynamics of Levodopa through Parkinson's disease progression* présenté au Chapitre 2.

B.1 Parameters values

The parameters values for the different parts of the model are presented in the tables below.

Tableau 16. Parameters values of the pharmacokinetic model (equations 2.1,2.2 and 2.3 in the paper)

Parameter	Value [**1**]
Q_{12}	9.11 L/min
Q_{21}	10 L/min
Q_{13}	0.0021 L/min
CL_{e3}	0.006 L/min
CL_{e1}	0.7979 L/min
V_1	12 L
V_2	32 L
V_3	2 L
$k_0(t)$	3.33 mg/min for $0 \leq t \leq 30$min
	0 mg/min for $t \geq 30$min

Tableau 17. Parameters values for the dopamine dynamics model (equations 2.4 and 2.6)

Parameter	Value	Reference
$I_{DAendogenous}$	0.9963 μmol/L/s	[**4**]
V_{max}	4 μmol/L/s	[**4**]
k_m	0.16 μmol/L	[**4, 7**]
k_{rem}	0.04 1/s	[**2, 4**]
k_D^{D1}	1 μmol/L	[**6**]
k_D^{D2}	0.01 μmol/L	[**6**]
B_{max}^{D1}	0.007 μmol/L	[**3**]
B_{max}^{D2}	0.015 μmol/L	[**5**]

Tableau 18. Values of the synaptic weights and of the membrane time constant (τ) in the neurocomputational model of basal ganglia (equation 2.7)

Parameter	Value	Reference
w^{CS}	$\begin{bmatrix} 1.1 & 0.2 \\ 0.2 & 1.1 \end{bmatrix}$	
L	$\begin{bmatrix} 0 & -1.2 \\ -1.2 & 0 \end{bmatrix}$	
w^{CT}	$\begin{bmatrix} 4 & 0 \\ 0 & 4 \end{bmatrix}$	
w^{GC}	$\begin{bmatrix} 0.48 & 0 \\ 0 & 0.48 \end{bmatrix}$	
w^{GS}	$\begin{bmatrix} 0.9 & 0 \\ 0 & 0.9 \end{bmatrix}$	
w^{NC}	$\begin{bmatrix} 1.08 & 0 \\ 0 & 1.08 \end{bmatrix}$	[**1**]
w^{NS}	$\begin{bmatrix} 0.1 & 0 \\ 0 & 0.1 \end{bmatrix}$	
w^{EN}	$\begin{bmatrix} -2.42 & 0 \\ 0 & -2.42 \end{bmatrix}$	
w^{IE}	$\begin{bmatrix} -3 & 0 \\ 0 & -3 \end{bmatrix}$	
w^{IG}	$\begin{bmatrix} -12 & 0 \\ 0 & -12 \end{bmatrix}$	
w^{TC}	$\begin{bmatrix} 3 & 0 \\ 0 & 3 \end{bmatrix}$	
w^{TI}	$\begin{bmatrix} -3 & 0 \\ 0 & -3 \end{bmatrix}$	
k_E	7	
w^{STNE}	-1	
w^{ESTN}	1	
w^{ISTN}	14	
w^{GCHI}	-1	
w^{NCHI}	1	
τ	24 ms	
τ_L	120 ms	

Tableau 19. Values of the external input to the neurons (equation 2.7)

Parameter	Value	Reference
I^E	$\begin{bmatrix}1\\1\end{bmatrix}$	[**1**]
I^I	$\begin{bmatrix}3\\3\end{bmatrix}$	
I^H	1.25	

Tableau 20. Parameters values related to dopamine effect in the basal ganglia (equation 2.7) and to the sigmoid function (equation 2.8)

Parameter	Value	Reference
υ^G	0.3	[**1**]
α	404.6143	
β	-65	Modified for scaling
γ	-65	

Références

[1] Chiara Baston, Manuela Contin, Giovanna Calandra Buonaura, Pietro Cortelli et Mauro Ursino : A mathematical model of levodopa medication effect on basal ganglia in parkinson's disease : An application to the alternate finger tapping task. *Frontiers in Human Neuroscience*, 10, jun 2016.

[2] Evgeny A Budygin, Carrie E John, Yolanda Mateo et Sara R Jones : Lack of cocaine effect on dopamine clearance in the core and shell of the nucleus accumbens of dopamine transporter knock-out mice. *The Journal of neuroscience : the official journal of the Society for Neuroscience*, 22:RC222, mai 2002.

[3] Y H Chou, P Karlsson, C Halldin, H Olsson et L Farde : A pet study of d(1)-like dopamine receptor ligand binding during altered endogenous dopamine levels in the primate brain. *Psychopharmacology*, 146:220–227, septembre 1999.

[4] J. K. Dreyer : Three mechanisms by which striatal denervation causes breakdown of dopamine signaling. *Journal of Neuroscience*, 34(37):12444–12456, sep 2014.

[5] Hiroto Kuwabara, Mary E McCaul, Gary S Wand, Christopher J Earley, Richard P Allen, Elise M Weerts, Robert F Dannals et Dean F Wong : Dissociative changes in the bmax and kd of dopamine d2/d3 receptors with aging observed in functional subdivisions of the striatum : a revisit with an improved data analysis method. *Journal of nuclear medicine : official publication, Society of Nuclear Medicine*, 53:805–812, mai 2012.

[6] Torsten May : Striatal dopamine d1-like receptors have higher affinity for dopamine in ethanol-treated rats. *European Journal of Pharmacology*, 215(2-3):313–316, may 1992.

[7] Michael C. Reed, Janet Best et H. Frederik Nijhout : Passive and active stabilization of dopamine in the striatum. *Bioscience Hypotheses*, 2(4):240 – 244, 2009.

Annexe C

Cette annexe contient le matériel supplémentaire associé à l'article *A mechanistic model of ADHD as resulting from dopamine phasic/tonic imbalance during reinforcement learning* présenté au Chapitre 4.

C.1 Equations of the model and parameters values

C.1.1 Neurocomputational model of basal ganglia

The equations of the neurocomputational model describing the neuronal activity in each subregions of the basal ganglia is described in this section. Abbreviations for the name of each subregions are used and described in Table 21.

Tableau 21. Abbreviations for the subregions of the basal ganglia

Subregion's name	Abbreviation
Sensory input	S
Cortex	C
Cortex's lateral inhibition	L
Go part of striatum (D1 receptors)	G
NoGo part of striatum (D2) receptors	N
Globus pallidus internal	I
Globus pallidus external	E
Subthalamic nucleus	STN
Thalamus	T
Cholinergic interneurons	H

The equations describing the neuronal activity in each region are of type firing rate. There are four neurons in each subregions to represent the four action channels except for the subthalamic nucleus and for the cholinergic interneuron. Let i be the number of

the postsynaptic neuron in the subregion k receiving current from the presynaptic neuron number j in the subregion m with a weight of w^{km}. The general form of the equations are the following :

$$\tau \frac{u_i^k}{dt} = -u_i^k + \sum_{j=1}^{4} w_{ij}^{km} y_j^m. \tag{.0.32}$$

The post synaptic variable u_i^k is transformed into the activity of the neuron (scaled between zero and one) by the following sigmoidal function :

$$\begin{aligned} y_i^k &= \zeta(u_i^k), \\ &= \frac{1}{1 + e^{-a(u_i^k - u_0)}}. \end{aligned} \tag{.0.33}$$

The value of the parameters of the sigmoïdal function are presented in Table 22.

Tableau 22. Values of the parameters of the sigmoïdal function

Parameter	Description	Value	Reference
a	Parameter affecting the central slope	4	[**5**]
u_0	Value to obtain a y_i^k of 0.5	1	

Here are the equations for the neuronal activity in each subregions :

Cortical neurons :

$$\tau_L \frac{du^L}{dt} = -u^L + Ly^C, \tag{.0.34}$$

$$\tau \frac{du^C}{dt} = -u^C + w^{CS} S + u^L + w^{CT} y^T, \tag{.0.35}$$

$$y_i^C = \zeta(u_i^C) \; i \in \{1,2,3,4\}, \tag{.0.36}$$

Go neurons :

$$\tau \frac{u^G}{dt} = -u^G + w^{GS}S + w^{GC}y^C + \alpha \cdot D_1(y^G - v^G) + w^{GH}y^H \begin{bmatrix} 1 \\ 1 \\ 1 \\ 1 \end{bmatrix}, \tag{.0.37}$$

$$y_i^G = \zeta(u_i^G)\ i \in \{1,2,3,4\}, \tag{.0.38}$$

NoGo neurons :

$$\tau \frac{du^N}{dt} = -u^N + w^{NS}S + w^{NC}y^C + \beta \cdot D_2 + w^{NH}y^H \begin{bmatrix} 1 \\ 1 \\ 1 \\ 1 \end{bmatrix}, \tag{.0.39}$$

$$y_i^N = \zeta(u_i^N)\ i \in \{1,2,3,4\}, \tag{.0.40}$$

GPe neurons :

$$\tau \frac{du^E}{dt} = -u^E + w^{EN}y^N + w^{ESTN}y^{STN} + I^E, \tag{.0.41}$$

$$y_i^E = \zeta(u_i^E)\ i \in \{1,2,3,4\}, \tag{.0.42}$$

GPi neurons :

$$\tau \frac{du^I}{dt} = -u^I + w^{IG}y^G + w^{IE}y^E + w^{ISTN}y^{STN} \begin{bmatrix} 1 \\ 1 \\ 1 \\ 1 \end{bmatrix} + I^I, \tag{.0.43}$$

$$y_i^I = \zeta(u_i^I)\ i \in \{1,2,3,4\}, \tag{.0.44}$$

STN neuron :

$$\tau \frac{du^{STN}}{dt} = -u^{STN} + k_E E + \sum_{i=1}^{4} w_i^{STNE} y_i^E, \tag{.0.45}$$

$$\text{with } E = y_1^C y_2^C + y_1^C y_3^C + y_1^C y_4^C + y_2^C y_3^C + y_2^C y_4^C + y_3^C y_4^C, \tag{.0.46}$$

$$y^{STN} = \zeta(u^{STN}), \tag{.0.47}$$

Thalamus neurons :

$$\tau \frac{du^T}{dt} = -u^T + w^{TI} y^I + w^{TC} y^C, \tag{.0.48}$$

$$y_i^T = \zeta(u_i^T)\ i \in \{1,2,3,4\}, \tag{.0.49}$$

Cholinergic interneuron :

$$\tau \frac{du^H}{dt} = -u^H + I^H + \gamma \cdot D_2, \tag{.0.50}$$

$$y^H = \zeta(u^H). \tag{.0.51}$$

See [**2, 3**] for a more detailed description of the model. The weights of connection between each subregions and membrane time constants are presented in Table 23.

The globus pallidus (intern and extern) [**4**] and the cholinergic interneurons [**1**] are tonically active, therefore there is an external input to these neurons. The value of these external inputs are presented in Table 24.

The value of the weight of dopamine effect of the Go, NoGo and cholinergic interneurons are defined in Table 25.

Tableau 23. Values of the synaptic weights and of the membrane time constants (τ) in the neurocomputational model of basal ganglia

Parameter	Description	Value	Reference
w^{CS}	Weight between S and C	$\begin{bmatrix} 1 & 1 & 1 & 1 \\ 1 & 1 & 1 & 1 \\ 1 & 1 & 1 & 1 \\ 1 & 1 & 1 & 1 \end{bmatrix}$	
L	Lateral inhibition weight	$\begin{bmatrix} 0 & -1.2 & -1.2 & -1.2 \\ -1.2 & 0 & -1.2 & -1.2 \\ -1.2 & -1.2 & 0 & -1.2 \\ -1.2 & -1.2 & -1.2 & 0 \end{bmatrix}$	
w^{CT}	Weight between T and C	$\begin{bmatrix} 4 & 0 & 0 & 0 \\ 0 & 4 & 0 & 0 \\ 0 & 0 & 4 & 0 \\ 0 & 0 & 0 & 4 \end{bmatrix}$	
w^{EN}	Weight between NoGo and GPe	$\begin{bmatrix} -2.2 & 0 & 0 & 0 \\ 0 & -2.2 & 0 & 0 \\ 0 & 0 & -2.2 & 0 \\ 0 & 0 & 0 & -2.2 \end{bmatrix}$	
w^{IE}	Weight between GPe and GPi	$\begin{bmatrix} -3 & 0 & 0 & 0 \\ 0 & -3 & 0 & 0 \\ 0 & 0 & -3 & 0 \\ 0 & 0 & 0 & -3 \end{bmatrix}$	[**5**]
w^{IG}	Weight between Go and GPi	$\begin{bmatrix} -36 & 0 & 0 & 0 \\ 0 & -36 & 0 & 0 \\ 0 & 0 & -36 & 0 \\ 0 & 0 & 0 & -36 \end{bmatrix}$	
w^{TC}	Weight between C and T	$\begin{bmatrix} 3 & 0 & 0 & 0 \\ 0 & 3 & 0 & 0 \\ 0 & 0 & 3 & 0 \\ 0 & 0 & 0 & 3 \end{bmatrix}$	
w^{TI}	Weight between GPi and T	$\begin{bmatrix} -3 & 0 & 0 & 0 \\ 0 & -3 & 0 & 0 \\ 0 & 0 & -3 & 0 \\ 0 & 0 & 0 & -3 \end{bmatrix}$	
k_E	Energy weight in STN	7	
w^{STNE}	Weight between GPe and STN	-1	
w^{ESTN}	Weight between STN and GPe	1	
w^{ISTN}	Weight between STN and GPi	30	
w^{GH}	Weight between ChI and Go	-1	
w^{NH}	Weight between ChI and NoGo	1	
τ	Time constant	15 ms	
τ_L	Time constant for lateral inhibition	75 ms	

Tableau 24. Values of the external input to the neurons

Parameter	Description	Value	Reference
I^E	External input to GPe	$\begin{bmatrix}1\\1\\1\\1\end{bmatrix}$	[**5**]
I^I	External input to GPi	$\begin{bmatrix}2.5\\2.5\\2.5\\2.5\end{bmatrix}$	Modified from [**5**]
I^H	External input to ChI	1	[**5**]

Tableau 25. Parameters value related to dopamine effect in the basal ganglia

Parameter	Description	Value	Reference
υ^G	Threshold of Go neurons	0.35	[**5**]
α	Dopamine weight to Go neurons	20	Modified from [**5**]
β	Dopamine weight to NoGo neurons	-12.5	Modified from [**5**]
γ	Dopamine weight to ChI	-6.25	Modified from [**5**]

C.2 Evolution of synaptic weights figures

Figures of synaptic weights evolution with each epoch as described in the paper.

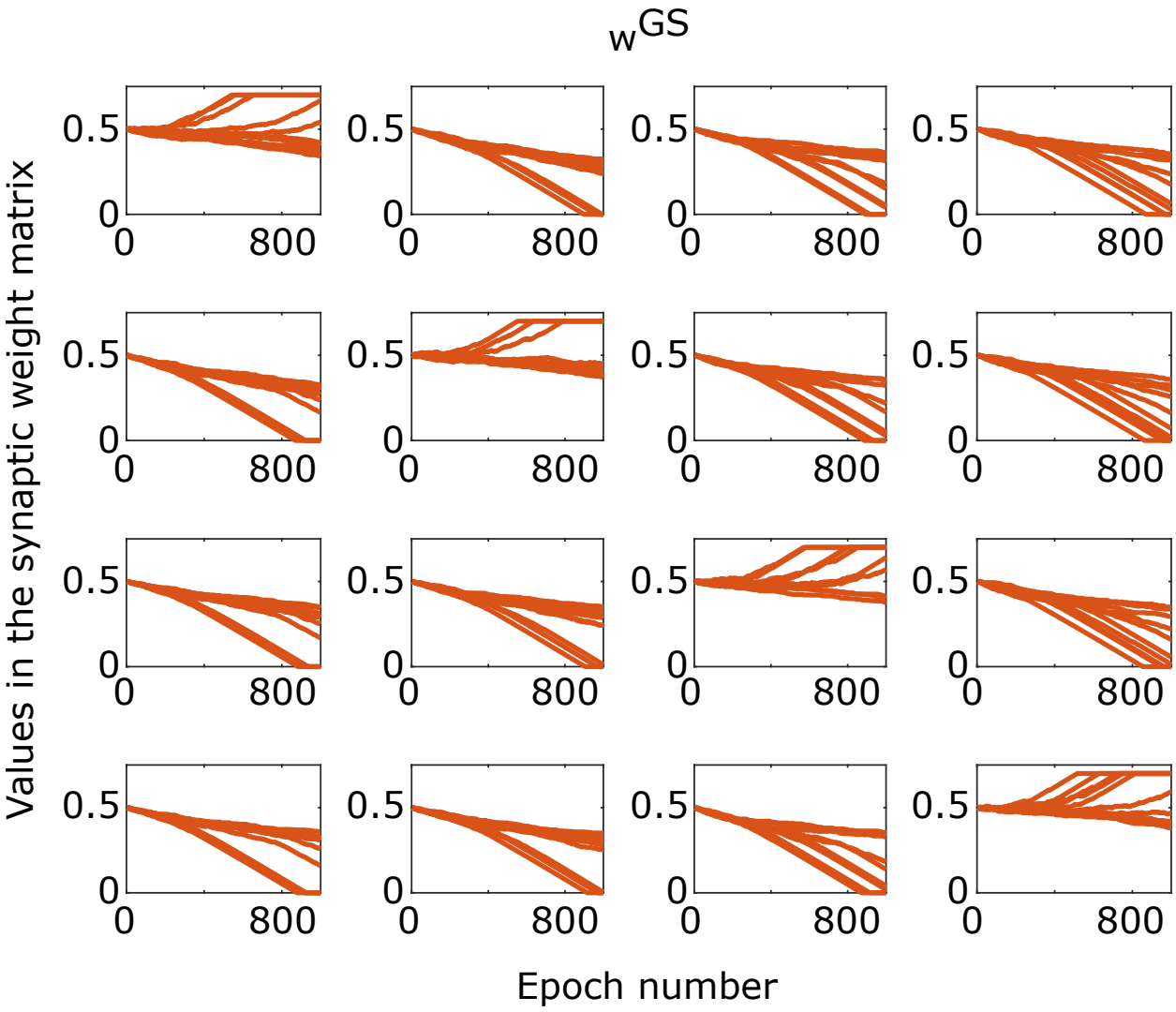

Figure 50. Evolution of the values in the w^{GS} matrix of each individual in the dopamine imbalance group

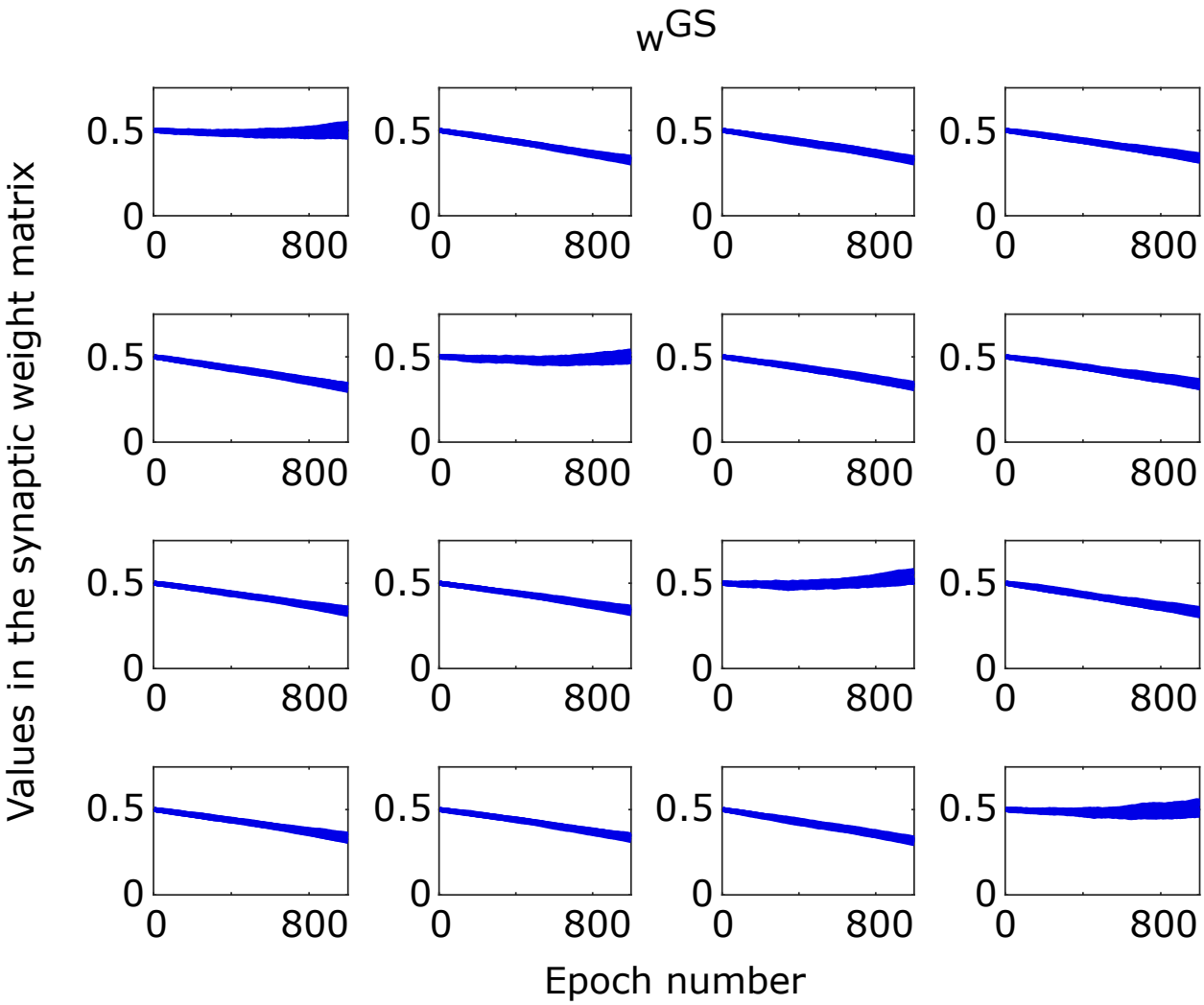

Figure 51. Evolution of the values in the w^{GS} matrix of each individual in the control group

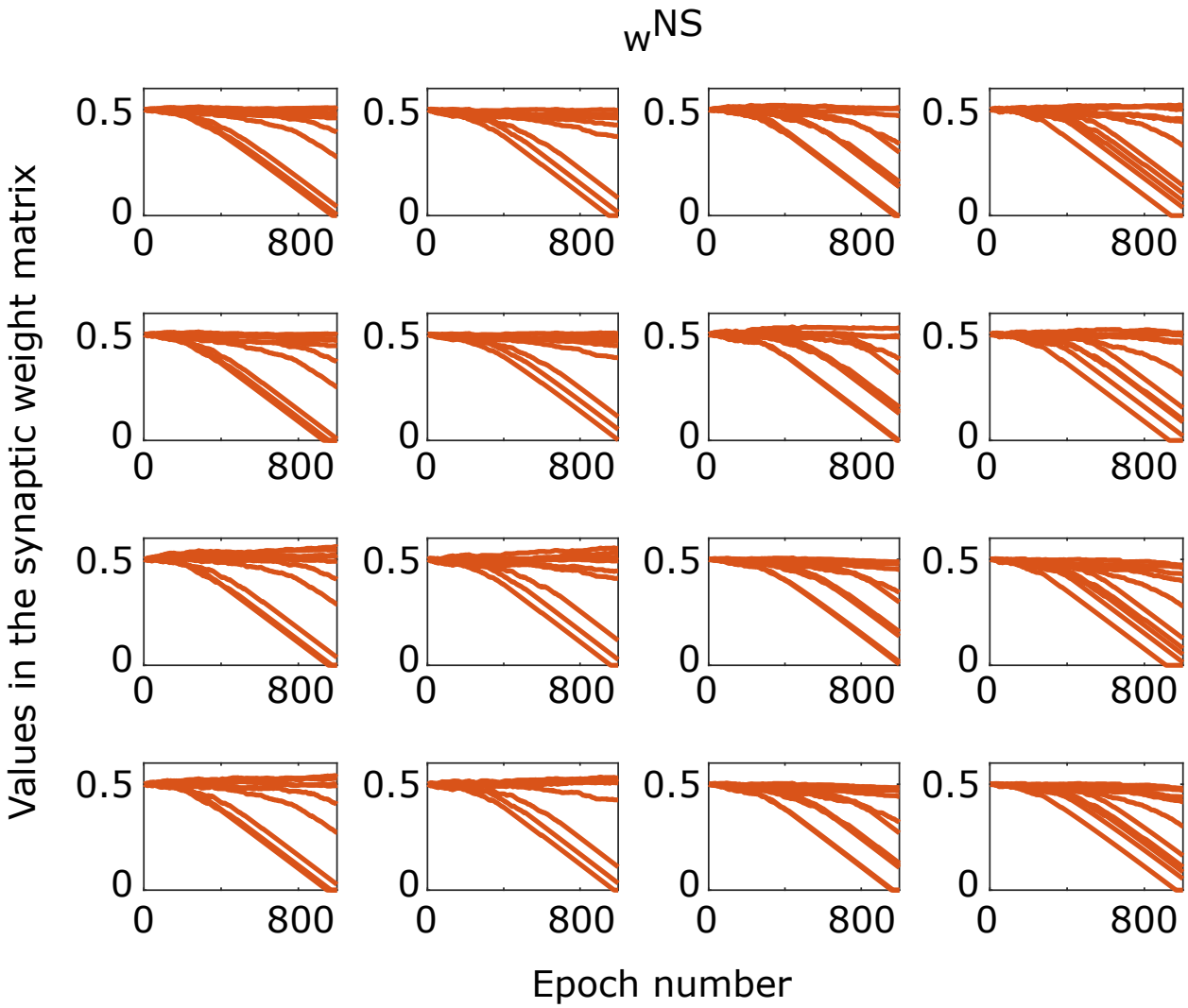

Figure 52. Evolution of the values in the w^{NS} matrix of each individual in the dopamine imbalance group group

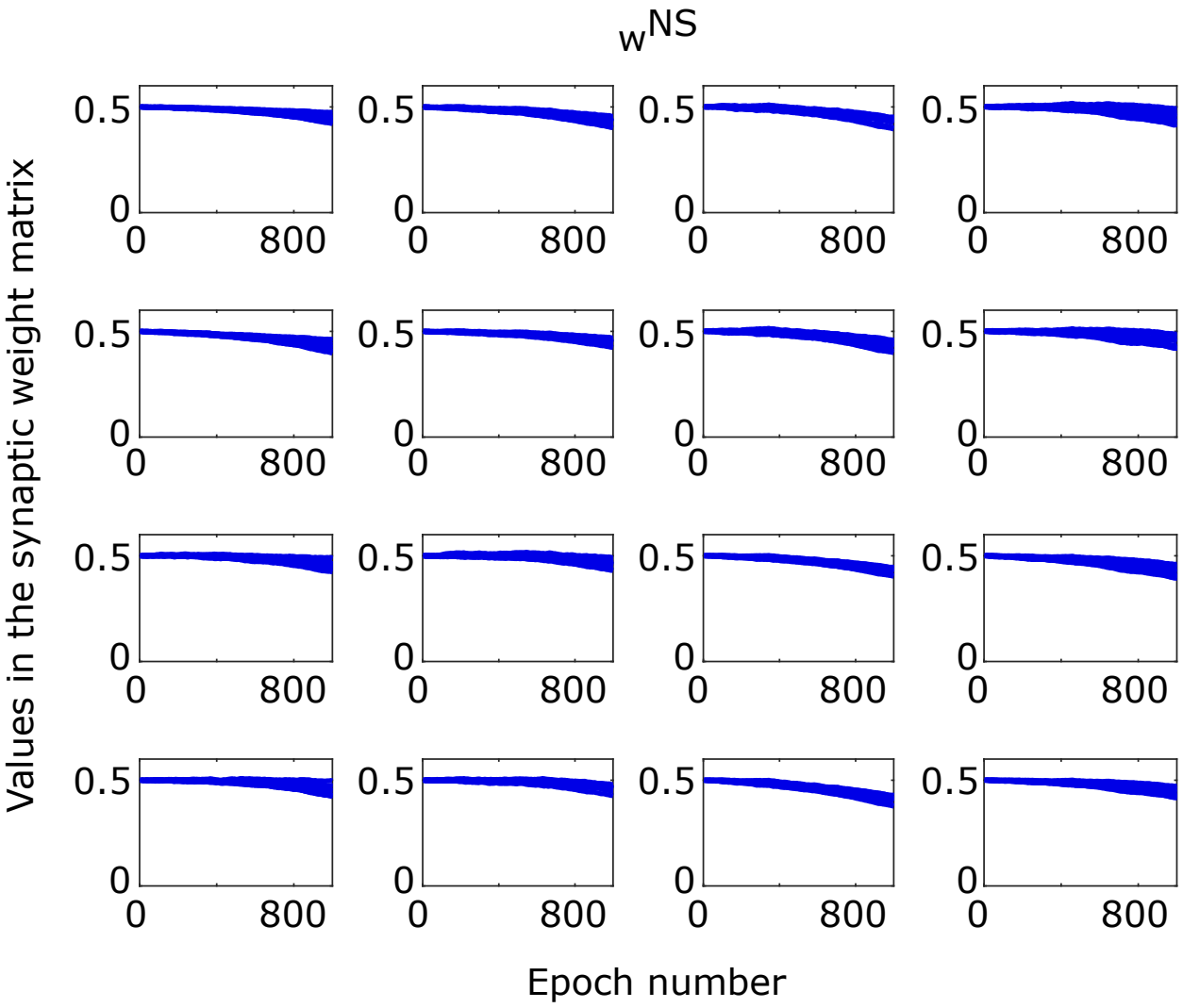

Figure 53. Evolution of the values in the w^{NS} matrix of each individual in the control group

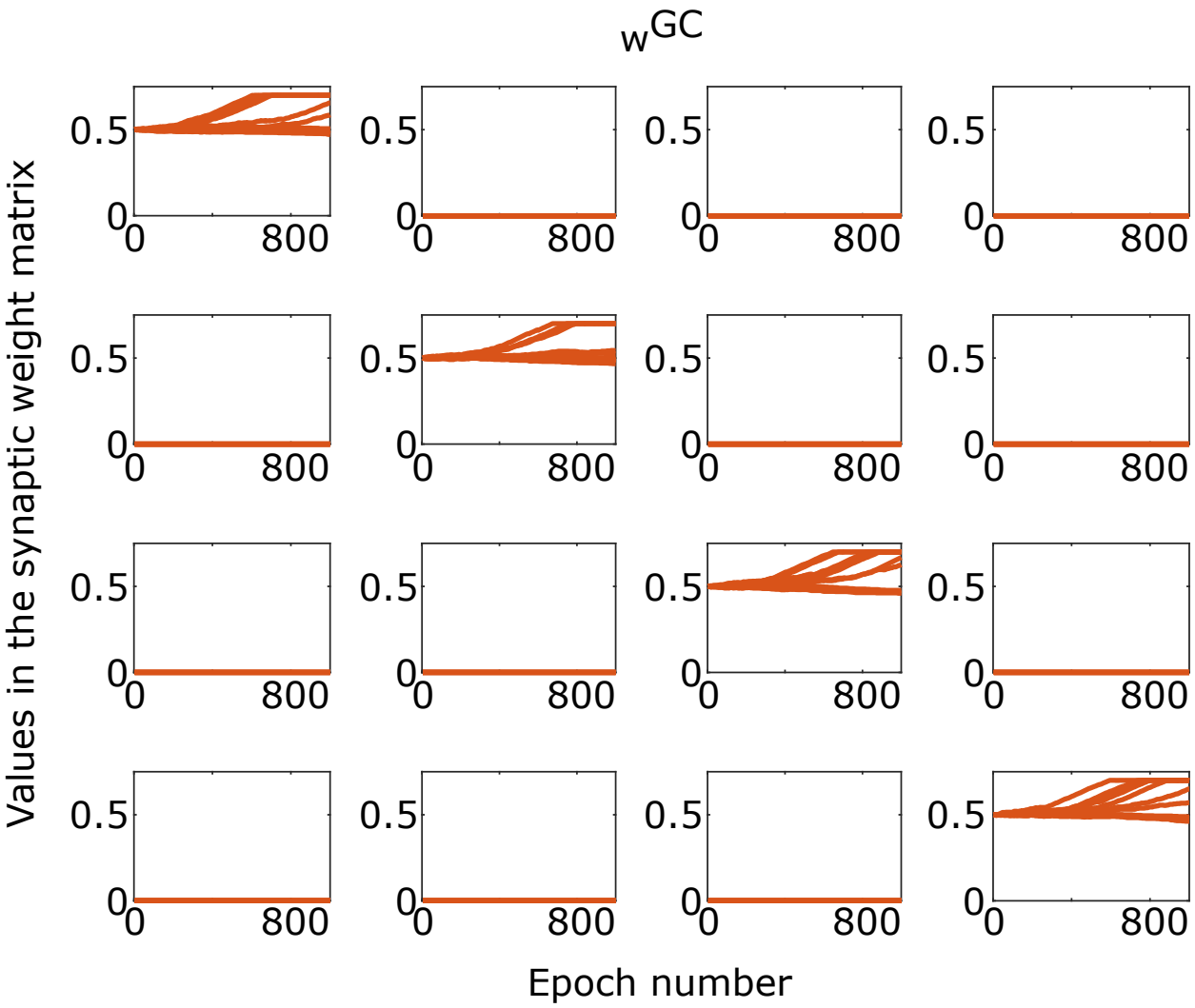

Figure 54. Evolution of the values in the w^{GC} matrix of each individual in the dopamine imbalance group

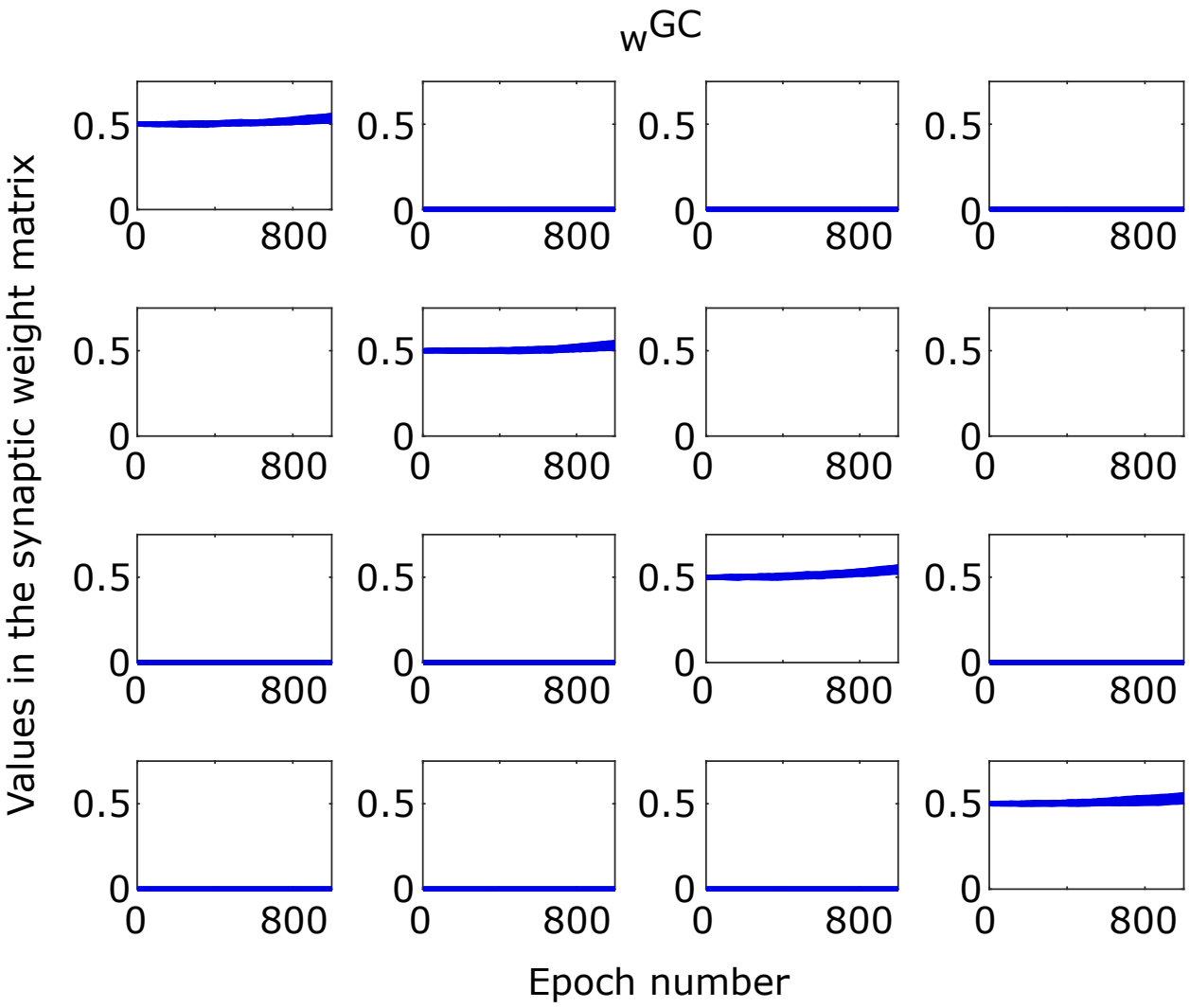

Figure 55. Evolution of the values in the w^{GC} matrix of each individual in the control group

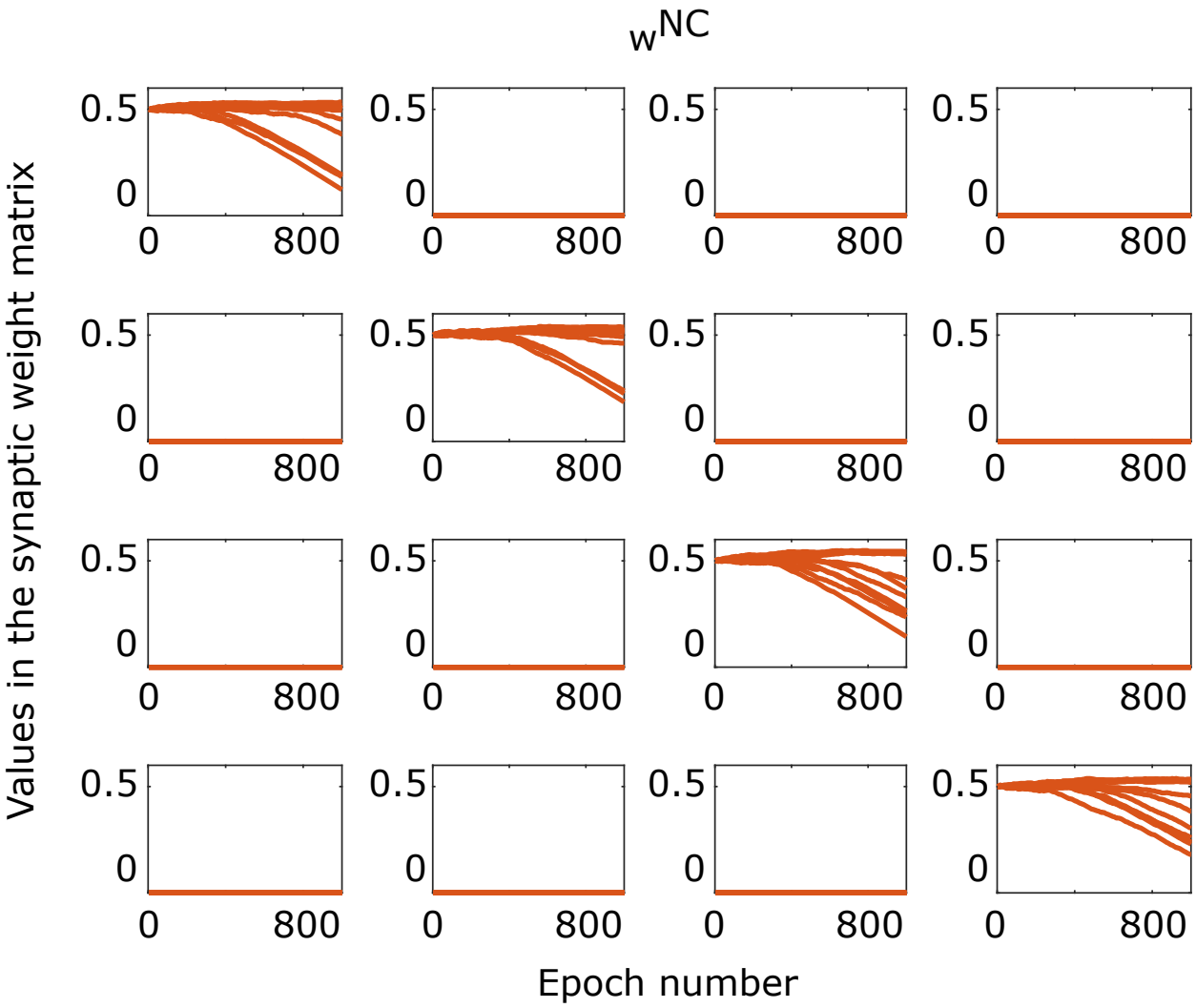

Figure 56. Evolution of the values in the w^{NC} matrix of each individual in the dopamine imbalance group

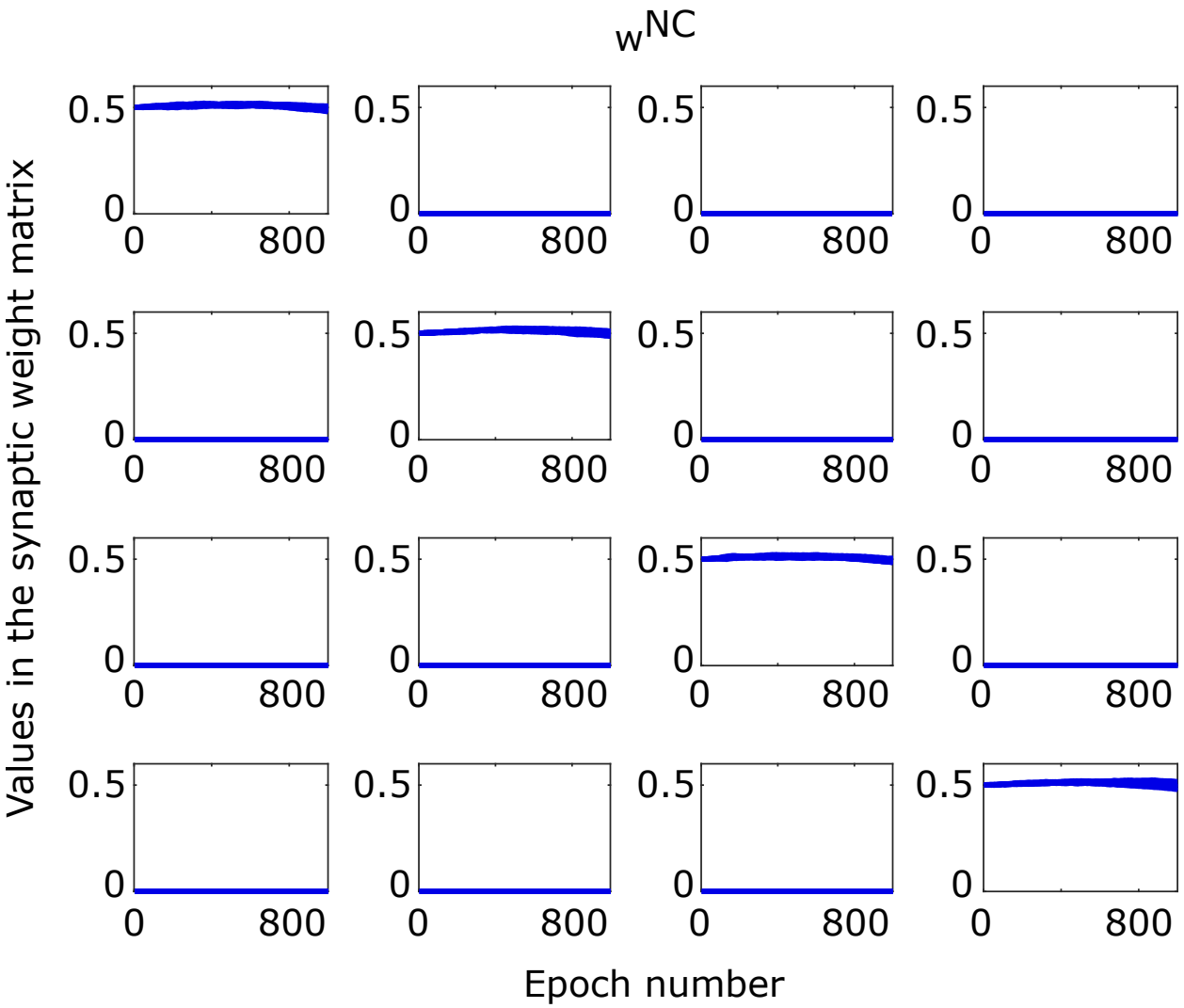

Figure 57. Evolution of the values in the w^{NC} matrix of each individual in the control group

Références

[1] Teemu Aitta-Aho, Benjamin U Phillips, Elpiniki Pappa, Y Audrey Hay, Fiona Harnischfeger, Christopher J Heath, Lisa M Saksida, Tim J Bussey et John Apergis-Schoute : Accumbal cholinergic interneurons differentially influence motivation related to satiety signaling. *eNeuro*, 4, 2017.

[2] Chiara Baston, Manuela Contin, Giovanna Calandra Buonaura, Pietro Cortelli et Mauro Ursino : A mathematical model of levodopa medication effect on basal ganglia in parkinson's disease : An application to the alternate finger tapping task. *Frontiers in Human Neuroscience*, 10, jun 2016.

[3] Chiara Baston et Mauro Ursino : A biologically inspired computational model of basal ganglia in action selection. *Computational Intelligence and Neuroscience*, 2015:1–24, 2015.

[4] R Mark Richardson, Curt R Freed, Shoichi A Shimamoto et Philip A Starr : Pallidal neuronal discharge in parkinson's disease following intraputamenal fetal mesencephalic allograft. *Journal of neurology, neurosurgery, and psychiatry*, 82:266–271, mars 2011.

[5] Mauro Ursino et Chiara Baston : Aberrant learning in parkinson's disease : A neurocomputational study on bradykinesia. *The European journal of neuroscience*, 47:1563–1582, juin 2018.